# PURIFICATION AND CHARACTERIZATION OF A NOVEL ANTILITHIATIC PROTEIN FROM THE SEEDS OF DOLICHOS BIFLORUS AND ITS VALIDATION IN RAT UROLITHIATIC MODEL

**by**


## RAKESH KUMAR BIJARNIA


**A THESIS SUBMITTED IN FULFILLMENT OF THE REQUIREMENTS FOR THE DEGREE OF**

**DOCTOR OF PHILOSOPHY**

**IN**

**BIOTECHNOLOGY AND BIOINFORMATICS**



**JAYPEE UNIVERSITY OF INFORMATION TECHNOLOGY**
**WAKNAGHAT**


**AUGUST 2008**

JAYPEE UNIVERSITY OF INFORMATION TECHNOLOGY
(Established by H.P. State Legislative vide Act No. 14 of 2002)
Waknaghat, P.O. Dumehar Bani, Kandaghat, Distt. Solan – 173215 (H.P.) INDIA
Website : www.juit.ac.in
Phone No. (91) 07192-257999 (30 Lines)
Fax: (91) 01792 245362

# CERTIFICATE

This is to certify that the thesis entitled, "**PURIFICATION & CHARACTERIZATION OF A NOVEL ANTILITHIATIC PROTEIN FROM THE SEEDS OF DOLICHOS BIFLORUS AND ITS VALIDATION IN RAT UROLITHIATIC MODEL"** which is being submitted by **Rakesh Kumar Bijarnia** in fulfillment for the award of degree of **Doctor of Philosophy** in **Biotechnology and Bioinformatics** by **Jaypee University of Information Technology**, is the record of candidate's own work carried out by him under my supervision. This work has not been submitted partially or wholly to any other University or Institute for the award of this or any other degree or diploma.

**Supervisor**
**Dr. C.Tandon**
Associate Professor
Biotechnology & Bioinformatics
Jaypee University of Information Technology,
Waknaghat, Solan

**Co-Supervisor**
**Dr. S.K. Singla**
Professor
Department of Biochemistry
Panjab University,
Chandigarh

*To my parents*

*The voice of parents is the voice of gods, for to their children*
*they are heavensliutenants*

# Acknouledgement

Writing a thesis is like going on a mountain trip, never certain to reach the summit, but always aware of difficulties lying ahead. Since past few years, I have worked with a great number of people whose contribution in assorted ways to the research and in making of my thesis deserved special mention. It is a pleasure to convey my gratitude to all of them with my humble acknowledgment.

First of all, I wish to thank my advisor, Dr. C. Tandon, for his advice and support. I especially appreciate the laboratory atmosphere of intellectual independence with friendly collaboration that he fostered. Above all and the most needed, he provided me unflinching encouragement and support in various ways. He has been a constant oasis of ideas and valuable suggestions in science and everyday life, which exceptionally inspire and enrich my growth as a student, a researcher and a person. I am indebted to him more than he knows. I gratefully acknowledge Dr. S.K. Singla for his advice, supervision, and crucial contribution, which made him an important contributor of this research and so to this thesis. I wish to thank him for making generous provisions of lab facilities at Panjab University and timely help during course of my research.

I express my earnest gratitude to, Professor R.S. Chauhan, Head of the Department of Biotechnology and Bioinformatics, Jaypee University of Information Technology, for his constructive comments, for his important support during the course of this work and finally for setting up good standards of research in the whole department.

I would like to record my gratitude to Brig (Retd.) Balbir Singh, Registrar, Jaypee University of Information Technology for being a supportive person and providing all financial help on right time, required for the experimental work. I express my earnest gratitude to Dr. D.S. Chauhan, Vice Chancellor and Dr. Y Medury, former Vice Chancellor of Jaypee University of Information Technology for providing excellent facilities required to accomplish this endeavor. I want to extend a word of thanks to Dr. P.K. Naik for his meticulous efforts in completing the *in silico* work of this thesis.

I am also thankful to Dr. S.K. Singh, Department of Urology, Post Graduate Institute of Medical and Education research (PGIMER), Chandigarh, India for providing

clinical calcium oxalate stones, Dr. Girish Sahni, Director, Institute of Microbial Technology (IMTECH), Chandigarh, India for amino acid analysis, Dr. P. Rama Rao, Director, National Institute of Pharmaceutical Education and research (NIPER), SAS Nagar, India for MALDI-TOF MS and Mr. Navtej Singh of Sophisticated Analytical Instrumentation Facility (SAIF), Panjab University, Chandigarh, India for microscopic imaging.

I also benefited by unreserved suggestion and constructive criticism of all the teachers of our department during the semester end seminars. Furthermore, I would like to thank all the technical staff of the department for their unstinted help and generous cooperation.

I was fortunate enough to have friends like Hans Raj (Hansie), Amit, Deepak, Sunil, Parvinder, Nishu & Sapna for their everlasting love, synergy, moral boosting and invaluable help whenever it was most needed. I wish to thank Hansie for his support, unreserved suggestions and moral boosting. Thank you Hansie for constant supply of papers whenever I required, I could never have accomplished the research I started without them. Collective and individual acknowledgments are also owed to my colleagues whose presence somehow perpetually refreshed and cherished me. Many thanks go in particular to Afroz, Priyadarshini, Hemant, Priyanka for giving me such a pleasant time when working together with them. Thanks to all the bubbly juniors Aarti, Payal, Nidhi, Mani, Krishna, Saurabh, Mamta, Tamana & Anshoo, who made working in the lab a pleasure.

I also know that I would not be here today, if not for the love and support of my fiancé, Tanzeer. When things got difficult, she pushed me, inspired me, and made me a better person and scientist. I am lucky to have not only a companion, but a colleague who always understands me. In addition to advisors and colleagues, a person's success is often a result of the strength and support of their family. Finally, I would like to thank my parents. It is the result of their guidance and unconditional love, that I have achieved great successes in my life. Mahinder, Suman bhabi, Kailash and Dr.Vijay, thanks for the support and care you have always bestowed upon me.

To all acknowledged, I solemnly owe this work.

**Rakesh Kumar Bijarnia**

# TABLE OF CONTENTS

# LIST OF TABLES

# LIST OF FIGURES

Page

## LIST OF ABBREVIATIONS

| | |
|---|---|
| **AP** | Alkaline Phosphatase |
| **BSA** | Bovine serum albumin |
| **$Ca^{2+}$** | Calcium ion |
| **CaOx** | Calcium oxalate |
| **CaP** | Calcium phosphate |
| **CAT** | Catalase |
| **CGU** | Carboxy glutamic acid |
| **CNX** | Calnexin |
| **COD** | Calcium oxalate dihydrate |
| **COM** | Calcium oxalate monohydrate |
| **DAP** | *Dolichos biflorus* antilithiatic protein |
| **DTNB** | 5-5′’-Dithio-bis (2-nitrobenzoic acid) |
| **E.g.** | *Exempli gratia* (for example) |
| **EDTA** | Ethylenediaminetetraacetic acid |
| **EG** | Ethylene glycol |
| **ELISA** | Enzyme linked immunosorbant assay |
| **ESWL** | Extra corporeal shock wave lithotripsy |
| **FEB** | Free energy of binding |
| **FTIR** | Fourier transform infrared spectroscopy |
| **GAGs** | Glucosaminoglycans |
| **Gla** | Gamma carboxy glutamic acid |
| **GSH** | Reduced glutathione |
| **GSSG** | Oxidized glutathione |
| **HE** | Haemotoxylin & Eiosin |
| **HPLC** | High pressure liquid chromatography |

| | |
|---|---|
| **$HPO_4^{2-}$** | Phosphate ion |
| **i.e.** | *id est* (that is) |
| **LDH** | Lactate dehydrogenase |
| **LP** | Low pressure |
| **LPO** | Lipid peroxidation |
| **MALDI-TOF** | Matrix assisted laser desorption ionization time of flight |
| **MDA** | Malondialdehyde |
| **MDCK** | Madin-Darby canine kidney |
| **MOE** | Molecular operating environment |
| **MS** | Mass spectroscopy |
| **NAC** | N-acetylcysteine |
| **NBT** | Nitro blue tetrazolium |
| **$NH_4Cl$** | Ammonium chloride |
| **OD** | Optical density |
| **OPN** | Osteopontin |
| **PAGE** | Polyacrylamide gel electrophoresis |
| **PDB** | Protein Data bank |
| **pI** | Isoelectric point |
| **PMSF** | phenylmethane sulphonyl fluoride |
| **ROS** | Reactive oxygen species |
| **SEM** | Scanning electron microscopy |
| **SD** | Standard deviation |
| **SDS** | Sodium dodecyl sulphate |
| **SOD** | Super oxide dismutase |
| **TBA** | Thiobarbituric acid |
| **TCA** | Trichloroacetic acid |

| | |
|---|---|
| **TEM** | Transmission electron microscopy |
| **TFA** | Trifloroacetic acid |
| **UV** | Ultraviolet |
| **w.r.t.** | with respect to |

## Common abbreviations for the twenty amino acids

| | |
|---|---|
| **Ala** | Alanine |
| **Arg** | Arginine |
| **Asp** | Aspartic acid |
| **Asn** | Asparagine |
| **Cys** | Cysteine |
| **Glu** | Glutamic acid |
| **Gln** | Glutamine |
| **Gly** | Glycine |
| **His** | Histidine |
| **Ile** | Isoleucine |
| **Leu** | Leucine |
| **Lys** | Lysine |
| **Met** | Methionine |
| **Phe** | Phenylalanine |
| **Pro** | Proline |
| **Ser** | Serine |
| **Thr** | Threonine |
| **Trp** | Tryptophan |
| **Tyr** | Tyrosine |
| **Val** | Valine |

# Abstract

Stone formation in the kidney is one of the oldest and most wide spread diseases known to man. Kidney stone formation also called as urolithiasis is a common chronic disorder affecting 10-15% of the general population world wide. Advancement in various treatments of urolithiasis has tried to sort out the problem to some extent, but recurrence and persistent side effects after the treatment restrict their use. An alternate, using phytotherapy which is advantageous, safe and culturally acceptable is being sought. Many medicinal plants have been employed since ages to treat urinary stones. The rationale behind their use is not well established through systematic and pharmacological studies, except for some composite herbal drugs and plants. The discovery and elucidation of the mechanism of action, in particular the clinical role of these herbal remedies can make an important contribution to treatment of urinary stone disease as an alternative or adjunct therapy. Till date, various plant extracts have been studied to reduce the incidence of urolithiasis but the identification of naturally occurring calcium oxalate inhibitory biomolecules from plants was hampered in the past by limitations in identification method.

*Dolichos biflorus* seeds, which are used as dietary food in the northern region of India, possess antilithiatic properties. The present study is aimed at examining the efficacy of *Dolichos biflorus* on calcium oxalate and calcium phosphate crystallization *in vitro* and further validating it in rat urolithiatic model. By combining conventional biochemical methods with recent advances in mass spectrometry, a novel calcium oxalate (CaOx) and calcium phosphate (CaP) crystal growth inhibitor was purified and characterized from the seeds of *Dolichos biflorus*. In the present study, a dimeric antilithiatic protein from seeds of *Dolichos biflorus* was purified by three step purification scheme; ammonium sulfate fractionation, anion exchange chromatography and molecular sieve chromatography based on its ability to inhibit CaOx and CaP crystallization *in vitro*. The molecular weight of *Dolichos biflorus* antilithiatic protein (DAP) was calculated to be 98 kDa by using size exclusion chromatography on HPLC. The isoelectric point of DAP was calculated to be 4.79. Amino acid analysis of *Dolichos biflorus* antilithiatic protein (DAP) showed an abundant presence of acidic amino acids

like glutamate and aspartate. Matrix-assisted laser desorption/ionization-time-of-flight mass spectrometry (MALDI-TOF) of the DAP showed maximum sequence similarity with a calcium binding protein, calnexin (CNX) of *Pisum sativum*.

Finally, the efficacy of DAP was validated using rat urolithiatic model. DAP was found to restore renal functioning by maintaining creatinine clearance and serum urea level in ethylene glycol induced urolithiatic rats. Polarization microscopy of urine and kidney tissue of rats revealed a drastic decrease in the number of calcium oxalate monohydrate (COM) and calcium oxalate dihydrate (COD) crystals in DAP administered animals. DAP also reduced the renal injury caused by ethylene glycol and ammonium chloride exposure, which was evident from the normalization of renal injury marker enzymes viz. alkaline phosphatase and lactate dehydrogenase. In addition, the histology of renal tissue clearly indicates the effectiveness of DAP in reverting the manifestations caused by renal injury, like shrunken glomerulus, distorted renal tubule and inflammation in kidney tissue.

The antioxidant efficacy of DAP was also evaluated and compared with a known antioxidant N-acetylcysteine (NAC) under the conditions of oxidative stress induced hyperoxaluria. Similar to NAC, DAP also reduced lipid peroxidation, maintained activity of antioxidant enzymes and restored the level of reduced glutathione and redox ratio in the kidney tissue of these animals. Thus, the antilithiatic nature of a novel protein from *Dolichos biflorus* is clearly demonstrated and further indicates its potential as a therapeutic biomolecule for the treatment of urolithiasis.

# Chapter 1
# Review of Literature

## 1.1. KIDNEY STONE

Kidney stones also called renal calculi, are solid concretions (crystal aggregations) of minerals present in urine.These calculi can form anywhere in the urinary tract, from kidneys to the bladder but in the industrialized and affluent countries, they are generaly restricted to the kidneys. The term *urolithiasis* refers to the presence of calculi in the urinary tract, as shown in figure 1.1. It is a widespread disease afflicting mankind and continues to pose a universal health problem even today.

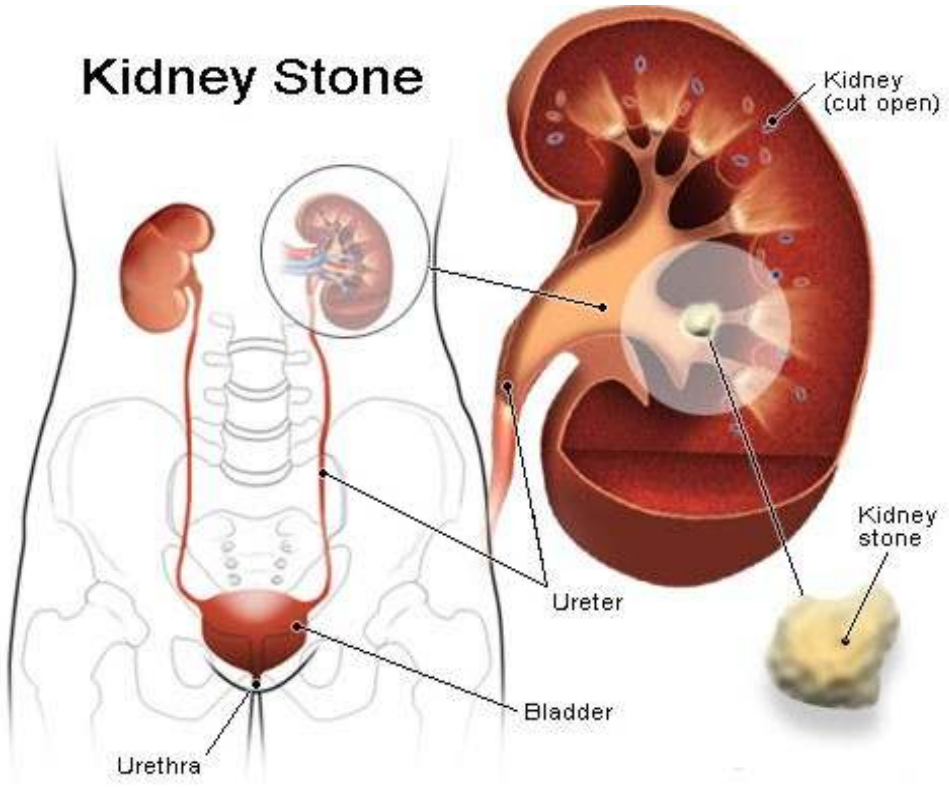


**Figure 1.1.** Common location of Kidney Stones

### *1.1.1. Overview*

Kidneys are a pair of organs that are primarily responsible for filtering metabolites and minerals from the circulatory system. These secretions are then passed to the bladder and out of the body as urine. Some of the substances found in urine are able to crystallize, and in a concentrated form these chemicals can precipitate into a solid deposit attached to the kidney walls. These crystals can grow

through a process of accretion to form a kidney stone and the fundamental cause for all stones is supersaturation of urine [1]. In medical terminology these deposits are known as renal calculi (Latin *renal*, "kidney" and *calculi*, "pebbles") [2].

Renal calculi can vary in size from as small as grains of sand to as large as a golf ball [3]. Kidney stones typically leave the body by passage in the urine stream, and many stones are formed and passed without causing symptoms. If stones grow to sufficient size before passage (on the order of at least 2-3 millimeters) they can cause obstruction of the ureter. The resulting obstruction with dilation or stretching of the upper ureter and renal pelvis as well as spasm of muscle, trying to move the stone, can cause severe episodic pain, most commonly felt in the flank, lower abdomen and groin (a condition called renal colic). Renal colic can be associated with nausea and vomiting due to the embryological association of the kidneys with the intestinal tract. Hematuria (bloody urine) is commonly present due to damage to the lining of the urinary tract.

Kidney stones affect approximately 12 percent of men and 5 percent of women by age 70. Recurrence can occur at a rate of up to 5 percent per year in people who are not treated. Within the United States, about 10–15% of adults are diagnosed with a kidney stone [4] and the total cost for treating this condition was US$2 billion in 2003 [5]. An unanticipated result of global warming is the likely northward expansion of the present-day southeastern U.S. kidney stone "belt." The fraction of the U.S. population living in high-risk zones for nephrolithiasis will grow from 40% in 2000 to 56% by 2050, and to 70% by 2095 [6].

### *1.1.2. History*

The existence of kidney stones has been recorded since the beginning of civilization, and lithotomy for the removal of stones is one of the earliest known surgical procedures [7]. In 1901, a stone was discovered in the pelvis of an ancient Egyptian mummy, and was dated to 4,800 BC. Medical text from ancient Mesopotamia, India, China, Persia, Greece and Rome all mentioned calculous disease. Part of the Hippocratic oath contains an admonition about the dangers of operating on the bladder for stones. The Roman medical treatise *De Medicina* by Cornelius Celsus contained a description of lithotomy, and this work served as the

basis for this procedure up until the 18th century [8]. New techniques in lithotomy began to emerge in 1520, but the operation remained risky. It was only after Henry J. Bigelow popularized the technique of litholopaxy in 1878 and after that the mortality rate dropped from about 24% down to 2.4%. However, other treatment techniques were developed that continued to produce a high level of mortality, especially among inexperienced urologists [8, 9]. In 1980, Dornier MedTech introduced extracorporeal shock wave lithotripsy for breaking up stones via acoustical pulses, and this technique has come into widespread use [10]. Among the famous leaders who were kidney stone sufferers are Emperor Napoleon Bonaparte, Emperor Napoleon III, Peter the Great, Louis XIV, George IV, Oliver Cromwell, and former U.S. President Lyndon B. Johnson. Other notable individuals who endured stones include Benjamin Franklin, the philosopher Sir Francis Bacon, the scientist Sir Isaac Newton, the civil servant and diarist Samuel Pepys, the physicians William Harvey and Herman Boerhaave, and the anatomist Antonio Scarpa [9]. Interestingly, astronauts seem to have a higher risk of developing kidney stones during or after long duration space flights.[11].

### *1.1.3. Types of kidney stones*

There are about six major types of crystalline substances involved in kidney stone formation (Figure 1.2). These are (A) Calcium oxalate (monohydrate-Whewellite, dihydrate-Weddelite), (B) Calcium phosphate (Brushite, Apatite, Whitlockite, Octacalcium-phosphate), (C) Magnesium ammonium phosphate (Struvite, Newberryite), (D) uric acid (uric acid dihydrate, urate monohydrate, ammonium acid urate, xanthine), (E) Cystine and others (F) miscellaneous types, occurs with drug metabolites such as xanthine, Crixivan etc. [12].

#### *A. Calcium oxalate (monohydrate & dihydrate)*

About 70% to 80% of all kidney stones are composed of calcium, usually combined with oxalate. Calcium oxalate (CaOx) develops in acidic urine with pH less than 6.0. Hypercalciuria or increased calcium in the urine may lead to calcium stone formation. It is stated that the amount of calcium in a person's urine is an important contributing factor in the formation of both types of kidney stones.

| | | |
|---|---|---|
|  |  |  |
| Calcium oxalate monohydrate | Calcium oxalate monohydrate over silica | Calcium Oxalate Dihydrate |
|  |  | 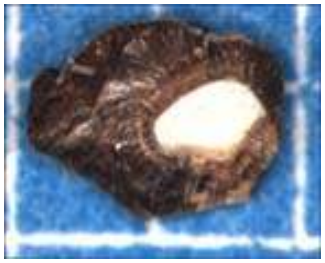 |
| Carbonate Apatite | Tricalcium Phosphate | Calcium Oxalate Monohydrate over apatite |
|  |  | 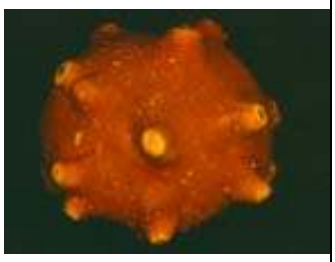 |
| Struvite | Brushite | Uric Acid |
|  |  |  |
| Uric Acid Dihydrate | Xanthine | Cystine |

**Figure 1.2.** Types of Kidney stones

But high levels of oxalate in the urine, or hyperoxaluria, is even more important to stone formation than high levels of calcium or hypercalciuria, since oxalate forms an insoluble complex with calcium to develop a calcium oxalate stone. Excessive intake of food and drink containing oxalate leads to calcium oxalate stones. Also, excessive intake of vitamin C which is metabolized to oxalate may lead to hyperoxaluria and an increase in stone formation.

***B. Calcium phosphate (Brushite, Apatite, Whitlockite, Octacalcium-phosphate)***

Calcium phosphate (CaP) develops in alkaline urine with pH greater than 7.2. Calcium phosphate stones typically occur in patients with metabolic or hormonal disorders such as hyperparathyroidism and renal tubular acidosis. These stones are of two types, Apatite [$Ca_5$ $(PO_4)_3OH$] and Brushite [$CaHPO_4.H_2O$]. Apatite is a very frequent component with 33%. Brushite constitutes 1-2% of the calcium stones. The other calcium phosphates, such as whitlockite and octacalcium phosphate are very rare.

***C. Struvite***

Struvite crystals are also known as magnesium ammonium phosphate, triple phosphate or "infection stones" with a frequency of 10-15%. Unlike other calculi, struvite crystals are caused by a urinary tract infection. The bacteria that cause the urinary tract infection affect urine chemistry and neutralize urine acids. This allows the bacteria to grow even more, resulting in struvite masses. They are the only types of calculi that are treated medically as if they were infected foreign particles. The basis of struvite stones formation is the presence of urea-splitting bacteria. *Proteus mirabilis* is one of the most common urea splitting bacteria. Apart from *Proteus mirabilis,* there are other bacteria such as *Klebsiella, Serratia, Providencia* species that can split urea into ammonia. This process of splitting urea into ammonia decreases the overall acidity of the urine and thus resulting in the favorable conditions that help in the formation of struvite kidney stones. Struvite formations are more common in women than men, mainly because the female urinary tract system is more susceptible to infections.

### *D. Uric acid stones*

Uric acid is an end product of purine metabolism. It is the same crystal that causes gout, an arthritic condition. If the acid level in the urine is high or too much acid is excreted, the uric acid may not dissolve and uric acid stones may form. Genetics may play a role in the development of uric acid stones, which are more common in men. Approximately 10% of patients with kidney stone disease develop this type of stone. Foods high in purines like red meat, fish, and chicken are the main causes behind uric acid stone formation. The solubility of uric acid depends on the acidity or alkalinity of the urine. In acidic urine, pH less than 5.5, uric acid crystals precipitate leading to stone formation. If urine is alkaline, uric acid remains soluble and do not precipitate out. Knowledge of this fact is the basis of the medical treatment of uric acid stones. Factors that increase the risk for uric acid stones are given below.

1. Low urine output.
2. A diet high in animal protein, such as red meat.
3. Increased consumption of alcohol.
4. Gout
5. Inflammatory bowel disease

### *E. Cystine stones*

Cystine stones are rare since less than 1% of kidney stones are made of them. Cystine can build up in the urine to form a stone. It runs in families who are more likely to develop a metabolic condition that produces excess cystine in the urine (cystinuria). Cystine stones may be prevented or dissolved with medication but this may be difficult and not very effective. If the stones cause blockage or are too large, then removal of the stone will be needed. Appropriate prevention measures will reduce the risk of recurrence. Drugs such as penicillamine can be administered to make cystine more soluble and drug captopril can be used to make cystine less likely a reason to cause stones.

### *1.1.4. Organic matrix of stones*

Morphologically, the organic matrix exists as either amorphous or fibrous forms. The organic matrix is investigated to be a mucoprotein in nature and has been designated as uromucoid [13].The matrix is found to be formed of 64% protein, 9.6% non-amino sugars, 5% glycosamine, 10% bound water and traces of lipids with organic ash as remainder [14]. The proteins are generally characterized by high glutamic acid and aspartic acid contents and the frequent occurrence of gamma-carboxy glutamic acid. In matrices of calcium phosphate crystals, the principal proteins are Tamm-Horsfall protein followed by albumin, prothrombin-related proteins and osteopontin. However, when crystals were induced in the urine of stone formers, albumin was the major component of the organic matrix of both CaOx and CaP crystals [15]. Moreover, nine of the 13 proteins were found in all types of stone: human serum albumin, alpha 1-acid glycoprotein, alpha 1-microglobulin, immunoglobulins, apolipoprotein A1, transferrin, alpha 1-antitrypsin, retinol-binding protein and renal lithostathine. The beta 2-microglobulin was present only in calcium oxalate and uric acid stones [16].An *in vitro* study shows that the canine renal distal tubular cell line Madin-Darby canine kidney (MDCK) forms calcium phosphate stones during a long-term culture which is found to contain osteopontin (OPN) and calprotectin [17]. In another study an extracellular protein, produced from Pseudomonas fluorescens strain D with molecular mass of 41.5 kDa was partially purified from stones [18]. The organic matrix of calcific stones is also found to contain significantly more acidic and complexed phospholipids than uric acid and struvite stones. Osteopontin was undetectable in calcium oxalate monohydrate (COM) extracts, but clearly visible in calcium oxalate dehydrate (COD). Prothrombin fragment 1 was abundant in COM, but present in COD in lesser amounts than osteopontin [19].

### *1.1.5. Inhibitors of renal stones*

Although the kidney is supersaturated with calcium and oxalate, the basic components of kidney stones, only three to five percent of people in the world form them. Most people pass microscopic calcium oxalate crystals with their urine before

they can grow into dangerous masses. It is the natural fate of supersaturated solutions to grow crystals, however, something must be working to prevent this in the kidneys and these are inhibitory biomolecules. These inhibitors are also present in soft tissues like tendons, aorta etc. An *in vitro* study demonstrates that flexor tendons of rabbit contain an acidic polypeptide which inhibits the mineralization [20].

In an another study the inhibitory activity of the aorta extract was found to be primarily due to the presence of three biomolecules having molecular weights of 66, 45, and 27-29 kDa. These inhibitory biomolecules loosely associated with aorta may be involved in the control of calcification associated with arteriosclerosis [21]. The crystallization inhibitors help in avoiding or delaying calculi development [22].

An ELISA based assay system study shows that a potent inhibitor having molecular weight between 14.2 and 16.2 kDa was found to be primarily responsible for the differences observed in the urinary inhibitory activity between normal persons and kidney stone patients. This assay system can be used to screen human beings for potential stone formers [23]. Among the most prominent inhibitors is citrate, which, by forming a soluble complex with calcium, reduces the amount of available calcium to form an insoluble complex with oxalate [24].

High molecular weight inhibitors are also investigated which inhibit one or more phases of stone formation *in vitro*, includes several urinary proteins viz. Tamm-Horsfall protein, uropontin, prothrombin F1 peptide [19], uronic acid rich protein (Bikunin), nephrocalcinetc and glycosamino- glycans [25] viz. chondroitin sulfate and heparan sulfate. The bone matrix protein like Osteocalcin, Osteonectin and γ-Carboxyglutamic acid (Gla) protein are also known to inhibit stone formation process. An anti-inflammatory protein called calgranulin, play a key role in the prevention of kidney stones. Calgranulin present, even in minute amounts stop the growth of calcium oxalate crystals, which is the major component of kidney stones. It is made up of two distinct subunits, which are often defective in stone-formers [26].

Another potent inhibitor is inter-alpha-trypsin trimer which could be a mechanism contributing to the differences in CaOx urolithiasis between sexes [27]. Recently, it is investigated that some oxalate binding protein like, histone H (1B)

(27.5kDa), nuclear membrane protein (68 kDa) and nuclear pore complex protein (205 kDa) present in nucleus were having the oxalate binding properties.

The oxalate binding proteins were thought to modulate the crystallization process in a hyperoxaluric condition similar to calcium specific binding protein modulators [28]. It has been observed that cations as well as anions also inhibit *in vitro* mineralization which are $Mg^{2+}$, $P_2O_7^{4-}$,$CrO_4^{2-}$, $SrO_4^{2-}$ etc [29]. Studies showed that these inhibitors act by getting absorbed on the surface of microcrystalline calcium salts.

### *1.1.6. Epidemiology of kidney stones: its causes and distribution*

Kidney stone is a clinical disorder which is known to be caused by multiple etiologic factors. People with kidney stones may first have dysfunction or damage to some of the collecting tubes in the kidney. The epidemiology of renal stones includes preurinary and urinary risk factors.

#### *1.1.6.1. Urinary factors*

Urinary factors include the condition and composition of urine which could result in formation of kidney stones. These factors can be concentration of ions in urine, volume of urine, pH of urine, enzymes concentration and level of various stone formation inhibitors in urine.

#### *A. Concentration of salts in urine*

The key process in the development of kidney stones is supersaturation. This process involves salts that are carried in urine such as calcium oxalate, uric acid, cystine, or xanthine. These salts can become extremely concentrated under certain circumstances. If the volume of urine is significantly reduced or abnormally high amounts of crystal-forming salts are present, the concentration levels reaches the point at which the salts no longer dissolve, they precipitate out and form crystals.

An *in vitro* study has shown that oxalate, either in crystalline or in soluble form triggers a spectrum of responses in renal cells that favor stone formation, including alterations in membrane surface properties that promote crystal attachment and alterations in cell viability that provide debris for crystal nucleation. Activation of

cytosolic phospholipase A2 appears to play an important role in oxalate actions, triggering a signaling cascade that generates several lipid mediators by (arachidonic acid, lysophosphatidyl choline, ceramide) acting as key intracellular targets (mitochondria, nucleus).

The net effect is increased production of reactive oxygen molecules (that in turn affect other cellular processes), an increase in cell death and an induction of a number of genes in surviving cells, some of which may promote proliferation for replacement of damaged cells or may promote secretion of urinary macromolecules that serve to modulate crystal formation. [30]. Further, it was found that calcium oxalate monohydrate gets precipitated at membrane lipid rafts [31].

***B. Volume of urine***

Increased urinary volume is an important tool in the prevention of calcium renal stones. Urine dilution considerably reduces crystallization phenomena induced *in vitro* by an oxalate load in both calcium stone-formers and normal subjects [32].

***C. pH of urine***

Uric acid stones occur especially in patients with very low urine pH (below pH 5.0) and in those with hyperuricosuria. Uric acid is very insoluble in urine at pH 5.0, but becomes significantly more soluble in urine at pH 7.0. Any combination of low urine pH, concentrated urine, and increased urinary uric acid excretion, make one at risk for uric acid stone disease. In some patients this very low urine pH is caused by a defect in renal ammonia secretion that results in less buffering of secreted hydrogen ion and lower urine pH [33] suggested that the very low urine pH is in some way related to the insulin resistance

***D. Enzymes in urine***

The initial step in the pathogenesis of urolithiasis must be the precipitation of an organic matrix of mucoprotein. An important factor in this process may be the activity and/or concentration of the urinary enzyme urokinase which would affect the level of urinary mucoprotein. A decrease has been observed in urinary urokinase concentration of renal stone patients which, once again, underlines the possible involvement of urokinase in renal stone formation [34]. Increased excretion of urinary

enzymes like lactate dehydrogenase, alkaline phosphatase, γ-glutamyl transpeptidase and beta glucuronidase in calculogenic rats indicates membranuria and damage to proximal tubules during stone formation [35].

#### *1.1.6.2. Preurinary factors*

The preurinary factors could be both intrinsic and extrinsic. Intrinsic factors include the heredity, age and sex. Extrinsic factors, on which the incidence of renal stones occurrence depends are geographical distribution, climatic factors and dietary factors which includes water intake.

#### *A. Age and sex*

The inhibition of calcium oxalate crystal growth is influenced by a complex combination of gender and age. With age the vigorous ability to inhibit crystallization is reduced. Men are at higher risk for kidney stones then women. Urinary citrate and magnesium excretion were lower, and glycosaminoglycan and zinc excretion were higher, in stone formers than in controls. The citrate:creatinine excretion ratio was significantly higher in women than men. The higher citrate excretion in women may explain the lower incidence of calcium stones in women [36]. Another known reason attributing to the higher incidence of kidney stones in men then women is inter-alpha-trypsin trimer. It was shown that the inter-alpha-trypsin trimer is a CaOx binding inhibitor which is a function of age and sex-hormone status in males and females. In males a decrease in inter-alpha-trypsin trimer was associated with the onset of adulthood and entry into the 'stone-forming years'. Females did not show this decrease, and neither sex showed an increase in inter-alpha-trypsin trimer in the above 60 group [27].

#### *B. Geographical distribution*

The overall probability of stone forming people differs in various parts of the world: 1-5% in Asia, 5-9% in Europe, 13% in North America, 20% in Saudi Arabia. The composition of stones and their location in the urinary tract, bladder or kidneys may also significantly differ in different countries. Stones in the upper urinary tract appear to be related to the life-style, being more frequent among affluent people, living in developed countries, with high animal protein consumption. Bladder stones

are nowadays mainly seen in the Third World, on account of very poor socio-economic conditions [37]. A high frequency of stone formation among hypertensive patients has been reported, and among those with high body mass as well [37]. In India, two high incidence stone belts have been reported. The first belt starts from Amritsar in North and while passing through Delhi and Agra ends up in Uttar Pradesh. The other belt which starts from Jamnagar in west coast extends inwards towards Jabalpur in central India. Very low incidence areas have been in West Bengal and coastal areas of Maharashtra, Karnatka, Kerala, Tamil Nadu, and Andhra Pradesh

***C. Climatic factors***

While determining the geographic variability in rates of kidney stones in the United States, authors found that ambient temperature and sunlight levels are important risk factors for stones. The differences in exposure to temperature and sunlight may contribute to geographic variability Reasons for higher incidence in summers could be an increased conversion of vitamin D3 to its active metabolites resulting in increased calcium absorption from intestines and decrease in urine production due to loss of water as sweat causes supersaturation of urine with stone constituents [38].

***D. Dietary factors***

Diet plays an important role in the pathogenesis of kidney stones. As the metabolism of many dietary factors, may change with age, the relation between diet and kidney stones may be different in older adults. Uncertainty also remains about the association between many dietary factors, such as vitamin C, magnesium, and animal protein, and the risk of kidney stone formation.

The relative risk for men who consumed 1000 mg or greater of vitamin C showed higher risk of kidney stone formation whereas magnesium at dose 1000mg or more per day showed decreased risk of kidney stone formation, thus indicating that magnesium intake decreases and total vitamin C intake increases the risk of symptomatic nephrolithiasis [39]. Currently, the recommended upper limit for ascorbic acid intake is 2000 mg/d. However, because vitamin C is endogenously converted to oxalate and appears to increase the absorption of dietary oxalate, supplementation may increase the risk of kidney stones. The 1000 mg vitamin C

twice each day increased urinary oxalate and calcium oxalate crystals as kidney stones in 40% of participants when both stone formers and non-stone formers given oxalate and vitamin C for 24 hr [40]. Vitamins have been associated with the kidney stones disease in various references. The potential benefits of dietary or supplemental calcium and vitamin D in reducing the risk of recurrence kidney stones have been documented [41]. It was also suggested that idiopathic renal stone genesis could be generated by vitamin A deficiency [42].

Vitamin K deficiency has also been associated with stones of renal origin. Vitamin K has been known to promote the formation of gamma carboxy-glutamic acid which has high affinity for calcium. A reduced carboxylase activity was observed in the urolithic patients, this suggests its important role in the course of renal calcium oxalate urolithiasis [43]. A number of investigators have shown that increased water intake and increased urinary output decreases the incidence of urinary calculi. Recently, it was shown that the "stone clinic effect" which encourages a high intake of fluid and recommended diet, significantly decreased urinary supersaturation for calcium oxalate and the formation of new kidney stones in 80% of patients during first year of follow-up [44].

***E. Hereditary factors***

Nephrolithiasis is a complex phenotype that is influenced by both genetic and environmental factors. There are several rare, heritable causes of nephrolithiasis that result in the onset of oxalate stone disease early in childhood and frequently lead to renal failure. A study done by Goldfarb et al [45] showed that kidney stones are genetically linked. Their study done on dizygotic and monozygotic twins showed that the heritability of the risk for stones was 56%. Many instances have also showed that nephrolithiasis disproportionately affects white patients. Whites have a higher prevalence of hypercalciuria compared with nonwhites [46]. Previous studies suggest a familial incidence in a subset of persons who have recurrent urinary tract stone disease. Identification and characterization of families of recurrent stone formers is essential for the identification of unique genetic, environmental and metabolic factors that predispose individuals to recurrent calcium oxalate stone formation. As oxaluria and calciuria have a prominent role in calcium stone formation, any genes that

influence their excretion can be considered prime candidates in calcium nephrolithiasis. Among the determinants of urine calcium salt saturation, the rate of urine oxalate excretion is an important risk factor for the development of renal calcium lithiasis. Genetic studies have identified a small group of individuals with known inherited metabolic disorders who develop recurrent calcium oxalate stones at a very early age. Recently a new suggestive gene locus for autosomal dominant nephrolithiasis, have been discovered. It is localized on chromosome 9q33.2-q34.2. The responsible gene will provide new insights into the molecular basis of nephrolithiasis [47]. Low serum phosphate concentrations due to decrease in renal phosphate reabsorption have been reported in some urolithiatic patients with defect in gene coding for the type 2a sodium-phosphate co-transporter [48].

As it is known that there exist many inhibitors in our urine which prevent stone formation. These inhibitors are encoded by genes, so a genetic abnormality of these genes can increase the risk of stone formation. Such protenacious inhibitors are bikunin, a glycoprotein crystal adhesion inhibitor, heparin, a recently found anti-inflammatory protein called calgranulin, made up of two distinct subunits, and many more. The genes encoding them are often defective in stone-formers.

The majority of urinary tract stones are composed of calcium oxalate. The genetic contribution to development of this, is more prevalent, calcium oxalate stone diseases of adult can be due to increased calcium and oxalate absorption. Since vitamin D3 plays a central role in calcium metabolism in the intestine, kidneys and bone, and its plasma levels are usually increased in stone patients [49], a genetic disorder in its pathway was a most attractive hypothesis to explain this trait; the candidate genes contributing to hypercalciuria and, hence, calcium stone formation, could involve some steps of the vitamin D pathway, or anomalies in its receptors, or in its synthesis or activation. Formation of kidney stones is hypothesized to be associated with the vitamin D receptor gene (VDR). On evaluating the association between calcium stone disease and the polymorphism VDR gene in a North Indian population, it was found that the VDR FokI polymorphism may be a good candidate for a marker for calcium oxalate-stone disease [50].

Oxalate is transported into the cells through chloride bicarbonate exchanger band 3 protein 'AE1'. Oxalate competes with chloride for the same transporter [51]. Oxalate is also found to be a substrate of sulfate transport system due to its negative charge and structure. Oxalate is transported across the mitochondrial membrane by a phosphate linked, carrier-mediated system similar to or identical to the dicarboxylate transporter [52]. The affinity of oxalate to these transporters is much less as compared to their respective substrate but due to some mutations in their respective genes, an increase may occur in their transportation.

APRT (Adenine phosphoribosyl transferase) deficiency, is known to cause dihydroxyadenine (2, 8-DHA) urolithiasis. APRT catalyses the synthesis of AMP from adenine and 5'-phosphoribosyl-1-pyrophosphate in the presence of $Mg^{2+.}$ In APRT deficiency, adenine is oxidized to 2,8-dihydroxyadenine (2,8-DHA) by xanthine dehydrogenase (XDH). This defect is inherited as a recessive autosomal trait. The gene is located on chromosome 16q24. Caucasian species predominantly show this defect [53].

The genes responsible for several uncommon but important kidney stone diseases have been cloned, including those for cystinuria, primary hyperoxaluria, hereditary distal renal tubular acidosis, X-linked nephrolithiasis (Dent's disease), and hereditary hypomagnesemia-hypercalciuria. Each of these diseases is inherited as a single Mendelian trait and has clinical features that distinguish it from other causes of kidney stones. Primary Hyperoxaluria is inherited as an autosomal recessive trait and is caused by a mutation in the gene for alanine:glyoxalate aminotransferase. Inactivation or impairment of this enzyme's activity increases the risk of calcium oxalate stones and nephrocalcinosis leading to renal failure.

Cystinuria is inherited autosomal recessive traits that impair renal reabsorption of cystine. It is of two types viz type I and non-type I. Type I disease is caused by a mutation in the solute carrier family 3 gene, SLC3A1 encoding heavy subunit (rBAT) of the heterodimeric transporter. Cystinuria non-type I, is caused by mutations in the SLC7A9 gene. Cystinuria is a heterogeneous disorder at the molecular level as a patient is a compound heterozygote for one SLC3A1 and one SLC7A9 mutation [54]. The inherited autosomal dominant form of distal renal tubular acidosis (dRTA) is

caused by mutations in a gene for the basolateral anion exchanger (AE1) responsible for bicarbonate transport. AE1 mutations can result in both recessive and dominant dRTA, possibly depending on the position of the amino acid change in the protein [55]. The first molecular defect associated with hypercalciuric stone formation was in the voltage-gated chloride channel protein, ClC-5. The product of a gene on the X chromosome, ClC-5 is predominantly expressed in the kidney, primarily in the sub apical endosomes of proximal tubule cells.

In Dent's disease, defects in the ClC-5 channel inhibit chloride entry into the endosomes. This prevents the acidification needed for post-endocytotic degradation of low-molecular-weight proteins [56]. The gene responsible for hereditary hypomagnesemia-hypercalciuria, a syndrome characterized by magnesium and calcium wasting in the urine, nephrolithiasis, nephrocalcinosis, and muscle weakness, encodes a protein, paracellin-1, that may function either as a component or a regulator of a cation channel for paracellular reabsorption of magnesium and calcium in the loop of Henle and distal tubule. Homozygous mutations of PCLN-1 results in a selective defect of paracellular Mg and Ca reabsorption in the thick ascending loop [57].

Up to 40% of patients with idiopathic hypercalciuria have a family history of kidney stones. Patients have excessive intestinal calcium absorption, or renal calcium leak, some may also have secondary hyperparathyroidism. This shows involvement of genes such as those for the calcium-sensing receptor [58] renal sodium-phosphate co-transporter, vitamin D-receptor, renal 1-alpha-hydroxylase (vitamin D-activating enzyme), or factors affecting bone mineralization.

### *1.2. Treatments of kidney stones*

Kidney stones that do not occur as a result of a genetic or metabolic disorder are considered to be due to diet-related condition. Proper nutrition can support healthy kidney function and may discourage stone formation, and natural therapies may help ease the pain and spasm that accompanies stone passage. Initial treatment for symptomatic kidney stones is similar for all patients. However, measures to prevent future stones vary depending upon a person's risk of recurrence. During the initial

phase of kidney stone symptoms, many patients require only pain medication and fluids until the stone is passed. Nonsteroidal anti-inflammatory drugs (NSAIDs, such as ibuprofen or naproxen) may be prescribed for pain and can be taken in pill form. The treatments available for kidney stones include: drinking lots of water, surgical treatments and herbal Medicine.

### *1.2.1. Drinking of water*

Water intake is useful in preventing stone disease [59]. Drinking lots of water (two and a half to three pints per day) and staying physically active are often enough to move a stone out of the body. With increased water intake the kidney stones, of small size and appropriate shape can be passed out with urine. Increased water intake between meals to prevent renal stone recurrence should preferably be achieved with relatively low calcium water and calcium-rich mineral water should be avoided [60].

**Figure 1.3** Water to treat kidney stone

### *1.2.2. Surgical treatment*

Surgery is only an option when the stone attains a size or shape that will prevent its passage and blocks the flow of urine or when it causes damage to the kidney or another part of the urinary tract. Recovery time is longest with open surgery. Today, treatment for these stones is greatly improved and in many cases do not require major surgery and the recovery time is also reduced. Such treatments include, Ureteroscopic, Percutaneous Nephrolithotomy and Extracorporeal Shockwave Lithotripsy.

### *A. Ureteroscopic*

It is usually needed for mid- and lower-ureter stones. No incision is made in this procedure. Instead, the surgeon passes a small fiberoptic instrument called an ureteroscope through the urethra and bladder into the ureter as shown in figure 1.4. The surgeon then locates the stone and either removes it with a cage-like device or shatters it with a special instrument that produces a form of shock wave.

A small tube or stent may be left in the ureter for a few days to help the lining of the ureter heal. Before fiber optics made ureteroscopy possible, physicians used a similar "blind basket" extraction method. But this outdated technique should not be used because it may damage the ureter. Simultaneous combined use of flexible ureteroscopy and percutaneous nephrolithotomy to reduce the number of access tracts in the management of complex renal calculi.

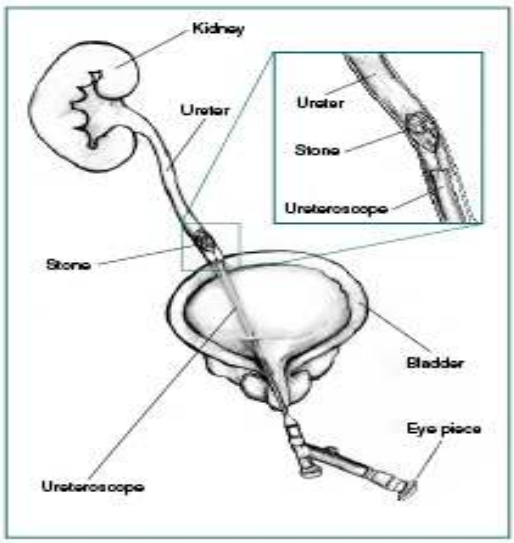


**Figure 1.4.** Treatment of kidney stones by Ureteroscopy

***B. Extracorporeal shock wave lithotripsy (ESWL)***

Extracorporeal shock wave lithotripsy was first applied successfully in a patient with gallbladder stones in January 1985 and revolutionized for treatment of stones throughout the urinary tract. More than 1 million patients are treated annually with ESWL in USA alone. In recent years extracorporeal shock wave therapy is also used in veterinary medicine especially in equine orthopedics [61]. ESWL produces high pressure shock waves which pass through the body. When wave encounters the calculus, the pressure causes the stone to be stressed, then fractured and eventually disintegrated (Figure 1.5). A fluoroscopic x-ray system is used to direct the focus of the waves precisely on the stone. A lithotriptor is a medical device used in the non-invasive treatment of kidney stones (urinary calculosis) and gallstones. It works best with stone between 4 mm and 2 cm in diameter located in the kidney. Lithotripsy offers many advantages over kidney stone removal through surgery, with lithotripsy, there is a sizable reduction in complications and pain. The trauma, inconvenience and pain of a surgical incision are avoided. Post-treatment complications are minimized and recuperation time after treatment is greatly reduced. Recuperation with lithotripsy usually takes only a few days compared to the average of three to six weeks following surgery.

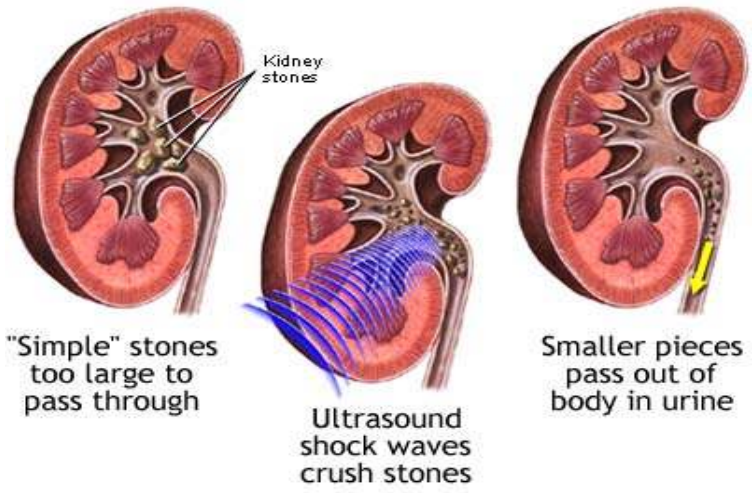


**Figure 1.5.** Treatment of kidney stones by extracorporeal shock wave lithotripsy

Lithotripsy is of two types, shock wave and laser. A shock wave is transmitted through the patient's skin and passes harmlessly through the patient's soft tissue. The shock wave passes through the kidney and strikes the stone. At the stone boundary, energy is lost and this causes small cracks to form on the edge of the stone. Laser lithotripsy disintegrates the kidney stones using a pulsed laser. An endoscope (small tube) is inserted in the urinary tract next to the stone. With the endoscope in place, the laser fiber is inserted to touch the stone. The laser uses short rapid pulses of energy to break up the kidney stone into smaller particles allowing the body to flush the stone naturally. Sometimes, when kidney and urinary tract stone fragments are being passed, urine flow from the kidney can be blocked. If this causes severe pain or blockage of the kidney, a tube called stent may be placed through the back and into the kidney to keep the kidney drained until all the fragments pass out.

***C. Percutaneous nephrolithotomy***

Sometimes a procedure called percutaneous nephrolithotomy is recommended to remove a stone. This treatment is often used when the stone is quite large or in a location that does not allow effective use of ESWL.

In this procedure, the surgeon makes a tiny incision in the back and creates a tunnel directly into the kidney as shown in figure 1.6.

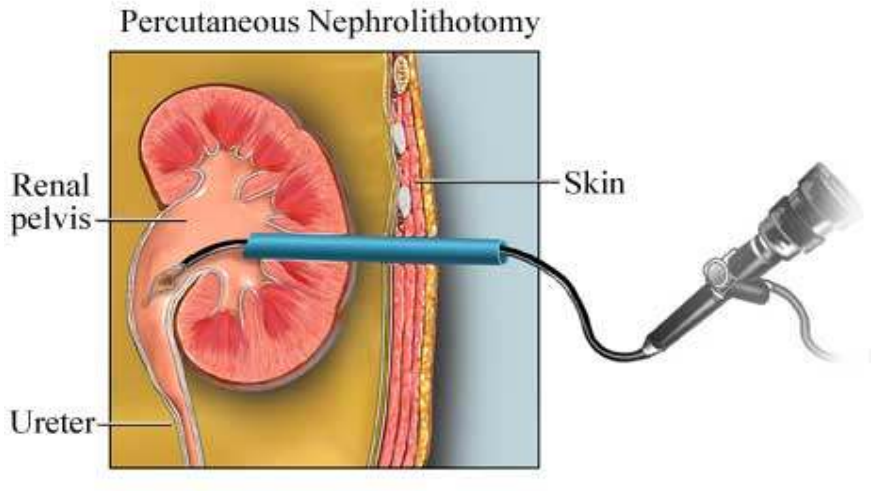


**Figure 1.6.** Percutaneous nephrolithotomy for treatment of kidney stones

Using an instrument called a nephroscope, the surgeon locates and removes the stone. For large stones, some type of energy probe (ultrasonic or electrohydraulic) may be needed to break the stone into small pieces. One advantage of percutaneous nephrolithotomy over ESWL is that the surgeon removes the stone fragments instead of relying on their natural passage from the kidney.

### *1.3. Drawbacks of current treatments*

The extracorporeal shock waves lithotripsy is fundamental in the treatment of lithiasis. However, there are evidences that it can produce renal damage [62]. High-energy shock waves (HESW) when applied to rat did not inhibit the animal growth but caused transitory histological lesion in spleen (proliferative changes in the red pulp) and in liver (cloudy swelling of hepatocytes) [63]. Shockwaves can enhance metastasis of tumors and this effect is attributable to cavitations. It has been reported that extracorporeal shock wave lithotripsy also leads to reduced sperm concentration and motility in men [64]. The effects of ESWL, on patients undergoing renal stone treatment have been studied using activities of glucose-6-phosphate dehydrogenase, superoxide dismutase, catalase and levels of malondialdehyde in the erythrocyte haemolysate. Recent study revealed that ESWL can induce erythrocyte lipid peroxidation and antioxidative defense mechanism may be transiently impaired by it

[65]. A case study also shows an unusual complication like rupture of the kidney observed after extracorporeal shock wave lithotripsy [66].

### *1.4. Crystals of calcium oxalate in plants*

Calcium oxalate crystals are widespread minerals in higher plants [67, 68, 69, 70, 71]. These crystals exhibit specific morphological patterns suggesting a genetically controlled formation [72,73,74,75] induced by the plant. These crystals are typically developed within a crystal chamber in the vacuole of specialized cells called idioblasts [76,77]. The microenvironment into this chamber is believed to play an important role in the crystal nucleation and morphology. For instance, the size and shape of the chamber in which crystals form determine the macromolecules and ions that are present in solution into the chamber [72,73,78]

The specific biological function of calcium oxalate crystals in plants has neither been well characterized nor fully understood. In recent studies, it has been proposed that these crystals can perform diverse biological functions in plants such as storage of calcium, deposit of secondary metabolites, and molecular container of metallic ions that are found in toxic levels inside tissues or cells [71,79]. Additionally, these crystals seem to have specific functions in different plants such as to promote the formation of air chambers in aquatic plants [80], provide structural support [81] or protect against herbivores by their association with irritating chemicals or with proteolytic toxins [82,83,84].

The precise patterns exhibited by plants that produce calcium oxalate reflect multiple levels of organism and cellular control over the crystallization process [77] Extensive observations indicate that calcium oxalate does not result from random precipitations wherever appropriate levels of calcium and oxalate happen to meet but that certain cells within the plant become specialized to accumulate calcium and crystallize calcium oxalate in a controlled and defined manner. The features of calcium oxalate crystals, their functions, and the plant cells that produce them have interested plant biologists for more than a century [85,86]

### *1.4.1. Calcium oxalate crystallization and calcium regulation*

Why do plants sequester calcium oxalate? Calcium is very abundant in the natural environment in which most plants grow. A required element for plant growth and development, calcium plays many important roles, for example, as a structural component of cell walls [87], a signal in various physiological and developmental pathways [88] and an osmoticum [89]. Nonetheless, cytosolic free calcium must be restricted to levels of ~$10^{-7}$ M or less [90], because higher concentrations interfere with a variety of crucial cell processes, including calcium- dependent signaling [88], phosphate-based energy metabolism [90], and microskeletal dynamics [91].

Although the mechanisms controlling calcium absorption at the root are controversial, plants accumulate calcium in excess of cytosolic requirements and limits [89]. In addition, most plants, unlike animals, do not have well-developed excretory systems to dispose of excess calcium. Instead, higher plants appear to modulate differences between the natural abundance of environmental calcium and the very low levels required for cytosolic free calcium by controlling the distribution of calcium and its compartmentation within the cell [92]. The cell wall and the vacuole provide major sinks for calcium in plants [89].

Many plants accumulate crystalline calcium oxalate in response to surplus calcium [93]. With a solubility product of 1.3 X $10^{-9}$ in water, calcium oxalate provides a relatively insoluble, metabolically inactive salt for calcium sequestration [89]. Calcium oxalate thus provides a high-capacity repository for calcium, and plants may accumulate this salt in substantial amounts, up to 80% of their dry weight [94] or 90% of total calcium [93]. The extent of calcium partitioning into calcium oxalate varies among different taxonomic groups of plants. In many species examined so far, calcium oxalate content was found to be about 6.3% of plant dry weight [94]. Numerous studies [95] also indicate that crystals do not only form an inert, non-retrievable pool but they can also be re-dissolved. However, despite the significance of calcium oxalate in sequestering and storing calcium, little is known about factors that direct calcium to this pool.

### *1.4.2. Variation of distribution and morphology of CaOx crystals*

Calcium oxalate crystals may form in any organ or tissue within plants. For example, crystals occur in roots, stems, leaves, flowers, fruits, and seeds [69] and within epidermal [96], ground, and vascular [97] tissues. Calcium oxalate often forms in idioblasts cells that develop in isolation, with distinct structure or content from surrounding cells [98]. In other instances, crystals may develop in defined groups of cells, as in files of bundle sheath cells [99], for example, or in a single layer of the seed coat [100]. Less often, entire tissues such as endosperm [101] or leaf epidermis [102] accumulate calcium oxalate in every cell or in a majority of cells.

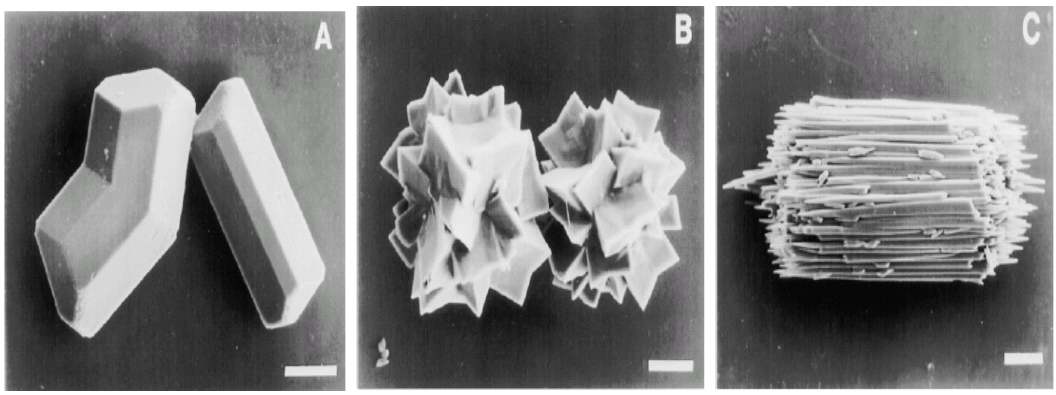


**Figure 1.7.** Characteristic morphologies of calcium oxalate crystals isolated from plants.

Plant crystals display an astonishing variety of morphologies, most of which confirm to one of the following categories defined by botanists [69]; (1) prisms, consisting of simple regular prismatic shapes (Figure 1.7 A) (2) druses, which are spherical aggregates of crystals (Figure 1.7 B) (3) styloids, acicular crystals that form singly (4) raphides, acicular crystals that form in bundles (Figure 1.7 C) (5) crystal sand, small tetrahedral crystals that form in clusters. Some of the characteristic morphological features of calcium oxalate in plants are shown in figure 1.7. Calcium oxalate exists in two chemical forms, monohydrate and dihydrate, and both of these occur in plants [103,104]. The observed morphologies represent elaborations and modifications of basic crystal structure for either the monohydrate or dihydrate form. The monohydrate is more stable and is more commonly found in plants than is the dihydrate.

### *1.4.3. Matrix of calcium oxalate crystals*

Webb and Arnott [78] showed that grape druse crystals have a nonmineralized core material of unknown but presumably organic composition. Webb et al. [73] demonstrated that a complex organic matrix was present within the vacuole of grape raphide idioblasts and this matrix could facilitate crystal formation. On treatment of isolated calcium oxalate crystals from plants with EDTA, the calcium oxalate is partially or completely dissolved and examination of the samples with TEM reveals a non mineral matrix. This non mineral matrix retains the shape of the original crystal, thus, it is referred as "crystal matrix ghost." The crystal matrix ghost even remains intact during processing of the sample for TEM but it is flexible and can be bent at a 90° angle, unlike the crystal, indicating that it is made of an interconnected macromolecular complex. Often the central region of the raphide crystals do not de-mineralize so that a small block of crystal remains. Partial dissolution with EDTA can also leave behind small "plates" of Ca Ox along the matrix. It is also observed that if a crystal matrix ghost is incubated with calcium and oxalate, a crystal forms with essentially the same shape as the ghost, although often the surfaces are rough or have micro-crystals projecting from them. The druse crystals also have a central core of material [105], and after dissolution of the mineral with EDTA, this core material can also initiate crystallization, although the crystal morphology is very irregular.

Microautoradiography of crystals or crystal matrix exposed to radioactive calcium or oxalate further demonstrates the ability of the matrix to bind these ions. Recently, Bouropoulos et al. [106] found that crystals of tomato and tobacco contain macromolecules that can promote CaOx nucleation. Macromolecular matrix materials can hold important implications with respect to crystal morphology and, as pointed out by Arnott and Webb [83], crystal stability.

Most calcified tissues in animal systems undergoing controlled mineralization have been found to have an organic matrix associated with them [107], which includes various classes of proteins shown *in vitro* to be able to control crystal growth and morphology. Such proteins have been found to be integrated into the structure of biominerals of invertebrate organisms such as sponge spicules [108], mollusk shells [109], sea urchin spines [110], and also in CaOx renal stones that form in humans

[111]. Although macromolecules appear to be involved in nucleation and modifying growth patterns [112,113], it is also possible that they may have inhibitory effects in the case of CaOx in the urinary tract [114,115].

It is interesting to note that the acidic proteins from animal matrix have some physical properties similar to the matrix protein of plant crystals, such as poor solubility of some of the animal matrix proteins, a tendency to aggregate, and poor staining on SDS-PAGE [112]. It is hypothesized by Li et al [116] that the protein isolated from plant CaOx crystals have a similar function to some of the animal matrix proteins in terms of affecting crystal growth. They suggested that crystal matrix protein has calcium binding properties, which would be important to their integration into the crystalline matrix. More recently [117] four proteins from the organic matrix of CaOx crystals present in the seeds of *Phaseolus vulgaris*, have been isolated which inhibited the nucleation of CaOx crystallization in solutions. They have also shown that the isolated proteins modified the morphology of CaOx crystal mainly at {120} face (fastest growing face).

### *1.5. Hyperoxaluria induced oxidative stress*

Oxalate is a natural byproduct of metabolism and in normal individuals it is harmlessly excreted. However, increased urinary excretion of oxalate, hyperoxaluria, can be toxic largely because of its propensity to crystallize at physiological pH and form calcium oxalate (CaOx) crystal deposits in the kidneys [118]. In the kidneys, CaOx crystals can block the renal tubules, disrupt cellular functions and kill nearby cells. Hyperoxaluria is a result of either genetic (primary hyperoxaluria) or environmental factors (secondary hyperoxaluria). Enhanced absorption of oxalate, secondary to many gastrointestinal diseases, ileal resection, or jejuno-ileal bypass is called enteric hyperoxaluria [119]. Even though various hyperoxalurias have distinct origins, the pathologies they induce can often be indistinguishable, encompassing urolithiasis, nephrocalcinosis, metabolic acidosis, hematuria, pyelonephritis, hydronephrosis and renal failure. In case of primary hyperoxaluria, there is a systemic deposition of CaOx in almost all of the body tissues including kidneys, heart, bone, cartilage, teeth, vasculature and brain. Patients with primary hyperoxaluria eventually

develop end-stage renal failure, usually in childhood. Patients with enteric hyperoxaluria may also develop renal inflammation and end stage renal disease.

Recent research has shown that the response of renal epithelial cells to oxalate and CaOx crystals is biphasic and concentration dependent [120,121,122]. Oxalate by itself is mitogenic at low concentrations and toxic at higher concentrations as well as in association with CaOx crystals. Injury to the renal epithelial cells results in cellular degradation and the production of membranous vesicles [123]. The crystals are either passed as crystalluria particles or are endocytosed by the epithelial cells to be processed by their lysosomal system or transported to the interstitium. CaOx crystal deposition in the kidneys upregulates the expression and/or synthesis of macromolecules, which can promote inflammation and lead to fibrosis [124,125]. In animals and renal epithelial cells in culture, reaction to high oxalate and CaOx crystals is associated with the generation of free radicals [126,127]. Antioxidants reduce hyperoxaluria and CaOx crystal induced toxicity [128,129].

### *1.5.1. Oxidative stress and CaOx nephrolithiasis*

High concentrations of oxalate and CaOx crystals also provoke renal cells to increase the synthesis of various mediators of the inflammatory processes and extracellular matrix production, and modulators of crystallization [124,125,130]. Reactive oxygen species are involved in the activation of signaling molecules such as protein kinase C, c-Jun N-terminal kinase and p38 mitogenactivated protein kinase (MAPK), with influence over transcription factors such as NF-jB and activated protein- 1 (AP-1). Activation of these transcription factors leads to upregulation of genes and production of crystallization modulators such as osteopontin, bikunin, and microglobulin [124,125,130], which affect all aspects of nephrolithiasis including crystal formation, growth, aggregation as well as their retention within the kidneys.

Oxidative stress is injurious to all components of the cells. Figure 1.8 outlines the lithogenic effects of hyperoxaluria induced generation of reactive oxygen species (ROS). Previous studies from many laboratories indicate that damage to the urothelium may predispose to *de novo* crystallization and crystal retention in the kidneys.

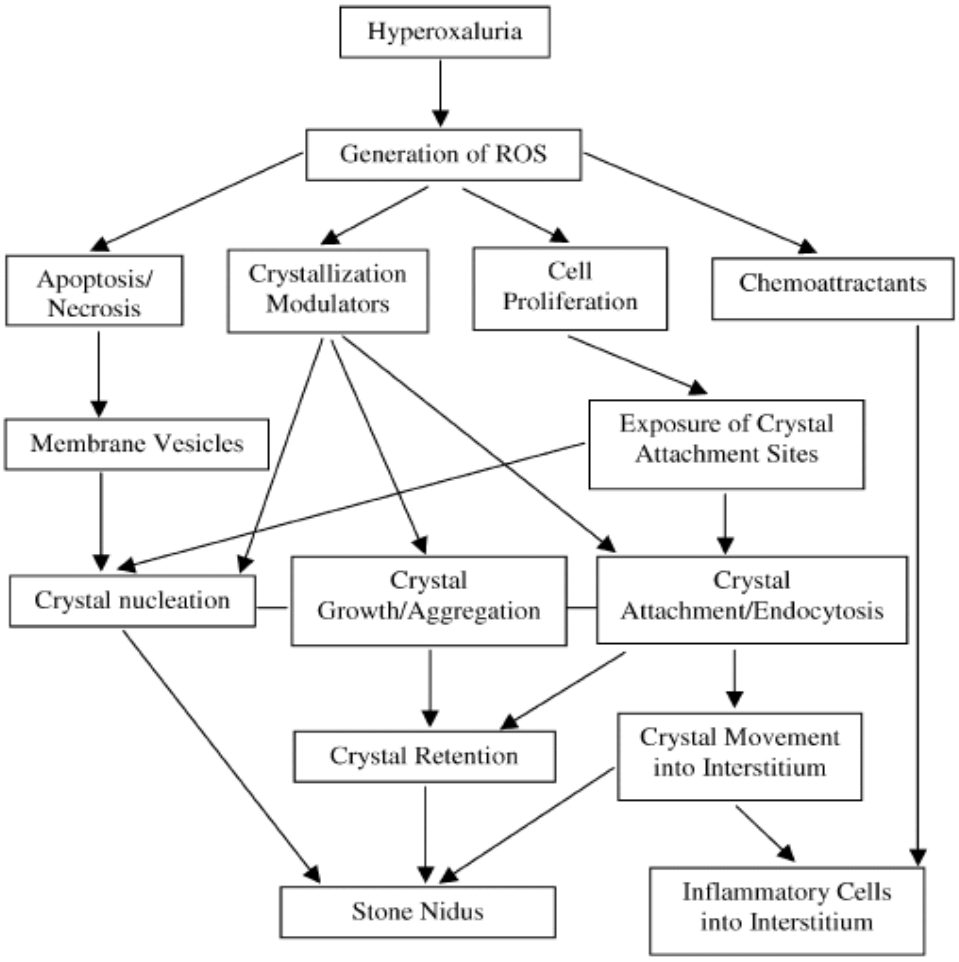


**Figure 1.8.** Hyperoxaluria induced generation of free radicals and their effect on various aspects of crystal formation

It has been demonstrated that experimentally induced hyperoxaluria in rats results in renal tubular cell damage and CaOx crystal deposition [123]. Both apoptotic and necrotic injuries have been detected [131,132]. Crystals always deposit at sites of tubular injury in association with membrane vesicles and are also seen attached to the exposed basement membrane [123,133,134]. Our *in vitro* studies have shown that membranes and lipids of cellular degradation products are excellent nucleators of CaOx crystals at supersaturation normally found in the renal tubular fluids [135]. Tissue culture studies in which renal epithelial cells were exposed to oxalate or CaOx crystals have shown that epithelial injury promotes attachment of CaOx crystals [136, 137]. This attachment is mediated by oxalate induced exposure of phosphatidylserine

on cell surfaces [138,139]. Interestingly, apoptosis involves the exposure of phosphatidylserine on cell surfaces [131].

### *1.5.2. Antioxidants for renal protection*

Figure 1.9 illustrates the stages in which specific antioxidants and other protective detoxification treatments have been shown to impede the development of hyperoxaluria- induced oxidative stress. Pretreatment with vitamin E along with mannitol abolished the deposition of CaOx crystals in the kidneys of rats injected with sodium oxalate [140]. Alanine-induced deposition of CaOx crystals in rat kidneys was blocked by dietary supplementation with vitamin E plus selenium [141]. Interestingly, vitamin E alone caused only a decrease in crystal deposition, while combined treatments totally abolished it. Treatment with methionine [142] or glutathione monoester [143] also reduced renal CaOx crystal deposits in the kidneys of hyperoxaluric rats. The reduction or total elimination of crystal deposition was associated with restoration of the anti-oxidation defenses of the kidneys by increasing activities of the enzymes SOD, catalase, glutathione peroxidase (GPx) and/or free radical scavengers, reduced glutathione (GSH), ascorbic acid, vitamin E and protein thiol groups. Vitamin E is the major lipid soluble antioxidant present in the cell membranes and acts synergistically with the other antioxidants. It can react with lipid radicals and stop the propagation of lipid peroxidation. Selenium is normally incorporated in GPx. Mannitol is a scavenger of hydroxyl radicals while methionine is a thiol generating compound.

Green tea has recently been shown to reduce CaOx crystal deposits in the kidneys of rats made hyperoxaluric by the administration of ethylene glycol [144]. Reduced crystal deposition was coupled with improved SOD activity. In addition, green tea consumption caused a decrease in apoptotic activity in the kidneys. It was concluded that antioxidants, catechins, present in green tea were mainly responsible for these improvements. Reduction of angiotensin production by inhibiting ACE or blocking angiotensin receptors has been shown to significantly reduce renal CaOx crystal deposition as well as the development of interstitial inflammation [145]. These treatments also resulted in a reduction in the oxidative stress measured as products of lipid peroxidation. Angiotensin II is implicated in causing oxidative stress by

activating membrane associated NADPH oxidase, which leads to the production of superoxide [146]. ROS generated through the activation of NADPH oxidase are also involved in the production of MCP-1, for the recruitment of monocytes/macropahges to the interstitium. Exposure of renal epithelial cells in culture to oxalate caused ROS dependent up regulation of theMCP-1 gene, and the production and secretion of the protein [147]. Antioxidant treatment for stone disease has not been clinically tested.

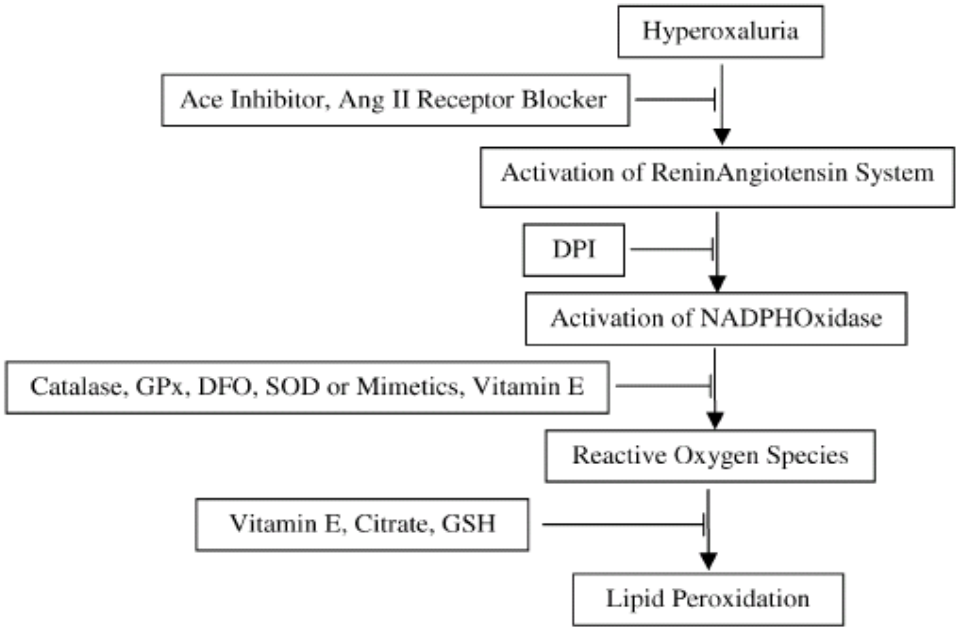


**Figure 1.9.** Antioxidant and other detoxification treatments to impede the development of hyperoxaluria induced oxidative stress

However, some well-known antioxidants such as citrate and allopurinol, have been evaluated in a number of prospectively randomized trials, and their efficacy has been established [148] in populations of recurrent stone formers. Citrate increases cellular nicotinamide adenine dinucleotide phosphate and reduced glutathione while allopurinol is a xanthine oxidase inhibitor.

### *1.6. Herbal medicine and urolithiasis*

Many remedies have been employed during the ages to treat urinary stones. In the traditional systems of medicine, most of the remedies were taken from plants and they were proved to be useful, though the rationale behind their use is not well established through systematic pharmacological and clinical studies except for some

composite herbal drugs and plants. The recent treatment procedures like surgical removal, percutaneous techniques and extracorporeal shock wave lithotripsy (ESWL) are prohibitively costly for the common man. With these procedures recurrence is quite common and the patient has to be subjected to careful follow up for a number of years. Pharmacotherapy has a potential to reduce the recurrence rate. The use of plant products with claimed uses in the traditional systems of medicine assumes importance.

### *1.6.1. Medical plants and Goethe*

Due to the adverse effects of the present day treatment strategies for kidney stone, alternative treatment modalities composed of herbal remedies have been the mainstay of medical therapy for thousands of years, especially in Eastern civilizations. Although it is believed that the resurgence of interest in phytotherapy became popular in the second half of the 19th century in Western countries, this complementary medical therapy was widely used in Europe much before that date. Johann Wolfgang von Goethe (1749 to 1832), the famous German poet, novelist, playwright, courtier and natural philosopher, was one of the greatest figures in western literature. Besides this, Goethe experienced urolithiasis all his life. The first renal colic episode was reported in 1795 and the most dramatic period was in February 1805. He experienced severe fever and was almost dying of urosepsis. Goethe performed a cure in Lauchstad in July under the supervision of Professor Johann Christien Reil, who prescribed a treatment composed of thermae carolinae, aqua calcis, *Hyoscyamus niger*, *Arum maculatum*, soda crystallisata, herbae subastringentes and uva-ursi. *Hyoscyamus niger* is a plant that grows in Europe and has relaxing, antispasmodic, anesthetic features that share the pharmacological effect of drugs prescribed for renal colic treatment even today. Uva-ursi was prescribed to Goethe because of its diuretic and antilithogenic effects. After this therapy colic disappeared but stone passage was not mentioned [149].

### *1.6.2. Social and economic impact of phytotherapy*

Only a decade ago, alternative medicine in America was still a distinctly counterculture phenomenon. It has now become an established presence in mainstream culture. In fact, a national survey was conducted in 1990 in US about the

use of unconventional therapies for health problems [150]. The survey recorded 1539 adults by telephone interview. One of three (34%) of respondents reported using, at least one unconventional therapy in the past year and 10.2% of them had seen providers for unconventional therapy. In 1998, this percentage has increased to 15.1% [151]. The frequency of use such therapy varied some what among socio-demographic groups with the highest use reported by non black persons who had relatively more education and higher incomes. The majority used unconventional therapy for chronic and serious conditions. The interesting thing in this study is the revelation that 70% of the respondents who used unconventional therapy did not inform their medical doctor that they had done so.

Clearly, the use of plant products as medicines is widespread and growing. In 1996, Brevoort estimated the size of the 1994 US herbal market at $1.6 billion [152]. By 1998, her estimate had increased to $3.9 billion. A 1996 survey by prevention magazine and ABC News reported that 1 in 3 Americans use herbal medicines, estimating the size of the annual herbal market at $3.2 billion [153]. Several national polls in 1997 and 1998 corroborated these estimates, reporting that 32% to 37% of Americans use medicinal botanicals in a given year. One of the among unconventional therapy that we will focus on is phytotherapy or the use of plants in the treatment of diseases especially kidney stone formation. Indeed, herbal medicine is as ancient as the history of man kind. From the very beginning, herbal treatment has been a favorite tool of naturopathically inspired practitioners. Of course, conventional medicine has also derived many of its drugs from plant sources. According to the World Health Organization, approximately 75% of the global population, most of the developing world, depends on botanical medicines for their basic healthcare needs [154]. Substances first isolated from plants account for approximately 25% of the western pharmacopoeia, with another 25% derived from modification of chemicals first found in natural products [155].

### *1.6.3. Scientific evidences of phytotherapy for urolithiasis*

As far as urolithiasis is concerned, acupuncture, herbal medicine, natural products and homeopathy have been used to treat and/or to alleviate symptoms of kidney stone patients. In case of herbal medicines, there is a large number of species

described in many pharmacopoeias of several countries in the world as remedies for urolithiasis. However, few investigators have devoted their efforts to study these plants by using objective and scientific methods. Such studies are needed to understand the mechanism by which these plants exert their effects and identify their active principles. The efficacy of rice-bran therapy was evaluated in patients with idiopathic hypercalciuria [156]. During the treatment, a reduction of urinary calcium excretion was noticed. These results were confirmed experimentally and clinically [157]. In another study conducted on hypercalciuric patients with calcium-containing urinary stones, the frequency of stone episodes was reduced dramatically from 0.462 to 0.101 per patient per year [158]. Urinary calcium excretion was considerably reduced while urinary phosphate and oxalate were slightly increased. Interestingly, the treatment was well tolerated and no side effects were observed even after conducting the therapy for up to 43 months for certain patients.

Grases and colleagues have studied the efficacy of a medicinal plant, *Rosa canina* on the urinary risk factors of calcium oxalate [159,160,161]. Except some little effect on calciuria and citraturia, no significant changes have been observed during the treatment on urinary chemistries. However, the important findings are that beneficial effect of this plant depends on diet.

To ascertain the beneficial effect of banana stem extract on urinary risk factors, a prospective study showed that the plant extract reduced significantly urinary oxalate in experimentally hyperoxaluric rats. Such effect could be beneficial in the treatment of patients with hyperoxaluria urolithiasis.

Another Chinese medicinal plant that has attracted more attention is Kampou medicine known to be used in the treatment of various diseases for hundreds of years. It had been also used for prevention and treatment of urinary calculus. An experimental study suggested a direct inhibitory effect of Kampou extracts of calcium oxalate crystallization *in vitro* and *in vivo* [162]. In this study, two species from Kampou, Takusya (*Alisma orientale*) and Kagosou (*Prunella vulgaris*), were employed to evaluate their stone prophylactic effect in an animal model. In the same study, Chorey-to which is a Chinese medicine that contains five Kampou plants including Takusya, has been evaluated *in vivo*. The low dose of this preparation

exhibited apparent anti-stone effect despite the disadvantage of decreasing citrate excretion. Takusya had been also used to examine the inhibitory effect of the formation of calcium oxalate renal stones induced by ethylene glycol and vitamin D3 in rats as well as on osteopontin expression that is identified as an important constituent of stone matrix [163]. The rate of renal stone formation is lower in the group receiving Takusya extracts than in the control group. The expression of osteopontin in the rat group receiving the plant was smaller than in stone group. This finding suggests that Kampou medicine action include decreasing on calcium oxalate aggregation and growth as well as proliferation.

In Brazil, *Phyllantus niruri* has been used to treat several pathological conditions [164]. The plant has been called "break stone" because it has been used for generations as an effective product to eliminate gallstones as well as kidney stones. Such observation has been confirmed in rat model of urolithiasis induced by the introduction of CaOx seed into the bladder [165]. Its effect was noticed particularly on crystal growth. The effect seemed to be independent of changes in the urinary excretion of citrate and magnesium but might be related to the higher incorporation of GAGs into calculi. The plant has been the subject of many phytochemical and pharmacological investigation in which different classes of compounds have been identified like alkaloids, flavonoids, lactones, steroids, terpenoids, lignans, and tannins.

Some researchers have demonstrated an antispasmodic and an analgesic activity in *Phyllantus niruri* which could explain the popular use of the plant for kidney and bladder stones [166]. The effect of an aqueous extract of *Phyllantus niruri* has also been investigated *in vitro* on a model of CaOx crystal endocytosis by Madin-Darby Canine Kidney cells (MDCK) in culture. The extract exhibited a potent and effective nonconcentration dependant inhibitory effect on CaOx crystal internalization [167]. The use of 68 medicinal plants belonging to 29 families and 58 genera were documented against the treatment of kidney and urinary disorders in the tribal communities of Ladakh region in India. The most common species were *Bergenia ligulata, Emblica officinalis, Mangifera indica, Punica granatum, Terminalia belerica, Terminalia chebula, Zingiber officinale* [168]. The fresh juice of *Coleus*

*aromaticus* was found to reduce the deposition of calcium and oxalate in the kidney of experimental rats [169]. Certain enzyme systems implicated in the process of calcification like ATPases and phosphohydrolases were affected by the juice proving its regulatory influence on calcium oxalate stone formation. Studies on various fractions of *Tribulus terrestris* have indicated that the aqueous methanolic fraction is more effective against experimentally induced urolithiasis by foreign body insertion method using glass beads in albino rats [170]. Investigation of the effect of aqueous extract of *Tribulus terrestris* on the oxalate metabolism in male rats fed with sodium glycolate, revealed a decrease in urinary oxalate excretion and a significant increase in urinary glyoxylate excretion and also a decrease in liver galactose oxidase and glutamic acid decarboxylase activities [171].

Studies on the stem juice of *Musa paradisiaca* were found to be effective in dissolving the phosphate type of stones in albino rats induced by foreign body insertion method using zinc discs [172]. In another experimental study, stem juice of Musa significantly reduced the incidence of oxalate urolithiasis by lowering the activity of the enzyme glycolic acid oxidase [173]. The stem juice of *Musa paradisiaca* reduced urinary oxalate, glycolic acid, glyoxylic acid and phosphorus excretion in hyperoxaluric rats [174]. *Agropyron repens* is another widely consumed extract for nephritis, urethritis and urinary calculi [161]. However, *Agropyron repens* infusion has not been assigned to any positive effect on urolithiasis risk factors. The decreased citriuria, increased calciuria and decreased magnesiuria, were observed by this treatment. This indicates contradiction towards consumption of this remedy for urolithiais [161]. Some most commonly used plants for kidney stone treatment are given in table 1.1. Another antilithogenic effect of some herbal remedies is antimicrobial properties. It must be emphasized that a deficit in the crystallization inhibitory effect of urine and the presence of promoters are considered the most important risk factors in the process of urinary stone disease [175] when these conditions favor stone formation, the anti-adherent layer of glycosaminoglycans acts as a protective barrier against urinary stone disease. If this layer is damaged, i.e. as a consequence of bacterial attack, a stone nucleus might develop, leading to a full stone in the urinary tract.

**Table 1.1.** Currently consumed phytotherapeutic agents and their mechanisms of action

| *Agent* | *Evaluated* | *Potential Beneficial Actions* |
|---|---|---|
| *Herniaria hirsuta* | Urine or cell culture *in vitro* | Removes crystals already attached to cell surface, results in higher COD vs COM excretion |
| *Cranberry juice* | Humans *in vivo* | Increases urinary citrate excretion, decreases urinary oxalate and calcium ion excretion |
| *Grapefruit juice* | Humans *in vivo* | Increases urinary citrate excretion |
| *Lemonade juice* | Humans *in vivo* | Increases urinary citrate excretion |
| *Dolichos biflorus* | Urine or cell culture *in vivo* | Decreases calcium phosphate precipitation |
| *Bergenia ligulata* | Urine or cell culture *in vivo* | Decreases calcium phosphate precipitation |
| *Vigna unguiculata* | Humans *in vivo* | Increases urinary magnesium |
| *Zea mays* | Animals *in vivo* | Diuretic |
| *Amni visnaga* | Animals *in vivo* | Diuretic |
| *Aerva lanata* | Animals *in vivo* | Decreases urinary calcium, oxalate, uric acid & phosphorus excretion |
| *Costus spiralis* | Animals *in vivo* | Decreases stone size with unknown mechanism, no diuretic effect |

At this point, some extracts that show antimicrobial properties can be considered antilithogenic by protecting the anti-adherent glycosaminoglycan layer covering the epithelium of the collecting system. In regard to this aspect Muangman et al evaluated *Andrographis paniculata*, an Eastern herb, for its bacteriostatic activity [176]. They prescribed this drug in patients who underwent SWL and noted a significant decrease in pyuria and hematuria. *Arctium lappa*, *Equisetum arvense* and *Arctostaphylos uva-ursi* exerted the same antiseptic activity, which prevented the retention of microcalculus on the kidney epithelium as the antilithogenic action [177]. Also, *Agropyron repens* has been thought to exert antimicrobial features, which might be responsible for its protective effect [161]. In addition, Melzig evaluated herbal remedies based on goldenrod (*Solidago virgaurea* L.) and found new mechanisms responsible for the antilithogenic activities of these remedies [178]. He reported that such remedies exert a rather complex action spectrum, such as antimicrobial and anti-inflammatory properties. It is highly recommended for infections and inflammations to prevent kidney stone formation.

The vast Ayurvedic literature claims a number of plants to be useful for urinary stones, still many plants need to be exploited for their pharmacological actions. Inspite of intensive research to establish the mechanisms of stone formation, dietary management, evaluation of medicinal plants and other agents in the treatment of urinary stones, still to date there is no standard drug available. The main drawbacks in the development of a standard drug may be attributed to multifactorial nature of urolithiasis, different biochemical disorders that lead to urolithiasis and different chemical forms of renal stones.

### *1.6.4. Herbal plants and diuretics*

The current role of diuretics in urolithiasis is limited. Although thiazides are commonly used to treat urolithiasis due to their hypocalciuric effects, certain diuretics might even have a negative effect on stone risk, e.g. urine calcium excretion increases in patients on a loop diuretic [179]. In fact, immediate improvement in hemodynamic variables and cardiac performance can be detected in patients with chronic heart failure following diuretic therapy, primarily due to decreases in plasma and extracellular fluid volumes. Plasma renin, angiotensin and aldosterone increase

maximally in week 1 but they attenuate during sustained therapy [180]. These findings suggest that diuretics cause volume contraction other than an increment in urine volume in a short period with a variable clinical outcome in the long term due to diuretic resistance [180]. Although many studies claimed that the diuretic effect of the herbs was responsible for the antilithogenic effect, still there was no study confirming that the long-term diuretic activity has a potential antilithogenic effect. On the other hand, the aim of many folk medicines is based on the increment of urine volume. It is considered that the critical step in idiopathic CaOx nephrolithiasis is the nucleation and growth of crystals on solid particles [181]. High urine volume after volume contraction in the short term might be an important factor because it can prevent nucleation and may be beneficial for the spontaneous passage of small fragments. Thus, extracts leading to increased volume of urine can be a part of the antilithogenic phytotherapy.

### *1.7. Herbal based commercial formulations for urolithiasis*

The marketed composite herbal formulations, Cystone (Himalaya Drug Company, India), Calcuri (Charak Pharmaceuticals, Bombay, India), Uriflush (Inti Sumatera Global, Indonesia), Uriflow (Discovery Herbs, USA) and Chandraprabha bati (Baidyanath, India) have been widely used clinically to dissolve urinary calculi in the kidney and urinary bladder. Pharmacological and clinical studies carried out on a composite herbal formulation, Trinapanchamool consisting of five herbal drugs namely *Desmostachya bipinnata, Saccharum officinarum, Saccharum nunja, Saccharum spontaneum and Imperata cylindrica* found it to be effective both as a prophylactic in preventing the formation and as a curative in dissolving the pre-formed stones in albino rats. The antiurolithiatic activity of this formulation has been attributed to its diuretic activity [182]. Cystone is a product of The Himalaya Drug Co. (Figure 1.10) which is often prescribed by the physicians to the patients suffering from urinary calculi. There are various studies which showed its ability to inhibit calcium phosphate and calcium oxalate mineralization [183]. The main components of Cystone are given in table 1.2.

**Table 1.2.** The components in one Cystone tablet [183]

| *Herb* | *Amount* |
|---|---|
| *Didymocarpus pedicellata* | 65 mg |
| *Saxifraga ligulata* | 49 mg |
| *Rubia cordifolia* | 16 mg |
| *Cyperus scariosus* | 16 mg |
| *Achyranthes aspera* | 16 mg |
| *Onosma bracteatum* | 16 mg |
| *Vernonia cinerea* | 16 mg |
| *Shilajeet* | 13 mg |
| *Hajrul yahood bhasma** | 16 mg |


**Figure 1.10.** Cystone: a herbal formulation for treatment of kidney stones.

*Hajrul yahood bhasma is prepared with *Ocimum basilicum*, *Tribulus terrestris*, *Mimosa pudica*, *Dolichos biflorus*, *Pavonia odorata*, *Equisetum arvense* and *Tectona grandis*.

In addition, its efficacy to reduce urolithiasis was also reported in male Wister rats [184]. In various reports, the anticalcifying properties of Cystone are used as a reference for evaluating the antilithiatic properties of other plants.

### *1.8. Herbal medicines: Aspects untouched*

Recent years have seen dramatic advances in phytotherapy for urolithiasis. An unavoidable interest in this, results in an expense of more than $1.5 billion annually in the United States [185]. Although phytotherapeutic extracts are popular in folk culture, review of literature suggests that very few studies have been done on the exact clinical role, efficacy and side effects of these herbs after long-term consumption. Correspondingly potential acceptance of this herbal therapy as an alternative or an adjunct to classic medical therapy remains to be determined. An increased excretion of urinary citrate, decreased excretion of urinary calcium and oxalate, and diuretic and antiseptic features are only some of the known mechanisms

of these extracts. A precise understanding of the mechanism of action of these herbal extracts would have diagnostic value with regard to the nature of this disease, in addition to the potential therapeutic implications in this future field of research. In this respect the absence of this information is a fruitful area for scientific research by willing investigators. Although preclinical research has proved that the efficacy of some of these herbs is truly mythical, all deserve innovative scientific study to clarify the mechanism of action because myths may always become reality in the future.

### *1.9. Dolichos biflorus*

*Dolichos biflorus* L. (Leguminosae-Papilionoideae), locally known as "Kulthi" in Himachal Predesh, India, is a fast growing annual herb. Its stems are nearly erect. Its branches climb and twine while producing clusters of pea-like yellow flowers which are 0.75" inch long. It makes flat, curved 2" long seed pods (Figure 1.11).

**Figure 1.11.** Plant of *Dolichos biflorus*

It is mainly found in tropical and subtropical regions in south Asian countries. Its immature seeds are widely consumed as food in south Asian countries including rural areas of India.

It is commonly used in folklore to treat urolithiasis. The seeds of Dolichos biflorus are also the component of various commercial drug formulations like Cystone. So far, only few investigators have studied its efficacy on calcium mineralization. More recently, the seeds of *Dolichos biflorus* were tested and compared with Cystone (commercial drug) for their *in vitro* antilithiatic and anticalcification activity on calcium phosphate precipitation [186]. The extract of *Dolichos biflorus* showed inhibitory activity almost equivalent to Cystone towards calcium phosphate precipitation. Similar *in vitro* study showed the possibility of more than one biomolecules in *Dolichos biflorus*, possessing the ability to inhibit calcium phosphate precipitation [187]. There are no reports in the literature of the exact clinical role and efficacy of this plant on *in vivo* urolithiasis. The present study is aimed at examining the efficacy of *Dolichos biflorus* and identification of the most potent biomolecule responsible for its antilithiatic property.

# Chapter 2
# Materials & Methods

## *2.1. Screening of most effective antilithiatic plant*

### *2.1.1. Materials*

Plants viz. *Achyranthes aspera, Dolichos biflorus, Tribulus terrestris*, *Cocos nucifera* were collected from local market and nearby fields, identified and then authenticated by microscopical and physiochemical data. The part of the plant used is given below in the table 2.1. All other reagents used were of analytical grade. The distilled water was obtained from Millipore Elix distillation system.

**Table 2.1.** Plants and their respective part used for current investigation

| | Plant | Part used |
|---|---|---|
| 1 | *Achyranthes aspera* | Roots |
| 2 | *Dolichos biflorus* | Seeds |
| 3 | *Tribulus terrestris* | Fruit |
| 4 | *Cocos nucifera* | Liquid endosperm |

### *2.1.2. Preparation of extracts*

The respective part of three plants viz. *Achyranthes aspera, Dolichos biflorus* and *Tribulus terrestris* were weighed and soaked in double-distilled water (10%w/v) overnight at $4^{o}$C. The extract so obtained was filtered through muslin cloth and subjected to centrifugation at 3000 rpm for 30 min at $4^{o}$C in a cold centrifuge. The supernatant thus obtained was referred to as aqueous extract. *Cocos nucifera* extract was prepared by centrifugation of its milky water at 3000 rpm for 30 min at $4^{o}$C in a cold centrifuge.

### *2.1.3. Homogenous system of calcium phosphate mineralization*

To determine the extent of calcium phosphate (CaP) precipitation, homogenous mineralization system was used to study the extent of *in vitro* mineral phase formation in the absence of any matrix [188]. This *in vitro* homogeneous assay system was modified by replacing 17.5 mM barbital buffer with 0.1 M Tris buffer (pH 7.4). The homogenous system consisted of 5 mM $CaCl_2$ and 5 mM $KH_2PO_4$. After incubating this system at $37^0$C, precipitates obtained were centrifuged and the pellets were resuspended in 0.1N HCl. The calcium ($Ca^{2+}$) and phosphate ions ($HPO_4^{2-}$) concentration in the precipitate represented the extent of precipitation (crystallization) of these ions and the sample containing inhibitory biomolecule(s) minimized the extent of their precipitation. The $Ca^{2+}$and $HPO_4^{2-}$ ions were estimated by the methods of Trinder [189] and Gomori [190] respectively (as given in sections 2.1.3.1 and 2.1.3.2.).

#### *2.1.3.1. Determination of calcium ions*

The calcium ions in a sample were determined by the method of Trinder [189].

*Principle*

Calcium ions get precipitated as naphthyl hydroxamate by directly adding slight excess of calcium reagent. After centrifugation excess of reagent is removed by decantation and unwashed precipitates are dissolved in EDTA. Addition of ferric nitrate results in development of an orange red color, intensity of which is measured as the amount of calcium ions present in the sample.

*Reagents*

- Calcium reagent – Prepared by mixing two components and the volume was raised to 1000 ml by adding distilled water, the mixture was filtered and stored in dark reagent bottle. The components were:

  (a) 280 mg of Naphthylhydroxamic acid in 100 ml of (95 ml distil water + 5 ml ethanolamine + 2 gm of tartaric acid)

  (b) 9 gm of NaCl in 500 ml of distilled water.

- Color reagent – 60 gms $FeNO_3$ was dissolved in 500 ml of acidified distilled water (485 ml distil water with 15 ml of conc. $HNO_3$). Then, the volume was raised to 1000 ml with distilled water.
- Working standard – 2 mM of calcium chloride
- EDTA – 2 gm EDTA was dissolved in 1000 ml of 0.1 N NaOH

*Procedure*

- 0.1 ml of sample was dissolved in 2.5 ml of calcium reagent and incubated at room temperature for 30 mins.
- The precipitates were obtained after centrifugation and then dissolved in 1.0 ml of 0.2% EDTA with boiling for 10 mins.
- Finally, 3 ml coloring reagent was added and the absorbance was measured at 450 nm.

*Calculations*

The concentration of calcium ions (mM) was calculated using following formula.

$$\frac{\text{Absorbance of test}}{\text{Absorbance of standard}} \times \text{concentration of standard}$$

***2.1.3.2. Determination of phosphate ions***

The phosphate ions concentration in the sample was determined by the method of Gomori [190].

*Principle*

Phosphate reacts with molybdic acid to form phosphomolybdic acid. Treatment of 2-methyl-4aminosulfate causes reduction of phosphomolybdic acid to form deep blue colored complex which gives absorption maxima at 660 nm.

*Reagents*

- Molybdic acid – Prepared by mixing 2.5% ammonium molybdate dissolved in distilled water and 10 N $H_2SO_4$ in the ration of 10:4.
- Metol reagent – Prepared by mixing 5% $NaHSO_3$ and 1% metol in distilled water.
- Working standard – 2 mM of potassium dihydrogen phosphate

*Procedure*

- 1.2 ml of molybdic acid was added to 0.2 ml of sample and incubated at room temperature for 10 mins. The sample was diluted by 6.8 ml of distilled water.
- Then, 0.5 ml of metol reagent was added and the solutions were mixed properly.
- Finally, the mixture was kept at room temperature for 20–30 mins and absorbance was measured at 660 nm.

*Calculations*

The concentration of phosphate ion (mM) was calculated using following formula

$$\frac{\text{Absorbance of test}}{\text{Absorbance of standard}} \text{ X concentration of standard}$$

***2.1.3.3. Determination of percentage inhibition of calcium phosphate mineral phase***

The percentage inhibition of CaP mineralization in the presence of test sample was calculated using following formula.

$$\%\text{age Inhibition} = [(C\text{-}T)/C] \text{ X } 100$$

where,

*'C'* is the concentration of $Ca^{2+}$or $HPO_4^{2-}$ ion of the precipitate formed in control system which had distilled water.

'*T'* is the concentration of $Ca^{2+}$or $HPO_4^{2-}$ ions of the precipitate formed in the assay system with the test sample.

### *2.1.4. Homogeneous system of growth and demineralization of calcium phosphate mineral phase*

The growth and demineralization of the preformed mineral phase consisting of calcium phosphate required initial precipitates of these minerals as obtained by method given above in section 2.1.3. In order to study the growth of the preformed mineral phase, the precipitates formed by the above method were resuspended in the same assay system having calcium and phosphate along with respective plant extract. This assay system was incubated at $37^0$C for 30 minutes after which estimation of $Ca^{2+}$ and $HPO_4^{2-}$ ions concentration represented the growth of precipitation of these ions over the previously formed mineral phase.

For demineralization, the preformed mineral phase was resuspended in the assay system with plant extract but without further addition of calcium and phosphate ions. This assay system was incubated at $37^0$C for 12 hrs. $Ca^{2+}$ and $HPO_4^{2-}$ ions concentration were estimated in supernatant to determine the demineralization of mineral phase by all four plant extracts.

Varied volumes of plant extract were added in the homogenous assay system compensated by water. The calcium and phosphate level of all the five plants were estimated and their concentrations were balanced in the assay system. For every volume of plant extract, five test tubes were taken. The concentration of calcium and phosphate ions of the mineral phase in these test samples was determined. In case of growth of pre-formed mineral phase, concentration of $Ca^{2+}$ and $HPO_4^{2-}$ ions of preformed mineral phase was deducted from the final concentration of $Ca^{2+}$ and $HPO_4^{2-}$ ions. The percentage inhibition or stimulation caused by different volumes of each plant extract was calculated with respect to control system which has distilled water instead of plant extract. In case of demineralization, the percentage of $Ca^{2+}$ and $HPO_4^{2-}$ ions demineralized was calculated in the supernatant.

### *2.1.5. Calcium oxalate (CaOx) crystal growth*

Inhibitory activity against CaOx crystal growth was measured using the seeded, solution-depletion assay described previously by Chutipongtanate et. al [191] and

Nakagawa et al [192]. The slurry of COM crystal (FTIR identified clinical kidney stones) was added to a solution containing 1 mM calcium chloride ($CaCl_2$) and 1 mM sodium oxalate ($Na_2C_2O_4$). The reaction of $CaCl_2$ and $Na_2C_2O_4$ with crystal seed would lead to deposition of CaOx on the crystal surfaces, thereby decreasing free oxalate that is detectable at $\lambda_{214}$ nm. When a test sample containing calcium oxalate inhibitor is added into this solution, depletion of free oxalate ions will decrease if it inhibits CaOx crystal growth.

Rate of reduction of free oxalate was calculated using the baseline value and the value after 5 mins incubation with or without protein. The relative inhibitory activity was calculated as follows:

$$\% \text{ Relative inhibitory activity} = [(C–S)/C] \times 100$$

Where, C is the rate of reduction of free oxalate without any test sample.

*S* is the rate of reduction of free oxalate with a test sample.

### *2.1.6. Separation of biomolecules on the basis of their molecular weight*

All plant extracts were centrifuged by using Amicon Ultra-4 centrifugal separating tubes (Millipore) of 10 kD cut off molecular weight. The separated fractions were resuspended in original volume to keep concentration same (10%w/v). Both (less than and more than 10 kD molecular weight) fractions were assayed by initial homogenous system of mineralization.

### *2.1.7. Qualitative identification of biomolecules*

Various chemical tests were carried out in the aqueous extract using standard procedures to identify the constituents such as saponins, tannins, terpenoids, flavonoids, alkaloids and proteins as described by Trease & Evans [193] and Harborne [194]. Below are the methods used to identify the presence of biomolecules.

#### *2.1.7.1. Test for saponin*

About 10 ml of aqueous extract was taken in a test tube and then filtered. The filtrate was mixed with 5 ml of distilled water and shaken vigorously for a stable

persistent froth. The frothing was mixed with 3 drops of olive oil and shaken vigorously, and the samples were observed for the formation of emulsion.

***2.1.7.2. Test for tannins***

About 10 ml of aqueous extract was taken in a test tube and then filtered. A few drops of 0.1% ferric chloride were added and observed for brownish green or a blue-black coloration.

***2.1.7.3. Test for flavonoids***

Two methods were used to determine the presence of flavonoids in the plant sample [194,195]. 5ml of dilute ammonia solution were added to a portion of the aqueous filtrate of each plant extract followed by addition of concentrated $H_2S0_4$. A yellow coloration observed in each extract indicated the presence of flavonoids. The yellow coloration disappeared on standing.

***2.1.7.4. Test for terpenoids***

The Salkowski test was used to determine the presence of terpenoids. Five ml of each extract was mixed in 2 ml of chloroform and 3 ml of concentrated $H_2S0_4$ was carefully added to form a layer. A reddish brown coloration at the inter face was formed to show positive results for the presence of terpenoids.

***2.1.7.5. Test for alkaloids***

The amount of alkaloids was estimated by using Mayer's reagent (Mercuric-potassium iodide) which causes precipitation of alkaloids and appearance of cream colored precipitate indicates the presence of alkaloids.

***2.1.7.6. Test for proteins***

The Lowry's [196] method was used for the qualitative estimations of proteins.

*Principle*

The phenolic group of tyrosine and tryptophan residues (amino acid) in a protein produces a blue purple color complex with Folin-Ciocalteau reagent which is consisted of

sodium tungstate molybdate and phosphate. Thus the intensity of color depends on the amount of these aromatic amino acids present and the absorption is measured at 660 nm.

*Reagents*

- BSA stock solution (1 mg/ml),
- Lowry's reagent: It was prepared by mixing 98 ml of component (a) and 2.0 ml of component (b).
  - (a) 50 ml of 2% sodium carbonate mixed with 50 ml of 0.1 N NaOH solutions (0.4 gm in 100 ml distilled water.)
  - (b) 10 ml of 1.56% copper sulphate solution mixed with 10 ml of 2.37% sodium potassium tartarate solution.
- Folin-Ciocalteau reagent solution (1 N) was prepared freshly by diluting commercial reagent with water in the 1:1 ratio.

*Procedure*

- 0.2 ml of test solution was taken in a test tube.
- 5.0 ml of Lowry's reagent was added in to it.
- The solution was mixed & allowed to stand for 10 mins at 37 $^0$C.
- Finally, 0.5 ml of follin's reagent was added. The solution was mixed again and put at 37$^0$C for 30 mins. Similarly standard and blank tubes were run in parallel and then, absorbance of all samples was measured at 660 nm.

*Calculations*

The concentration of protein (mg/ml) was calculated using following formula

$$\frac{\text{Absorbance of test}}{\text{Absorbance of standard}} \text{ X concentration of standard}$$

***2.1.8. Data analysis***

The data are represented as the mean ± standard deviation of five replicates.

## *2.2. Purification of antilithiatic protein*

The schematic representation used for the purification, characterization and validation of most potent antilithiatic protein is shown in figure 2.1. The fractions obtained after each step of purification were assayed for their antilithiatic properties by employing *in vitro* homogenous system of calcium phosphate mineralization (CaP) [188] and *in vitro* calcium oxalate (CaOx) crystal growth [191,192]. The protein content was determined by Lowry's method and the extent of purity of the active fractions was determined by SDS-PAGE analysis.

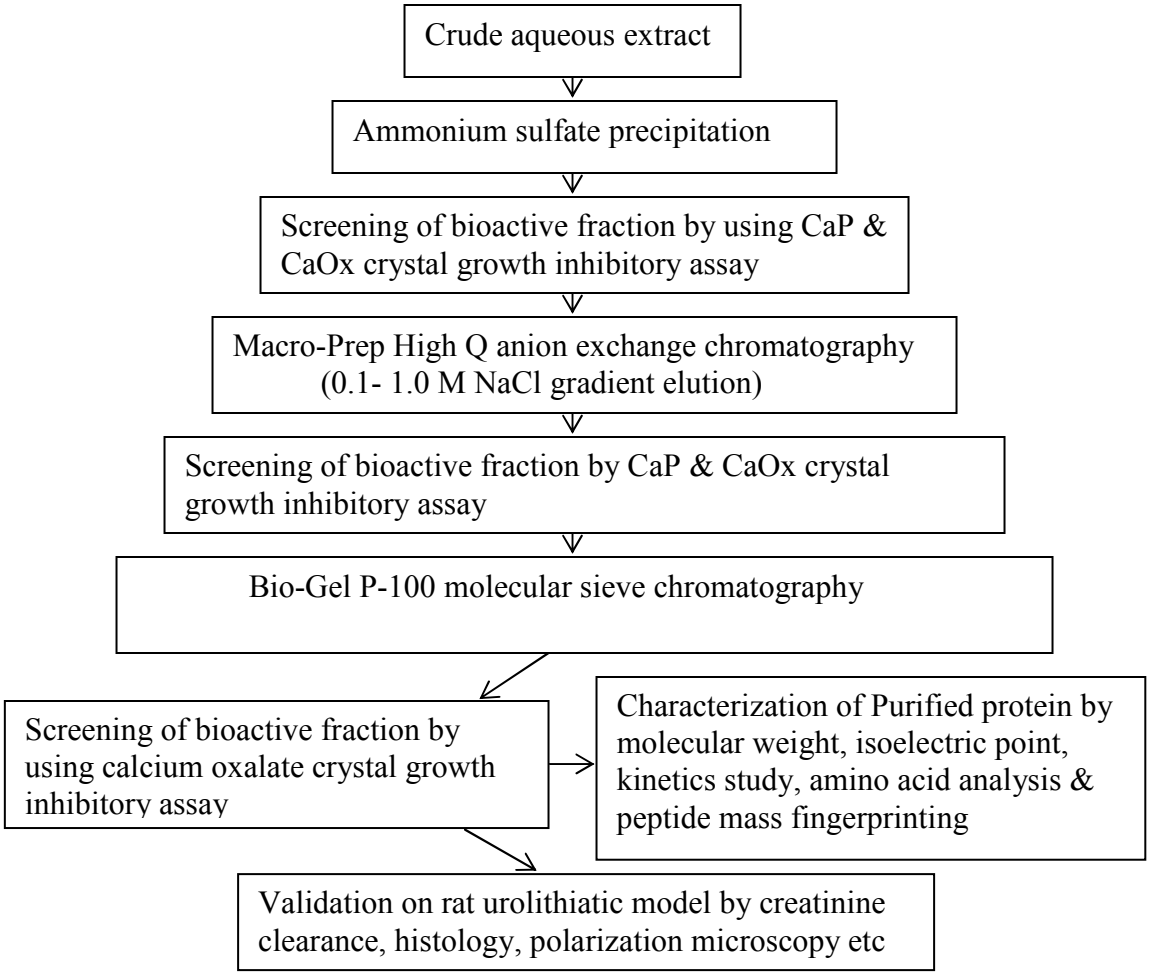


**Figure 2.1.** Schematic representation used for the purification, characterization & validation of most potent antilithiatic protein from seeds of *Dolichos biflorus*

***2.2.1. Materials***

Materials required were Macro Prep® 25 Q strong anion exchanger (Bio-Rad laboratories), Bio gel® P-100 gel (Medium, 90-180 μm) molecular sieve support (Bio-Rad laboratories), Solvents used were of HPLC grade.

***2.2.2. Extraction***

Seeds of *Dolichos biflorus* were dried, grinded and passed through muslin cloth to obtain its finely grounded powder. To obtain crude protein extract, 30 gms of finely grounded powder was then extracted with extraction buffer [50 mM Tris-Cl buffer (pH 7.4), containing 0.25 M NaCl, 1 mM PMSF and 0.01% sodium azide]. The slurry so formed was then stirred continuously for 24 hrs at $4^0$C. After 24 hrs of continuous stirring, the slurry was centrifuged at 10,000 g for 20 min at $4^0$C. The supernatant was removed and stored at $-20^0$C for further experimentation. This supernatant was referred to as the crude extract of *Dolichos biflorus*.

***2.2.3. Ammonium sulfate precipitation***

Ammonium sulfate was added to the total volume of homogenate to obtain a precipitate formed between 0 to 25% saturation, 25 to 50% saturation, 50 to 75% saturation and greater than 75% saturation. The precipitates obtained were dialyzed overnight against 20 mM Tris buffer (pH 7.4) containing 25 mM NaCl. The dialyzed samples were checked for calcium phosphate and calcium oxalate inhibitory activity by the method as described in section 2.1.3 and 2.1.5 respectively. After obtaining the sample having highest inhibitory activity towards both calcium phosphate and calcium oxalate crystallization, it was stored at -20 $^0$C and used for further purification of antilithiatic protein.

***2.2.4. Ion exchange chromatography***

The active dialyzate obtained from ammonium sulfate precipitation was centrifuged at 10,000 rpm for 15 min at 4 $^0$C to remove insoluble material and then filtered by whattman filter paper. The Macro Prep® 25 Q strong anion exchanger, after removal of ethanol, was pre-equilibrated with 20 mM Tris buffer containing 0.1 M NaCl at pH 7.4. The column (20 X 1.5 cm) was packed with pre-equilibrated strong anion

exchanger and washed with same buffer by two bed volumes of anion exchanger. Total 96 mg of protein sample was loaded in injecting loop and the column was eluted with buffer A and B [Buffer A- 20mM Tris-Cl buffer containing 0.1M NaCl (pH 7.4); Buffer B- 20mM Tris-Cl containing 1.0 M NaCl (pH 7.4)]. The column was eluted by a linear gradient of 0.1-1.0 M sodium chloride at a flow rate of 1.5 ml/min using Automated Biologic LP system (as shown in figure 2.2.). A total of 140 fractions (1ml) were collected. The absorbance at 280 nm for each fraction was read and the elution profile was made using LP Data view software version 1.03. The fractions under each peak were pooled and checked for their inhibitory potency towards both calcium phosphate and calcium oxalate crystallization and the active fraction was dialyzed against the buffer A to remove the excess salt.

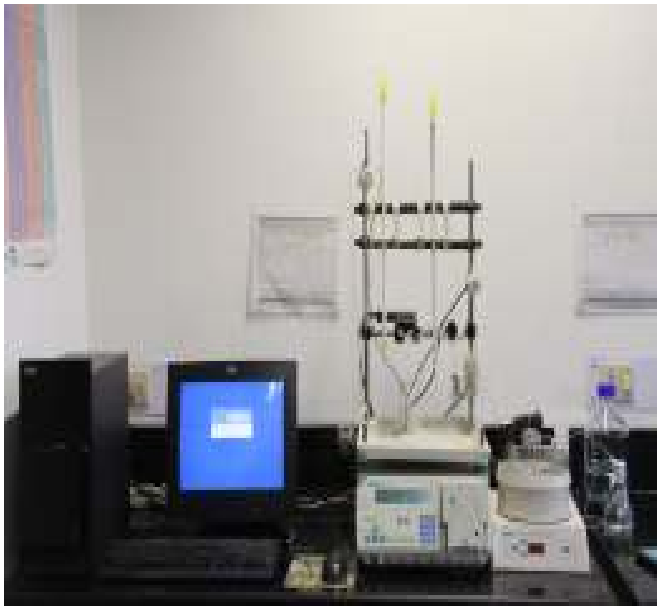

**Figure 2.2.** Automated Biologic LP system (BioRad)

**Table 2.2.** Method used for Anion exchange chromatography

| *Time (minutes)* | *Flow rate (ml/min)* | *Buffer* |
|---|---|---|
| 0-30 | 1.5 | Buffer A |
| 30-100 | 1.5 | 0-90% gradient from Buffer A to Buffer B |
| 100-120 | 1.5 | Buffer B |
| 120-140 | 1.5 | Buffer A |

***2.2.5. Molecular sieve chromatography***

The lyophilized powder of the fraction with the highest CaOx and CaP inhibitory activity obtained after anion exchange chromatography was dissolved in 1.5 ml of 20 mM Tris-Cl buffer (pH 7.4) and centrifuged at 10,000 rpm for 15 min at room temperature to remove insoluble material. The molecular sieve resin [Bio gel® P-100 gel (Medium, 90-180 µm), BioRad laboratories] was equilibrated with 240 ml of above mentioned buffer. A total 16.5 mg protein was loaded on the molecular sieve column (70 X 2.5 cm) and eluted with same buffer using Biologic LP system (as shown in figure 2.2.) at a flow rate of 25 ml/hr. Fractions of 2 ml were collected throughout the elution. The absorbance at 280 nm for each fraction was read and the elution profile was made using LP Data view software version 1.03. The calcium oxalate and calcium phosphate inhibitory activity was checked in each fraction. Fractions with CaOx and CaP inhibitory activity were freeze-dried.

***2.2.6. SDS-PAGE***

Electrophoresis of active fraction obtained after ammonium sulfate precipitation, anion exchange and molecular sieve chromatography was carried on 10% gel under denaturizing conditions in the presence of reducing agent. Electrophoresis separation was accomplished in a BioRad Mini protein gel system at 100 V for an average of 1.5 hour. Gels were stained with Coomassie Brilliant Blue R-250 [197].

***2.2.7. Native-PAGE***

The electrophoresis of the fraction obtained after molecular sieve chromatography was performed maintaining the native configuration of protein biomolecule(s). The gel for Native-PAGE was used in the concentration of 10% without using SDS or 2-mercaptoethanol (reducing agent). The molarity of the electrophoresis buffer used for native gels was 50 mM Tris-Cl and 284 mM glycine. The gels were over-run for 15 minutes and stained with Coomassie Brilliant Blue R-250. Total protein amount of the ammonium sulfate precipitation fractions, anion exchange and molecular sieve chromatography fractions was determined by the method of Lowry's [196] as described in section 2.1.7.6.

## *2.3. Characterization of purified antilithiatic protein*

### *2.3.1. Materials*

Protein molecular weight markers like carbonic anhydrase, alcohol dehydrogenase & bovine serum albumin were purchased from Sigma, St. Lois, USA, Trypsin profile IGD kit (Sigma, St. Lois, USA) was used for protein trypsinization, Macro Prep® 25 Q Strong cation exchanger (Bio-Rad laboratories) was used for isoelectric point determination, softwares used were Sigma plot & Mascot search engine. HPLC column used were Protein Pak 125, Pico Tag of Waters. Solvents used were of HPLC grade. All other chemicals were of analytical grade.

### *2.3.2. Kinetics of inhibitory activity of Dolichos biflorus antilithiatic protein*

The inhibitory activity of *Dolichos biflorus* antilithiatic protein was evaluated using *in vitro* homogenous system of CaP mineralization and CaOx crystal growth assay system as given in section 2.1.3 and 2.1.5 respectively. The inhibitory activity of the purified protein was tested at a varying concentration of 50 µg/ml, 100 µg/ml, 200 µg/ml, 350 µg/ml and 450 µg/ml subsequently.

### *2.3.3. Molecular weight determination*

The molecular mass of purified inhibitory protein was determined by using HPLC (Figure 2.3), in which pre-equilibrated with 20 mM sodium phosphate buffer (pH 7.4) Protein Pak 125 (300 mm x 7.8 mm) column was used. The elution was carried out at a flow rate of 25 ml/hr. The protein was detected at 280 nm using Waters 2996 photodiode array detector. The column was calibrated using standard proteins

**Figure 2.3**. High Pressure Liquid Chromatography.

(carbonic anhydrase 29 kDa; Bovine serum albumin 68 kDa; alcohol dehydrogenase 150 kDa). A graph was plotted between retention times (in minutes) versus log of molecular mass for each standard protein. Finally, the molecular mass of purified protein was calculated on the basis of its retention time.

### *2.3.4. Isoelectric point determination*

Isoelectric point was determined by the method of Yang and Langer [198]. Fully hydrated (20% v/v ethanol) Macro Prep® 25 Q Strong cation exchanger supports were utilized for determination of isoelectric point. After washing of matrix with distilled water, it was equilibrated with 40 mM sodium phosphate buffer of varying pH values ranging from pH 3 to pH 7. The purified protein, buffered with varying pH values corresponding to those of previously prepared resins were mixed and incubated at room temp, for 10 min with the corresponding matrix. The supernatant was removed by centrifugation at 2,500 g for 5 minutes and assayed at 280 nm for the presence of protein at all pH range. A graph was plotted between pH versus absorbance using sigma plot and isoelectric point was calculated using following equation.

$$pI=1/m[\{(Y_H + Y_L)/2\}-b]$$

where,

$Y_H$ = absorbance value of higher plateau of the absorbance-pH plot

$Y_L$ = absorbance value of lower plateau of the absorbance-pH plot

m = slope of straight line

b = y-intercept of straight line

### *2.3.5. Total amino acid composition*

Total amino acid content in the protein was estimated after acid hydrolyses of purified protein sample by the method of Elkin & Wasynczuk [199]. For hydrolysis, 200 µl of HCl/Phenol solution was added and the sample was dried in nitrogen gas prior to its hydrolysis at $105^0$C in oven for 24 hrs. This causes release of free amino acids from the protein. Derivatization of free amino acids after hydrolysis was performed by

phenylisothiocyanate (PITC), ethanol, water and triethylamine in ratio of 1:7:1:1. The derivarized sample was loaded on silica based Pico Tag (Waters; 3.9 mm X 15 cm) column. Before loading, the sample was diluted with solution made up of disodium hydrogen phosphate with 5% acetonitrile. About 20 µl of this solution was loaded on the column, thus indicating that about 1µg of protein is loaded. Elution was done under high pressure using a gradient of sodium acetate trihydrate in 6% acetonitrile and 60% acetonitrile as shown in table 2.3. The detection was done at a wavelength of 254 nm and the temperature was kept at $46^0$C during the separation procedure.

Eluent A: Sodium acetate trihydrate containing 6% acetronitrile

Eluent B: 60% acetronitrile in water

**Table 2.3.** The gradient program used for amino acid analysis

| *Time (mins)* | *Flow (ml/min)* | *% A* | *%B* |
|---|---|---|---|
| | 1 | 100 | 0 |
| 12 | 1 | 54 | 46 |
| 14 | 1 | 0 | 100 |
| 16 | 1.5 | 0 | 100 |
| 18 | 1 | 100 | 0 |
| 20 | 1.5 | 100 | 0 |
| 20.5 | 0.1 | 100 | 0 |

### *2.3.6. Peptide mass fingerprinting*

Peptide mass fingerprinting was done using Matrix-Assisted Laser Desorption/ Ionization-Time of Flight Mass Spectrometry (Figure 2.4). It is a very sensitive technique and can determine the molecular mass of a protein even in pico mole amount. In peptide mass fingerprinting, protein is digested with trypsin and various small peptides thus obtained are subjected to Matrix-Assisted Laser Desorption/Ionization-Time of Flight

Mass Spectrometry which determines the molecular weight of each peptide of the trypsinized protein.

The protein band obtained after purification was excised and subjected to in-gel tryptic digestion by using Trypsin profile IGD kit (Sigma). The resulting peptide mixtures were eluted on the sample plate with the matrix solution (10 mg/ml of α-cyano-carboxycinnamic acid in 50% acetonitrile/0.1% trifluoroacetic acid). Matrix and samples were deposited on the MALDI probe and allowed to air-dry. The spectrum was then recorded on Bruker Ultraflex MALDI–TOF/TOF mass spectrometer operating at 20,000V with the nitrogen laser focused at 337 nm. At least fifty shots were averaged to obtain a decent spectrum of antilithiatic protein of *Dolichos biflorus*.

**Figure 2.4**. Bruker Ultraflex MALDI TOF MS

### *2.3.7. Peptide Matching*

Peptide matching was performed using the MASCOT search engine (http://www.matrixscience.com) assuming that peptides were monoisotopic, carbamidomethylated at cysteine residues, and oxidized at methionine residues. A mass tolerance was 120 parts per million, and only 1 maximal cleavage was allowed for peptide matching. Probability-based MOWSE (Molecular Weight SEarch) score was calculated using the formula [–10log (*P*)], where *P* is the probability that the observed match was a random event.

## *2.4. In-silico study on interaction of antilithiatic proteins with COM*

### *2.4.1. Materials*

Molecular modeling was performed using Molecular Operation Environment (MOE) software package (Chemical Computing Group, Montreal, Canada), The Cif. format of 3 dimensional COM crystal structure data was downloaded from American Data Base and visualized in Mercury 1.4.2 Crystal structure Visualization and Exploration (Cambridge Crystal Database, University of Cambridge), The interactions between ligand and protein with in a docked structure, shown by hydrogen bonds and by hydrophobic contacts was depicted by LIGPLOT program (Lawrence Livermore National Laboratory)

### *2.4.2. Formation of calcium oxalate structure*

The unit cell structure of calcium oxalate monohydrate (COM) was prepared using crystallographic data derived and predicted by Tazzoli and Domeneghetti [200]. The low temperature monoclinic structure with space group $P2_1/c$ was selected. Since, hydrogen atoms were not included in the COM crystal structure format downloaded from American data base so they were computationally added to COM structure. Energy minimization was preformed to calcium oxalate monohydrate structure by using force field MM2 with dielectric constant equal to 1.2 to obtain the most stable structure of COM. This minimized (energy) structure of COM was treated as a ligand for further docking simulations. Figure 2.5 represents the structure of COM crystal observed by Mercury crystal structure, the green color bond is between calcium and oxygen (Ca-O), red bond is between two oxygen atoms, grey color bond is present in oxalate group, between carbon and oxygen and white color bond is depicting the hydrate moiety i.e. the bond between hydrogen and oxygen in water molecule. The figure 2.5 also represents free calcium binding sites for further growth which will be denoted as growth points or the site of further growth of COM

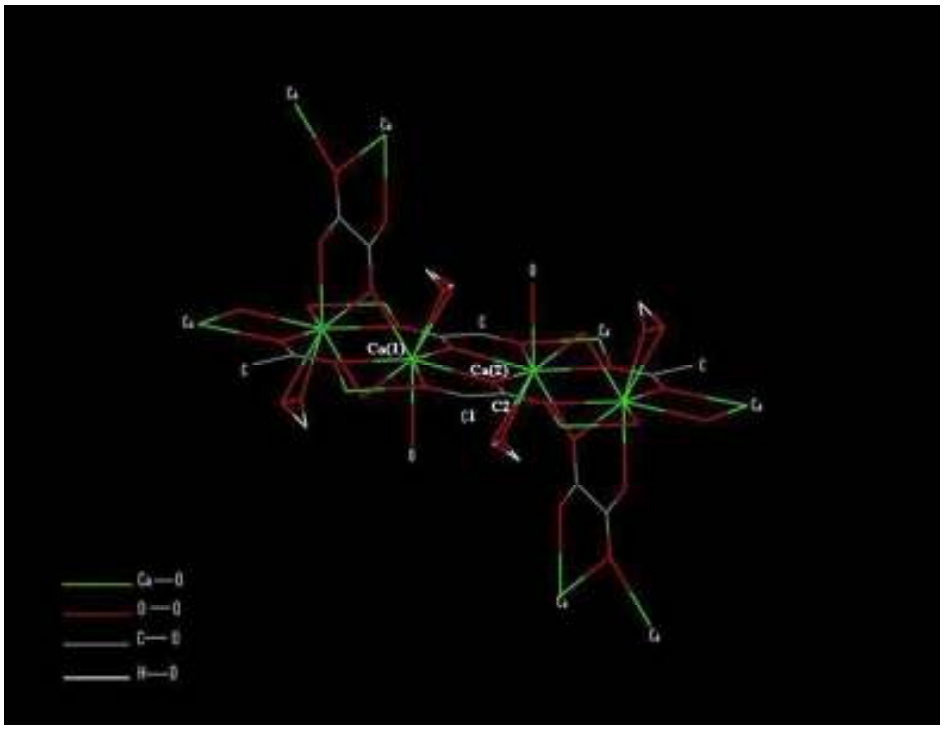


**Figure 2.5.** Structure of Calcium oxalate monohydrate (COM) unit cell showing coordination polyhedra of atoms Calcium 1 [Ca (l)] and Calcium 2 [Ca (2)].

### *2.4.3. Prediction and modeling of binding sites*

The coordinates of inhibitory proteins viz. bikunin (PDB ID:1BIK ), osteonectin (PDB ID:1SRA ), urinary prothrombin (PDB ID:2PF2), CD59 (PDB ID:2J8B ), MAp19 (PDB ID:1SZB) was taken from Protein Data Bank (www.rcsb.org) (Table 2.4). After addition of hydrogen atoms, Amber99 force field was used to assign partial charge on protein and all structure minimizations. Different binding sites of each protein were predicted with MOE-Site Finder which predicts hydrophilic and hydrophobic interaction sites and cavities. After adding the hydrogen atoms and prior to the docking calculations, an energy minimization using MMFF94 forcefield was performed on all the binding sites using the minimization protocol of Steepest Descent (SD), Conjugate Gradient (CG) and Truncated Newton (TN) methods. During the minimization, non-hydrogen atoms were held fixed and the RMSD gradient used in SD was 1,000, in CG was 100, and in the TN step the RMSD was 0.1. The iteration limits in SD and CG are 100 in TN 200.

### *2.4.4. Docking simulations*

Docking simulations were done using MOE-Dock which utilizes a Monte Carlo simulated annealing process for the docking calculation. A docking energy is calculated from a set of energy grids centered in the binding site of the protein. The protein coordinates were fixed during calculation, while the ligand is flexible and moves on the grid and searches the grid to locate the best binding orientation and conformation based on the docking energy. In all docking calculations, a docking box with a grid consisting of 60 X 60 X 60 points was employed. The spacing of the grid was 0.375 Å.

**Table 2.4.** Information of proteins procured from Protein data Bank (www.rcsb.org)

| | *Protein* | *PDB ID* | *Resolution (Å)* | *Source organism* |
|---|---|---|---|---|
| 1 | Osteonectin | 1SRA | 2.00 | *Homo sapiens* |
| 2 | CD59 | 2J8B | 1.15 | *Homo sapiens* |
| 3 | Bikunin | 1BIK | 2.50 | *Homo sapiens* |
| 4 | Urinary Prothrombin | 2PF2 | 2.20 | *Bos Taurus* |
| 5 | MAp19 | 1SZB | 2.50 | *Homo sapiens* |

The iteration limit was set to 20,000, the numbers of cycles were set to 20 and numbers of runs were set to 25, producing a molecular database with 25 docked configurations for each calculation. After a preferable binding structure was obtained

from docking simulation, the complex was used to determine atoms involved in hydrogen bonds and distance between atoms were determined using LIGPLOT [201].

### *2.4.5. Molecular mechanics and binding free energies*

For the calculations of free energy of binding (FEB) of the ligand within the corresponding binding sites, only the docking result and the best scoring pose of the ligand was taken into consideration. eMBrAcE developed by Schrodinger was used for the physics-based rescoring procedure [202] For each binding site, the energy of protein–ligand complex (*E*lig–prot), the free protein (*E*prot) and the free ligand (*E*lig) were all subjected to energy minimization in implicit solvent (water) using the OPLS_2001force field with a constant dielectric electrostatic treatment of 1.0 [203,204]. It uses traditional MM methods to calculate ligand–receptor interaction energies (*Gele, GvdW, Gsolv*) by a GB/SA method [205] for the electrostatic part of solvation energy and solvent-accessible surface for the non-polar part of solvation energy. A conjugate gradient minimization protocol with default values was used in all minimization. eMBrAcE minimization calculations were performed using an energy difference mode, in which the calculation is performed first on the receptor, then on the ligand and finally on the complex, taking complexes obtained after docking analysis (MOE-dock outputs) as input. The energy difference is then calculated using the equation:

$$\Delta G_{binding} = E_{complex} - E_{ligand} - E_{protein}$$

Where,

$E_{complex}$ = Energy of docked complex

$E_{ligand}$ = Energy of ligand

$E_{protein}$ = Energy of protein

$\Delta G_{binding}$ = Free energy of binding

## *2.5. Validation in rat urolithiatic model*

### *2.5.1. Materials*

Healthy male rats of the Wistar strain weighing between 150-175 gm of equivalent age groups were obtained from the central animal house of Panjab University Chandigarh, India. The animals were acclimatized for one month in polypropylene cages under hygienic conditions and were provided standard animal feed and water *ad libitum*. All procedures were done in accordance with ethical guidelines for care and use of laboratory animals and were approved by the local care of Experimental Animals Committee.

### *2.5.2. Experimental groups*

All animals were divided into two major groups i.e Group A and Group B on the basis of the treatment given for 9 and 15 days respectively. Another Group C was given hyperoxaluric dose for 24 hrs to check only oxidative stress. Each major group was further subdivided into four groups having 8 animals in each and named as group A1, A2, A3, A4; B1, B2, B3, B4 and C1, C2, C3, C4 respectively. The flowchart representation of all three major groups and their subgroups is given in figure 2.6.

The description of each group with its respective dose and period of treatment is given below

**Group A1**: The control animals which were given standard animal feed and water *ad libitum* for 9 days.

**Group A2:** The stone forming rats which were given 0.4% ethylene glycol with 1.0% ammonium chloride (EG + $NH_4Cl$) in their drinking water for 9 days.

**Group A3:** The rats were given intraperitoneal dose of *Dolichos biflorus* purified protein at a dosage of 1mg/kg body weight in addition to 0.4% ethylene glycol with 1.0% ammonium chloride (EG + $NH_4Cl$) in their drinking water for 9 days.

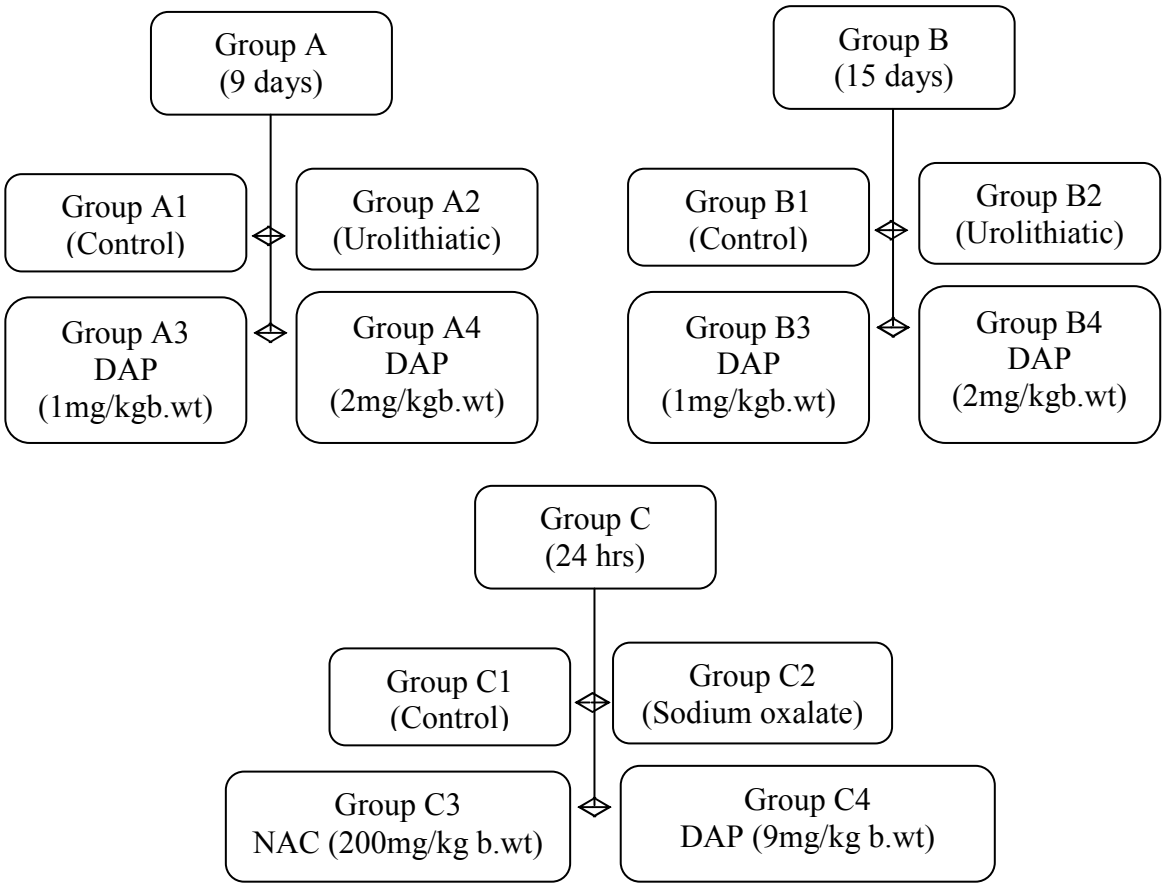


**Figure 2.6.** Flowchart of animal grouping for *in vivo* studies

**Group A4:** The rats were given intraperitoneal dose of *Dolichos biflorus* purified protein at a dosage of 2 mg/kg body weight in addition to 0.4% ethylene glycol with 1.0% ammonium chloride (EG + $NH_4Cl$) in their drinking water for 9 days.

**Group B1**: The control animals which were given standard animal feed and water *ad libitum* for 15 days.

**Group B2:** The stone forming rats which were given 0.4% ethylene glycol with 1.0% ammonium chloride (EG + $NH_4Cl$) in their drinking water for 15 days..

**Group B3:** The rats were given intraperitoneal dose of *Dolichos biflorus* purified protein at a dosage of 1 mg/kg body weight in addition to 0.4% ethylene glycol with 1.0% ammonium chloride (EG + $NH_4Cl$) in their drinking water for 15 days.

**Group B4:** The rats were given intraperitoneal dose of *Dolichos biflorus* purified protein at a dosage of 2 mg/kg body weight in addition to 0.4% ethylene glycol with 1.0% ammonium chloride (EG + $NH_4Cl$) in their drinking water for 15 days.

**Group C1:** The control animals which were given single intraperitoneal dose of normal saline

**Group C2:** The rats in this group were given single intraperitoneal dose of sodium oxalate (70mg per Kg body weight) for 24 hrs.

**Group C3:** The rats in this group were given single intraperitoneal dose of sodium oxalate (70mg per Kg body weight) and single intraperitoneal dose of *Dolichos biflorus* purified protein (9 mg per kg body weight) after half hour of sodium oxalate injection. The treatment was given for 24 hrs.

**Group C4:** The rats in this group were given single intraperitoneal dose of sodium oxalate (70mg per Kg body weight) and single intraperitoneal dose of N-acetylcysteine (200mg per kg body weight) after half hour of sodium oxalate injection. The treatment was given for 24 hrs.

Before sacrificing the rats, the blood was taken from the orbital sinus of rat's eye with the help of capillaries. The rats were anaesthetized with diethyl ether and sacrificed by decapitation after 24 hours of above treatment. Urine from the urinary bladder was directly obtained by syringe.

Both the kidneys were removed and perfused with ice cold normal saline (0.9 % NaCl) to remove residual blood. The transverse section from both the kidneys were cut and fixed in formaldehyde for histological analysis.

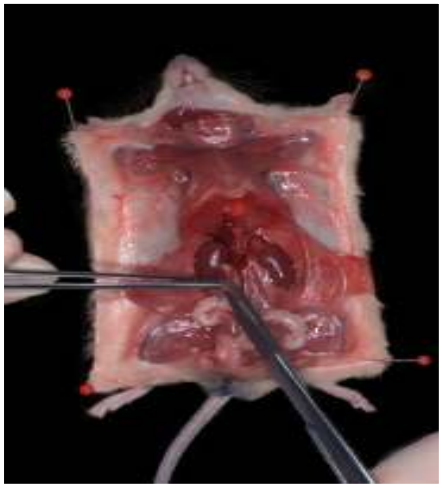

**Figure 2.7.** Location of kidney and urinary bladder observed after dissection

### *2.5.3. Body weight*

The animals in various groups were monitored for their physical health and dietary intake. The change in body weight was recorded everyday for animals in all the groups.

### *2.5.4. Serum parameters*

#### *2.5.4.1. Preparation of serum*

Before sacrificing the rats, the blood was taken from orbital sinus into a centrifuge tube without anticoagulant and allowed to clot at room temperature for 15 minutes and then centrifuged for 15 minutes at 3000 rpm. The supernatant was collected as serum for the estimation of creatinine and urea.

#### *2.5.4.2. Estimation of creatinine*

It was estimated by the method of Bonseves and Taussky [206].

*Principle*

Creatinine in alkaline solution reacts with picric acid to form an orange red compound. Rate of development of color is proportional to the concentration of creatinine in the sample and absorbance of color was measured at 530 nm.

*Reagents*

- Picric acid: Saturated solution of picric acid was prepared by dissolving excess of picric acid in glass distilled water.
- Sodium hydroxide: 10 g of NaOH was dissolved in 250 ml of distilled water to prepare 1 M NaOH solution
- Creatinine standard: Prepared by dissolving 10 mg of creatinine in 10 ml of distilled water.

*Procedure*

- To 0.1 ml of sample, 0.1ml of 1 M NaOH was added.
- The contents were mixed and 0.2 ml of saturated picric acid solution was added.
- The solutions were mixed and allowed to stand for 10minutes.
- The volume was made to 10 ml with distilled water.
- Absorbance was measured at 530 nm.
- Appropriate blank and standard were also run in parallel.

*Calculation*

The concentration of creatinine (mg/dl) was calculated using following formula.

$$\frac{\text{Absorbance of test}}{\text{Absorbance of standard}} \times \text{concentration of standard}$$

***2.5.4.3. Estimation of urea***

Urea in serum was estimated by diacetylmonoxime method as described by Marsh [207].

*Principle*

Urea reacts directly with diacetylmonoxime under strong acidic conditions to give yellow condensation product. The reaction is intensified by the presence of ferric ion and thiosemicarbazide and red complex is formed whose absorbance is measured at 520nm.

*Reagents*

- Working urea standard- 200 mg of urea was dissolved in water and final volume was made to 100ml
- The acid reagent was made by mixing Stock A (0.5 ml) with 1 litre of Stock B

- Acid reagent (stock A) – 5gm of ferric chloride ($Fecl_3, 6H_2O$) was dissolved in about 20 ml of water. This 20 ml solution was then transferred to a 250ml measuring flask in which 100 ml of phosphoric acid (85%) was added slowly with swirling and the final volume was made to 250 ml with water.
- Acid reagents (stock B) – 200 ml of concentrated $H_2SO_4$ was added to 800 ml of water in one liter conical flask slowly, with swirling and cooling.
- The Color reagent was made by mixing 6.7 ml of stock A with 6.7 ml of stock B and made to 100 ml with distilled water. Both the solutions were prepared fresh every time.
- Color reagent (stock A) – 2 gm of Diacetyl monoxime was dissolved in 100 ml distilled water and then filtered to remove any suspended insoluble particles.
- Color reagent (stock B) – 5 gm of thiosemicarbazide was dissolved with one liter distilled water.

*Procedure*

- The sample (0.1 ml) was taken in test tube and it was diluted by adding 9.9 ml of distilled water.
- The contents were mixed thoroughly on vortex.
- 2 ml of mixed color reagent was added in test tube followed by 2 ml of mixed acid reagent.
- The solutions were mixed again and kept on boiling water bath for 20 minutes.
- The standard and blank tubes were run in parallel by taking 0.1 ml standard urea and 0.1 ml water respectively.
- All the tubes were cooled and their absorbance was measured at 520 nm.

*Calculation*

The concentration of urea (mg/dl) was calculated using following formula.

$$\frac{\text{Absorbance of test}}{\text{Absorbance of standard}} \quad X \quad \text{concentration of standard}$$

### *2.5.5. Urinary parameters*

#### *2.5.5.1. Urine collection/ processing*

After the end of treatments period, the rats were placed in metabolic cages and urine was collected for 24 hour period with 20 µl of 20% sodium azide as a preservative. After measuring urinary volume, an aliquot of urine was acidified by the addition of 3 N HCl for the determination of urinary creatinine. The remaining urine was frozen at $-20^0$ C and used for determination of alkaline phosphatase (AP), lactate dehyrogenase (LDH).

#### *2.5.5.2. Estimation of lactate dehydrogenase*

The activity of Lactate dehydrogenase was estimated by the method of Vassault [208].

*Principle*

$$CH_3CO\ COO^- + NADH + H^+ \longleftrightarrow CH_3.CHOH.COO^- + NAD^+$$

Pyruvate Lactate

Lactate dehydrogenase activity is determined by measuring the rate of disappearance of NADH when pyruvate is converted to lactate. Enzyme activity is measured by estimating the concentration of NADH present in the reaction mixture. NADH absorbs light at 340 nm (molar absorbtivity = 6.22 X $10^3$ $M^{-1}$ $cm^{-1}$) whereas $NAD^+$ does not. The equilibrium for the reaction lies very strongly in the direction of reduction of pyruvate and hence the reaction is followed by measuring the rate of decrease in absorbance of NADH at 340 nm.

*Reagent*

- Substrate – 3.5 gm of $K_2HPO_4$, 0.45 gm of $KH_2PO_4$, 5.35 gm NaCl (pH 7.2) and 31mg of sodium pyruvate were dissolved in 450 ml distilled water.
- NADH – 42 mg of NADH was dissolved in 4.5 ml of 1% $NaHCO_3$.

*Procedure*

- To a cuvette, 3 ml of substrate, 50µl of NADH and 200 µl of sample were added.
- The solutions were mixed rapidly and a decrease in absorbance was measured at 340 nm.

*Calculations*

The activity of lactate dehydrogenase was calculated using following formula

$$\text{Activity (Units/min/mg protein)} = \frac{\text{Absorbance/min}}{\text{6.22 X mg protein/ml of sample}}$$

***2.5.5.4. Estimation of alkaline phosphatase***

The activity of enzyme alkaline phosphatase was measured by the method of Bessey et al [209].

*Principle*

Alkaline phosphatase causes the conversion of p-nitrophenol to p-nitrophenylphosphate. The rate of formation of the yellow colour of p-nitrophenol produced by hydrolysis of p-nitrophenylphosphate in alkaline solution is measured spectrophotometrically at 405nm to calculate the activity of enzyme.

*Reagents*

- Buffer –3.16 gm 2-Amino -2 Methyl propane was dissolved in 80 ml distilled $H_2O$, pH was adjusted to 10.25 (Adjust with 1 M NaOH) and then 40.6 mg $MgCl_2.6H_2O$ was added and dissolved. Finally the volume was raised to 100 ml.

- Substrate – 105mg disodium-p-nitrophenylphosphate per ml distilled $H_2O$ was dissolved & stored on ice.

*Procedure*

- To a cuvette, 2.8ml of buffer and 100µl substrate was added for 5 mins.
- 100µl of sample was added to the cuvette and rate of increase in absorbance was recorded at 405nm for 5 mins.

*Calculations*

The activity of alkaline phosphatase was calculated using following formula

$$\text{Units/min/mg protein} = \frac{\Delta A_{340}/\text{min}}{18.8 \times \text{mg protein/ml of sample}}$$

***2.5.5.5. Collection & Polarization microscopy of Urine from Urinary Bladder***

The rats were anaesthetized with diethyl ether and sacrificed by decapitation after 24 hours of above treatment. Urine from the urinary bladder was directly obtained by puncturing with a 5/8 inch needle attached to a 1ml tuberculin syringe and directly used under polarization microscope to see presence of crystals in urine. A drop of urine obtained from bladder was spread on a glass slide, covered with glass slide and visualized under polarized light using Leica DM3000 light microscope.

**Figure 2.8.** Leica DM3000 light microscope

***2.5.6. Creatinine clearance***

Creatinine clearance determines the amount of creatinine excreted out of body per unit time and per unit volume. Creatinine clearance was calculated according to standard clearance formula

$$\mathbf{C = (U/S) \times V}$$

Where,

U is the urinary concentration of creatinine,

S is the concentration of creatinine in the serum,

V is the urinary volume in mL/min.

### *2.5.7. Preparation of homogenate*

Tissues were weighed, excised into small pieces and added into ice cold 0.1 M Tris buffer to make 10% (W/V) homogenate in Poter Elevejhem Homogenizer by using motor driven teflon pastle rotated at 3000 rpm. Finally, homogenate was taken in labeled plastic vials and stored in refrigerator for estimations of lipid peroxidation (LPO), superoxide dismutase (SOD), catalase (CAT), reduced glutathione (GSH) and redox ratio (GSH/GSSG).

#### *2.5.7.1. Lipid peroxidation assay*

Lipid peroxide formation was assayed by the method of Buege and Aust [210].

*Principle*

The sample under test is heated with TBA at low pH and a pink chromogen develops (a TBA malondialdehyde adduct), which is measured by its absorbance at or close to 532 nm.

*Reagents*

- 0.1 M Tris-HCl Buffer (pH 7.4)
- 10% (w/v) Trichloroacetic acid (TCA)
- 0.67% (w/v) Thiobarbituric acid (TBA)

*Procedure*

- 0.5 ml of tissue homogenate (10% w/v) was diluted to 1.0 ml using 0.1 M Tris-HCl buffer (pH 7.4).

- Samples were incubated at 37$^{o}$C for 2 hours with constant shaking.
- At the end of the incubation, 1.0 ml of ice cold 10% TCA was added and after thorough mixing, the reaction mixture was centrifuged at 800 g for 10 minutes.
- To 1.0 ml of supernatant, 1.0 ml of 0.67% TBA was added and colour developed at 100 C for 10 minutes.
- Samples were cooled and diluted with 1.0 ml doubled distilled water. The absorbance was read at 532 nm.

*Calculations*

The amount of Malondialdehyde formed was calculated on basis of molar extinction coefficient of MDA-TBA chromophore (1.56 X $10^5$ $M^{-1}$ $cm^{-1}$) and results were expressed as nmoles of MDA/ mg protein.

***2.5.7.2. Superoxide dismutase (SOD) assay***

Superoxide dismutase assay was performed according to the method of Kono [211].

*Principle*

The reduction of nitro blue tetrazolium (NBT) to blue formazon mediated by hydroxylamine hydrochloride was measured under aerobic conditions. Addition of super oxide dismutase inhibits the reduction of NBT mediated by hydroxylamine hydrochloride and extent of inhibition was taken as measure of enzyme activity.

*Reagents*

- Solution A – 50 mM Sodium Carbonate in 0.1 mM EDTA (pH 10.8).
- Solution B – 96 mM Nitro Blue Tetrazolium (NBT) in Solution A.
- Solution C – 0.6% Tritan X-100 (v/v)

- Solution D – 20 mM Hydroxylamine hydrochloride.

*Procedure*

The assay system contained 1.3 ml of solution A, 0.5 ml of solution B and 0.1 ml of solution C. The reaction was initiated by the addition of 0.1ml of solution D. The rate of NBT reduction in the absence of enzyme source was recorded for 4-5 minutes. Then small aliquots of the tissue homogenate were added to the test cuvette as well as the reference cuvette (did not contain solution D). The absorbance was recorded at 550 nm. The percentage inhibition on the rate of NBT reduction by 50% was defined as one unit of activity.

*Calculation*

1 unit of enzyme is defined as amount of enzyme inhibiting the rate of reaction by 50%. Enzyme activity was expressed as units/mg protein.

***2.5.7.3. Catalase (CAT) enzyme estimation***

Catalase was estimated by UV spectrophotometer method described by Luck [212].

*Principle*

On decomposition of $H_2O_2$ by catalase, the absorbance decreases with time, this can be used for determination of enzyme activity. Since the ultraviolet absorption of $H_2O_2$ solution can be easily measured at 240nm, thus the decrease in enzyme activity can be calculated, the reaction can be followed spectrophotometrically at 240 nm.

$$2\ H_2O_2 \longrightarrow 2H_2O + O_2$$

*Reagents*

- 50 mM Phosphate buffer (pH 7.0).

- 12.0 mM $H_2O_2$ in Phosphate buffer: 0.20 ml of $H_2O_2$ (30% w/v) was diluted by 100 ml of 50 mM phosphate buffer. The O.D. of this solution should be around 0.5 at 240 nm.

*Procedure*

The assay system contained 3.0 ml of $H_2O_2$ containing phosphate buffer and enzyme source. The rate of decomposition of $H_2O_2$ by catalase was measured by recording the time (in seconds) required for 0.05 decreases in optical density at 240 nm. Catalase activity was expressed in international units i.e. units/mg protein.

*Calculations*

The amount of $H_20_2$ decomposed was calculated on the basis of molar extinction coefficient of $H_2O_2$ (0.71 $M^{-1}$ $cm^{-1}$) and results were expressed as μ moles of $H_2O_2$ decomposed/min/mg protein.

***2.5.7.4: Estimation of reduced glutathione (GSH)***

Estimation of GSH was performed in the tissue homogenate by the method of Takeuchi et al [213].

*Principle*

The level of total sulfhydryl groups in the tissue were estimated with Ellman's reagent (DTNB). This method is based on the principle that DTNB is reduced by SH groups to form 1 mole of 2-nitro-5-mercaptobenzoic acid per mole of –SH which has an intense yellow color with absorbance maximum at 412 nm.

*Reagents*

- 0.2 M Phosphate buffer (pH-8.0)
- 0.6 mM 5, 5'-dithiobis (2-nitrobenzoic acid), (DTNB)

- TCA (25%)

*Procedure*

- The assay was performed by mixing 100 µl of 2.5% homogenate and TCA.
- The precipitated proteins were separated by centrifugation at 2000 g for 15 minutes.
- 0.1ml supernatant was diluted to 1 ml with 0.2 M phosphate buffer (pH 8.0).
- To this, 2 ml of freshly prepared 0.6 mM 5, 5'-dithiobis (2-nitrobenzoic acid) (DTNB) in buffer was added.
- Optical density of yellow colored complex was formed by the reaction of GSH and DTNB (Ellmen's reaction) was measured at 412 run on UV-visible recording spectrophotometer against reference which contained 0.1 ml of 5% TCA instead of sample.

***2.5.7.5. Total glutathione content***

The analysis was done by the method of Zahler and Cleland [214].

*Principle*

This method is bailed on the reduction with dithioerythritol and determination of the resulting monothiols with DTNB in the presence of arsenite. The arsenite forms a light complex with dithiols but not with monothiols.

*Reagents*

- 0.003 M Dithioerythritol
- l M Tris(pH 8.1)

- 0.005 M sodium arsenite
- 0.003 M DTNB
- 0.05 M Sodium Acetate (pH 5.0)

*Procedure*

- The disulphide in 0.2 ml solution was mixed with 0.1 ml of dithioerythritol and the reduction was allowed to proceed for 20 minutes or for the time for the disulphide to be reduced.
- After reduction, 0.2 ml of Tris, 1.5 ml of sodium arsenite and 0.9 ml water was added to give volume of 2.9 ml and the solution is mixed and allowed to stand for two minutes.
- 0.1 ml of DTNB prepared in Sodium Acetate was then added and the absorbance was recorded for at least three minutes.

*Calculations*

The absorbance resulting from the monothiols was determined by extrapolation of the linear plot of the curve of the time of addition of DTNB and subtractions of a blank value for a sample containing no disulfide.

***2.5.7.6. Oxidized glutathione (GSSG)***

Oxidized glutathione was quantitated by subtraction the values of the reduced glutathione from total glutathione.

***2.5.7.7. Redox ratio (GSSG/GSH)***

Redox ratio was determined for all the four groups by taking the ratio of oxidized glutathione/reduced glutathione.

### *2.5.7.8.* Statistical analysis

Statistical analysis was performed by unpaired, 2-tailed Student 't' test. It estimate whether the difference between the mean values of two groups are statistically significant or not.

### *2.5.8. Histology*

*Procedure*

- Fixation – small pieces of kidney tissue, after removal of extraneous material were fixed in Bouin. These were then dehydrated in various grades of ethanol, cleared in benzene and embedded in paraffine wax (M.P.60-62$^0$ C). The paraffin sections of appropriate thickness (8 μ) were cut.

- Histological Staining [Delafield's Haemotoxylin/Eiosin (HE)] – First of all, the sections were de-paraffinised in xylene and down graded through different grades alcohols to water. These were then stained in D. Haematoxylin for 15-17 minutes and then kept under running tap water. The nuclei of the cells were differentiated in acidic water and ammonia water till these stained blue. The slides were upgraded in 70% ethanol, dipped in eosin for 1 minute, differentiated in 90% alcohol and upgraded to absolute alcohol, cleared in xylene and mounted in DPX. The nuclei, nucleoli and chromatin material stained blue whereas the cytoplasm stained pink.

- The stained slides were viewed under light microscope and polarizing microscope.

# Chapter 3
# Results

## *3.1. Screening of most effective antilithiatic plant*

The 10% aqueous extract of all the four plants were screened on the basis of their ability to inhibit calcium phosphate (CaP) mineralization. The water as a solvent for extraction was chosen because of its properties for being a universal solvent. The effect towards CaP mineralization was evaluated at different volumes of aqueous extract of each plant on initiation of CaP mineralization and further on growth & demineralization of preformed mineral phase.

### *3.1.1. Effect of crude extracts of four different plants on in vitro mineralization*

Figure 3.1 shows the effect of plants extract towards initial mineral phase formation, it could be inferred from the figure 3.1a and 3.1b that *Achyranthes aspera* (84% for $Ca^{2+}$ and 76% for $HPO_4^{2-}$) and *Dolichos biflorus* (57% for $Ca^{2+}$ and 53% for $HPO_4^{2-}$) show the maximum inhibition towards CaP mineralization with as less as 0.25 ml of extract followed by *Cocos nucifera* and *Tribulus terrestris* which show lesser percentage inhibition of both calcium and phosphate ions at this volume of plant extract.

From the figure, it could be inferred that with increase in volume of plant extract, the inhibition of mineralization by *Achyranthes aspera* and *Dolichos biflorus* remained almost constant and marginally increased up to 83.8% and 87.4% for $Ca^{2+}$ and $HPO_4^{2-}$ ion (*Achyranthes aspera*) and 83.8% and 87.4% for $Ca^{2+}$ and $HPO_4^{2-}$ ion (*Dolichos biflorus*) respectively at 1.25 ml of crude plant extract.

Although *Cocos nucifera* also showed high inhibitory potency towards both calcium and phosphate ions at 1.25ml of its extract but its activity at lower crude volume was very low. *Tribulus terrestris* showed maximum inhibitory potency for both calcium (41%) and phosphate (38%) ions at 0.75ml of crude extract. In addition, *Tribulus terrestris* showed a peculiar fall in its inhibitory activity at higher volume of aqueous extract against the homogeneous system of CaP mineralization.

**Figure 3.1a**

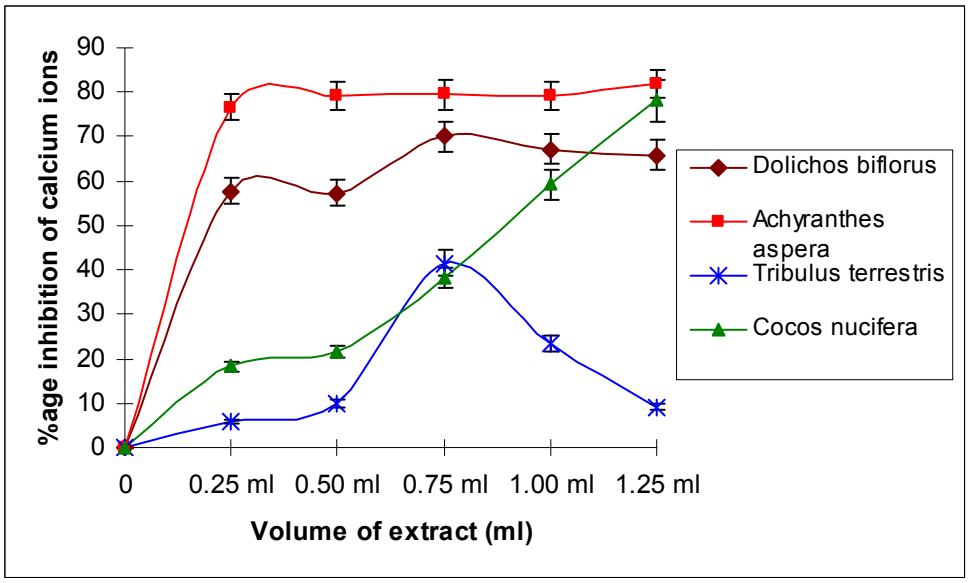


**Figure 3.1b**

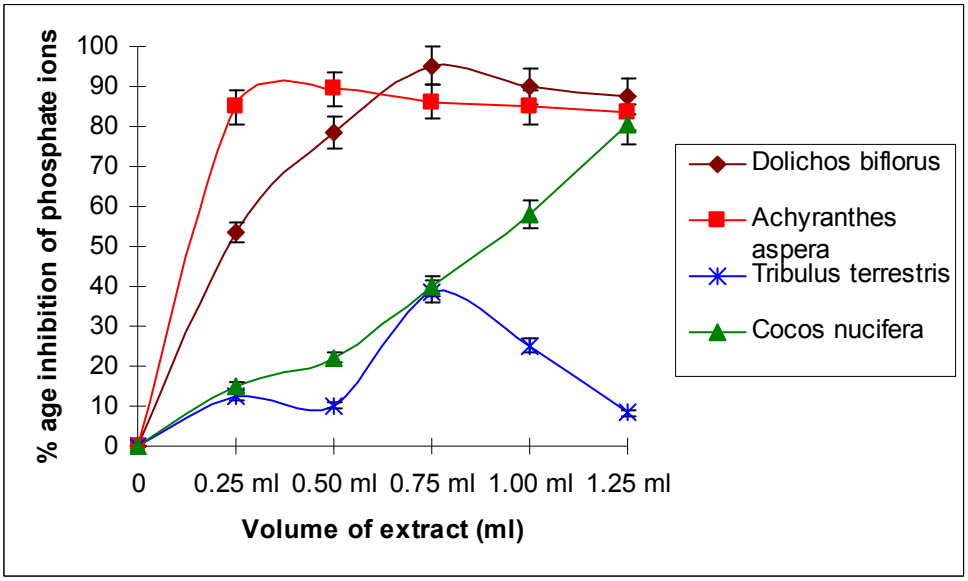


**Figure 3.1.** Effect of varied volumes of four plant extracts on initial mineral phase formation. Figure 3.1a. Percentage inhibition of calcium ions by four plant extracts. Figure 3.1b. Percentage inhibition of phosphate ions by four plant extracts. (Values are mean ± SD, n = 5)

**Figure 3.2a**

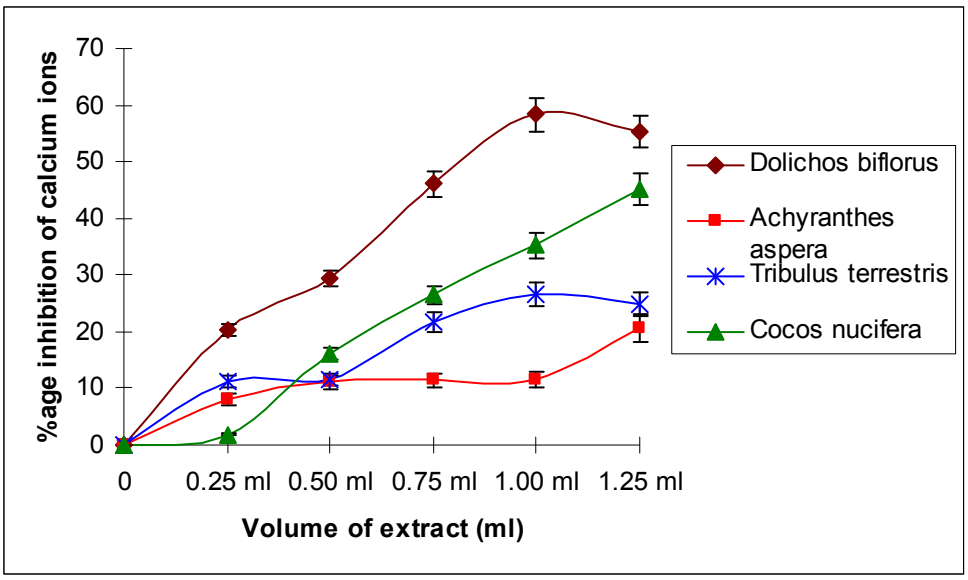


**Figure 3.2b**

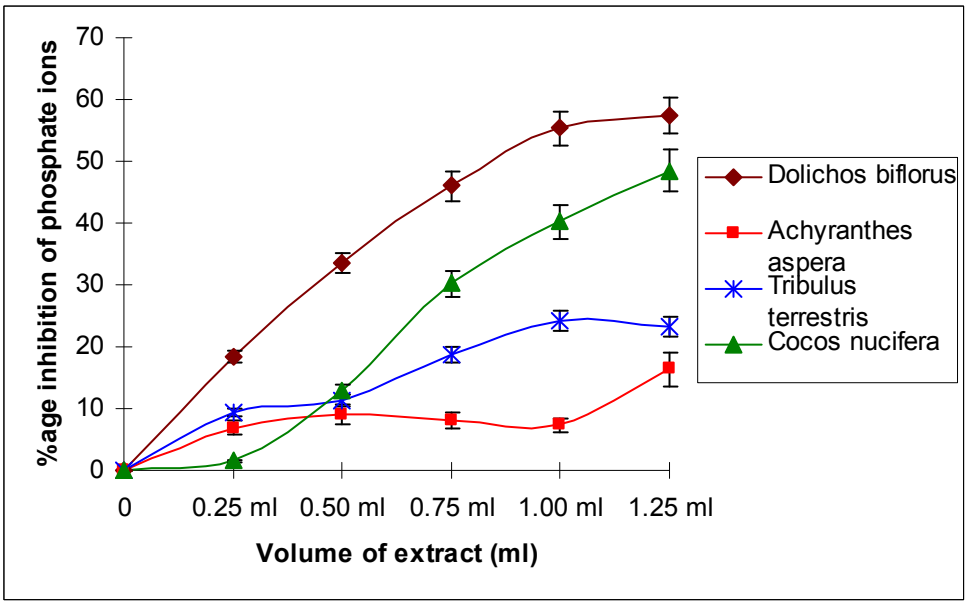


**Figure 3.2**. Effect of varied volumes of four plant extracts on the growth of preformed mineral phase. Figure 3.2a. Percentage inhibition of calcium ions by four plant extracts. Figure 3.2b. Percentage inhibition of phosphate ions by four plant extracts. (Values are mean ± SD, n = 5)

The same volume of aqueous extracts of all the four plants was further tested for their potential to inhibit growth of calcium phosphate mineralization. The figure 3.2 shows the percentage inhibition of growth of minerals over preformed mineral phase by all the four plants.

It is evident from the figure 3.2, that maximum inhibition of further growth over mineral phase is shown by *Dolichos biflorus* which was found to be 20.2% for $Ca^{2+}$ and 18.3% for $HPO_4^{2-}$ ions at 0.25 ml of aqueous extract and it progressively increased up to 55.33% and 57.51% for $Ca^{2+}$ and $HPO_4^{2-}$ ions respectively with subsequent increase in 0.5, 0.75, 1.00 and 1.25 ml of plant extract. On the other hand, *Achyranthes aspera* and *Tribulus terrestris* showed comparable inhibition of growth over preformed mineral phase. The maximum percentage inhibition of deposition of $Ca^{2+}$ and $HPO_4^{2-}$ ions over a preformed mineral phase by *Achyranthes aspera* was found to be 20.7% and 16.3% respectively. Moreover, *Tribulus terrestris* showed the maximum percentage of inhibition of deposition of $Ca^{2+}$ and $HPO_4^{2-}$ ions over a preformed crystal phase by 24.8% and 23.1% respectively. *Cocos nucifera* showed the inhibitory activity of 45.17% and 48.52% for $Ca^{2+}$ and $HPO_4^{2-}$ ions respectively, which can be considered as an adequate inhibitory activity of its extract.

The inhibitory potential of *Achyranthes aspera,* towards initial mineral phase formation was shown to be as high as 84% for $Ca^{2+}$ and 76% for $HPO_4^{2-}$ ions but the potential to inhibit further growth of preformed mineral phase with calcium and phosphate ions depositions was significantly low by the aqueous extract of this plant. However, *Dolichos biflorus* retained the consistency of inhibiting growth of mineral phase as compared to other plant extracts. In addition, all other plants showed similar effects towards inhibition of growth of mineral phase as that shown by their inhibitory potential towards initial CaP mineral phase formation.

**Figure 3.3a**

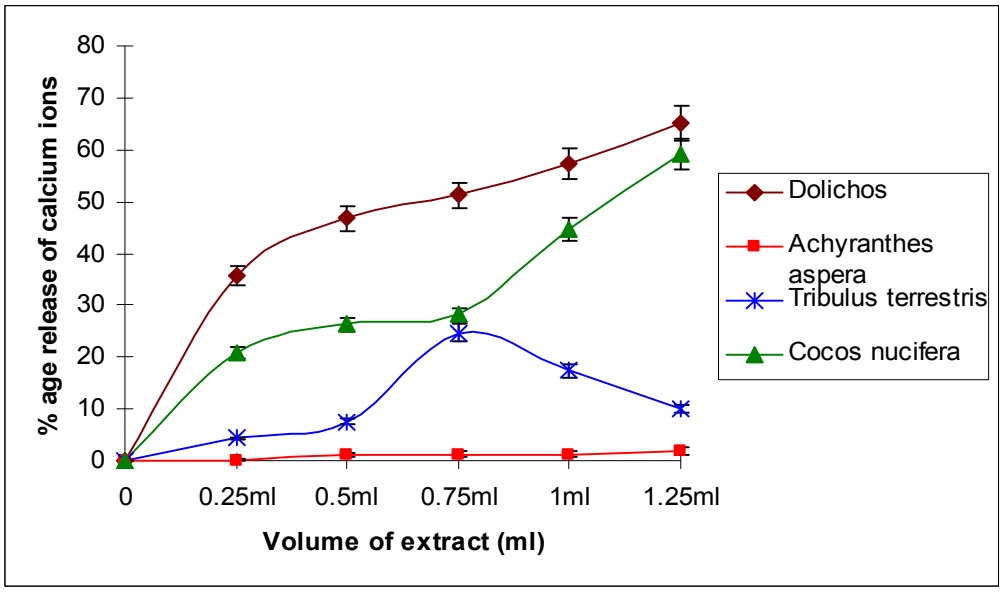


**Figure 3.3b**

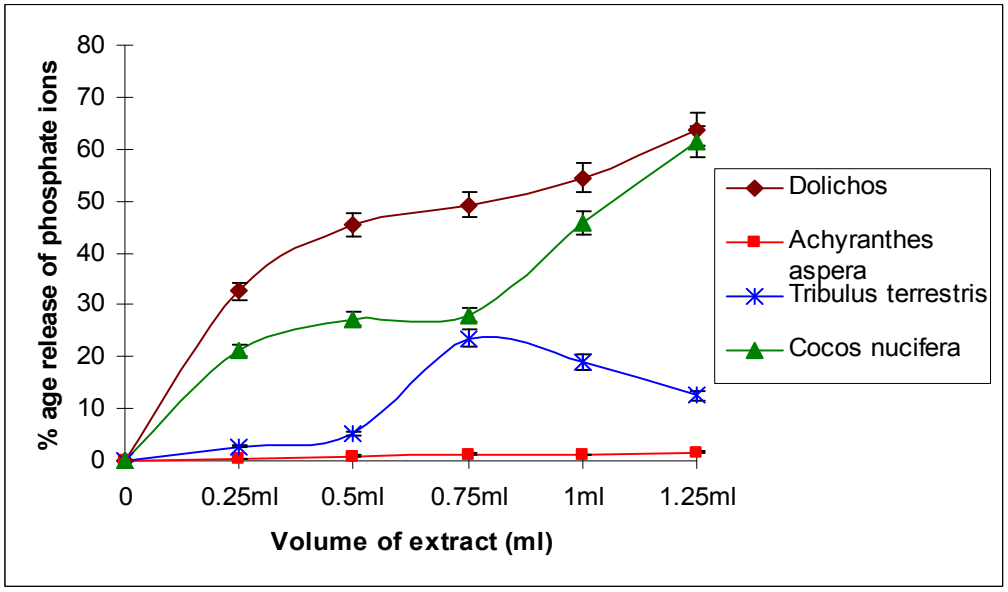


**Figure 3.3.** Effect of varied volumes of four plant extracts on demineralization of preformed mineral phase. Figure 3.3a. Percentage of calcium ions demineralized by four plant extracts. Figure 3.3b. Percentage of phosphate ions demineralized by four plant extracts. (Values are mean ± SD, n = 5)

The ability to demineralize preformed mineral phase by all four plant extracts is depicted in figure 3.3a and 3.3b. *Dolichos biflorus* showed the maximum demineralization towards both calcium and phosphate ions release from the preformed CaP mineral phase. The release of $Ca^{2+}$ and $HPO_4^{2-}$ ions with 0.25ml of aqueous extract of *Dolichos biflorus* was to the tune of 35.6% & 32.1% respectively and 1.25ml of its aqueous extract released about 65.2% of $Ca^{2+}$ & 63.7% of $HPO_4^{2-}$ ions from the preformed mineral phase.

After *Dolichos biflorus*, *Cocos nucifera* has also shown comparable demineralization of preformed mineral phase having the ability to release about 59.1% of $Ca^{2+}$ and 61.3% of $HPO_4^{2-}$ ions with 1.25ml of its extract. Although lower volume of *Cocos nucifera* extract did not show adequate demineralization ability.

On the other hand, *Tribulus terrestris* showed average ability to demineralize the preformed mineral phase of CaP. The maximum release of $Ca^{2+}$ and $HPO_4^{2-}$ ions from the mineral phase by its aqueous extract was 24.7% and 23.5% respectively by 0.75ml of aqueous extract. However, by increasing the volume of its aqueous extract to 1.25ml, a decrease in its ability to demineralize $Ca^{2+}$ and $HPO_4^{2-}$ ions was observed.

In contrast to the maximum ability of *Achyranthes aspera* to inhibit initial mineral phase formation, the ability of its aqueous extract to demineralize preformed mineral phase of CaP was shown to be very low and with the volume of 1.25ml, the maximum release of $Ca^{2+}$ and $HPO_4^{2-}$ ions was observed to be 1.92% and 1.62% respectively.

Among all the four plants (viz. *Achyranthes aspera*, *Dolichos biflorus*, *Cocos nucifera*, *Tribulus terrestris*), the seeds of *Dolichos biflorus* showed highest percentage of inhibition towards growth & demineralization of calcium phosphate and significantly good inhibition towards initiation of CaP mineral phase formation. Although *Achyranthes aspera* also possess equal ability to inhibit initiation of CaP, but its ability to inhibit the growth and demineralization of preformed mineral phase was very less.

Alternatively, *Cocos nucifera* showed adequate inhibition of CaP mineral phase formation at all the three stages (initiation, growth and demineralization). But its inhibitory activity was less at lower volume of extract. *Tribulus terrestris* on the other hand has a moderate ability to inhibit CaP mineral phase at all the three stages. Consecutively, *Dolichos biflorus* was selected to fractionate the biomolecule(s) possessing the ability to inhibit calcium phosphate and calcium oxalate crystals.

### *3.1.2. Effect of less than and more than 10kDa fractions of Dolichos biflorus on in vitro mineralization*

To have a perception of the type of biomolecules possessing anticalcifying properties, the aqueous extract of *Dolichos biflorus* which showed inhibitory potency towards CaP mineral phase was fractionated to more than 10kDa and less than 10kDa fractions. The activity of both these fractions was estimated towards CaP mineralization to check which molecular weight fraction is active. After fractionation of aqueous extract into more than and less than 10kDa fractions, the concentration of the sample was maintained at 10% w/v for further investigations. Figure 3.4 shows the inhibition of initiation of CaP mineral phase formation by the fraction of aqueous extract of *Dolichos biflorus* having less than 10kDa molecular weight biomolecules. Here, again the activity was estimated using different volumes of plant extract. From figure 3.4 it could be seen that the less than 10kDa molecular weight extract of *Dolichos biflorus* showed high percentage of inhibition of both $Ca^{2+}$ and $HPO_4^{2-}$ ions. The volume of extract at 0.25ml was inhibiting 40% and 46% of $Ca^{2+}$ and $HPO_4^{2-}$ ions respectively. The percentage inhibition by this extract increased linearly with increase in the volume till 82% for $Ca^{2+}$ and 88% for $HPO_4^{2-}$ ions with 1.25 ml of less than 10 kDa extract.

It could be observed that the less than 10kDa molecular weight fraction of aqueous extract of *Dolichos biflorus* has comparable inhibitory potential towards initial mineral phase formation as shown in figure 3.4.

**Figure 3.4a**

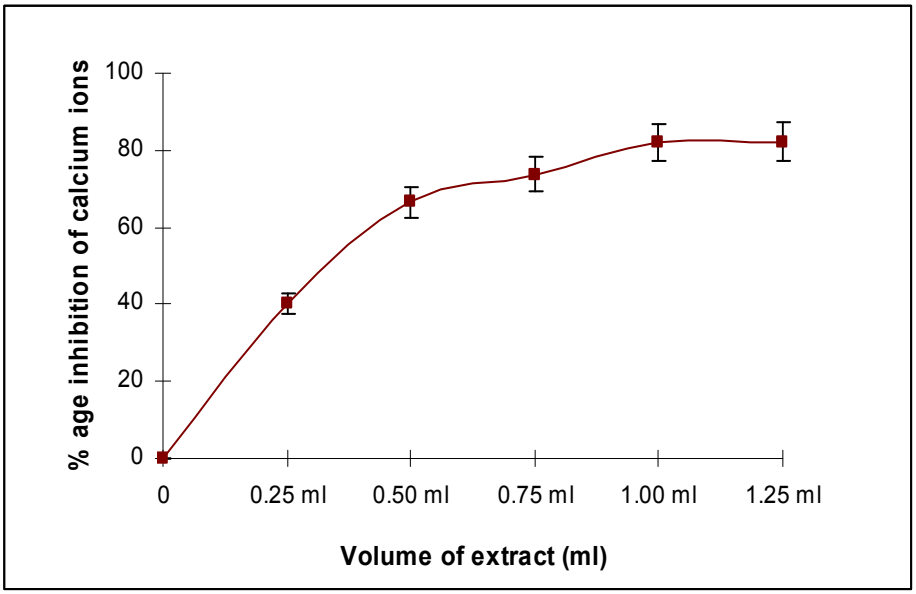


**Figure 3.4b**

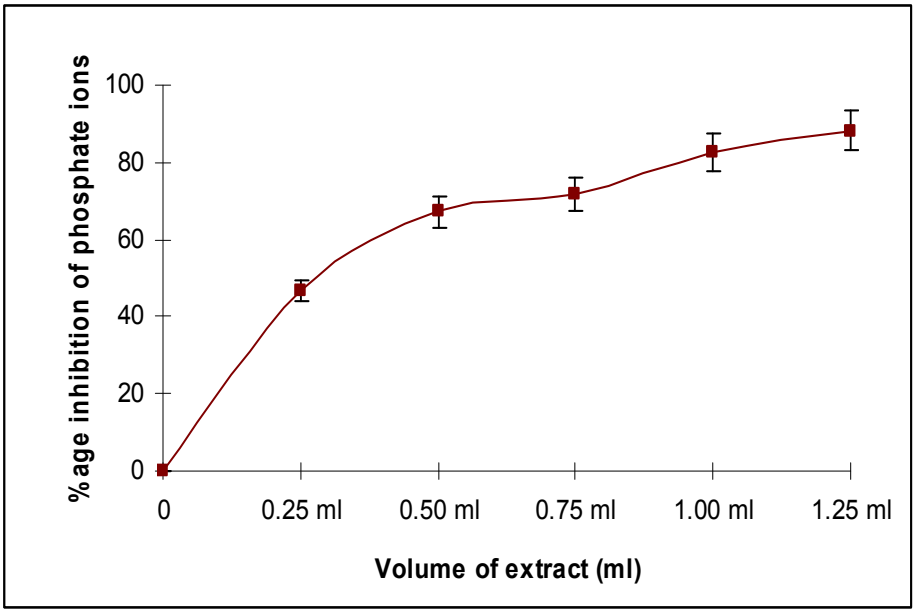


**Figure 3.4:** Effect of varied volumes of less than 10 kDa molecular weight fraction of plant extract on initial mineral phase formation. Figure 3.4a. Percentage inhibition of calcium ions by less than 10 kDa molecular weight fraction of plant extracts. Figure 3.4b. Percentage inhibition of phosphate ions by less than 10 kDa molecular weight fraction of plant extracts. (Values are mean ± SD, n = 5)

**Figure 3.5a**

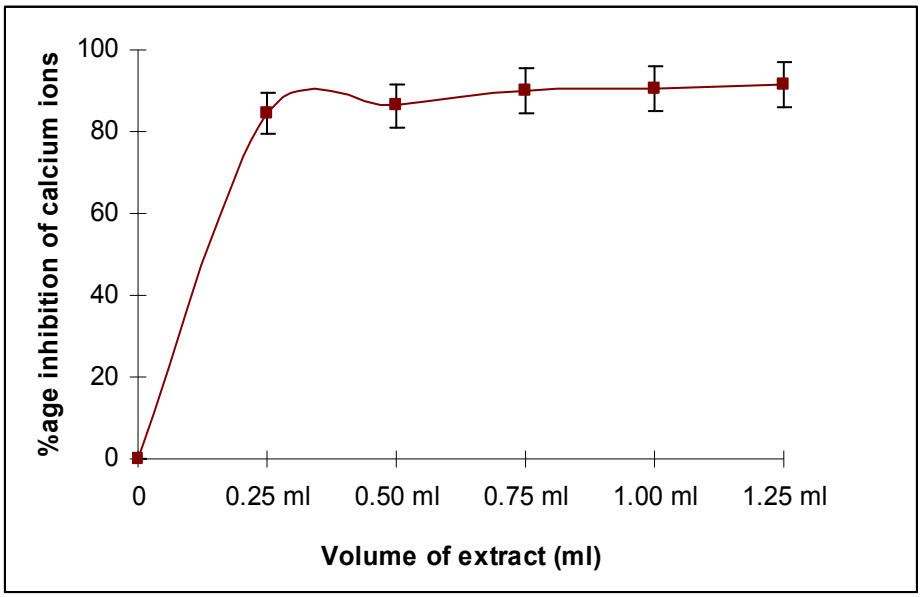


**Figure 3.5b**

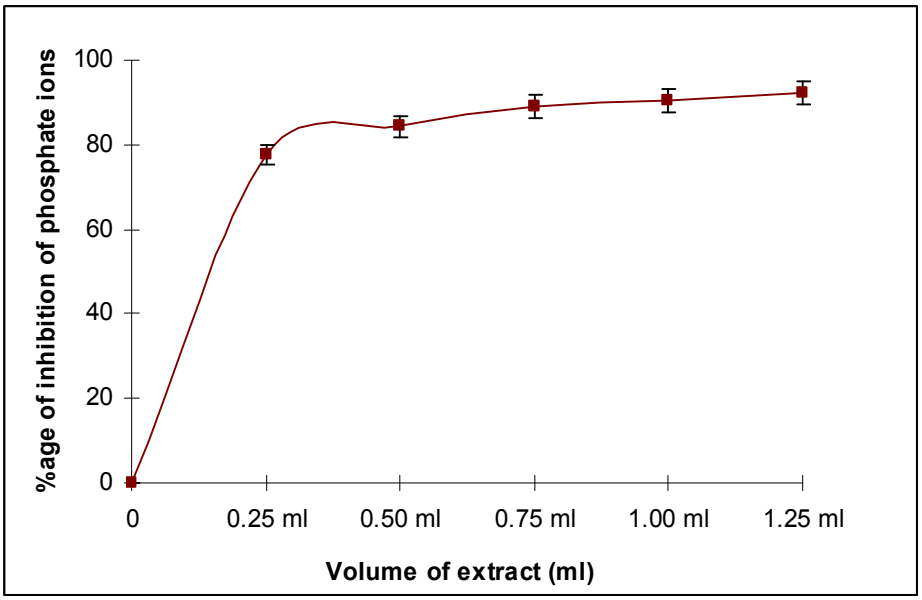


**Figure 3.5**: Effect of varied volumes of more than 10 kDa molecular weight fraction of plants extract on initial mineral phase formation. Figure 3.5a. Percentage inhibition of calcium ions by more than 10 kDa molecular weight fraction of plant extracts. Figure 3.5b. Percentage inhibition of phosphate ions by more than 10 kDa molecular weight fraction of plant extracts. (Values are mean ± SD, n = 5).

The figure 3.5 shows the effect of more than 10kDa fraction of aqueous extract of *Dolichos biflorus*. The more than 10 kDa molecular weight fraction clearly shows strong inhibition for both calcium and phosphate ions towards the initiation of CaP mineral phase formation. The 0.25ml of more than 10kDa molecular weight fraction showed very high inhibitory potency, an inhibition of 84.4% for $Ca^{2+}$ and 77.2% for $HPO_4^{2-}$ ions was observed. As the volume of more than 10kDa extract increases from 0.25ml to 1.25ml, the percentage inhibition of $Ca^{2+}$ and $HPO_4^{2-}$ ions increases to 91.3% and 92.6% respectively. On comparing the inhibitory potential of more than 10kDa molecular weight fraction of *Dolichos biflorus* with its crude aqueous extract (Figure 3.1), it can be inferred that more than 10kDa fraction has higher inhibitory potency.

After that, the more than 10kDa and less than 10kDa fractions of *Dolichos biflorus* were qualitatively screened for proteins and various phytochemicals viz. tannins, saponins, terpenoids, flavonoids and alkaloids by the method as described in section 2.1.7. The presence and absence of above mentioned biomolecules is depicted in table 3.1. The table clearly indicates that more than 10kDa fraction contains proteins and tannins whereas less than 10kDa extract contains many other biomolecules like saponins, tannins and flavonoids.

**Table 3.1.** Qualitative analysis of the biomolecules in more than and less than 10kDa fraction

| | tannins | saponins | terpenoids | flavonoids | alkaloids | proteins |
|---|---|---|---|---|---|---|
| *More than 10kDa* | + | - | - | - | - | + |
| *Less than 10kDa* | + | + | + | + | - | - |

## *3.2. Purification of antilithiatic protein*

Calcium oxalate crystal growth inhibitory proteins have been proposed to play an important role in renal stone disease for several decades. While some progress has been made in the characterization of these inhibitors but the knowledge of proteins that can inhibit stone formation is limited to a relatively small number of proteins. Identification of additional stone-inhibitory proteins was hampered in the past by limitations in protein identification methods, which meant that low abundance components or novel proteins could not be identified without some prior knowledge of their involvement.

Exploratory studies using modern technologies to define novel calcium oxalate crystal growth inhibitors are therefore necessary and may lead to better understanding of the pathophysiology of nephrolithiasis.

From the results shown in section 3.1, it was inferred that *Dolichos biflorus* seeds have more than one biomolecules that showed inhibition towards calcium phosphate mineralization. The probable types of biomolecules possessing the antilithiatic properties were expected to be proteins in more than 10 kDa fraction. So, an antilithiatic protein biomolecule from the seeds of *Dolichos biflorus* was purified using conventional protein purification methods including ammonium sulfate precipitation, ion exchange chromatography and molecular sieve chromatography.

The schematic representation used for the purification of most potent antilithiatic protein is shown in figure 2.1. The fractions obtained after each step of purification were assayed for their antilithiatic properties by employing *in vitro* homogenous system of CaP mineralization and *in vitro* calcium oxalate crystal growth assay. The protein content was estimated by Lowry's method [196] and the extent of purity of the active fractions was determined by SDS-PAGE analysis.

### *3.2.1. Ammonium sulfate precipitation*

The first step carried out to purify an anticalcifying protein from *Dolichos biflorus* was the fractionation of the crude extract using ammonium sulfate precipitation. Table 3.2, illustrates the data obtained throughout the ammonium sulfate precipitation procedure which shows that the precipitates obtained between 0 to 25% saturation with ammonium sulfate and the non-precipitated fraction (>75%) have the lowest total protein content. The precipitates obtained between 25 to 50% and between 50 to 75% saturation with respect to ammonium sulfate showed the highest total protein content among the precipitated fractions (Table 3.2).

**Table 3.2.** Extent of inhibition of CaP and CaOx crystals after ammonium sulfate precipitation of *Dolichos biflorus* crude extract.

| *Precipitation range (%)* | *Total protein content* | *CaP inhibitory activity (1000µg/ml of Protein Sample)* | | *CaOx inhibitory activity (1000µg/ml of Protein Sample)* |
|---|---|---|---|---|
| | | *%age inhibition of $Ca^{+2}$ ions* | *%age inhibition of $HPO_4^{2-}$ ions* | |
| 0-25 | 17.13 mg | 52.16 ± 3.14 | 49.20 ± 21 | 55.07 ± 2.34 |
| 25-50 | 85.37 mg | 31.24 ± 1.97 | 29.27 ± 1.87 | 44.0 ± 2.07 |
| **50-75** | **96.03 mg** | **61.52 ± 4.13** | **59.64 ± 2.17** | **73 ± 5.28** |
| >75 | 47.03 mg | 21.20 ± 1.15 | 19.23 ± 1.07 | 15.07 ± .091 |

* %age inhibition of CaP and CaOx represents results as mean ± SD (n = 6).

Almost all fractions obtained after ammonium sulfate precipitation showed some extent of inhibition towards both calcium phosphate and calcium oxalate *in vitro* assay system except for the fraction obtained after >75% ammonium sulfate saturation. But the precipitates obtained between 50 and 75% saturation showed maximum inhibitory potency towards both *in vitro* assay systems (Table 3.2).

### *3.2.2. Anion exchange chromatography*

The 50-75% ammonium sulfate precipitation fraction was loaded on a Macro Prep® 25 Q Strong anion exchanger (BioRad laboratories) column to separate the proteins present in the sample on the basis of their charge. Figure 3.6 shows the elution profile of anion exchange chromatography of 50-75% ammonium sulfate precipitation fraction. The fractions obtained after anion exchange chromatography were pooled and checked for their inhibitory activity.

In figure 3.6, the blue line represents the absorbance (A.U) of proteins present in the sample and red line represents the conductivity (mS/cm). The elution profile (figure 3.6) is showing a total of nine peaks of the sample after anion exchange chromatography. The method used during anion exchange chromatography in Biologic LP system is given in Table 2.2. The fractions under each peak were pooled and checked for their inhibitory potency towards both *in vitro* assay systems. Before estimating the inhibitory potential, the protein content of each peak was made to a concentration of 1000 µg/ml to maintain the consistency for comparing the activity of each sample.

The activity of each pooled peak towards calcium crystallization was estimated by the method given in section 2.1.3 and 2.1.5. The table 3.3 is showing the percentage inhibition of CaP initial mineral phase and percentage inhibition of CaOx crystals growth. From the table it could be seen that the fractions pooled between time intervals 96-106 minutes showed maximum percentage of inhibition towards both calcium phosphate mineralization and calcium oxalate crystal growth assay system. The most active fraction showed 81.06% inhibitory activity towards CaOx and the inhibition towards calcium & phosphate ions in CaP mineral phase was 70.18% and 72.11% respectively.

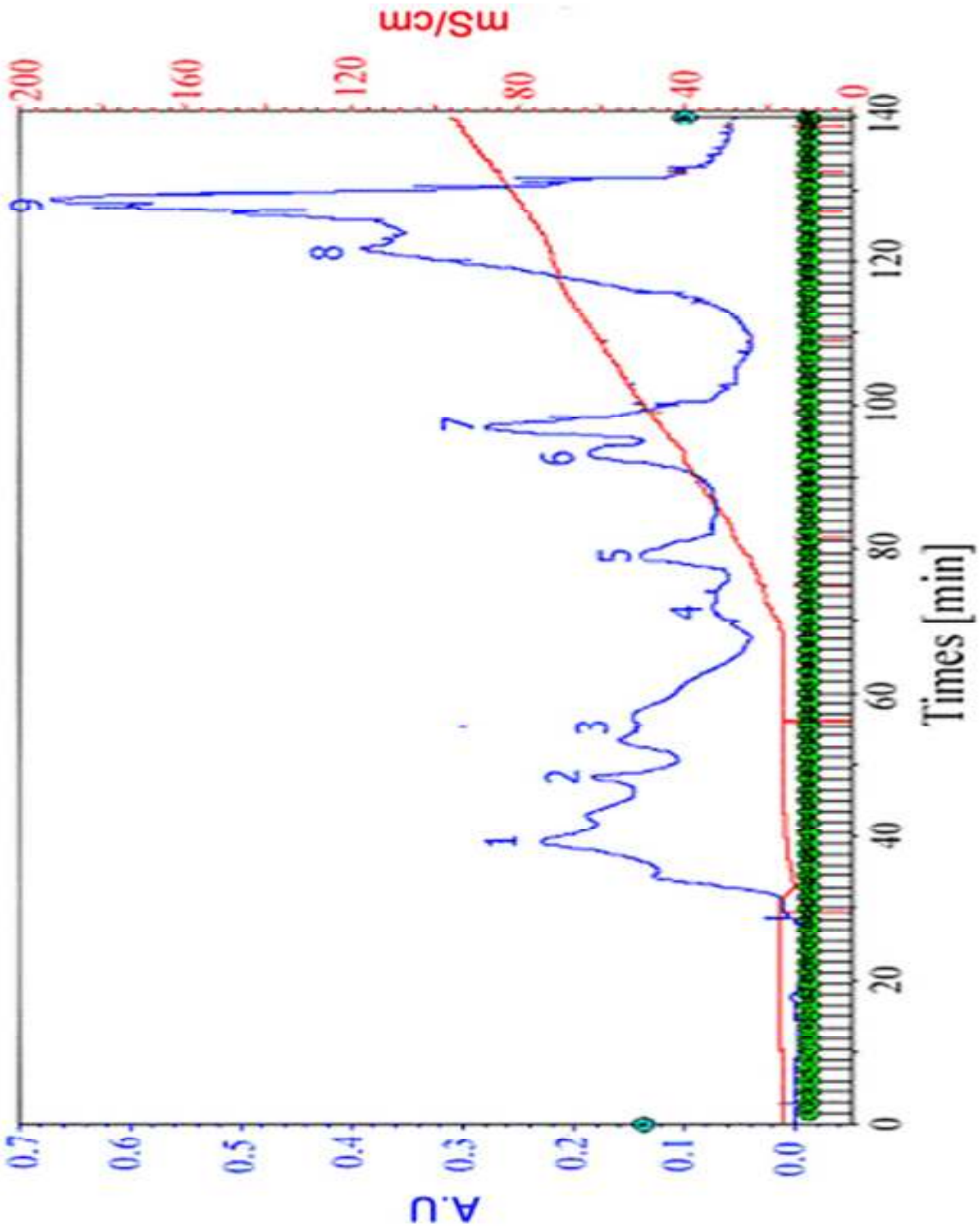


**Figure 3.6.** Elution profile of protein sample loaded on anion exchange chromatography column after ammonium sulfate precipitation. The eluting proteins were detected at 280nm. Each peak is marked consecutively as 1-9.

**Table 3.3.** Extent of CaP and CaOx inhibitory potential of fractions obtained after anion exchange chromatography.

| *Peak* | *Pooled fractions (mints)* | *Total protein content* | *CaP inhibitory activity (1000µg/ml of Protein Sample)* | | *CaOx inhibitory activity(1000µg/ml of Protein Sample)* |
|---|---|---|---|---|---|
| | | | *%age inhibition of $Ca^{+2}$ ions* | *%age inhibition of $HPO_4^{2-}$ ions* | |
| 1 | 39-44 | 9.01 mg | 21.57 ± 1.35 | 27.23 ± 1.65 | 15.29 ± 1.23 |
| 2 | 46-50 | 5.15 mg | 9.20 ± 0.75 | 11.27 ± 0.71 | 9.23 ± 0.9 |
| 3 | 55-68 | 7.23 mg | 17.16 ± 1.57 | 18.20 ± 1.25 | 13.03 ± 0.51 |
| 4 | 71-76 | 2.20 mg | 29.01 ± 2.01 | 29.85 ± 2.56 | 17.51± 2.31 |
| 5 | 78-83 | 4.23 mg | 35.27 ± 1.56 | 37.20 ± 2.35 | 21.25 ± 1.17 |
| 6 | 88-93 | 8.27 mg | 43.24 ± 2.36 | 41.14 ± 3.04 | 32.03 ± 1.91 |
| 7 | **96-106** | **16.5 mg** | **70.18 ± 4.11** | **72.11 ± 5.03** | **81.06 ± 3.11** |
| 8 | 117-122 | 18.26 mg | 42.28 ± 2.47 | 38.39 ± 1.91 | 50.32 ± 2.32 |
| 9 | 124-130 | 21.35 mg | 37.20 ± 2.61 | 33.02 ± 2.43 | 40.14 ± 2.03 |

* %age inhibition of CaP and CaOx represents results as mean ± SD (n = 6).

Since, 7th peak showed the most effective inhibition towards both CaP and CaOx assay system (Table 3.3), so it was subjected to SDS-PAGE analysis.

### *3.2.3. SDS-PAGE of 7th peak*

The SDS-PAGE analysis of the most active peak i.e peak 7th which was eluted between 96 mins to 106 mins at the conductivity of 52.50 mS/cm to 62.17 mS/cm is shown in figure 3.7. The first lane of the figure is showing the bands of 7th peak and the

second lane constitute molecular weight markers. From the SDS-PAGE analysis, the 7$^{th}$ peak is shown to have about 4 bands. Among the four bands, three are well resoluted whereas the fourth band seems to be merged or is present in a very high concentration in the fraction. Since, the four bands observed were showing marked difference in molecular weight, therefore, to further fractionate these proteins, molecular sieve chromatography was employed.

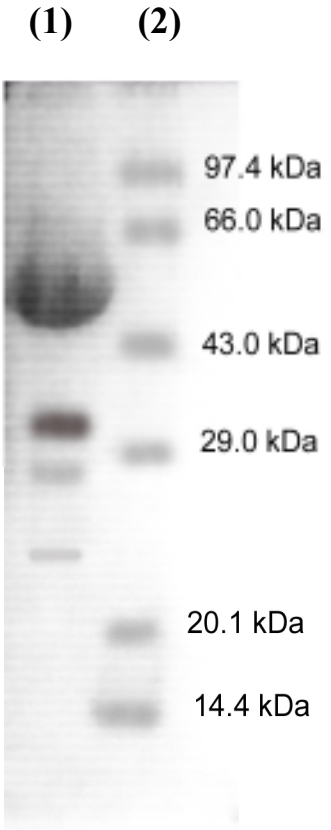


**Figure 3.7.** SDS-PAGE analysis of 7$^{th}$ peak (96-106 mins) after anion exchange chromatography.

(1) 7$^{th}$ peak (~ 20µg of protein was loaded)

(2) Molecular weight markers [molecular weight in kDa is shown on the right side of the figure]

### *3.2.4. Molecular sieve chromatography*

The pooled sample that contained the highest inhibitory activity was loaded on a Bio gel® P-100 gel (Medium, 90-180 μm) Molecular sieve support (BioRad laboratories) column in order to separate the mixture of proteins based on their molecular size. Figure 3.8 shows the elution profile of the molecular sieve chromatography. The highest peak was observed at 248.96 to 437.89mins of elution, followed by various other small peaks. The complete run of the sample in molecular sieve chromatography was till 2600 mins. During this run time a total of 8 peaks were eluted out. Each fraction was collected for 14 mins having 2 ml of fraction in it.

The peaks are numbered (as shown in figure 3.8) and the corresponding fractions were pooled as shown in table 3.4. The protein content in each pooled fraction was determined. The pooled fractions were then lyophilized after removal of salt from them. Finally, the fractions under each peak were suspended in buffer such that the final concentration of the sample is 1000 μg/ml. These fractions were then checked for their inhibitory potency towards *in vitro* CaP and CaOx assay system.

Table 3.4 is showing the percentage inhibition of CaP mineralization and CaOx crystal growth by various fractions obtained after molecular sieve chromatography. The sixth peak eluting at 1156mins to 1426mins showed highest inhibitory activity towards both *in vitro* assay systems. The inhibition by 1 mg/ml of protein by this peak was 92% for CaOx mineralization and for CaP, it showed about 86% inhibition towards $Ca^{2+}$ and 82% for $HPO_4^{2-}$ ions.

From the table 3.4, it can be seen that in addition to $6^{th}$ peak, peak 4, 5 and 7 are also showing some extent of CaP and CaOx inhibition. Extensive profiling of all these fractions with inhibitory activity against CaP and CaOx crystal growth and their characterization might throw light on current knowledge of other modulators of stone formation present in *Dolichos biflorus*.

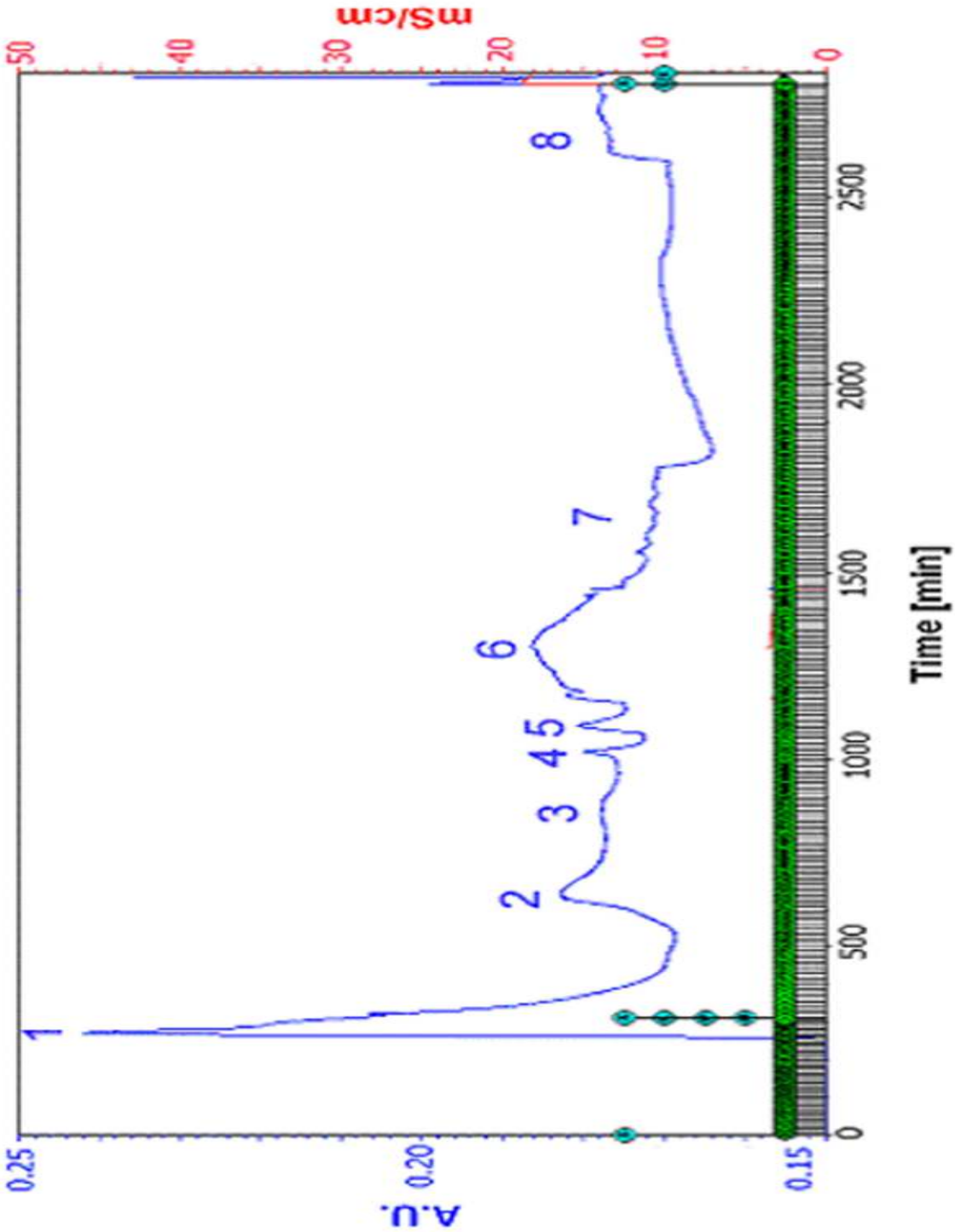


**Figure 3.8.** Elution profile of protein sample loaded on molecular sieve support after anion exchange chromatography. The eluting proteins were detected at 280nm. Each peak is marked consecutively as 1-8.

**Table 3.4.** Extent of CaP and CaOx inhibitory potential of fractions obtained after molecular sieve chromatography

| *Peak* | *Pooled fractions (mins)* | *Total protein content* | *CaP inhibitory activity (1000µg/ml of Protein Sample)* | | *CaOx inhibitory activity(1000µg/ml of Protein Sample)* |
|---|---|---|---|---|---|
| | | | *%age inhibition of $Ca^{+2}$ ions* | *%age inhibition of $HPO_4^{2-}$ ions* | |
| 1 | 248-437 | 4.27mg | 37.17 ± 2.31 | 30.20 ± 2.70 | 42.04 ± 1.21 |
| 2 | 554-740 | 0.52mg | 5.26 ± 0.31 | 7.14 ± 0.71 | 11.70 ± 0.65 |
| 3 | 781-963 | 0.12mg | 9.23 ± 0.73 | 7.24 ± 0.53 | 16.15 ± 1.03 |
| 4 | 1001-1055 | 0.17mg | 17.25 ± 1.71 | 15.26 ± 1.31 | 11.50 ± 0.97 |
| 5 | 1073-1127 | 0.19mg | 18.27 ± 2.57 | 21.32 ± 1.91 | 21.23 ± 2.14 |
| **6** | **1155-1426** | **1.47 mg** | **86.18 ± 3.71** | **82.11 ± 4.11** | **92.07 ± 3.73** |
| 7 | 1524-1776 | 0.35mg | 15.42 ± 1.31 | 18.29 ± 2.11 | 14.24 ± 2.10 |
| 8 | 2604-2767 | 0.47mg | 5.42 ± 0.71 | 3.02 ± 0.31 | 09.07 ± .47 |

* %age inhibition of CaP and CaOx represents results as mean ± SD (n = 6).

Since, the 6$^{th}$ peak showed maximum inhibitory activity towards both assay systems, so it was focused and further analyzed for purity by SDS-PAGE.

### *3.2.5. SDS-PAGE of 6$^{th}$ peak*

The protein profile of most active fraction after molecular sieve chromatography was performed using SDS-PAGE. The SDS-PAGE analysis of 6$^{th}$ peak (pooled fraction between 1155-1426 mins) showed two bands of molecular weight 58kDa and 34kDa.

Figure 3.9 shows the SDS-PAGE profile of 6$^{th}$ peak in lane 1, and molecular weight markers in lane 2.

Since, it is not anticipated that after molecular sieve chromatography, proteins of such huge difference in their molecular weight would elute together, therefore the active fraction was further tested for purity using Native-PAGE.

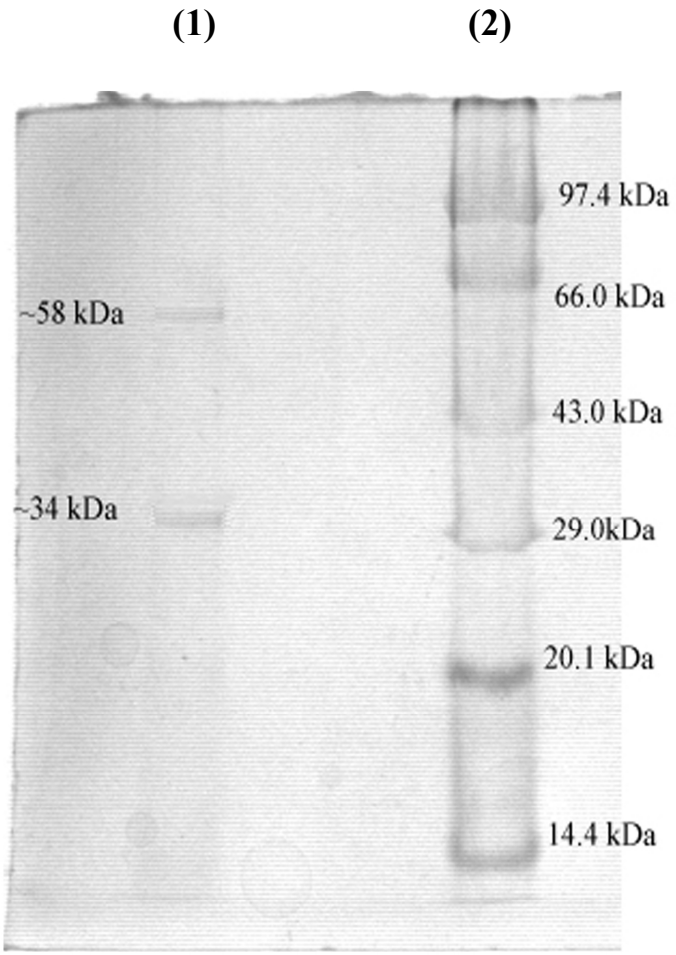


**Figure 3.9.** SDS-PAGE analysis of 6$^{th}$ peak (1155-1426 mins) pooled after molecular sieve chromatography.

(1) 6$^{th}$ peak (~ 20µg of protein was loaded)

(2) Molecular weight markers (molecular weight in kDa is shown on the right side of the figure)

**(1)**

**Figure 3.10.** Native-PAGE analysis of 6$^{th}$ peak (1155-1426 mins) pooled after molecular sieve chromatography.

(1) 6$^{th}$ peak (~ 20µg of protein was loaded)

Figure 3.10 is showing the Native-PAGE of pooled fraction under 6$^{th}$ peak. From this figure, it is clear that the fraction which showed two bands in SDS-PAGE, is showing a single band in Native-PAGE.

### *3.2.6. Purification of antilithiatic protein from the seeds of Dolichos biflorus*

The procedure used for purification of an antilithiatic protein from the seeds of *Dolichos biflorus* and the data obtained throughout the purification process are summarized in table 3.5. Finally, an antilithiatic protein was successfully purified, giving a single protein band on Native-PAGE (Figure 3.10). About 1.5 mg of antilithiatic protein was recovered from 30 gms of powdered *Dolichos biflorus* seeds, the yield (%) of this purification process was found to be 1.1.

**Table 3.5.** Summary of purification of inhibitory protein from the seeds of *D. biflorus*. %age inhibition of CaOx represents results as mean ± SD (n = 6). Data refer to the protein obtained during various stages of purification from 30gms of powdered *Dolichos biflorus* seeds.

| *Purification Steps* | *Total Protein (mg)* | *Yield (%)* | *CaP inhibitory activity (1000µg/ml of Protein)* | | *% Inhibition of CaOx by 1000µg/ml of protein sample* |
|---|---|---|---|---|---|
| | | | *%age inhibition of $Ca^{2+}$ ion* | *%age inhibition of $HPO_4^{2-}$ ions* | |
| Tris buffer extract | 137 | 100 | 41.52 ± 4.13 | 37.64 ± 2.17 | 65 ± 2.72 |
| 75 % $(NH_4)SO_4$ Precipitate | 96 | 70 | 61.52 ± 4.13 | 59.64 ± 2.17 | 73 ± 5.28 |
| Anion exchange Chromatography | 16.5 | 12 | 70.18 ± 4.11 | 72.11 ± 5.03 | 81 ± 3.11 |
| Molecular Sieve chromatography | 1.5 | 1.1 | 86.18 ± 3.71 | 82.11 ± 4.11 | 92 ± 3.73 |

## 3.3. Characterization of purified antilithiatic protein

### 3.3.1. Kinetics of inhibitory activity of Dolichos biflorus antilithiatic protein (DAP)

Figure 3.11 shows the inhibitory activity of *Dolichos biflorus* antilithiatic protein at varying concentrations of 50 µg/ml, 100 µg/ml, 200 µg/ml, 350 µg/ml and 450 µg/ml. From the figure, it can be observed that in comparison to control, the assay system having *Dolichos biflorus* antilithiatic protein (DAP) depicts significant inhibition of CaOx crystal growth from five minutes of incubation to one hour.

The figure clearly shows that, as time progressed, initially the oxalate concentration in assay system decreased linearly and then finally it became constant. Thus indicating that initially the rate of inhibition was dependant on DAP concentration and after long duration a constant rate of inhibition was achieved. The DAP was found to be effective even at a low concentration of 50 µg/ml.

On evaluating inhibitory potency of isolated protein on calcium phosphate mineralization, using similar concentrations of protein (50, 100, 200, 350 and 450 µg/ml), again an increase in percentage inhibition of both calcium and phosphate ions was observed as shown in figure 3.12. DAP was found to inhibit the initiation of CaP mineralization by decreasing both $Ca^{2+}$ and $HPO_4^{2-}$ ions by 8% and 12% respectively at very low concentration (50 µg/ml) and it showed inhibition towards CaP mineralization in a concentration-dependent manner.

From the figure 3.11 and 3.12, it can be inferred that with increase in concentration of DAP, its inhibitory potential increases and DAP is effective *in vitro* on both CaP and CaOx crystallization at as low as 50 µg/ml. In addition, the inhibition of both assay systems showed a similar trend i.e. the inhibition was found to increase in a concentration-dependent manner.

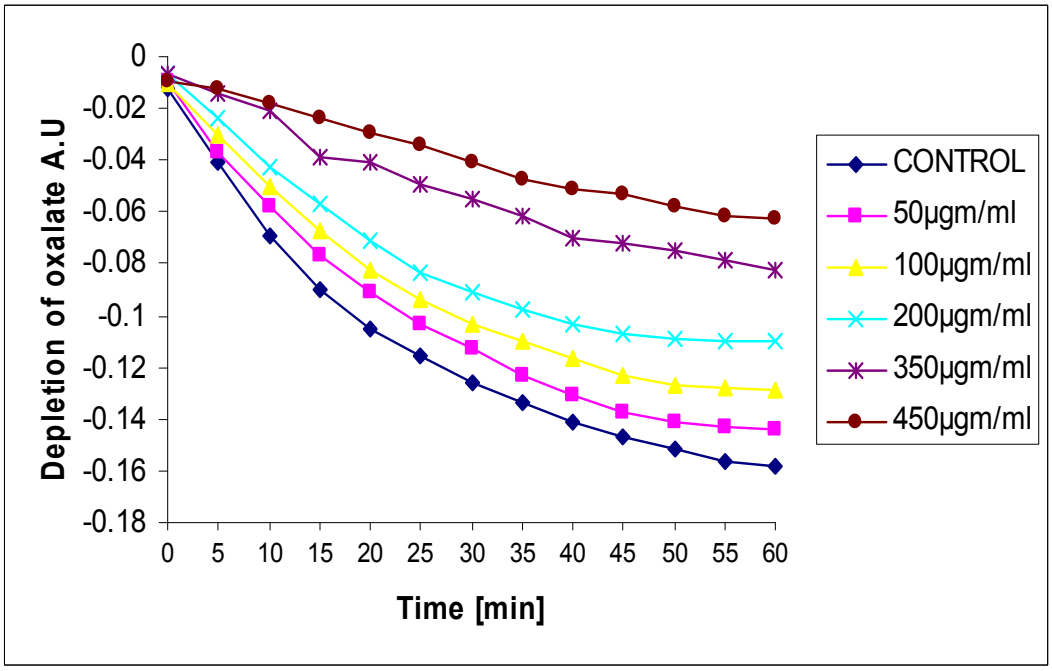


**Figure 3.11.** The inhibitory activity of *Dolichos biflorus* antilithiatic protein (DAP) at 50, 100, 200, 350 and 450 µg/ml.

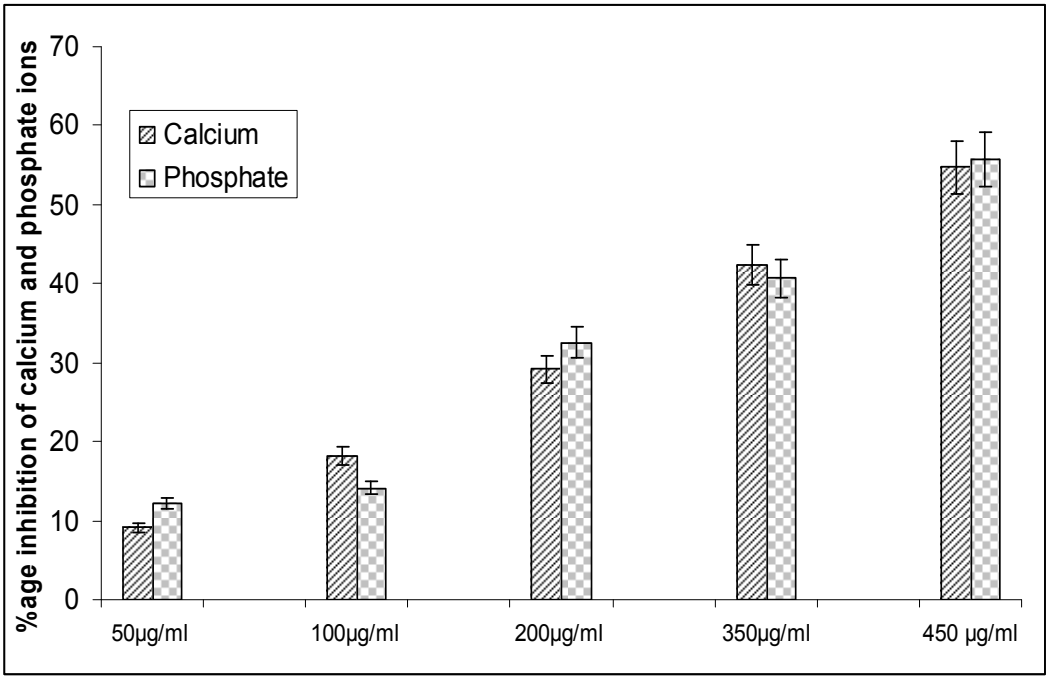


**Figure 3.12.** Percentage inhibition of calcium & phosphate ions by DAP at 50, 100, 200, 350 and 450 µg/ml of concentration.

### *3.3.2. Molecular weight determination*

The molecular weight of *Dolichos biflorus* antilithiatic protein is shown in figure 3.13. The log of molecular mass of standard proteins viz. carbonic anhydrase 29kDa; bovine serum albumin 68kDa; alcohol dehydrogenase 150kDa, was calculated to be 4.46, 4.83 and 5.17 respectively. On plotting the retention time of these standard proteins with respect to their log of molecular mass, a straight line was procured as shown in fig 3.13. The retention time of the *Dolichos biflorus* antilithiatic protein was 17.3. On extraplotting this retention time on y-axis of the graph, the molecular mass of the purified protein was calculated to be 98kDa.

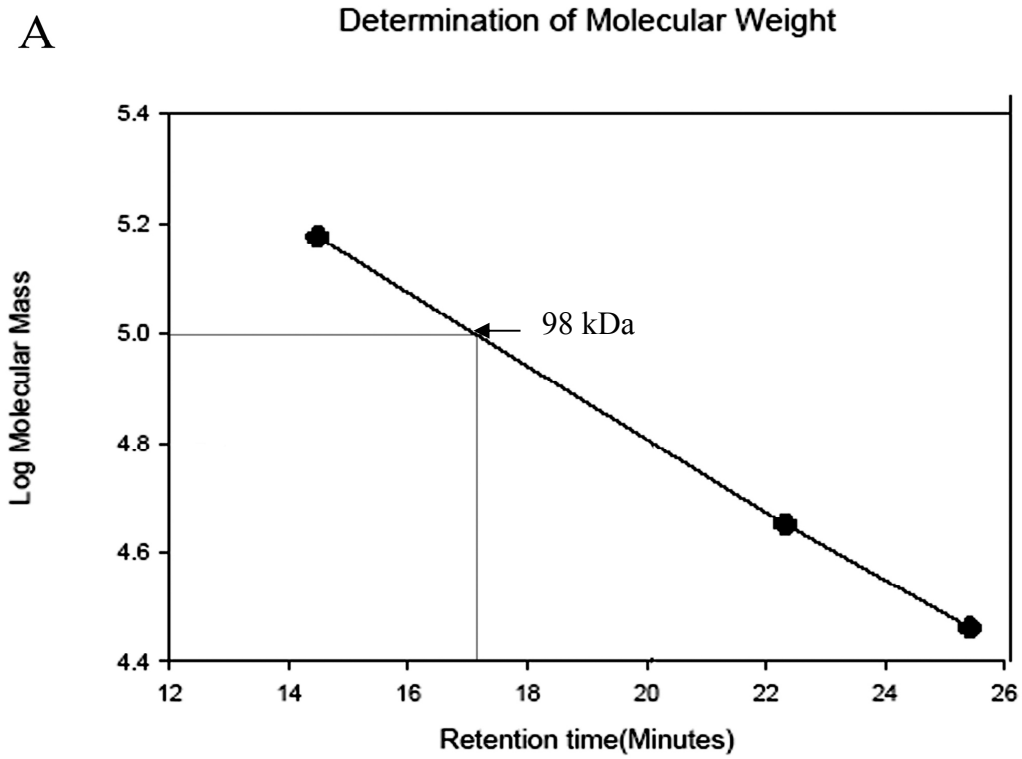


**Figure 3.13.** Determination of molecular mass of *Dolichos biflorus* antilithiatic protein (DAP) by using size exclusion HPLC. The molecular mass markers were in the range of 29 kDa-150 kDa. The graph represents standard curve and the mass of DAP is marked on the standard curve as 98 kDa.

### *3.3.3. Isoelectric point determination*

The isoelectric point of the purified protein was evaluated by the method of Yang & Langer [198]. Figure 3.14 shows the graph plotted between the pH of cationic resins and the absorbance of the supernatant representing unbound protein at the specific pH. The values of higher and lower plateau (as shown in the figure 3.14) are 0.682 and 0.021 respectively. From the straight line equation the slope (m) and Y-intercept (b) of straight line was calculated to be 0.5366 and -2.219 respectively,

Taking the values of higher & lower plateau and the values of m and b, the isoelectric point of protein was calculated as follows:

$$pI=1/0.5366\ [\{(0.021 + 0.682)/2\}+2.219] = 4.79$$

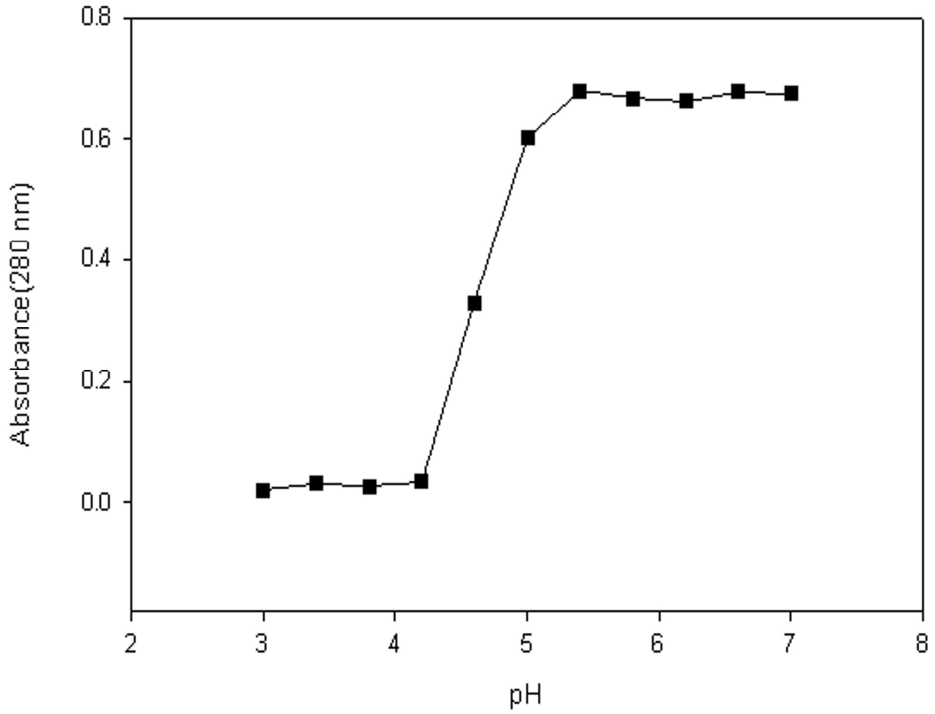


**Figure 3.14.** Determination of isoelectric point of *Dolichos biflorus* antilithiatic protein.

### *3.3.4. Total amino acid composition of Dolichos biflorus antilithiatic protein (DAP)*

The total amino acid analysis of DAP was done by using HPLC based method of Elkin & Wasynczuk [199]. The acid hydrolysis of DAP resulted in disintegration of the protein into free amino acids. These free amino acids on analysis by HPLC using a silica based column, gave peaks corresponding to their elution time. The peaks were identified using elution time with standards of every amino acid and the area under each peak gave the corresponding concentration of that amino acid in the acid hydrolyzate of DAP protein.

Figure 3.15 shows the elution profile of acid hydrolyzate of DAP protein after HPLC. In the figure, each peak is representing elution of a particular amino acid. The amino acids and their corresponding elution time is depicted over each peak in the figure. From the figure, it can be seen that there is no peak corresponding to amino acid tryptophan, this is because tryptophan is completely destroyed after acid hydrolysis of protein. Additionally, the glutamine and asparagine are converted into glutamic acid and aspartic acid respectively, so they appear as a single peak after elution.

The amino acid composition of DAP is shown in table 3.6. Acidic amino acids like aspartic acid (12.70%) and glutamic acid (12.69%) were found to be present in maximum amount in DAP protein. Among basic amino acids, lysine was present in good amount (10.15%) where as another basic amino acid arginine was just 0.63% of the total amino acids. Other than acidic amino acids, polar amino acid like serine was also present in adequate amount in DAP, it constituted about 8.74% of the total amino acids and tyrosine was 7.82%. The aliphatic amino acids were also present in DAP but in less amount. The content of amino acids viz. alanine, leucine, isoleucine and valine were 2.49 %, 5.91 %, 1.17 % and 3.97% respectively in the DAP.

The amino acid composition data and the isoelectric point of DAP, clearly shows that DAP has a higher content of acidic amino acids and consequently has negative charge at pH 7 which is in conformity with its pI ( 4.79).

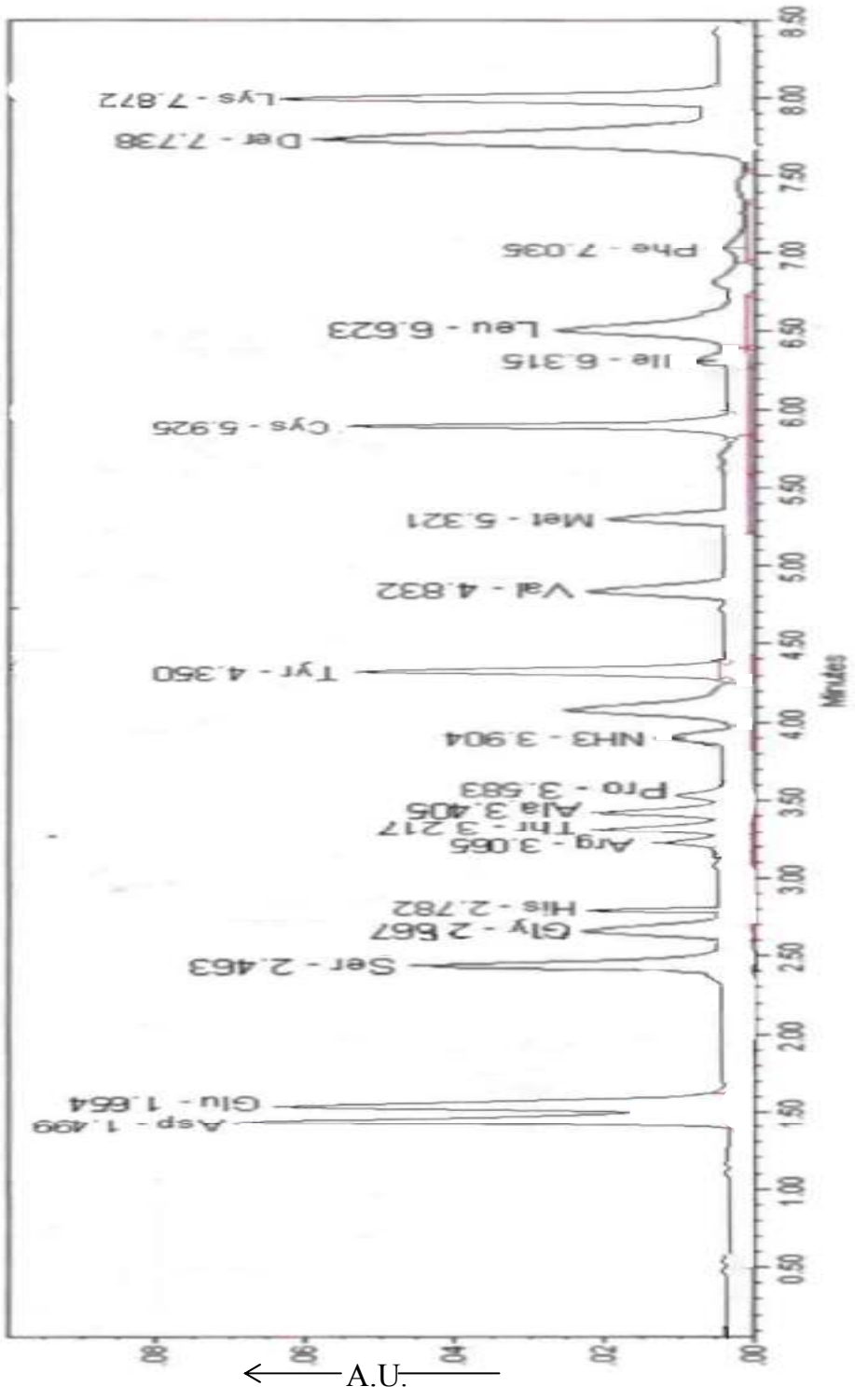


**Figure 3.15**. HPLC profile of amino acid analysis

**Table 3.6.** Amino acid composition of *Dolichos biflorus* antilithiatic protein (DAP)

| Amino Acids | % of Amino acid |
|---|---|
| Alanine (Ala) | 2.49 |
| Arginine (Arg) | 0.63 |
| Aspartic acid (Asp)* | 12.70 |
| Cysteine (Cys) | 7.72 |
| Glutamic acid (Glu)** | 12.69 |
| Glycine (Gly) | 3.99 |
| Histidine (His) | 1.65 |
| Isoleucine (Ile) | 1.17 |
| Leucine (Leu) | 5.91 |
| Lysine (Lys) | 10.15 |
| Methionine (Met) | 3.15 |
| Phenylalanine(Phe) | 2.77 |
| Proline (Pro) | 1.62 |
| Serine (Ser) | 8.74 |
| Threonine (Thr) | 2.50 |
| Tryptophan (Trp) | - |
| Tyrosine (Tyr) | 7.82 |
| Valine (Val) | 3.97 |

* include both aspartic acid and asparagine

** include both glutamic acid and glutamine

### *3.3.5. Peptide mass fingerprinting*

The trypsin digested DAP was loaded over MALDI-TOF MS for peptide mass fingerprinting. Figure 3.16 shows the peptide profile of DAP after trypsin digestion. MALDI TOF MS segregate the peptides on the basis of their mass to charge ratio. As a result each peptide moves with different speed in the analyzer and depending on their time of flight, the peptides reach at different times to the detector. Thus, with MALDI TOF MS we can detect the number of peptides and their m/z ratios. In figure 3.16, various peaks are shown with their corresponding m/z ratios.

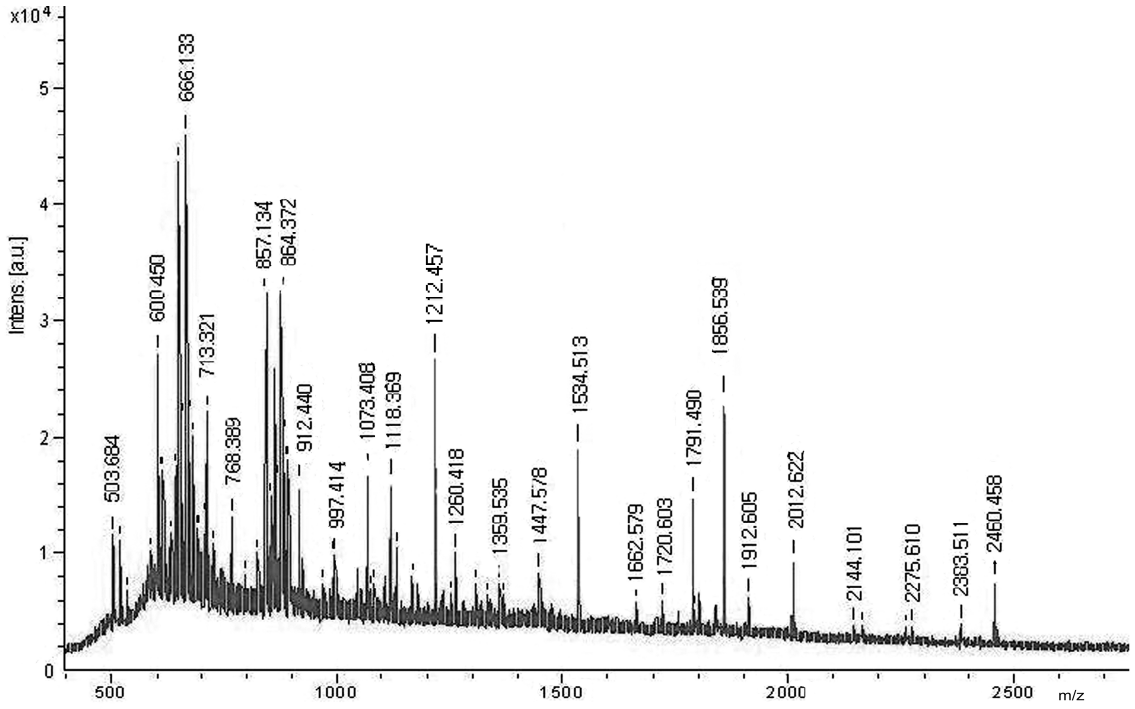


**Figure 3.16.** MALDI-TOF MS data obtained from DAP**.**

### *3.3.6. Peptide matching*

The m/z ratio of all peptides as observed by MALDI TOF MS, were loaded in mascot search engine. Mascot search engine compares the m/z ratios of all proteins in the data base, if they were digested with trypsin with the test m/z ratios. The parameters selected for mascot search are given in chapter 2, section 2.3.7. Figure 3.17 presents the

results obtained after Mascot search. The m/z ratios of DAP after searching with Mascot search engine showed the maximum similarity with calnexin protein of *Pisum sativum*. The match showed sequence coverage of 35% of DAP with calnexin of *Pisum sativum.*

# Mascot Search Results

Match to: **CALX_PEA** Score: **57** Expect: **8.6**
**Calnexin homolog precursor - Pisum sativum (Garden pea)**

Nominal mass ($M_r$): **62721**; Calculated pI value: **4.84**
NCBI BLAST search of CALX_PEA against nr
Unformatted sequence string for pasting into other applications

Taxonomy: Pisum sativum

Fixed modifications: Carbamidomethyl (C)
Variable modifications: Oxidation (M)
Cleavage by Trypsin: cuts C-term side of KR unless next residue is P
Number of mass values searched: **64**
Number of mass values matched: **33**
Sequence Coverage: **35%**

Matched peptides shown in **Bold Red**

```
  1 MVDRKEIPLA MGLLAVLLFF VASSSSFHLV RASDEVDDAI FYESFDEDFD
 51 NRWIVSGKEE YNGVWKHSKS EGHDDFGLLV SEPARKYAIV KELDAPVSLK
101 DGTVVLQFET RLQNGLECGG AYIKYLQTQE SGWKPKGFDN ESGYSIMFGP
151 DRCGATNKVH FIFRHKNPKT GKHVEHHLKF PPSVPSDKLS HVYTAVLKDD
201 NEVSILIDGE EKKKANFLSS EDFEPALIPS KTIPDPDDKK PEDWDERAKI
251 PDPEAVKPED WDEDAPREII DEEAEKPEPW LDHEPEVDDP EAKPEDWDDE
301 EDGEWEAPKI ENPKCEAAPG CGEWKRPTKS NPAYKGKWSA PYIDNPNYKG
351 IWKPQEIPNP EYFELEKPDF EPIAAIGIEI WTMQDGILFD NVLIAKDDKI
401 AESYRETTWK PKFNIEKEKQ KHEEEAAAAA AARSESEGIA GIQKKAFDLL
451 YKIADIAFLS GQKEKIIEII EKGEKQPNLT IGIIVSVVIV FVSIFFRLIF
501 GGKKPANVEA NVEKKKTNTE TTSKQDGGEK EDNKEKEETA NPPRRRPKRD
551 N
```

**Figure 3.17**. Using MASCOT search engine (www.matrixscience.com), peptide masses from DAP showed 35 % sequence similarity with calnexin protein

## *3.4. In-silico study on interaction of antilithiatic proteins with COM*

The matrix displays a variable and complex composition and a few proteins of matrix are common in various stones. It may act as a catalyst to induce mineral phase formation from metastable solutions or the biomolecules associated with the matrix may control mineralization by acting as inhibitors/stimulators. Various kidney stone inhibitory proteins are isolated from this organic matrix of kidney stones. These kidney stone inhibitory proteins may keep the crystals from aggregating or accumulating as additional layers and thus prevent their growth.

A growing body of evidence has linked a molecular feature of the proteins associated with mineralization, an abundance of carboxylate groups, to the modulation of biomineralization [215]. Many proteins that modulate the mineralization of calcium crystals in a variety of organisms have an abundance of aspartic acid residues [215]. Whether a protein or other macromolecule acts as an inhibitor of growth and aggregation or a promoter of nucleation and aggregation implies that there must be some mechanism to explain the interaction with the calcium oxalate surfaces. The attraction between calcium and amino acids is certainly plausible. Computer-based molecular modeling is required to determine the precise basis for the differences in the strength of such interaction [216].

The computational modeling helps to drive this evolution by providing a quantitative basis for new insights. In the following results, the interaction of COM with kidney stone inhibitory protein viz. bikunin, osteonectin, urinary prothrombin (prothrombin fragment 1), CD59, and MAp19 is depicted. The main focus of the present study is to investigate how well various active binding sites of these proteins interact with COM crystals (most prominent in kidney stones).

### *3.4.1. Structure of active binding sites*

On using MOE Site finder to depict active binding sites, each protein showed more than four such active binding sites and they were named arbitrarily. After their

energy minimization, these active binding sites were then proceeded for docking with COM unit cell to explore their mode of interactions.

### *3.4.2. Docking score and free energy of binding*

Table 3.7 represents docking score and the free energy of binding of those active binding sites which showed negative free energy of binding on interaction with COM as well as the amino acid sequence of binding sites.

**Table 3.7.** The docking score and estimated free energy of binding ($\Delta G_{binding}$) of functional motifs (from MOE site finder) with the unit cell of COM.

| | Protein | Active binding site | Sequence of active binding sites | Docking score (kcal/mol) | $\Delta G_{binding}$ (kcal/mol) |
|---|---|---|---|---|---|
| 1 | Bikunin | Bikunin-1 | YACETEYGCQG | -45.863 | -27.496 |
| | | Bikunin-2 | FGKCERCGV | -31.230 | -27.123 |
| 2 | CD59 | CD59-1 | YADCKNNFNE | -115.110 | -26.898 |
| | | CD59-2 | NFKCW | 467.665 | -1.531 |
| | | CD59-3 | KAGQENELT | 581.227 | -2.6 |
| 3 | MAp19 | Map-1 | YFTHFDQAPGKHH CHRA | -147.063 | -25.193 |
| | | Map-2 | YFTHFDQESPGKD HCHR | -212.368 | -26.46 |
| | | Map-3 | LELGQTEKF | 1053.544 | -14.28 |
| 4 | Osteonectin | Osteonectin-1 | FDIDGLKVI | 818.686 | -17.573 |
| | | Osteonectin-2 | RDWNAGDHLP | 48.608 | -24.937 |
| 5 | Urinary prothrombin | Uripro-1 | ANKGFLXXVRKG NLXRXCLXXPCSR XX | 47.726 | -27.22 |

The negative score of free energy of binding ($\Delta G_{binding}$) determines strong interaction of COM with the active binding site of the protein. The active binding sites which showed positive $\Delta G_{binding}$ are not included in the table 3.7. We observed that there is one or more than one binding site in each inhibitory protein that efficiently binds to COM (Table 3.7). Both active binding sites of bikunin and urinary prothrombin are showing the strongest interaction with COM crystal.

The amino acid marked as X in the binding site Uripro-1 of urinary prothrombin is the modified amino acid gamma carboxy glutamic acid which is abbreviated as CGU. The active binding site Uripro-1 of urinary prothrombin is the Gla binding domain of this protein identified by MOE site finder.

It is also observed that almost all sequences of active binding sites which showed negative $\Delta G_{binding}$ have one or more acidic amino acids in their sequences. Although increased number of acidic amino acids in a sequence have no influence on the $\Delta G_{binding}$, like Bikunin-2 (FGKCERCGV) active binding site have one acidic amino acid i.e Glu shows $\Delta G_{binding}$ to be -27.123 kcal/mol, whereas CD59-1 (YADCKNNFNE) active binding site have two acidic amino acids i.e Glu and Asp but still its $\Delta G_{binding}$ was calculated to be -26.898 kcal/mol, which is lower than Bikunin-2 active binding site.

### *3.4.3. LIGPLOT analysis*

Table 3.8 shows the amino acids of those active binding sites of the inhibitory proteins which showed minimum free energy of binding ($\Delta G_{binding}$) involved in hydrogen bonding and hydrophobic interactions with COM crystal. Table 3.8 also shows that calcium atom available at the growing sites of COM crystal is mainly forming hydrogen bonds with active site amino acids. On the other hand oxalate group of COM is involved in hydrophobic interaction with the active site amino acids.

**Table 3.8.** Geometry of hydrogen bonds and hydrophobic interaction of functional motifs (from MOE site finder) showing negative free energy of binding ($\Delta G_{binding}$).

| Hydrogen donar group (HD) | Hydrogen acceptor (A) | Distance (Å) | COM | Protein receptor | Distance (Å) |
|---|---|---|---|---|---|
| Bikunin (bikunin-1) | | | | | |
| 50 Ca | GLU A 69 OE1 | 2.89 | 54 C1 | GLU A 52 CB | 3.30 |
| | | | 54 C1 | GLU A 52 CA | 3.65 |
| Bikunin (bikunin-2) | | | | | |
| 48 Ca | GLY A 133 O | 2.03 | 53 C1 | VAL A 134 C | 3.79 |
| 48 Ca | ARG A 129 O | 2.47 | 53 C1 | ARG A 129 CD | 3.28 |
| | | | 53 C1 | ARG A 129 CG | 2.88 |
| | | | 16 C2 | ARG A 129 CG | 3.53 |
| | | | 53 C1 | ARG A 129 CB | 2.85 |
| | | | 53 C1 | ARG A 129 CB | 3.68 |
| | | | 53 C1 | PHE A 100 CE2 | 3.24 |
| CD59 (CD59-1) | | | | | |
| | | | 53 C1 | GLU A 73 CD | 2.61 |
| | | | 16 C2 | GLU A 73 CD | 3.34 |
| | | | 53 C1 | GLU A 73 CG | 2.79 |
| | | | 16 C2 | GLU A 73 CG | 3.06 |
| | | | 53 C1 | TYR A 4 CE1 | 3.44 |
| | | | 16 C2 | TYR A 4 CE1 | 3.58 |
| | | | 53 C1 | TYR A 4 CD1 | 2.75 |
| | | | 16 C2 | TYR A 4 CD1 | 3.40 |
| | | | 53 C1 | TYR A 4 CG | 3.07 |
| | | | 16 C2 | TYR A 4 CG | 3.88 |
| | | | 53 C1 | TYR A 4 CB | 3.41 |
| MAp19 (Map-1) | | | | | |
| 44 Ca | HIS A 140 ND1 | 2.98 | 63 C2 | HIS A 140 CE1 | 2.93 |
| | | | 3 C1 | HISA 140 CE1 | 3.45 |
| | | | 54 C1 | GLY B 87 C | 3.82 |
| | | | 64 C2 | ALA B 85 CB | 3.63 |
| | | | 24 C1 | GLN B 77 CG | 3.84 |
| | | | 64 C2 | GLN B 77 CB | 3.66 |
| | | | 24 C1 | GLN B 77 CB | 3.82 |
| | | | 64 C2 | GLN B 77 C | 3.72 |
| MAp19 (Map-2) | | | | | |
| 49 Ca | GLU A 78 OE1 | 2.58 | 5 C4 | HIS B 140 CG | 3.65 |
| 49 Ca | GLU A 78 0 | 2.30 | 5 C4 | HIS B 140 CB | 3.68 |
| 48 Ca | GLN A 77 OE1 | 3.33 | 63 C2 | LYS A 88 CE | 3.26 |
| | | | 3 C1 | LYS A 88 CE | 3.04 |
| | | | 63 C2 | LYS A 88 CD | 3.66 |
| | | | 4 C3 | LYS A 88 CD | 3.41 |
| | | | 3 C1 | LYS A 88 CD | 3.01 |
| | | | 4 C3 | LYS A 88 CG | 3.79 |
| | | | 53 C1 | GLU A 78 C | 3.32 |
| | | | 53 C1 | HIS A 48 CE1 | 3.89 |

**Table 3.8.** Continue…….

| Hydrogen bonding | | | Hydrophobic interaction | | |
|---|---|---|---|---|---|
| Hydrogen donar group (HD) | Hydrogen acceptor (A) | Distance (Å) | COM | Protein receptor | Distance (Å) |
| MAp19 (Map-3) | | | | | |
| | | | 26 C4 | PHE A 112 CZ | 3.46 |
| | | | 25 C3 | PHE A 112 CZ | 3.55 |
| | | | 26 C4 | PHE A 112 CE2 | 3.41 |
| | | | 63 C2 | GLU 109 CD | 3.86 |
| | | | 3 C1 | GLU 109 CD | 3.89 |
| Osteonectin (osteonectin-1) | | | | | |
| 48 Ca | PHE A 218 O | 3.32 | 53 C1 | ILE A 286 CD1 | 2.28 |
| | | | 16 C2 | ILE A 286 CD1 | 2.77 |
| | | | 53 C1 | ILE A 286 CG1 | 2.47 |
| | | | 16 C2 | ILE A 286 CG1 | 2.68 |
| | | | 53 C1 | ASP A 222 CG | 3.34 |
| | | | 53 C1 | ASP A 222 CB | 3.76 |
| Osteonectin (osteonectin-2) | | | | | |
| 48 Ca | PHE A 218 O | 3.32 | 53 C1 | ILE A 286 CD1 | 2.28 |
| | | | 16 C2 | ILE A 286 CD1 | 2.77 |
| | | | 53 C1 | ILE A 286 CG1 | 2.47 |
| | | | 16 C2 | ILE A 286 CG1 | 2.68 |
| | | | 53 C1 | ASP A 222 CG | 3.34 |
| | | | 53 C1 | ASP A 222 CB | 3.76 |
| Urinary prothrombin (uripro-1) | | | | | |
| 47 Ca | CGU A 7 OE1 | 3.31 | 53 C1 | CGU A 15 CD1 | 2.79 |
| 52 Ca | VAL A 9 O | 2.81 | 53 C1 | CGU A 15 CG | 3.74 |
| 50 Ca | SER A 24 OG | 2.46 | 53 C1 | CGU A 15 CB | 3.77 |
| | | | 53 C1 | CGU A 15 CA | 3.12 |
| | | | 17 C2 | CGU A 15 CD1 | 3.30 |
| | | | 54 C1 | ASN A 2 CG | 3.72 |
| | | | 37 C2 | ASN A 2 CG | 3.81 |
| | | | 63 C1 | ASN A 2 CB | 3.84 |
| | | | 63 C2 | ASN A 2 C | 3.86 |

From the table it could be seen that not only hydrogen bonding favors strong interaction of proteins with COM crystals, but purely hydrophobic interactions may also cause strong interaction of active binding site with COM crystal as is shown by active binding site CD59-1 of protein CD59. It shows the interactions of oxalate group of COM with amino acids glutamate and tyrosine in its active site. It is also certain that hydrogen bonding of calcium is always with a negatively charged oxygen atom of amino acids and the distance of hydrogen bond between calcium and oxygen is responsible for strong interaction of COM with that protein.

Bikunin-2 is also possessing comparable strong interactions with COM unit cell. Its Arg (basic amino acid) at position 129 is involved in both hydrogen bonding and hydrophobic interactions. Although Val and Phe are also involved in hydrophobic interactions as shown by LIGPLOT analysis, but still Arg at position 129 is forming the strongest interactions since its bond length is less i.e about 2.88 Å and 2.85 Å.

CD59-1 active binding site of CD59 has showed maximum attraction towards COM in comparison to its other active binding sites screened by MOE site finder. Although CD59-1 have Glu and Asp in its active binding site, yet only Glu showed hydrophobic interactions with COM and Asp is not at all involved (Table 3.8).

In case of Map-1, calcium ion is forming hydrogen bond with His at position 140 and the bonding is strong with the distance of about 2.98 Å. The hydrogen bonding by His is between $N^{\delta}$ of His and calcium at growing site in COM. His 140 of Map-1 is also involved hydrophobic interactions between its $C^{\varepsilon}$ and carbon of oxalate group of COM. The hydrophobic interactions by His 140 with COM are strongest in comparison to other amino acids involved in hydrophobic binding.

Figure 3.18 represents the interaction of amino acids of active binding site bikunin-1 with COM unit cell. From the figure can be seen clearly that Glu at $69^{th}$ position of this site is involved in hydrogen bonding with calcium through atom $O^{\varepsilon}$ and the calcium ion with which it is interacting is present at the growth sites of the COM crystal.

Alternatively, Glu at position 52 is involved in hydrophobic interactions with carbon atom (C1) of oxalate group in COM (Table 3.8). The $C^{\alpha}$ and $C^{\beta}$ of Glu 52, are involved in forming hydrophobic interactions with carbon atom of oxalate group of COM at position 54. The key representing the color of hydrogen bond (green dashed) and hydrophobic interactions (red radiating arc) is represented in figure 3.18. Calcium atoms are represented by green color, carbon by black and oxygen by red color.

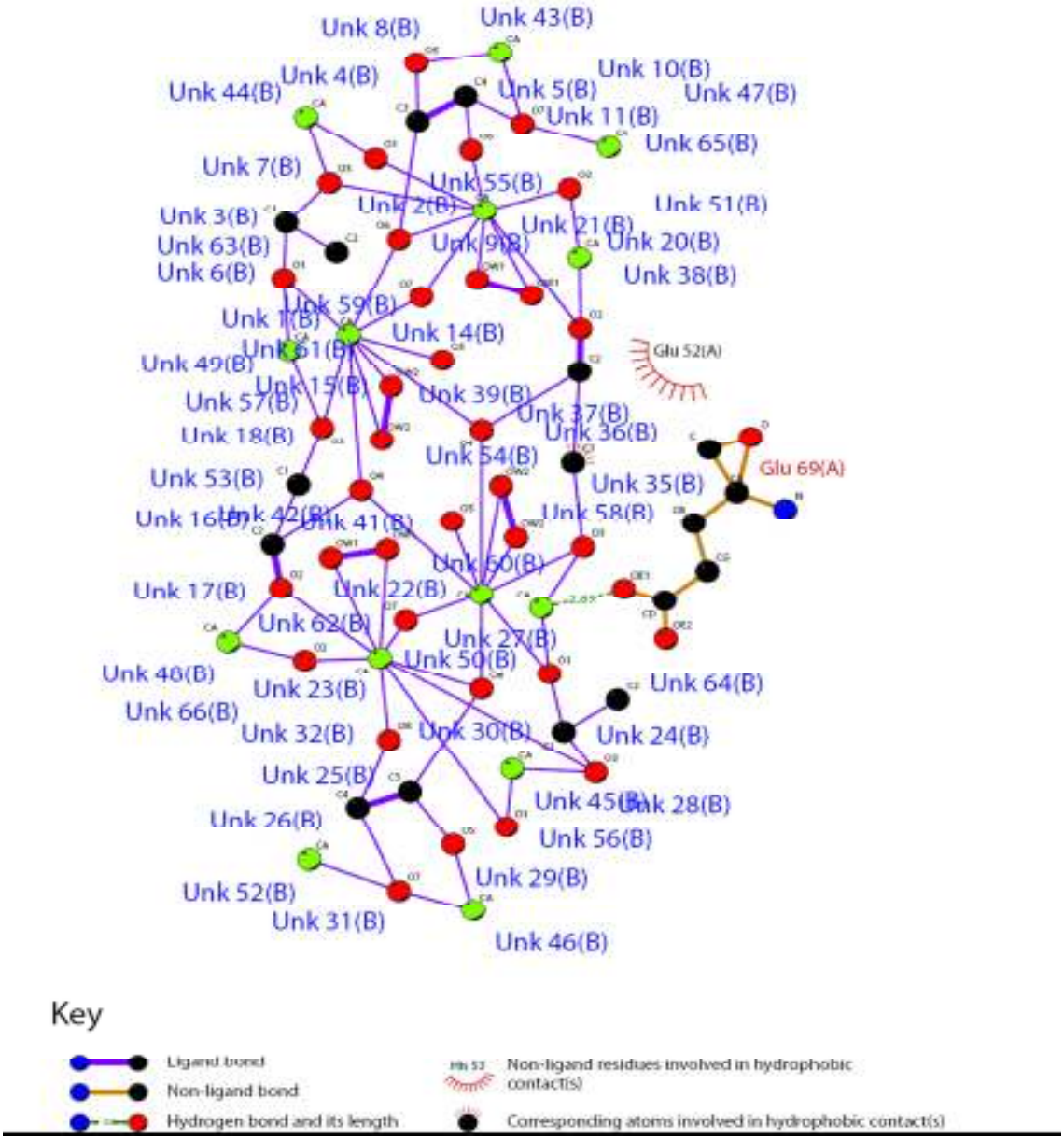


**Figure 3.18.** Two dimensional representations of the interactions observed between COM unit cell and active binding site bikunin-1 of protein bikunin. Dashed lines denote hydrogen bonds, and numbers indicate hydrogen bond lengths in Å. Hydrophobic interactions are shown as arcs with radial spokes. The figure was made using LIGPLOT.

Active binding sites of MAp19 identified by MOE site finder showed that out of all identified sites, Map-2 binding with COM unit cell is strongest followed by Map-1 and Map-3. Map-1 and Map-2 sites have quite similar sequences except for Glu and Asp present in Map-2 instead of Ala and His in Map-1. It is further observed that Glu of Map-2 is involved in hydrogen bonding with CA of COM. Although Map-3 active binding sites possess Glu in its sequence, still its Glu is not involved in hydrogen bonding, instead it is showing moderate hydrophobic interactions.

Figure 3.19 is showing the interactions of Map-2 with COM crystal. In the figure it can be seen that $O^{\varepsilon}$ of Glu at position 78 is forming strong bond with calcium ion at 49 of COM crystal. Similarly $O^{\varepsilon}$ of Gln at position 77 is also forming strong bond with calcium ion at 48 of COM crystal. Glu at position 78 is involved in forming two bonds with same calcium ion at position 49 in COM crystal. The strongest hydrogen bonding is shown by Glu at position 78 between its primary oxygen and calcium at 49 of COM, the distance of this bonding is 2.30Å as shown in figure 3.19.

In case of hydrophobic interactions between COM and amino acids in the active site of Map-2, basic amino acid Lys is found to actively participate in interacting with carbon of oxalate group in COM crystal. The carbon atoms of Lys at position 88 i.e $C^{\varepsilon}$, $C^{\delta}$ and $C^{\gamma}$ are actively involved in forming strong interactions with oxalate group of COM. In addition to Lys, His and Glu are also showing hydrophobic interactions with oxalate group of COM.

From the table 3.8, it is clearly depicted that Glu at position 78 of Map-2 is forming both hydrogen bonding as well as hydrophobic interactions with COM crystals. The Glu at position 78 of Map-2 active site is forming hydrophobic interactions with carbon at position 51 of COM.

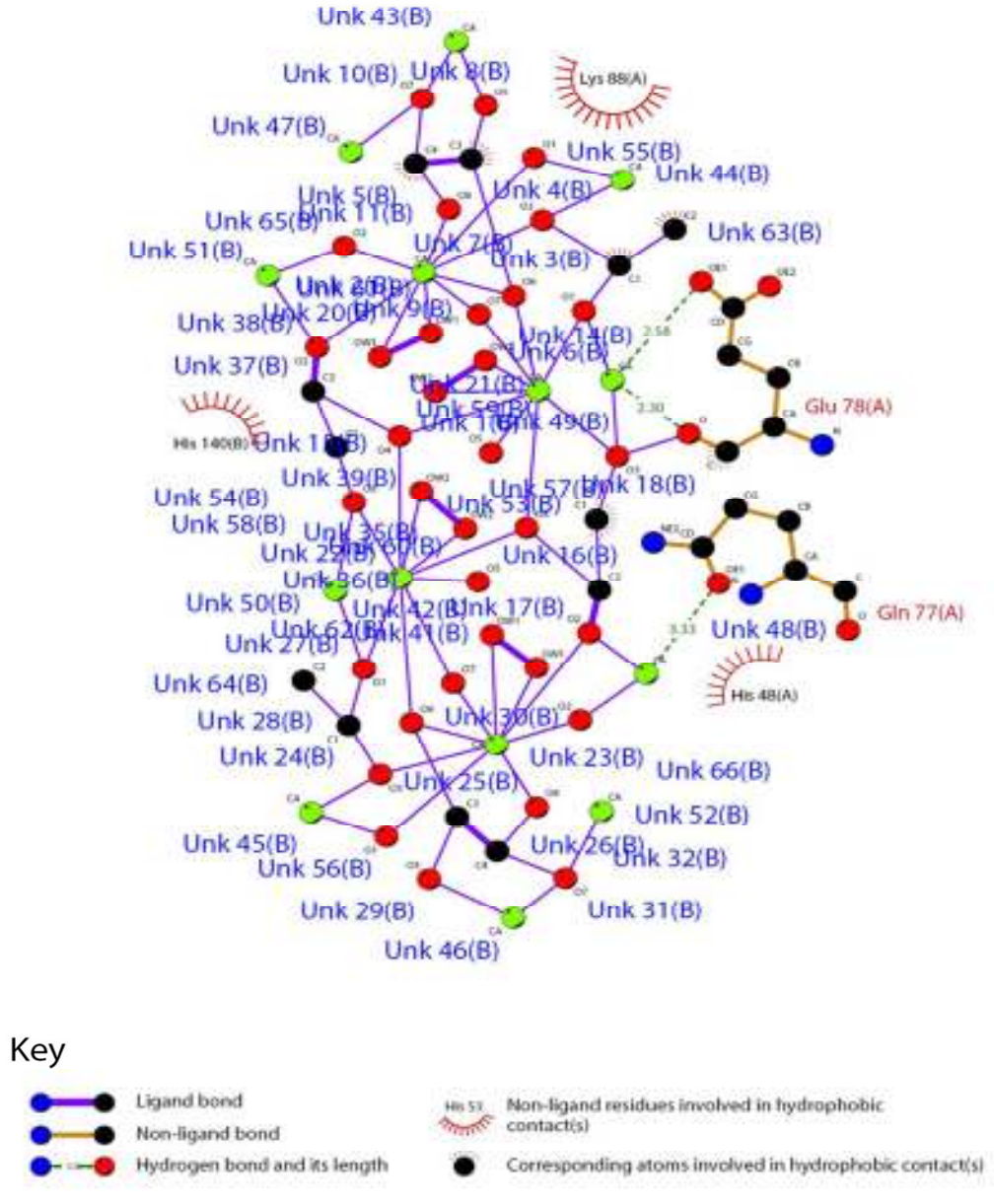


**Figure 3.19.** Two dimensional representations of the interactions observed between COM unit cell and active binding site Map-2 of MAp19. Dashed lines denote hydrogen bonds, and numbers indicate hydrogen bond lengths in Å. Hydrophobic interactions are shown as arcs with radial spokes. The figure was made using LIGPLOT.

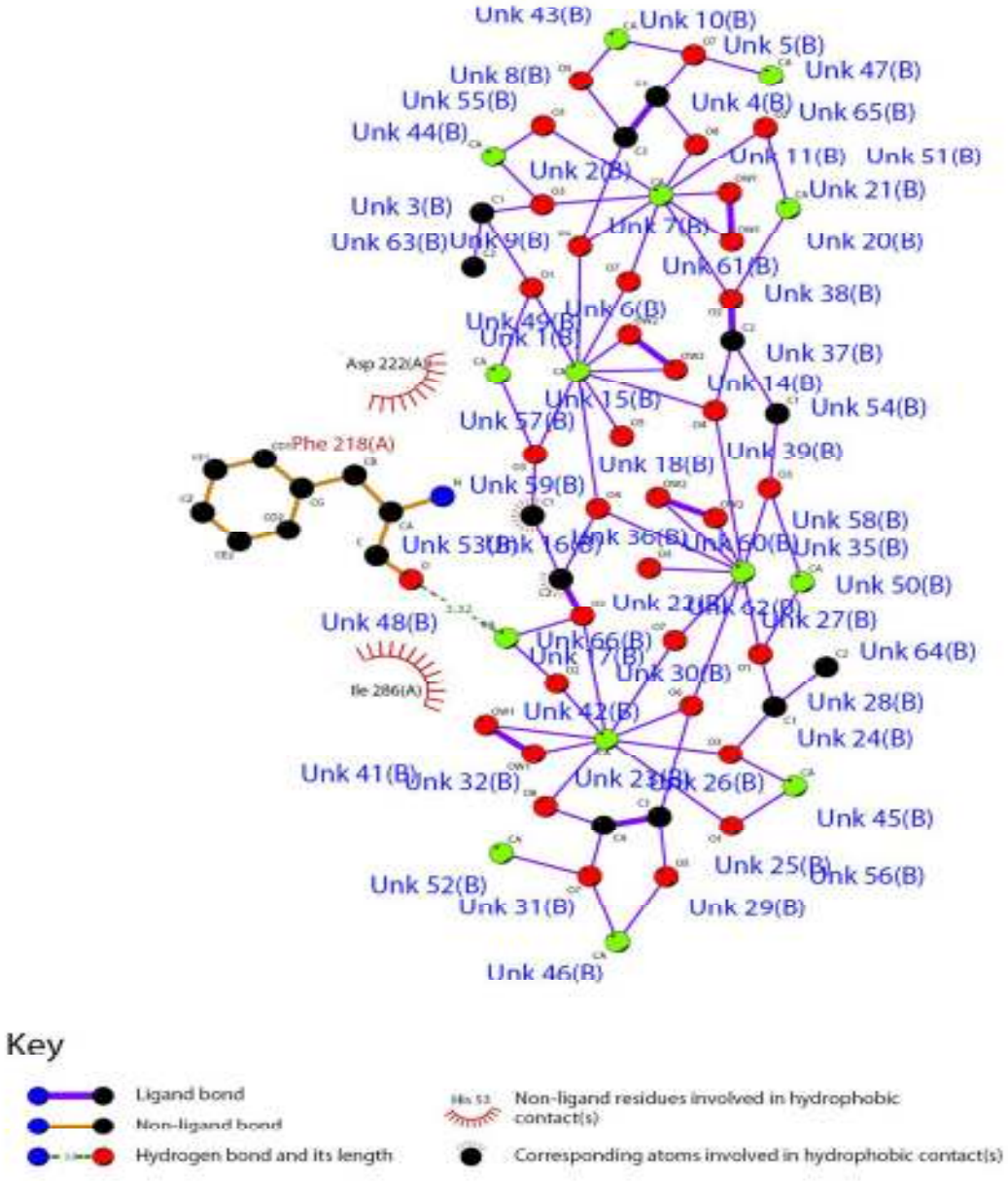


**Figure 3.20.** Two dimensional representations of the interactions observed between COM unit cell and active binding site osteonectin-1 of osteonectin protein. Dashed lines denote hydrogen bonds, and numbers indicate hydrogen bond lengths in Å. Hydrophobic interactions are shown as arcs with radial spokes. The figure was made using LIGPLOT

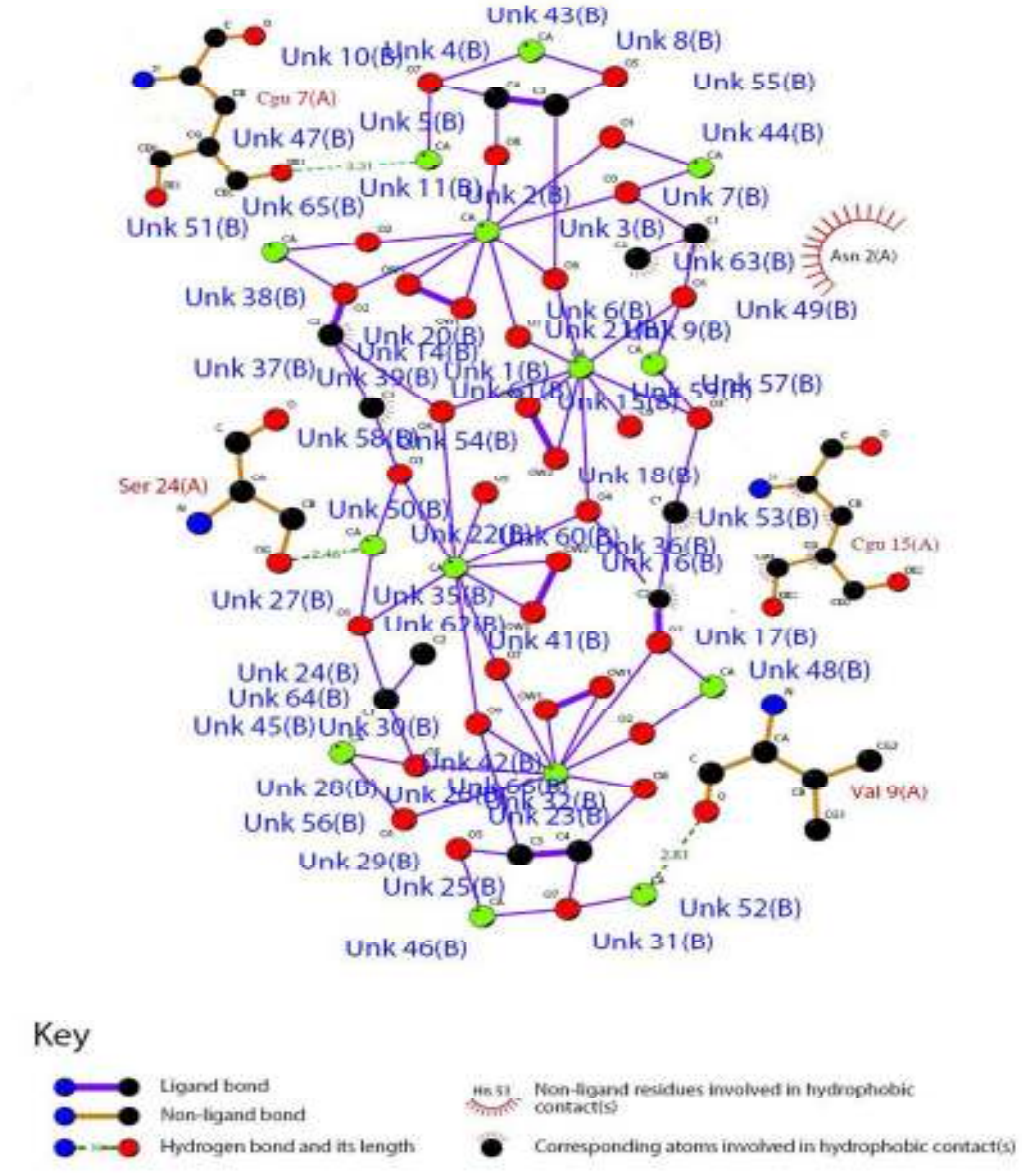


**Figure 3.21.** Two dimensional representations of the interactions observed between COM unit cell and active binding site uripro-1 of urinary prothrombin. Dashed lines denote hydrogen bonds, and numbers indicate hydrogen bond lengths in Å. Hydrophobic interactions are shown as arcs with radial spokes. The figure was made using LIGPLOT

On estimating the interaction between active binding sites of osteonectin and COM, it was observed that osteonectin-1 and osteonectin-2 showed comparable binding which is fairly strong. In addition to Glu and Asp, osteonectin-2 also showed involvement of aromatic amino acid Phe (Table 3.8). Involvement of aromatic amino acids in COM interactions is further supported by osteonectin-1 (Figure 3.20) active binding site where oxygen atom (O) of Phe is involved in hydrogen bonding with calcium ion of COM crystal.

In figure 3.20, the interactions of ostenectin-1 active binding site with COM crystal is shown. From the figure it is clearly visible that oxygen of phenylalanine (Phe) is forming hydrogen bond with calcium ion of COM crystal whereas Asp of osteonectin-2 is forming hydrophobic interactions with carbon at position 53 of COM crystal. In addition to Asp, Ile at position 286 is also involved in forming strong hydrophobic interactions with oxalate group of COM crystals.

In figure 3.21, the interactions of uripro-1 active binding site with COM crystal is visible. Only one active binding site uripro-1 of urinary prothrombin having gamma carboxy glutamic acid (CGU) showed strongest binding with COM in comparison to its other active binding sites. Gamma carboxy glutamic acid is involved in both hydrogen bonding and hydrophobic interactions (Table 3.8 and Figure 3.21). Carboxylic group in the side chain of CGU is forming hydrogen bond with calcium at $47^{th}$ position of COM crystal (Figure 3.20).

Carbon (C1) at position 53 and carbon (C2) at $17^{th}$ position of COM crystal are mainly forming hydrophobic interactions with $C^{\delta}$, $C^{\gamma}$, $C^{\beta}$ and $C^{\alpha}$ of CGU. The other two contributors of strong interactions of uripro-1 with COM crystals are Ser and Val. Here $O^{\gamma}$ at $24^{th}$ position of Ser forms hydrogen bonding with calcium ion at $50^{th}$ position and O of Val at $9^{th}$ position form hydrogen bond with calcium ion at $50^{th}$ position.

## *3.5. Validation in rat urolithiatic model*

Previous results showed that the purified protein from the seeds of *Dolichos biflorous* is effective towards both *in vitro* CaP mineralization and CaOx crystal growth inhibitory assay system. To check the efficacy of DAP *in vivo*, rat urolithiatic model was used as described in section 2.5. All animals progressed well during the treatment period. One or two animals out of 8 died in urolithiatic group A2 and B2. The animals in these urolithiatic groups also showed an abnormal coloration in their eyes and sparse body hair after the completion of treatment.

Following parameters were studied to assess the efficacy of *Dolichos biflorus* antilithiatic protein (DAP).

### *3.5.1. Body weight*

After treatment with ethylene glycol and $NH_4Cl$ for 9 days, a significant ($p<0.001$) decrease in body weight of group A2 animals was observed. They showed 23% decrease in body weight as compared to control animals (group A1). However, the animals of group A3 & A4 which were given purified protein from *Dolichos biflorus* (DAP) at the dose of 1mg/kg body weight and 2mg/kg body weight respectively, showed lesser decrease in their body weights. The body weight of these animals was quite close to the control group animals (group A1). Figure 3.22a shows the body weight of all group animals before and after treatment period of 9 days. Similarly, in group B2 animals, again a significant ($p<0.001$) decrease in body weight was observed at the end of treatment period. However, upon administration of DAP to the tune of 1mg/kg body weight and 2mg/kg body weight to ethylene glycol and $NH_4Cl$ exposed rats in group B3 and B4 respectively, again the body weights were almost comparable to control animals (B1). Figure 3.22b shows the changes in body weight of all groups before and after treatment period of 15 days. The dose for 15 days showed more adverse effect on body weight of urolithiatic group B2 animals than the animals in group A2. But the restoration of body weight after treatment with DAP to B3 and B4 group animals was comparable to group A3 and A4.

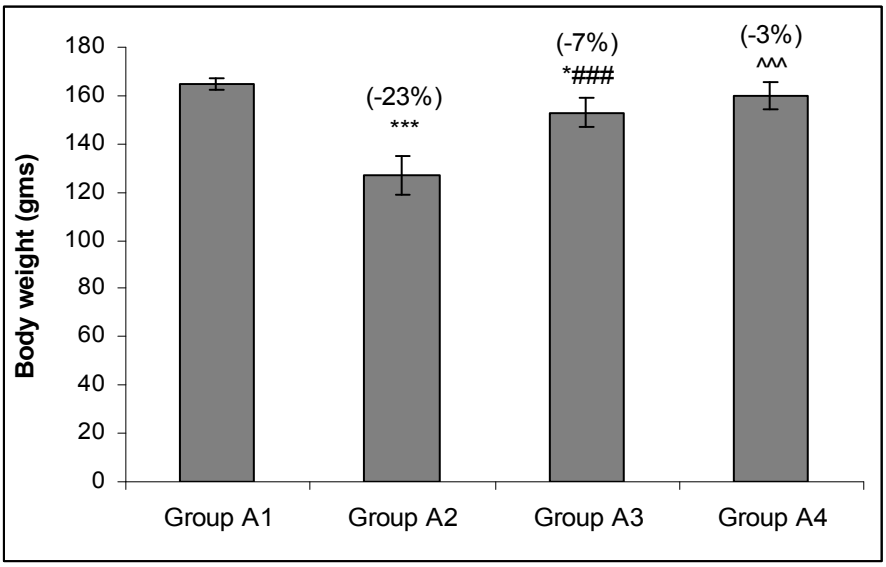


**Figure 3.22a.** Effect on body weight after treatment period of 9 days

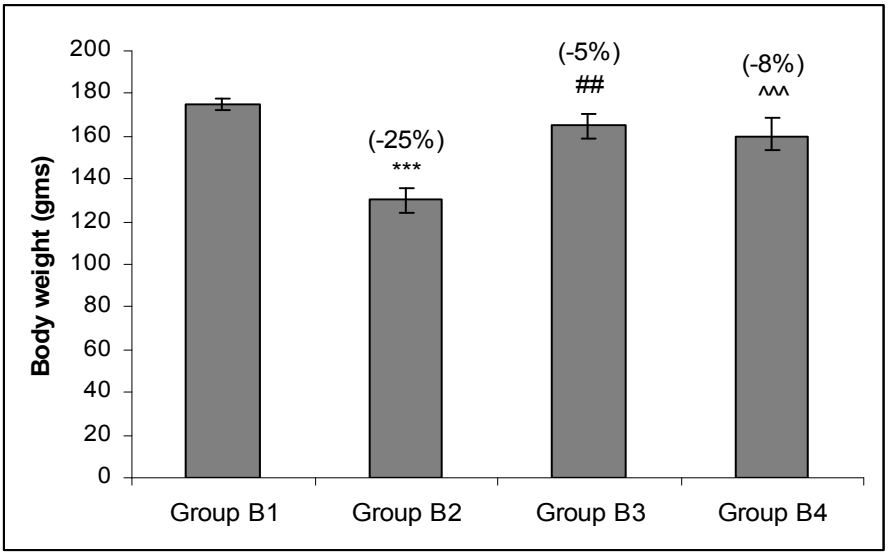


**Figure 3.22b.** Effect on body weight after treatment period of 15 days

**Figure 3.22.** Effect on body weight after treatment period for 9 and 15 days.

[*$p$< 0.05, **$p$< 0.01, ***$p$< 0.001: Indicate significant change in comparison to control group A1/B1. #$p$<0.05, ##$p$< 0.01, ###$p$< 0.001: Indicate significant change between group A2/B2 and A3/B3. ^$p$<0.05, ^^$p$< 0.01, ^^^$p$< 0.001: Indicate significant change between group A2/B2 and A4/B4. Values in brackets are % increase or % decrease as compared to group A1/B1].

### *3.5.2. Serum parameters*

#### *3.5.2.1. Creatinine content*

Figure 3.23a indicates the serum creatinine content after 9 days of treatment. From the figure, it can be seen that in group A2 animals, creatinine content in the serum increased by 64% in comparison to group A1 (control) animals. However, with treatment of DAP, creatinine content of group A3 and A4 was found to be lower in comparison to group A2.

Correspondingly, in group B2, a significant ($p$<0.001) increase of about 79% in creatinine content as compared to control group B1 animals was observed as shown in figure 3.23b. Although DAP in conjugation with ethylene glycol and $NH_4Cl$ has reduced the content of creatinine in serum of group B3 and B4 as compared to urolithiatic group B2 animals, but still these animals showed an increase of 51% and 46% respectively as compared to control group B1 animals.

The dosage of ethylene glycol and $NH_4Cl$ for 15 days caused a higher elevation in serum creatinine content as compared to 9 days treatment. In addition, the treatment of urolithiatic animals with DAP dose for 9 days resulted in higher reduction in creatinine content w.r.t urolithiatic animals as compared to 15 days treatment.

#### *3.5.2.2. Urea content*

The serum urea content estimated in the serum after 9 days exposure of ethylene glycol and $NH_4Cl$ showed an increase of 112% in group A2 as compared to control group A1 (Figure 3.24a). The treatment of urolithiatic animals with DAP in groups A3 & A4 showed significant decrease in urea content as compared to group A2 animals. Although, both groups A3 and A4 showed significant ($p$<0.001) increase (37% and 52% respectively) in urea content as compared to control group A1 animals, but still the serum urea content of these animals was significantly less with respect to urolithiatic group 2 animals.

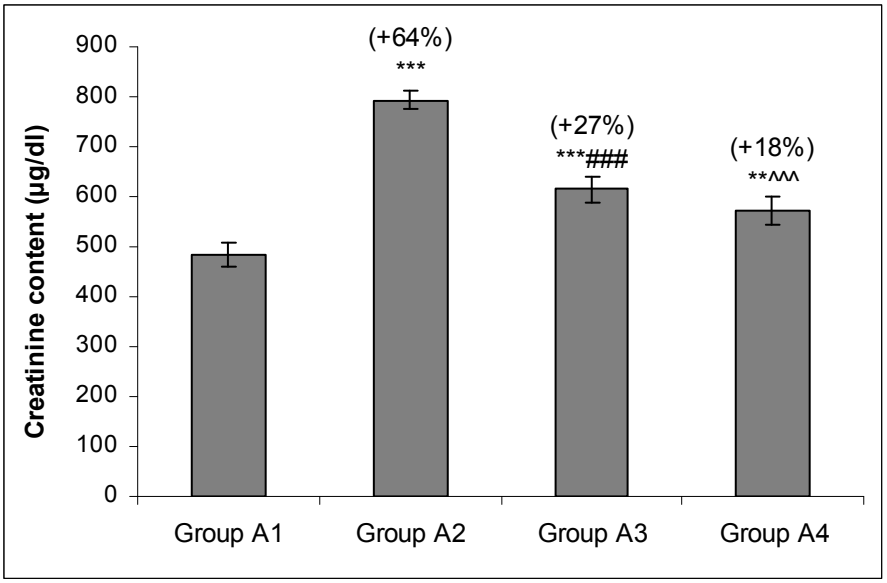


**Figure 3.23a.** The content of serum creatinine after 9 days of treatment period

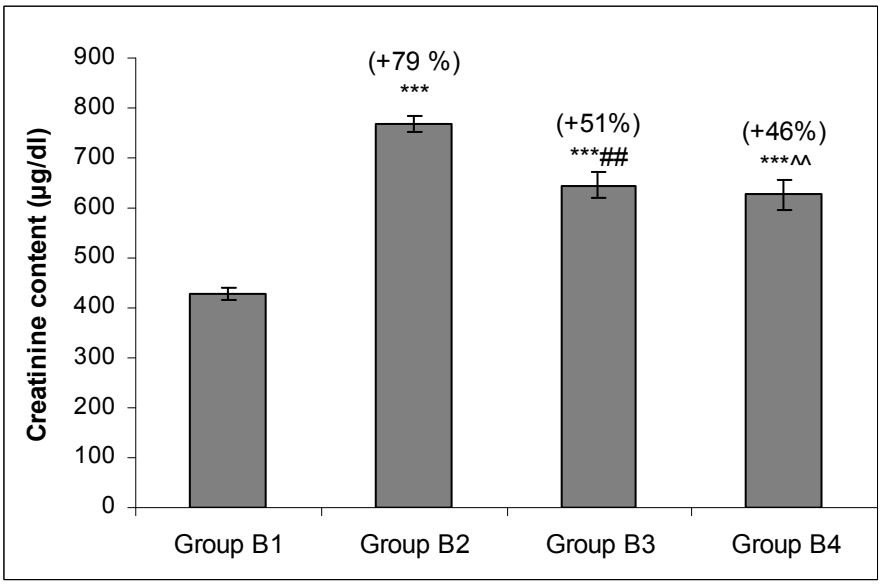


**Figure 3.23b.** The content of serum creatinine after 15 days of treatment period

**Figure 3.23.** Effect on serum creatinine content after the treatment period of 9 & 15 days

[*$p$< 0.05, **$p$< 0.01, ***$p$< 0.001: Indicate significant change in comparison to control group A1/B1. #$p$<0.05, ##$p$< 0.01, ###$p$< 0.001: Indicate significant change between group A2/B2 and A3/B3. ^$p$<0.05, ^^$p$< 0.01, ^^^$p$< 0.001: Indicate significant change between group A2/B2 and A4/B4. Values in brackets are % increase or % decrease as compared to group A1/B1].

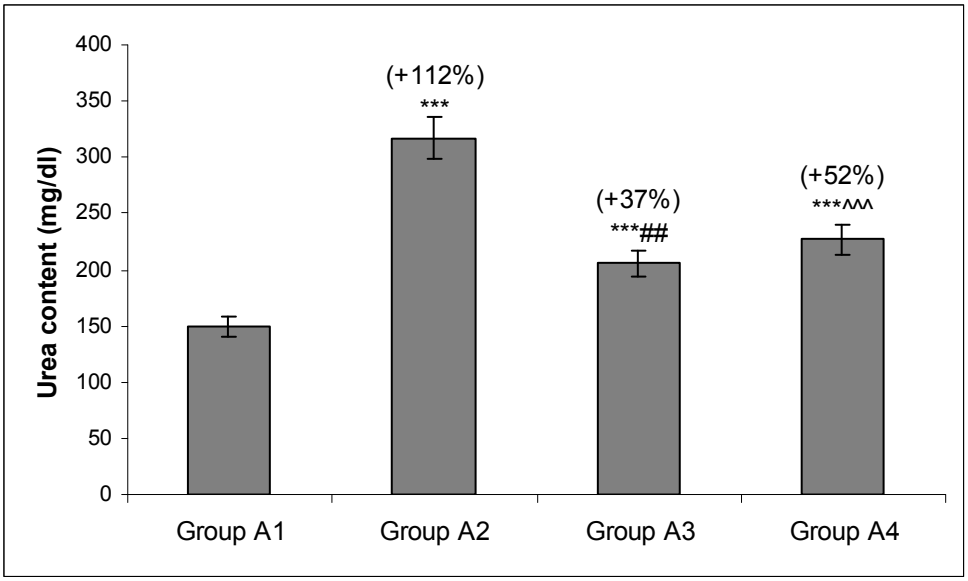


**Figure 3.24a.** The content of serum urea after 9 days of treatment period

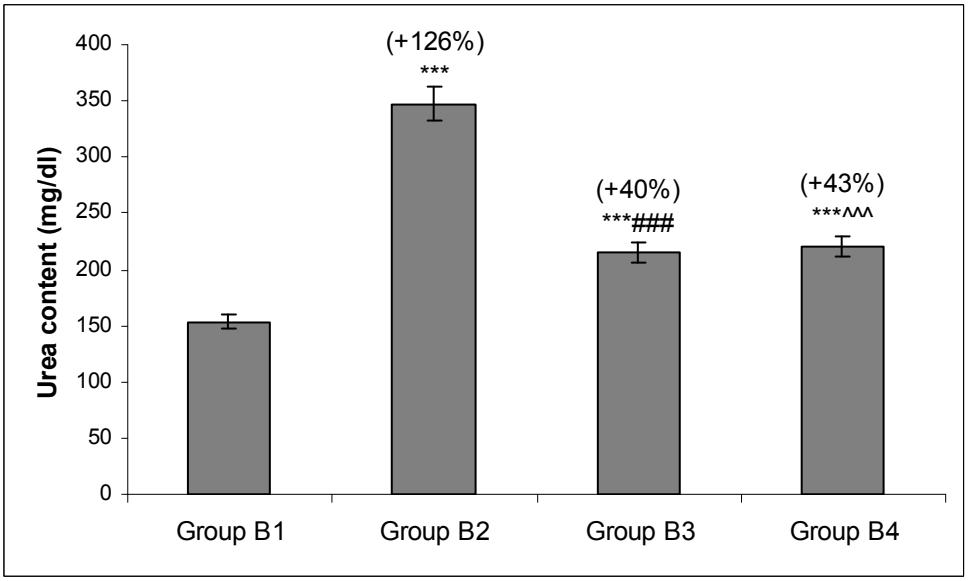


**Figure 3.24b**. The content of serum urea after 15 days of treatment period

**Figure 3.24.** Effect on serum urea content after the treatment period of 9 & 15 days

[*$p$< 0.05, **$p$< 0.01, ***$p$< 0.001: Indicate significant change in comparison to control group A1/B1. #$p$<0.05, ##$p$< 0.01, ###$p$< 0.001: Indicate significant change between group A2/B2 and A3/B3. ^$p$<0.05, ^^$p$< 0.01, ^^^$p$< 0.001: Indicate significant change between group A2/B2 and A4/B4. Values in brackets are % increase or % decrease as compared to group A1/B1].

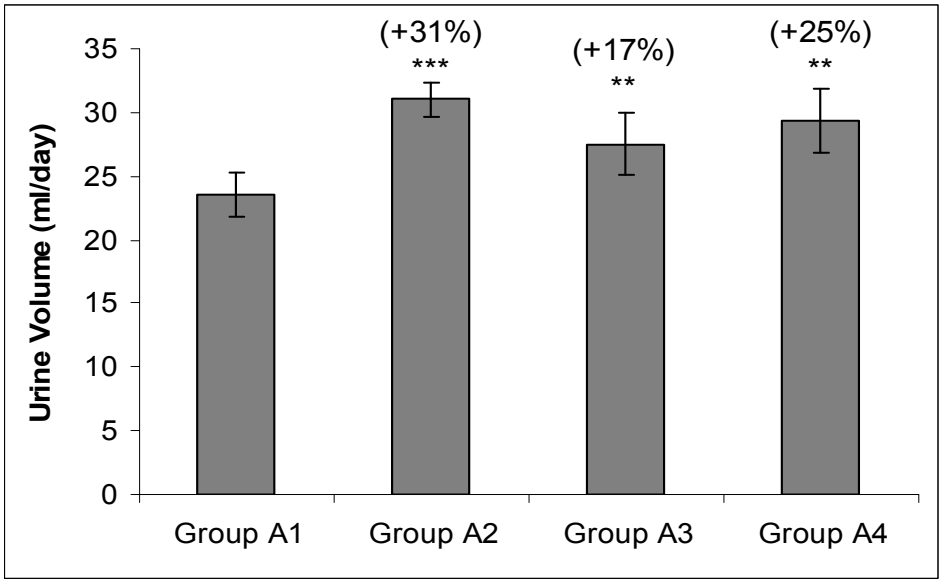


**Figure 3.25a.** Effect on 24 hr urine volume after treatment period of 9 days.

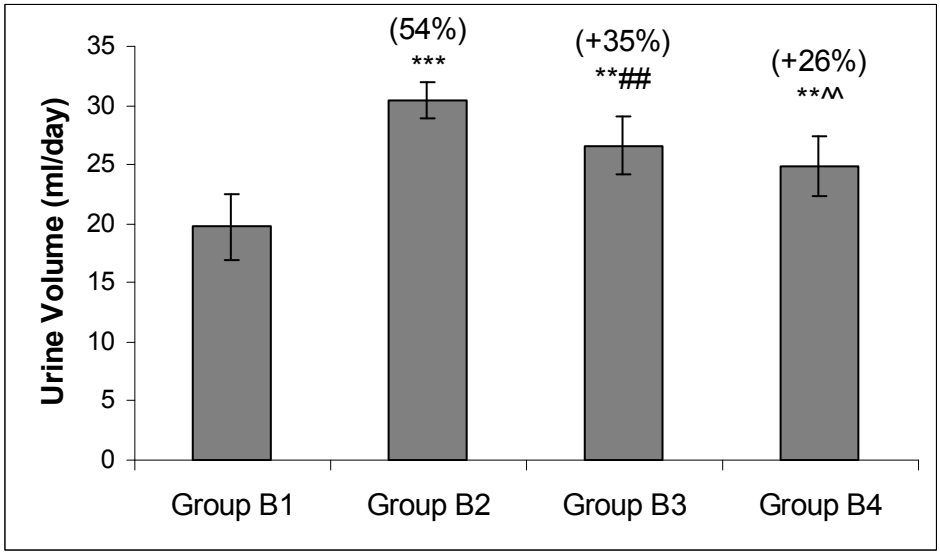


**Figure 3.25b.** Effect on 24 hr urine volume after treatment period of 15 days

**Figure 3.25**. Effect on 24 hr urine content after treatment period of 9 & 15 days

[*$p$< 0.05, **$p$< 0.01, ***$p$< 0.001: Indicate significant change in comparison to control group A1/B1. #$p$<0.05, ##$p$< 0.01, ###$p$< 0.001: Indicate significant change between group A2/B2 and A3/B3. ^$p$<0.05, ^^$p$< 0.01, ^^^$p$< 0.001: Indicate significant change between group A2/B2 and A4/B4. Values in brackets are % increase or % decrease as compared to group A1/B1].

In case of 15 days treatment, again a marked increase in blood urea level was observed as shown in figure 3.24b. Here again, the treatment of urolithiatic animals with DAP, reduced the serum urea level significantly ($p$<0.001) as compared to group B2 animals. It can be inferred that serum urea content in ethylene glycol & $NH_4Cl$ exposed animals was quite similar after 9 and 15 days treatment though the normalization of urea content after DAP treatment did not occur in a dose-dependant manner both after 9 and 15 days treatment (Figure 3.24a and 3.24b).

### *3.5.3. Urinary parameters*

#### *3.5.3.1. Urine volume*

All animals were kept in metabolic cages for 24 hrs and their urine was collected before the end of treatment period and a significant ($p$<0.001) increase in the urine volume was observed in urolithiatic group A2 and B2 as compared to the animals in control group.

The DAP dose showed little effect on urine volume in both of the treatment periods, the total volume of urine was higher as compared to control group animals. No significant difference in the urine volumes of DAP treated animals (A3, A4, B3 & B4) and urolithiatic animals (group A2 & B2) was observed (as shown in figure 3.25a & 3.25b).

#### *3.5.3.2. Alkaline phosphatase*

Figure 3.26a illustrates the activity of enzyme alkaline phosphatase (AP) in the urine of all groups after completion of their treatment period for 9 days. The treatment of ethylene glycol and $NH_4Cl$ for 9 days to group A2 animals (urolithiatic animals) has increased the activity of AP by about 97% as compared to control group A1 animals. Alternatively, with the dose of DAP the activity of AP in urine was found to be decreased in group A3 & A4 w.r.t. urolithiatic group A2 animals. Moreover, the A4 group animals, which were given 2mg/kg body weight DAP for 9 days, showed restoration of AP activity akin to the control group animals (group A1).

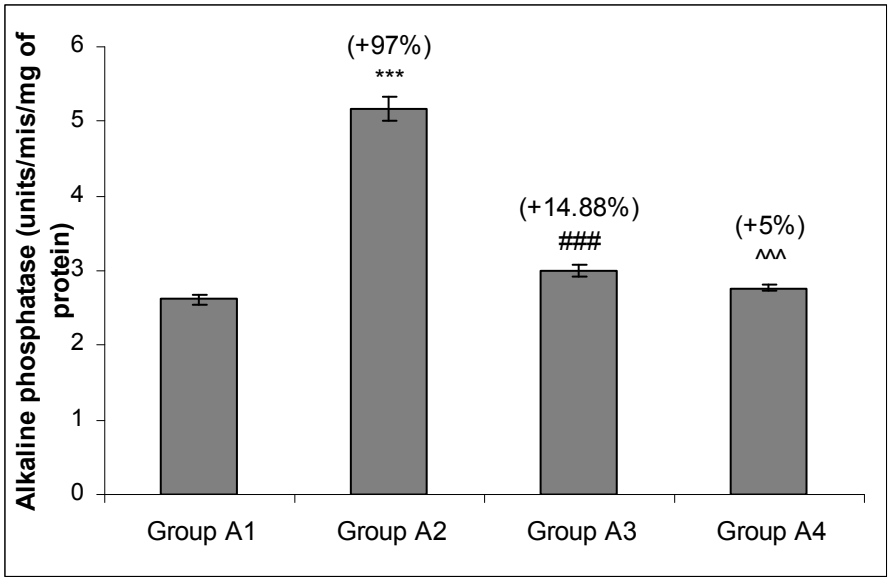


**Figure 3.26a.** Activity of alkaline phosphatase in all animals groups after 9 days

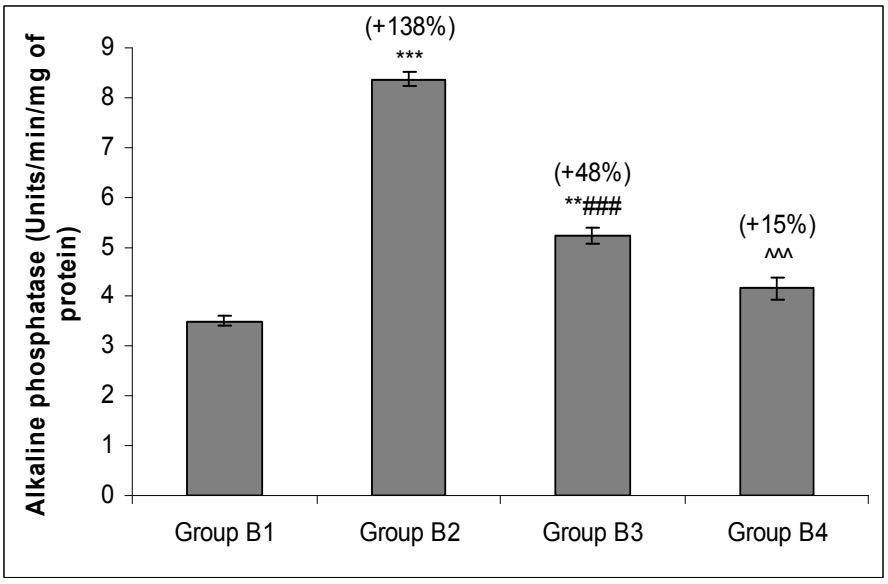


**Figure 3.26b.** Activity of alkaline phosphatase in all animals groups after 15 days

**Figure 3.26.** Activity of alkaline phosphatase in all animals groups after 9 & 15 days

[*$p$< 0.05, **$p$< 0.01, ***$p$< 0.001: Indicate significant change in comparison to control group A1/B1. #$p$<0.05, ##$p$< 0.01, ###$p$< 0.001: Indicate significant change between group A2/B2 and A3/B3. ^$p$<0.05, ^^$p$< 0.01, ^^^$p$< 0.001: Indicate significant change between group A2/B2 and A4/B4. Values in brackets are % increase or % decrease as compared to group A1/B1].

Correspondingly, group B2 animals showed a marked increase in AP activity as compared to A2 group animals (Figure 3.26b). The activity of AP was found to be elevated by 138 % in B2 group animals than in group A2 (97%) animals as compared to their respective control group. The DAP treated animals in group B3 and B4 showed a significant ($p$<0.001) decrease in AP activity as compared to group B2 animals. The dose of DAP given to group B3 & B4 for 15 days in addition to ethylene glycol and $NH_4Cl$ showed similar trend in decrease in the AP activity as that of group A3 & A4 after 9 days.

***3.5.3.3. Lactate dehydrogenase***

The activity of enzyme lactate dehydrogenase (LDH) in all group animals after 9 days treatment is indicated in figure 3.27a. From the figure it could be seen that the activity of LDH in group A2 animals was found to be significantly ($p$<0.001) increased by about 40% as compared to control group A1 animals. However, with the treatment of DAP at the dose of 1mg and 2mg per kg body weight to group A3 and A4, the animals showed a decrease in the activity of LDH as compared to urolithiatic group (A2) animals.

Correspondingly, figure 3.27b shows the activity of LDH in all group animals after 15 days of treatment. After the exposure of same dose of ethylene glycol and $NH_4Cl$ for 15 days, the activity of LDH in the group B2 animals was found highly elevated (85%) as compared to control group B1 animals. The animals of group B3 and B4 treated with DAP showed a significant ($p$<0.001) decrease in LDH activity with respect to B2 group (urolithiatic) animals. The DAP had tried to restore the LDH activity up to normal level in both 9 & 15 days treatment.

The dose of ethylene glycol and $NH_4Cl$ for 15 days showed higher elevation (85%) in the activity of LDH whereas the same dose for 9 days showed the increase in LDH activity by only 40% as compared to their corresponding control group animals. On the other hand, the treatment of these animals with DAP showed similar results.

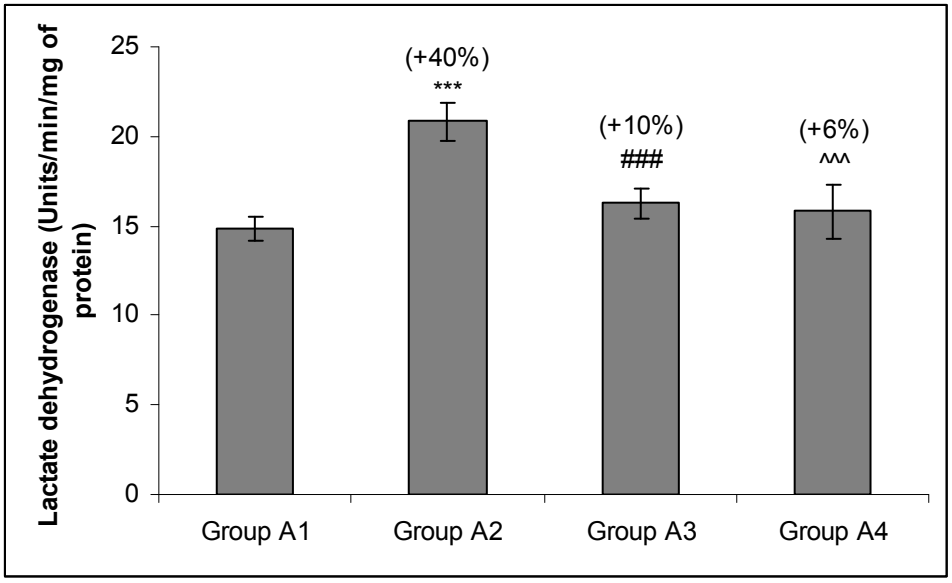


**Figure 3.27a.** Activity of lactate dehydrogenase in all four groups after 9 days

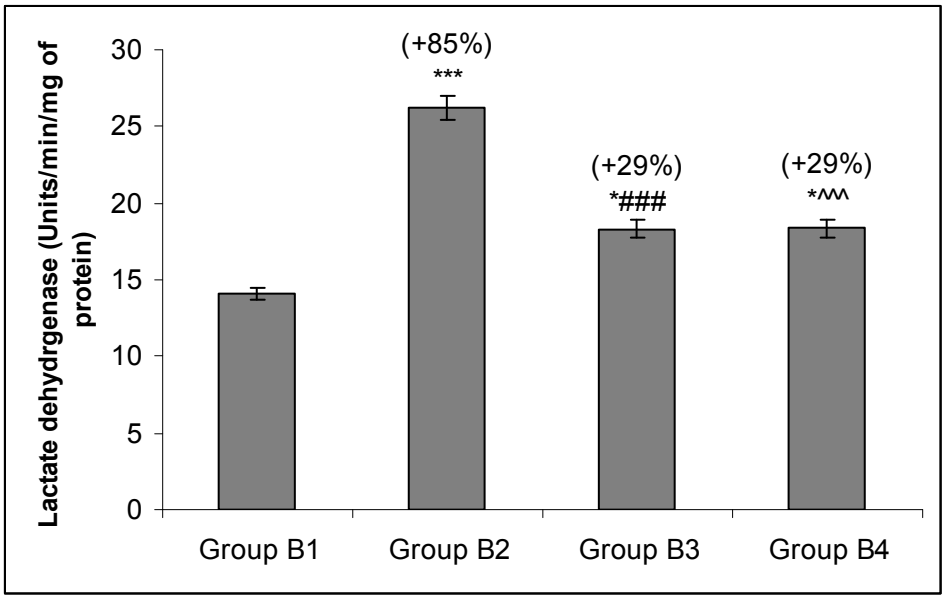


**Figure 3.27b.** Activity of lactate dehydrogenase in all four groups after 15 days

**Figure 3.27.** Activity of lactate dehydrogenase in all animals groups after 9 & 15 days

[*$p$< 0.05, **$p$< 0.01, ***$p$< 0.001: Indicate significant change in comparison to control group A1/B1. #$p$<0.05, ##$p$< 0.01, ###$p$< 0.001: Indicate significant change between group A2/B2 and A3/B3. ^$p$<0.05, ^^$p$< 0.01, ^^^$p$< 0.001: Indicate significant change between group A2/B2 and A4/B4. Values in brackets are % increase or % decrease as compared to group A1/B1].

***3.5.3.4. Polarization microscopy of rat urine***

Polarization light microscopy of bladder urine revealed that after experimental period of 9 days, urine of group A1 animals was more or less devoid of any crystal whereas in group A2 animals, the urine sample showed presence of abundant bipyramidal shaped COD & dumbbell-shaped COM crystals and at many instances, there aggregates were also visible as shown in figure 3.28a.

In the urine of group A3 and A4 animals, a drastic decrease in the number of urinary crystals was observed. Group A3 animals showed the presence of only few COD and a negligible number of COM crystals as shown in figure 3.28b. Similarly, group A4 animals illustrates the presence of only COD crystals and here again there number was very less as shown in figure 3.28c, in addition the size of COD crystals in A4 group animals were very small in comparison to COD crystals of group 2 animals.

Similarly, group B1 was also devoid of any crystal deposition but the animals of group B2 given ethylene glycol and $NH_4Cl$ for 15 days showed abundant COM and COD crystals as shown in figure 3.29a. The DAP treated urolithiatic animals of group B3 & B4 showed very few aggregates of COD or COM crystals (figure 3.29b & 3.29c). Although group B3 animals showed no aggregates, but their urine showed the presence of more COM and fewer COD crystals (Figure 3.29b).

Similarly, urolithiatic animals treated with DAP at 2mg/kg body weight (group B4) showed fewer crystals in the urine and here again COM crystals were pre-dominant. In the figure 3.29c, it is also shown that at many instances the crystals observed were broken and disintegrated. The size of COM crystals in these group animals was also very small as compared to urolithiatic group B2 animals.

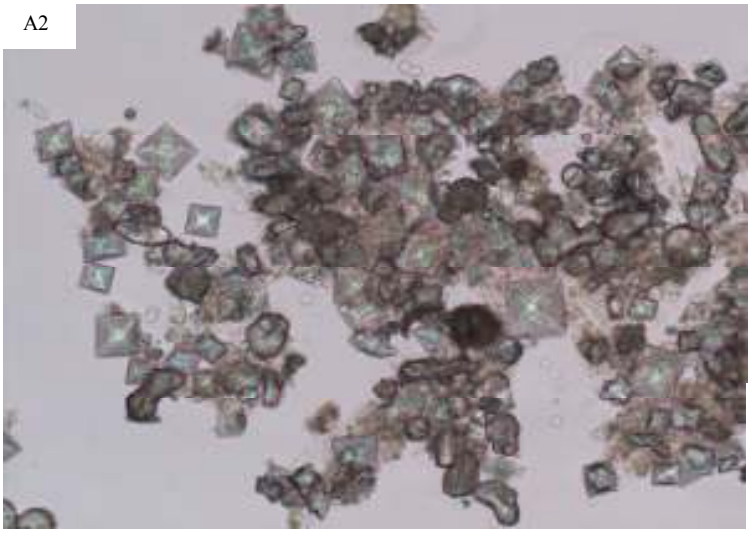


**Figure 3.28a**. Urine of EG and $NH_4Cl$ exposed rats for 9 days

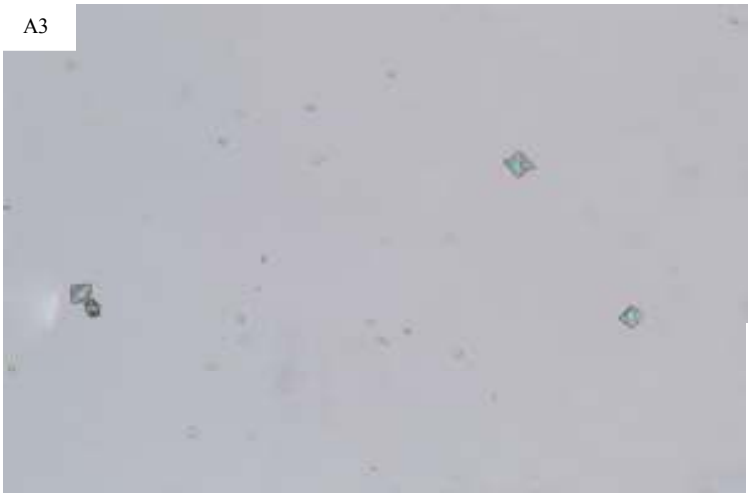


**Figure 3.28b**. Urine of EG and $NH_4Cl$ exposed rats treated with DAP 1mg/kg body weight rats for 9 days


**Figure 3.28c**. Urine of EG and $NH_4Cl$ exposed rats treated with DAP 2mg/kg body weight rats for 9 days

**Figure 3.28**. Polarization micrographs of rat's urine given treatment for 9 days

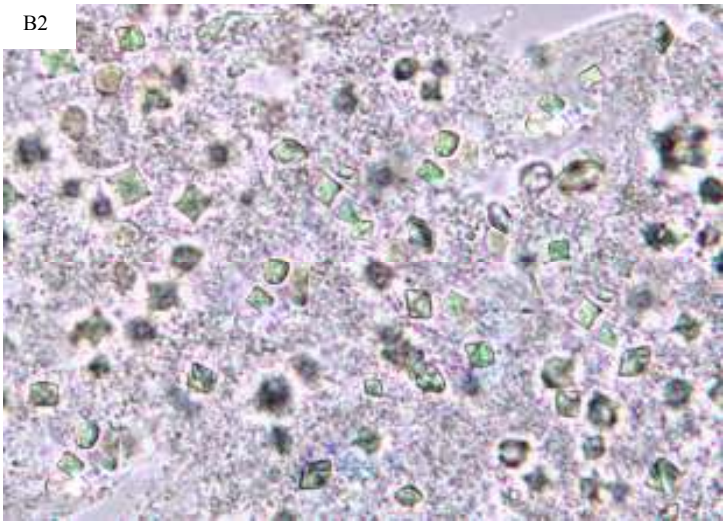


**Figure 3.29a**. Urine of EG and $NH_4Cl$ exposed rats for 15 days


**Figure 3.29b.** Urine of EG and $NH_4Cl$ exposed rats treated with DAP 1mg/kg body weight rats for 15 days

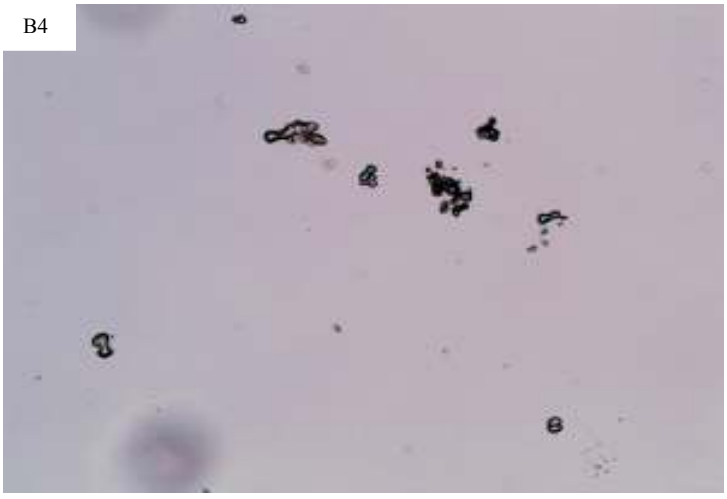


**Figure 3.29c**. Urine of EG and $NH_4Cl$ exposed rats treated with DAP 2mg/kg body weight rats for 15 days

**Figure 3.29**. Polarization micrographs of rat's urine given treatment for 15days

### *3.5.4. Creatinine clearance*

Creatinine clearance was calculated by the formula (as given in section 2.5.6) using serum and urine creatinine content and is graphically represented in figure 3.30a and 3.30b for the respective treatment period of 9 and 15 days. Figure 3.30a shows that after 9 days exposure of ethylene glycol and $NH_4Cl$, the animals in group A2 showed a marked decrease in creatinine clearance (-55%) as compared to control animals (group A1). Subsequently, treatment of ethylene glycol and $NH_4Cl$ exposed animals with DAP at the dose of 1mg and 2mg per kg body weight in group A3 & A4, an elevation in creatinine clearance was observed as compared to urolithiatic group A2 animals.

A similarly type of trend was observed in the case of rats treated for 15 days. The urolithiatic animals in group B2 showed significantly ($p<0.001$) decreased creatinine clearance which is about 57% less as compared to control group B1 animals. However, the treatment with DAP to group B3 and B4 showed enhanced creatinine clearance per unit time. The animals of group B3 given 1mg/Kg body weight of DAP were showing creatinine clearance of 3.5ml/min and group B4 animals given 2mg/kg body weight of DAP were showing the creatinine clearance of 3.8ml/min. This shows that DAP is showing dose-dependant effect in maintaining creatinine clearance level.

Although the dose of 15 days was having more adverse effect on creatinine clearance as compared to 9 days in case of urolithiatic groups B2 & A2 respectively but the DAP treatment for both 9 and 15 days experiment showed a similar response. The animals given treatment for 9 days showed similar level of creatinine clearance as the group given for 15 days treatment.

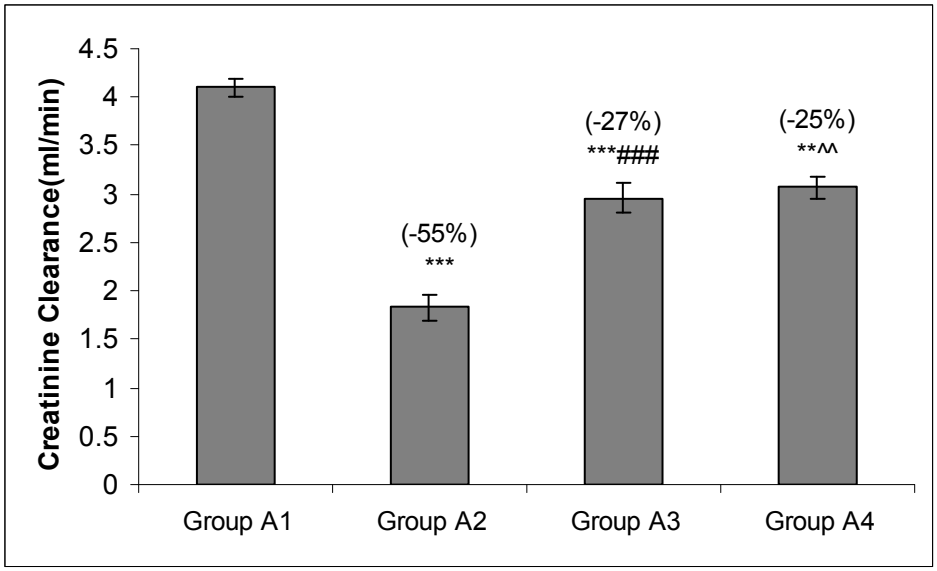


**Figure 3.30a.** The effect on creatinine clearance after treatment of 9 days

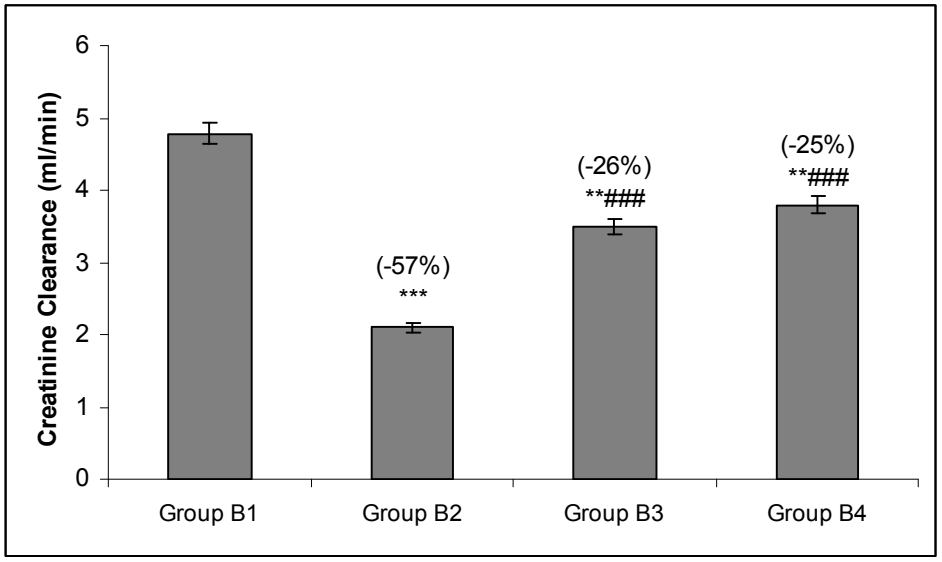


**Figure 3.30b.** The effect on creatinine clearance after treatment of 15 days

**Figure 3.30.** The effect on creatinine clearance after the treatment of 9 & 15 days.

[**p*< 0.05, ***p*< 0.01, ****p*< 0.001: Indicate significant change in comparison to control group A1/B1. #*p*<0.05, ##*p*< 0.01, ###*p*< 0.001: Indicate significant change between group A2/B2 and A3/B3. ^*p*<0.05, ^^*p*< 0.01, ^^^*p*< 0.001: Indicate significant change between group A2/B2 and A4/B4. Values in brackets are % increase or % decrease as compared to group A1/B1].

### *3.5.5. Renal histology under light microscope*

Light microscopy of renal tissue is shown in figure 3.31a, 3.31b, 3.31c and 3.31d. The figure 3.31a, illustrates the normal morphology of kidney tissues. The glomerulus within bowman's capsule was intact and the bowman's capsule was lined with a continuous lining of epithelial cells. The renal tubules showed intact lumen lined by cuboidal epithelial cells. No sign of inflammation and hemolysis was observed in the histology of control animals.

In contrast, the renal histology of urolithiatic animals (as shown in figure 3.31b) given ethylene glycol and $NH_4Cl$ showed distorted morphology. The glomerulus was shrunken and the lining of bowman's capsule was found to be broken at many instances. The renal tubules had lost their intact structure as no distinct lumen was observed. In addition to these morphological alterations, the histology of animals in this group showed marked inflammation and hemolysis. The cells were distorted and signs of edema were also observed at many instances in their histology.

However, the animals in group A3 which were treated with DAP at a dose of 1mg per kg body weight showed restored morphology as compared to control group animals (Figure 3.31c). The signs of inflammation were reduced and no hemolysis and edema was observed. The animals in this group showed normal size of glomerulus. Although, the loss of intact renal tubules was still prevalent.

In figure 3.31d, the histology of animals given DAP at the dose of 2mg/kg body weight is shown. From the figure, it could be clearly seen that the histology of these animals is comparable with control animals. The glomerulus is of appropriate size and lined by intact bowman's capsule. There are many instances of intact renal tubules lined by cuboidal epithelial cells and decrease in tissue injury was also observed. The renal histology of group A4 animals was more near to control animals than group A3 thus indicating that DAP showed a dose-dependant response

Figure 3.31a

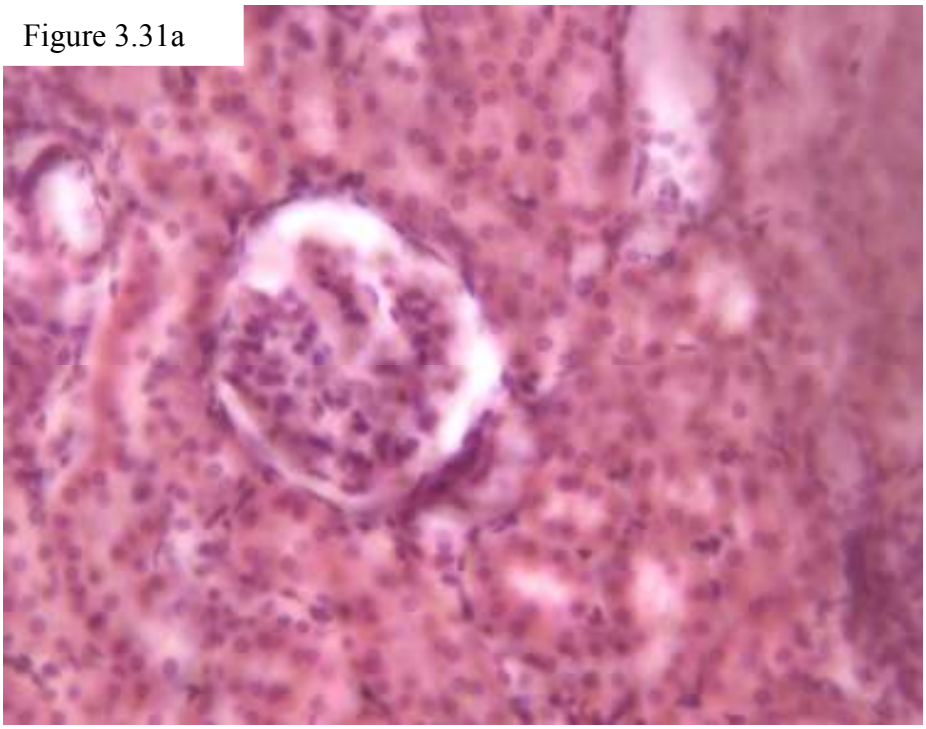

Figure 3.31b

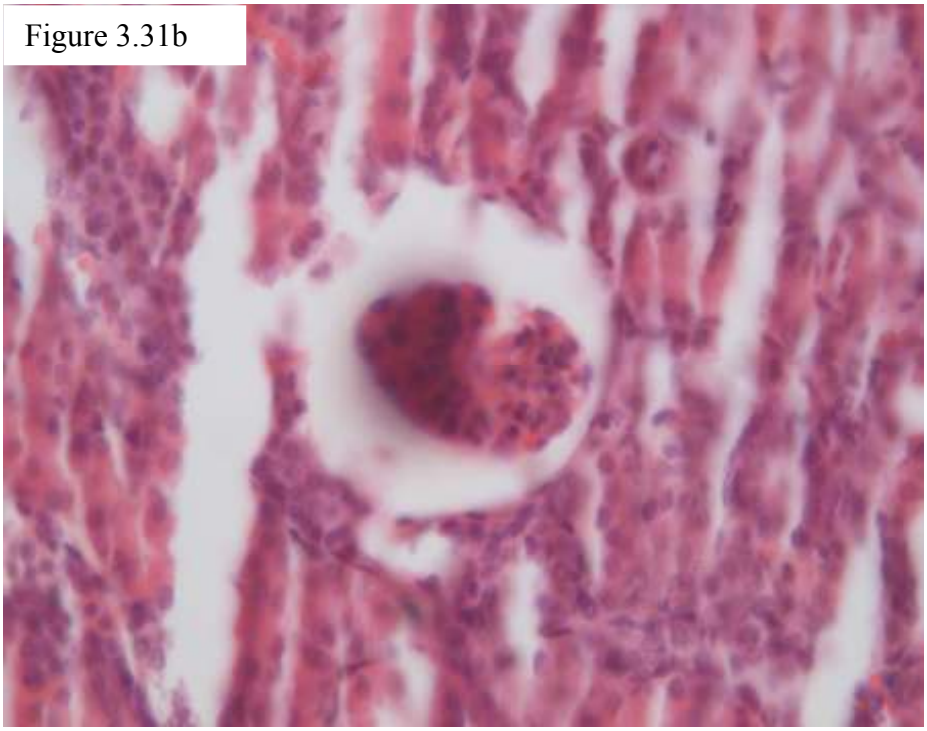

Figure 3.31c

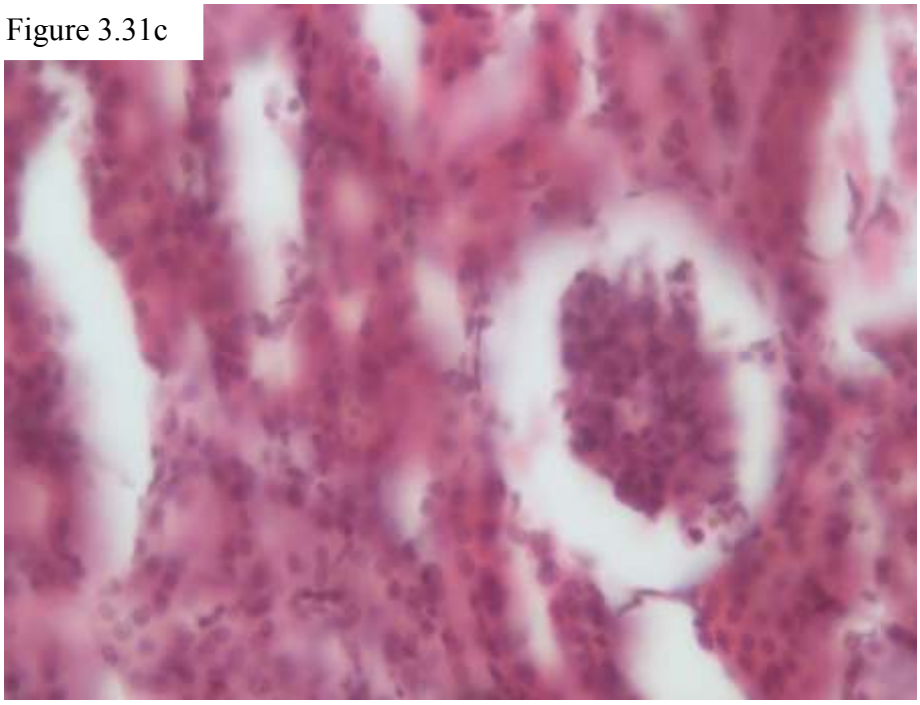

Figure 3.31d

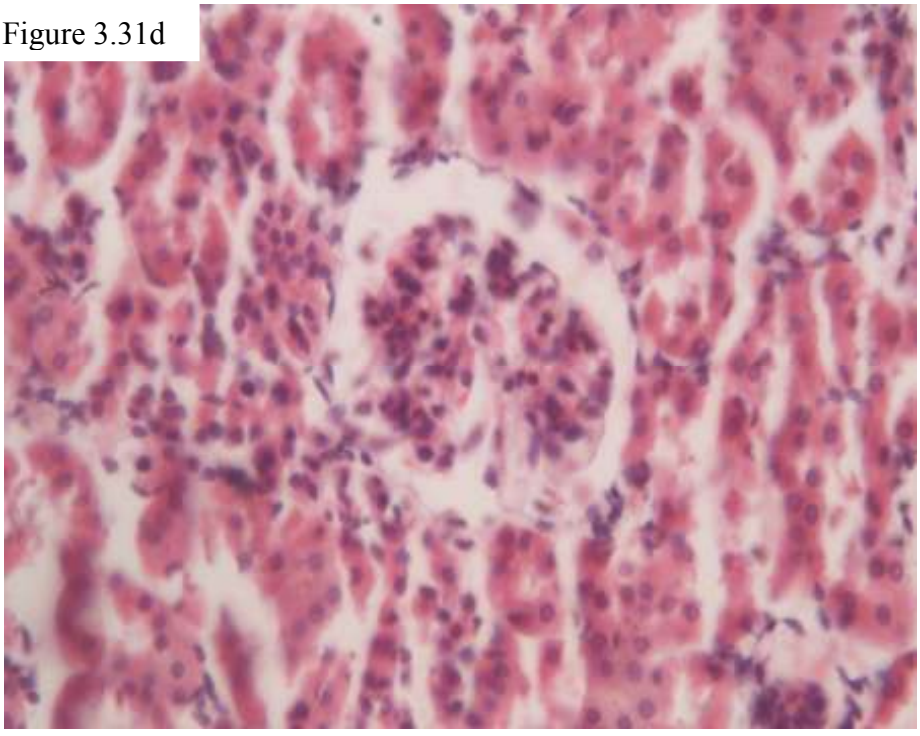

**Figure 3.31.** Renal histology under light microscope of rats given treatment for 9 days. a: group A1, b: group A2, c: group A3, d: group A4. (Magnification 200X)

Figure 3.32a

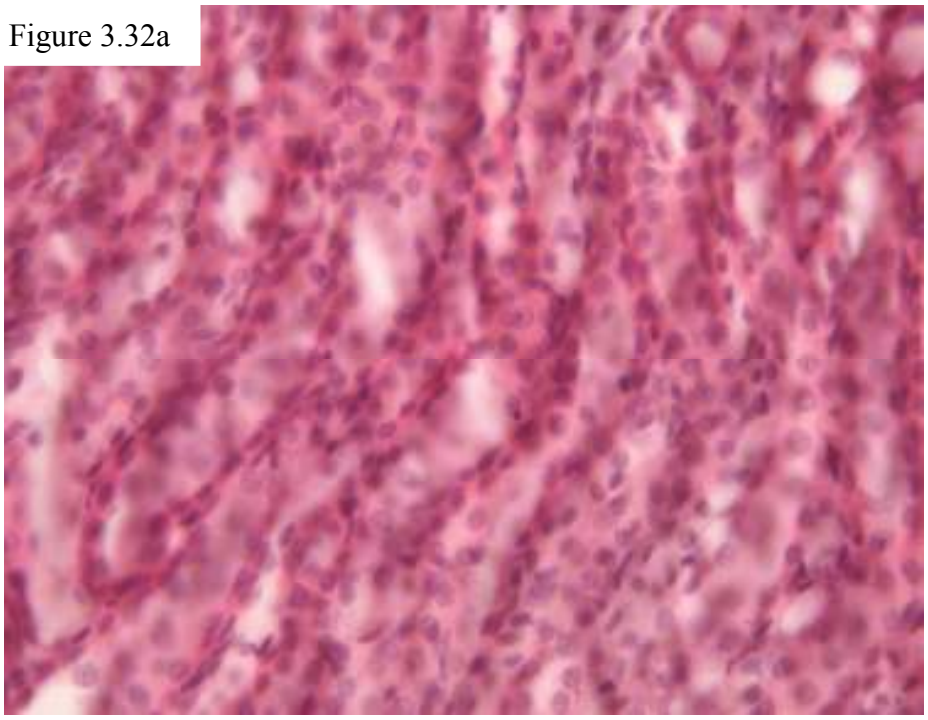

Figure 3.32b

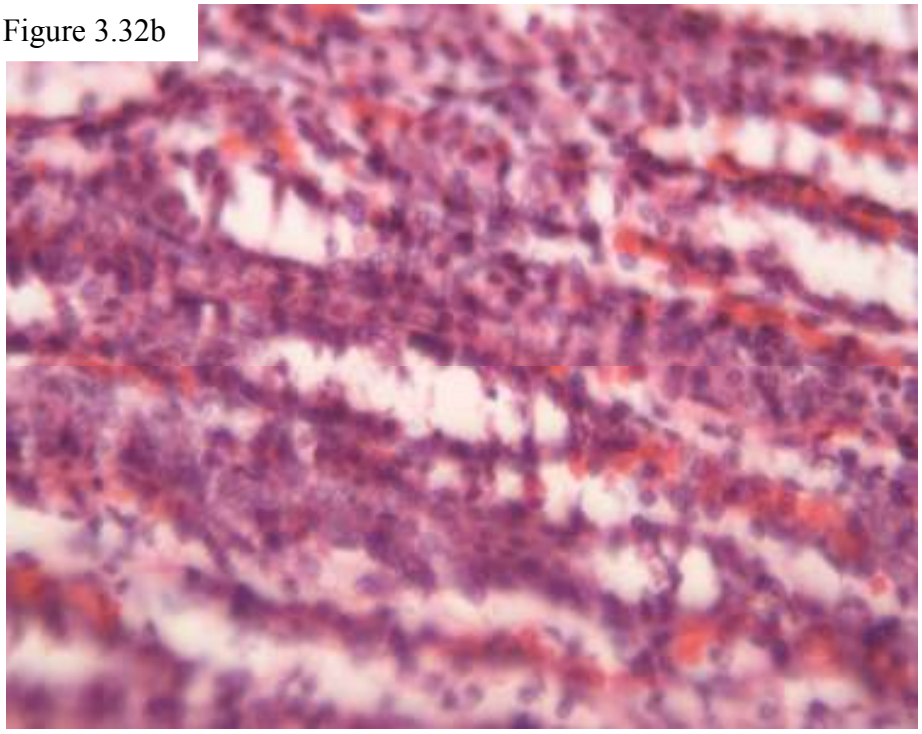

Figure 3.32c

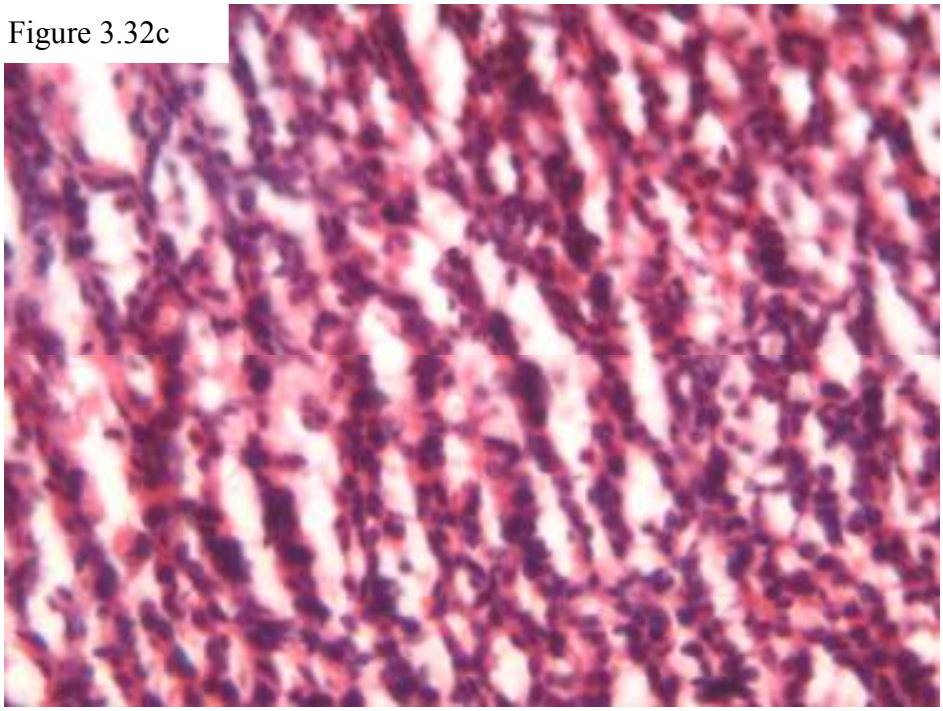

Figure 3.32d

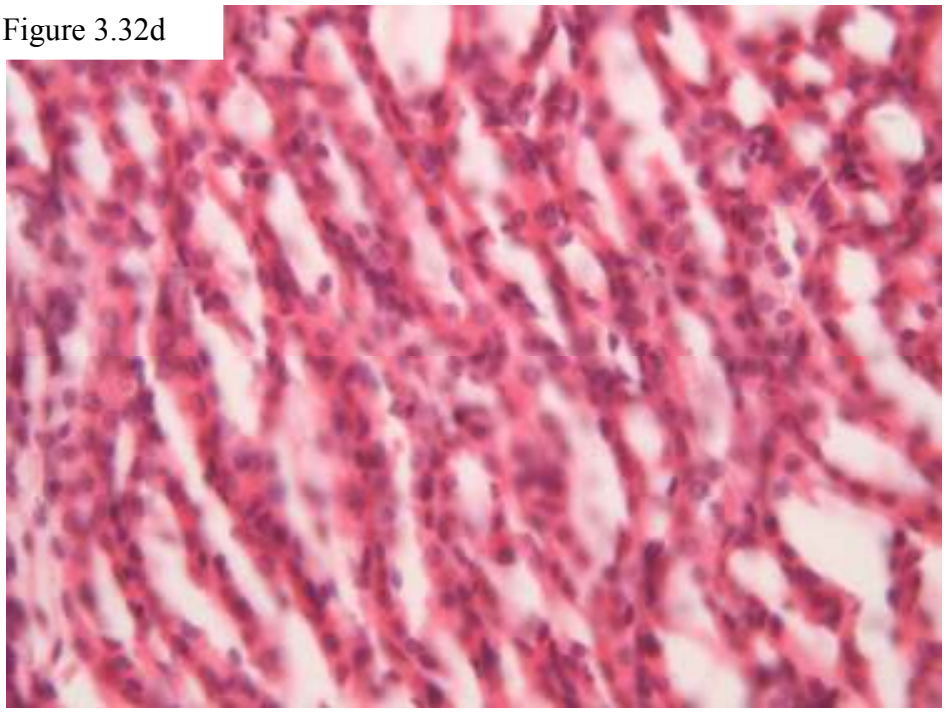

**Figure 3.32.** Renal histology of rats given treatment for 15 days under light microscope. a: group B1, b: group B2, c: group B3, d: group B4. (Magnification 200X)

Figure 3.32 is showing the renal histology of animals given treatment period for 15 days. The animals in control group B1 showed normal morphology as is shown in figure 3.32a. The figure shows that medulary rays are intact and arranged properly. The tubules of medullary rays are lined by continuous cuboidal epithelial.

On the other hand, animals given dose of ethylene glycol and ammonium chloride for 15 days showed marked changes in their histology. The renal tissue of these animals showed hemolysis at many instances. The tissues of these animals presented noticeable cell rupture as is shown in figure 3.32b. The arrangement of epithelial cells in their tissue was completely lost. The signs of inflammation and hemoloysis in these animals were significantly more than animals of group A2 given same dose for 9 days.

The animals given DAP dose at 1mg/kg body wt for 15 days to group B3 showed some marks of renal histology restoration. In group B3, the renal tissue presented a low level of hemolysis and inflammation. From figure 3.32c it can be suggested that, although the arrangement of epithelial cells is not completely restored, the rupturing of cells in their tissue is evidently less as compared to stone forming group B2 animal's renal tissue.

Figure 3.32d shows the histology of group B4 animals. The renal tissue of group B4, given DAP at a higher dose of 2 mg/kg b wt, showed an improved histology as compared to group B2. The cell rupturing was completely missing in these animal's renal tissues. The epithelial cells lining the renal tubules showed improved arrangement and the a marked decrease in inflammation of renal tissue was observed. These animals renal tissue showed no signs of hemolysis as shown by urolithiatic group B2.

On comparing the histology of group B4 and B3 given DAP at 1 and 2 mg/kg b. wt, it was clearly visible that DAP restored renal histology more at its higher dose.

### *3.5.6. Renal histology under polarization microscope*

The renal histology slides as observed under polarization microscope are shown in figure 3.33. Polarization microscopy focuses the crystal deposition in the kidney tissue. Figure 3.33a is showing the polarization micrographs of control group A1 animals. There was no mark of crystal deposition in the renal tissues of these animals.

In figure 3.33b, shows the histology of renal tissue of animals given ethylene glycol and $NH_4Cl$ for 9 days. In this figure, it is evidently clear that the animals in this group showed abundant crystal deposition in the tissue. The histology clearly shows that most of the crystals are deposited in the renal tubules and the tubules showed distorted morphology. There was no crystal deposition observed in the glomerulus. Since, renal tubules having crystal deposition is distorted, which indicates that either crystal deposition has caused renal tubule distortion/injury or the injury in the renal tubule has lead to crystal accumulation in these tubules.

Figure 3.33c shows the renal tissue of group A3 under polarization microscope. In group A3 which were given DAP at 1mg/Kg body weight, showed a marked decrease in number of crystal depositions in the kidney tissue. The crystals were observed at a few instances in renal tubules. The overall morphology of renal tissue was found to improve as compared to urolithiatic group A2 animals. The renal tubules were intact at many instances expect for those places where the crystal deposition was present.

Similarly, the DAP at a higher dose of 2mg/Kg body weight in A4 group animals showed again a decrease in number of crystals (figure 3.33d). Here, again the animals showed the deposition of crystals in renal tubules and as in group A3, the animals in this group also showed decrease in renal injury. The reduced size as well as number of crystals and decreased renal injury again showed the efficacy of this protein in a dose-dependent manner.

Figure 3.33a

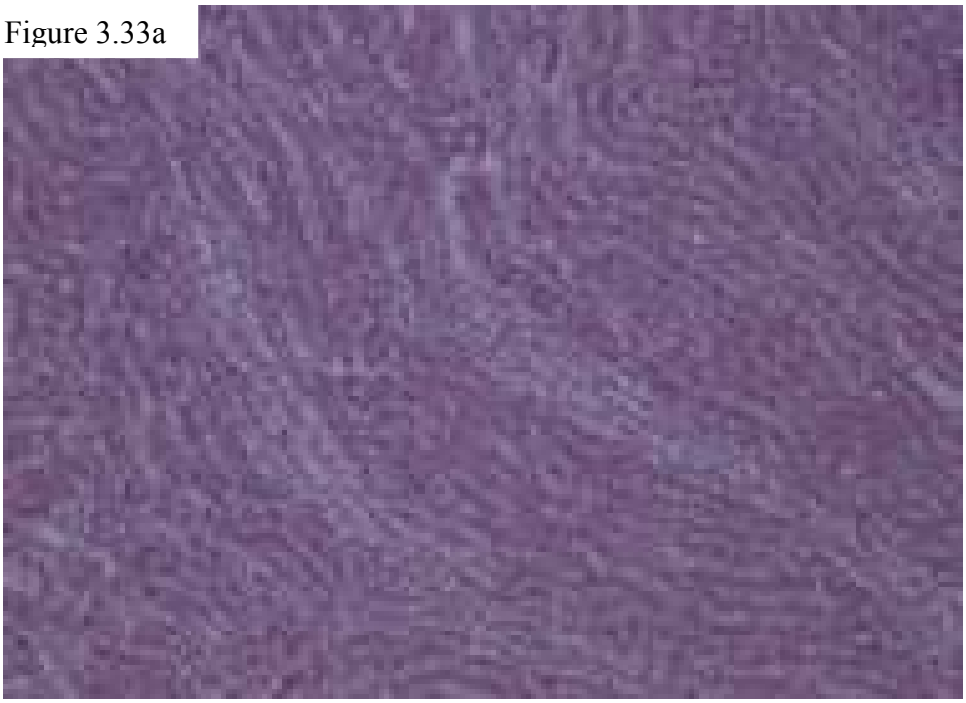

Figure 3.33b

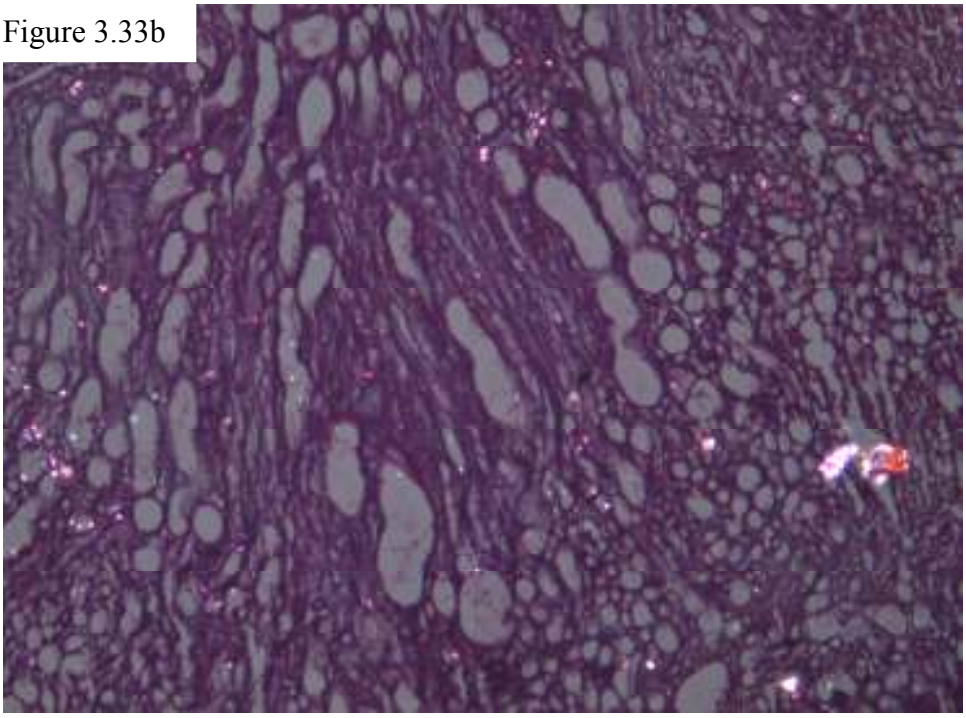

Figure 3.33c

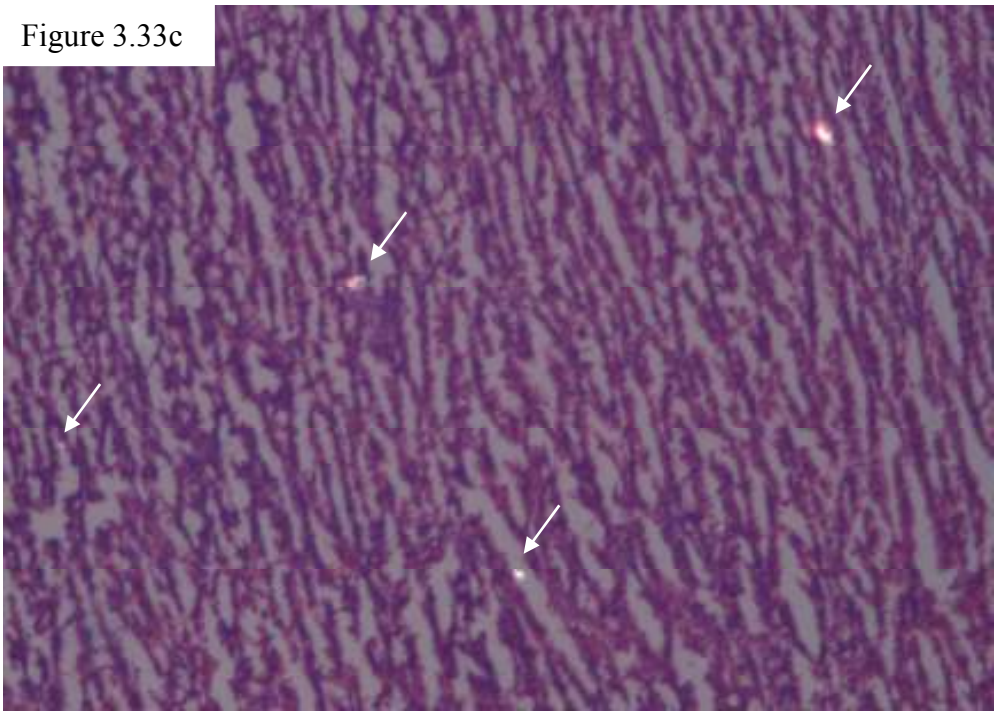

Figure 3.33d

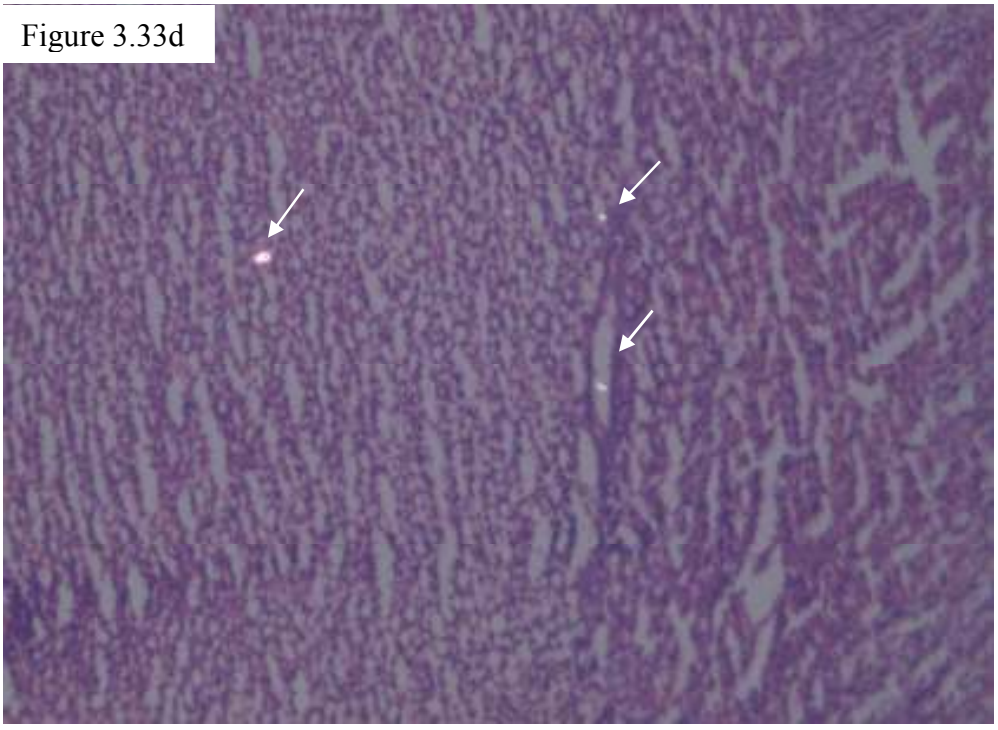

**Figure 3.33.** Renal histology under polarization microscope of rats given treatment for 9 days. a: group A1, b: group A2, c: group A3, d: group A4. (Magnification 200X)

### *3.5.7. Antioxidant properties of DAP*

To ascertain the antioxidant properties of DAP and its efficacy to maintain the antioxidant status of kidney tissue, it was compared with N acetylcysteine (NAC), a known antioxidant. The oxidative stress was induced in these rats by an acute dose of sodium oxalate (70 mg/kg b.wt). The dose of NAC was selected to be 200mg/kg b. wt and *Dolichos biflorus* antilithiatic protein (DAP) was given at a dose of 9mg/kg b. wt.

The oxidative stress in renal tissue was evaluated by lipid peroxidation. In addition, the effect of DAP on antioxidant defense system was also evaluated. The non enzymatic antioxidant like glutathione and enzymatic antioxidant like superoxide dismutase & catalase were estimated.

#### *3.5.7.1. Effect on lipid peroxidation*

Lipid peroxidation was evaluated by estimating the malondialdehyde (MDA) levels in renal tissue. Figure 3.34 shows that a single dose of sodium oxalate to group C2 animals had shown a significant increase ($p<0.01$) in MDA content of renal tissue as compared to control C1 animals. MDA status in this group was found to increase by 27%. Co-treatment of NAC with sodium oxalate have shown to significantly reduce ($p<0.01$) renal level of MDA in group C3 animals as compared to hyperoxaluric group C2. The increase in MDA levels in this group as compared to control group C1 is also significant ($p<0.01$).

Similarly the dose of DAP also maintained MDA level in renal tissue of group C4 animals. As shown in figure 3.34, the content of MDA in group C4 is significantly ($p<0.01$) lower than hyperoxaluric rats of group C2, thus indicating a decreased lipid peroxidation in group C4 animals. On comparing the decrease in MDA content of group C3 and C4 no significant difference was observed thus indicating that both NAC and DAP at their respective doses are having similar properties.

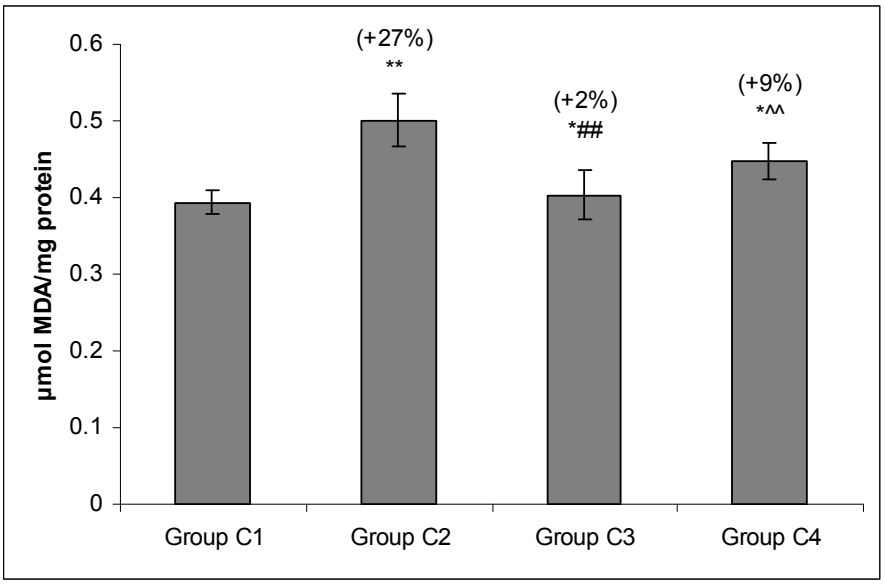


**Figure 3.34**. Effect on lipid peroxidation status of renal tissue after treatment of 24hrs.

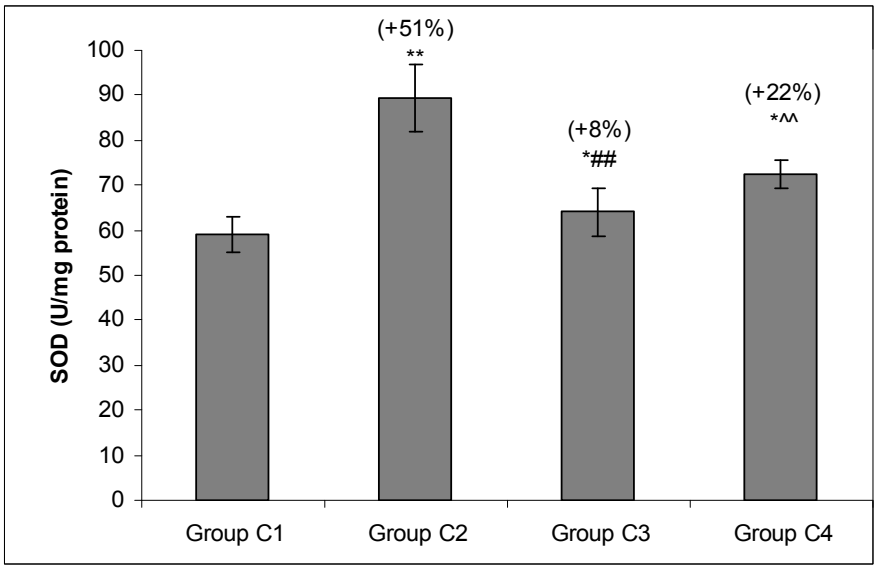


**Figure 3.35**. Effect on activity of SOD in renal tissue after treatment of 24hrs.

[*$p$<0.05, **$p$< 0.01, ***$p$< 0.001: Indicate significant change in comparison to control group C1. #$p$<0.05, ##$p$< 0.01, ###$p$< 0.001: Indicate significant change between group C2 and C3. ^$p$<0.05, ^^$p$< 0.01, ^^^$p$< 0.001: Indicate significant change between group C2 and C4. Values in brackets are % increase or % decrease as compared to group C1].

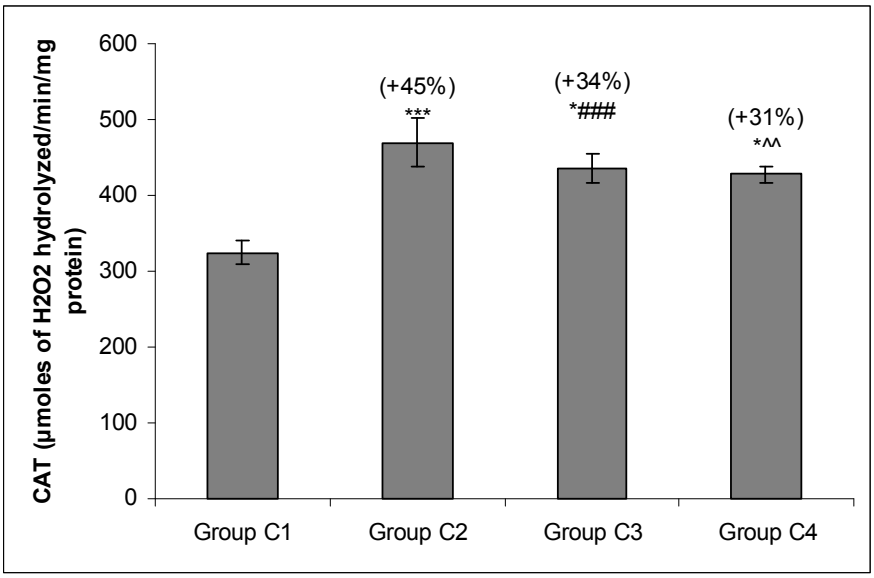


**Figure 3.36.** Effect on activity of catalase in renal tissue after treatment of 24hrs.

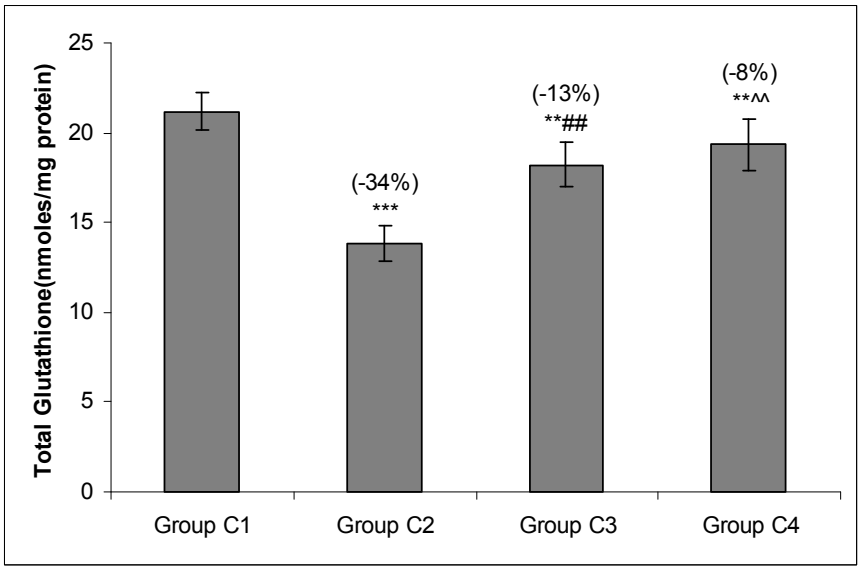


**Figure 3.37.** Effect on the content of total glutathione in the renal tissue.

[*$p$<0.05, **$p$< 0.01, ***$p$< 0.001: Indicate significant change in comparison to control group C1. #$p$<0.05, ##$p$< 0.01, ###$p$< 0.001: Indicate significant change between group C2 and C3. ^$p$<0.05, ^^$p$< 0.01, ^^^$p$< 0.001: Indicate significant change between group C2 and C4. Values in brackets are % increase or % decrease as compared to group C1].

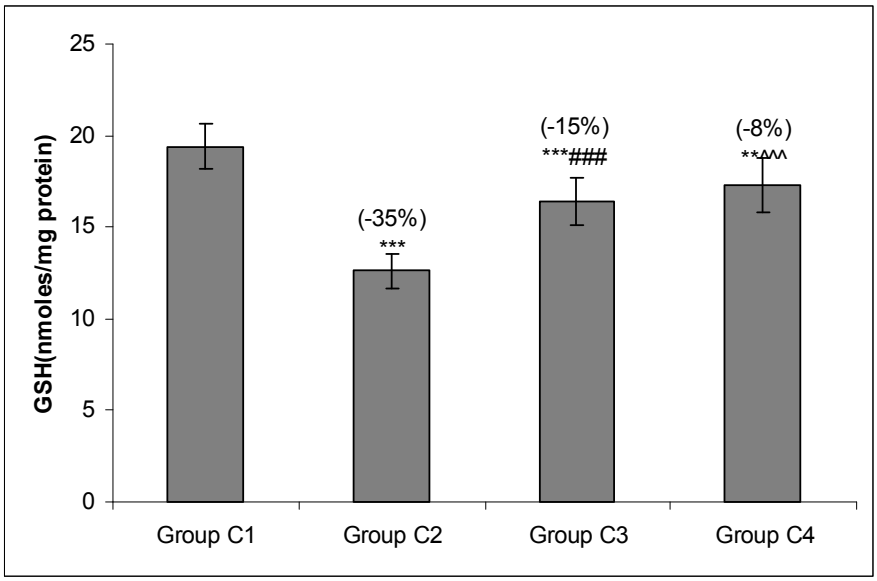


**Figure 3.38.** Effect on the content of reduced glutathione (GSH) after treatment of 24hrs.

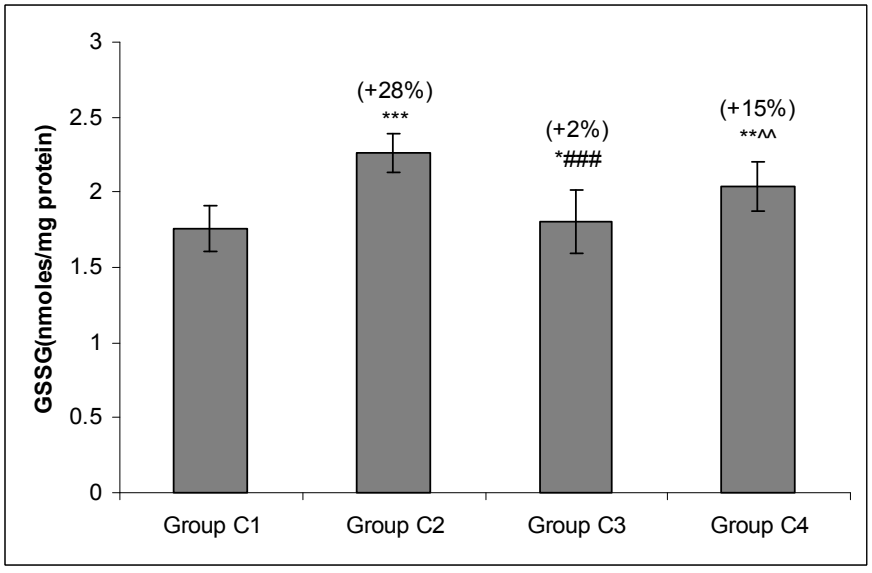


**Figure 3.39.** Effect on the content of GSSG after treatment of 24 hrs

[*$p$<0.05, **$p$< 0.01, ***$p$< 0.001: Indicate significant change in comparison to control group C1. #$p$<0.05, ##$p$< 0.01, ###$p$< 0.001: Indicate significant change between group C2 and C3. ^$p$<0.05, ^^$p$< 0.01, ^^^$p$< 0.001: Indicate significant change between group C2 and C4. Values in brackets are % increase or % decrease as compared to group C1].

### *3.5.7.2. Effect on the activity of superoxide dismutase (SOD)*

As a result of oxalate exposure to group C2 animals, the activity of enzyme superoxide dismutase (SOD) in the renal tissue was significantly elevated ($p<0.001$) as compared to control group C1 animals (Figure 3.35). The increase in SOD activity of group C2 was 51%. A marginal change of 8% in SOD activity was observed after NAC supplementation in group C3 animals when compared to control group C1. However on comparing the activity of SOD of group C3 with group C2 a significant ($p<0.01$) decrease was observed. The activity of SOD enzyme in group C4, given DAP in conjugation with sodium oxalate, was also significantly ($p<0.01$) lower as compared to group C2 (Figure 3.35).

### *3.5.7.3. Effect on the activity of catalase (CAT)*

The specific activity of catalase was significantly decreased ($p<0.01$) in sodium oxalate exposed rats of group C2 as compared to animals of control group C1. The activity of catalase in group C2 animals in comparison with control group C1 was found elevated by 45%.

After treatment of sodium oxalate exposed animals with NAC in group C3, a significant ($p<0.001$) decrease in the level of catalase activity from 45% to 34% (w.r.t control) was observed in comparison to hyperoxaluric group C2 animals. Correspondingly, group C4, in which animals are given treatment of DAP, displayed a significant decrease in catalase activity as compared to hyperoxaluric group C2 animals (Figure 3.36).

### *3.5.7.4. Effect on glutathione content*

Oxalate induction significantly depleted the levels of reduced (Figure 3.38) and total glutathione (Figure 3.37) in renal tissues ($p<0.001$). A decline of 35% in reduced glutathione (GSH) and 34% in total glutathione was found in group C2. On the other hand this decrease in both reduced and total glutathione was found to be stabilized in NAC treated group C3 animals.

Although both reduced glutathione and total glutathione level in the renal tissue of group C3 animals were significantly lower than control group C1 animals, but still, a significant increase in their content was observed as compared to hyperoxaluric group.

Similarly the level of both reduced and total glutathione was also restored in the DAP treated hyperoxaluric group 4 animals. On comparing the efficacy of DAP as compared to NAC in restoring glutathione level, it was found that DAP treated group C4 animals restored the level of glutathione in a relatively similar way as NAC treated group C3 animals.

The oxidized glutathione content (GSSG) of renal tissue after treatment period of 24 hrs is shown in figure 3.39. A marked elevation in the content of GSSG (28%) was observed after the oxalate exposure to group C2 animals. This increase in GSSG content was found significantly ($p$<0.001) decreased after NAC treatment to group C3 animals as compared to group C2. Similarly, DAP treatment also showed a decrease in content of GSSG as compared to group C2, after its dose.

The effect on redox ratio i.e GSSG/GSH is shown in figure 3.40. From the graph it can be observed that redox ratio is drastically high (113%) in group C2 animals. Whereas, in group C3 given NAC treatment, a significant ($p$<0.001) decrease in redox ratio was observed as compared to hyperoxaluric group C2. Likewise, in group C4 given DAP treatment, a normalized redox ratio was found. In addition, the redox ratio of DAP treated and NAC treated hyperoxaluric rats was highly comparable.

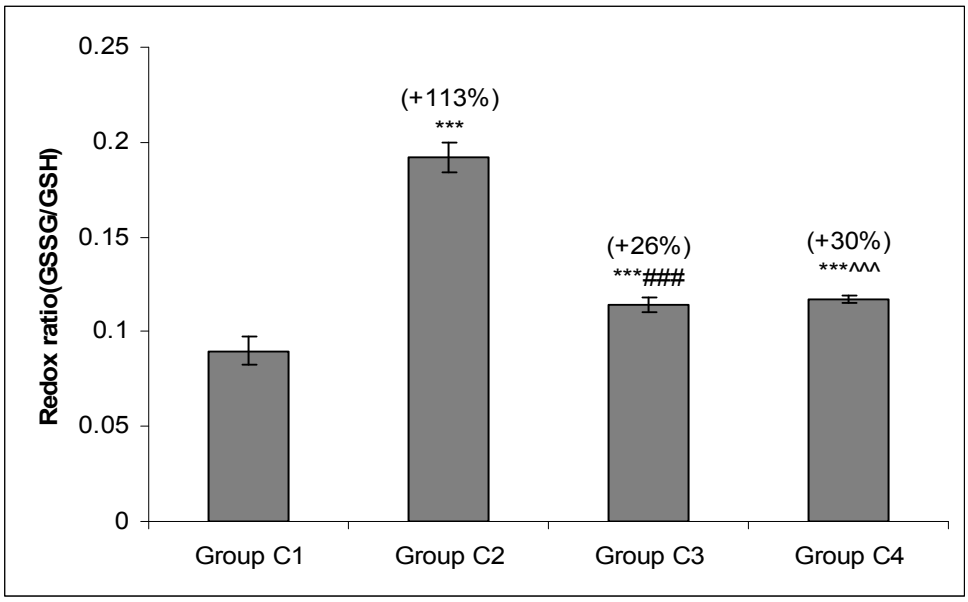


**Figure 3.40**. Effect on the redox ratio (GSSG/GSH) of renal tissue after treatment of 24 hrs.

[*$p$<0.05, **$p$< 0.01, ***$p$< 0.001: Indicate significant change in comparison to control group C1. #$p$<0.05, ##$p$< 0.01, ###$p$< 0.001: Indicate significant change between group C2 and C3. ^$p$<0.05, ^^$p$< 0.01, ^^^$p$< 0.001: Indicate significant change between group C2 and C4. Values in brackets are % increase or % decrease as compared to group C1].

# Chapter 4
# Discussion

Due to significant side effects and failure to prevent recurrence of kidney stones by the present day treatment procedures for urolithiasis, alternative treatment modalities by herbal products have assumed importance. Recent years have seen dramatic advances in phytotherapy for urolithiasis and many investigators have proposed to implicate scientific study on its efficacy [149]

There are various herbal drugs commercially available which are prescribed for treatment of kidney stones. The various drugs like Cystone, Uriflow, Renacare and Neeri are some examples of such drugs. These drugs are herbal composites and are prepared by mixing of various plant extracts in different proportions. Although, all these drugs have mixtures of more or less same plant extract but still they are not equally effective in all patients. In addition, some times the two different plants show antilithiatic effect individually but when they are mixed together, their efficacy is reduced. Like it is shown that *Bergenia ligulata* and *Dolichos biflorus* effectively inhibit calcium phosphate mineralization individually but together their efficacy is reduced [186] Since, alternative medication is not fully studied, so it is possible that the herbal plants known to have kidney stone inhibitory potential may also have certain toxins. *Salvia miltiorrhiza*, is a Chinese herb which is used to decrease the incidence of kidney stones. A small dose of this herb is usually recommended. In a case report by Wang and Yang [217], prescription of this herb in large amount by an unauthorized practitioner to a 15 years old boy for removal of kidney stone lead to severe neurological problems. He had severe dystonia in the trunk and limbs together with evident posture tremors. Chemical analysis showed that *Salvia miltiorrhiza* has a toxin named, Coumarin, which is toxic, mainly to the basal ganglia, and is possibly responsible for neurological symptoms in this patient. Clear analysis of herbs for their chemical component and testing each of them to determine what causes these clinical symptoms is of the utmost importance for preventing such tragedies. Identification of CaOx inhibitory biomolecules from herbs together with the chemical analysis for toxin compounds is very important to formulate an effective treatment for kidney stones.

Till date various plants extract have been studied to reduce the incidence of calcium stone deposition both *in vivo* and *in vitro* [218,219,220] but the identification of naturally occurring CaOx inhibitory biomolecules from plants was hampered in past by limitations in identification method. In the present research, an effective protein biomolecule from the seeds of *Dolichos biflorus* was isolated which has antilithiatic properties under both *in vitro* and *in vivo* conditions.

### *4.1. In vitro antilithiatic properties*

On comparing the antilithiatic ability of four plants viz. *Achyranthes aspera, Dolichos biflorus, Terminalia chebula*, *Cocos nucifera* using *in vitro* calcification assay, the seeds of *Dolichos biflorus* showed highest percentage of inhibition towards growth & demineralization of calcium phosphate and a significantly good inhibition towards initiation of CaP mineral phase formation (Figure 3.1, 3.2, 3.3). *Dolichos biflorus* seeds are common dietary food of north India and are known to have antilithiatic proficiency. There have been very few systematic studies on the antilithiatic properties of this plant [221,186,187]. Still, the constituents of *Dolichos biflorus* possessing antilithiatic property have not yet been identified. Based on *in vitro* antilithiatic potential of *Dolichos biflorus*, this study was aimed at purifying and characterizing the most potent biomolecule from it.

### *4.2. Protein from the seeds of Dolichos biflorus*

Various CaOx crystal growth inhibitors mostly proteins and glycosaminoglycans have been reported in humans to play an important role in renal stone diseases for several decades [222,223]. Most of these proteins have been isolated from CaOx kidney stones matrix itself in their active form [224,225]. Likewise, many plants are also known to produce CaOx as crystalline deposits [74,75] having an organic matrix constituting different proteins [116]. These proteins are believed to play an important role in the control of crystal growth and modification of crystal form [215]. More recently [117] four proteins from the organic matrix of CaOx crystals present in the seeds of *Phaseolus vulgaris*, have been isolated which inhibited the nucleation of CaOx crystallization in solutions. It was also shown that the isolated proteins modified the morphology of CaOx

crystals mainly at {120} face (fastest growing face). A well known CaOx inhibitor, citrate, has also shown to slow the growth of {120} face [226].

In the present study, an antilithiatic protein was isolated from the seeds of *Dolichos biflorus* inhibiting both calcium oxalate and calcium phosphate crystallization. The *Dolichos biflorus* antilithiatic protein (DAP) (98 kDa, pI 4.79) showed two bands of molecular weight 58 kDa & 34 kDa which clearly indicate its dimeric nature (Figure 3.9). Previous studies claim non-protein part to be responsible for antilithiatic nature [186, 187]. But our study showed the most active antilithiatic component to be a protein. There were certain other fractions which showed some extent of CaP and CaOx inhibition. Our focus was to find the most potent biomolecule, so we proceeded with the characterization protein fraction (DAP) having highest inhibitory potency. The MALDI–TOF MS analysis of DAP showed maximum similarity (35% sequence coverage) with calnexin (CNX) protein of *Pisum sativum* (CAA76741). Although molecular weight of CNX (62kDa) is not similar with DAP protein, but the pI of DAP is comparable with CNX (Figure 3.17) Since, many plant databases are still largely incomplete, many proteins present in *Dolichos biflorus* were found to be absent in those databases. So, DAP may not be homologous to CNX, but probably is a CNX like protein.

Calnexin, a type 1 membrane protein is as an interacting protein in the biogenesis of class I histocompatibility molecules in ER [227]. Calnexin is a predominant integral membrane protein of the ER and was first identified by its ability to bind $Ca^{2+}$ [228]. It has a long amino-terminal domain (460 amino acids) localized in the lumen of the ER, a single hydrophobic transmembrane domain, and a short, acidic cytosolic domain (91 amino acids). Calnexin may promote the proper assembly of protein complexes during transit through the ER. The retention and folding of such complexes is $Ca^{2+}$ dependent [229]. Calnexin has also been identified in nuclear membrane preparations [230], suggesting that it may also play a role in nuclear membrane trafficking or the regulation of nuclear $Ca^{2+}$ transients. Calnexin shares significant sequence similarity with calreticulin [231,232], the major $Ca^{2+}$ binding protein found in the lumen of the ER. Both calreticulin and calnexin lack "EF hand", a $Ca^{2+}$ binding motif found in the calmodulin

family of $Ca^{2+}$-regulated proteins [233]. However, these molecules contain unique subdomains that can be distinguished by charge, repeating motifs, and predicted secondary structure. A recently reported X-ray crystal structure shows that CNX consists of two domains, a globular domain and a long extended arm domain. Also, there are two disulfide bonds in the CNX structure, one in the globular domain, shown to be labile, and the second near the tip of the arm domain [234]. A lectin binding site was found within the concave surface of the globular domain and this it makes its structural similarity to legume lectin family. Additionally, a calcium binding site was also identified within the globular domain [235].

On exploring the inhibitory potency of DAP on calcium phosphate mineralization, again an effective inhibition was observed, thus clearly indicating that DAP is probably imparting its effect by binding to calcium ions. Probably DAP, which is CNX like protein has a calcium binding site, which might also be responsible for its ability to inhibit CaOx as well as CaP crystallization (Figure 3.11 & 3.12).

Lectins are particularly abundant in the seeds of legumes and they constitute upto 10% of soluble proteins in their seeds extract. *Dolichos biflorus*, a leguminous seed, has abundant lectins [236]. A report showed that adhesion of calcium phosphate and calcium oxalate crystals was inhibited by polyanions found in tubular fluid and by polycations and specific lectins that act on the apical cell surface of renal epithelial cells. They showed that lectins exerted their effect on the cell [237]. Treatment of cells with neuraminidase inhibited binding of crystals, suggesting that anionic cell surface sialic acid residues function as crystal receptor sites that can be blocked by specific cations or lectins [238]. This further strengthens the perspectives that DAP which is CNX like protein, possibly has a lectin domain that might be accountable for its calcium crystallization inhibitory properties as is observed during *in vivo* experiments.

It has been suggested that acidic amino acid residues such as Asp and Glu, that are expected to be deprotonated and negatively charged at urinary pH, are attracted to positively charged calcium ions of calcium stones [239]. Our data of amino acid analysis suggests that both CNX and DAP have higher acidic amino acids (Asp and Glu) content.

Thus, it could be argued that acidic amino acids present in the DAP, may possess the capability to inhibit calcium crystallization. A recent study by Wang et al. [216] presented that addition of serine spacer in poly-aspartate peptide increased its ability to inhibit COM crystallization. They suggested that the hydroxyl groups (-OH) of serine may have contributed in the interaction by directly binding to calcium ions and formation of hydrogen bonds. Another study says that phosphorylation of osteopontin is required for inhibition of calcium oxalate crystallization [252]. A significant amount of serine amino acids in DAP further ascertain its ability to inhibit CaOx crystallization.

### *4.3. Modeling of known kidney stone inhibitory proteins with COM crystal*

The use of molecular modeling and docking of compounds into the target sites of molecular models derived directly from resolved crystal structures has already proven valuable for discovering new ligands [240]. In the present study we have incorporated docking simulations to analyze the interactions between calcium oxalate monohydrate and proteins which are known to inhibit its growth. Docking energies are calculated as the sum of the intermolecular interactions (electrostatic + Van der Waals) plus the conformational energy of the ligand-domain complex determined by molecular mechanics [241]. More negative the docking score, stronger is the binding between ligand (COM in our study) and protein's active binding site. These strong interactions between protein active binding site and COM crystal, specifically at the growing sites would predict inhibition of COM crystal.

Each protein possessing the property of inhibiting COM crystallization taken in the present study showed diverse kind of interactions, supporting the fact that most of the kidney stone inhibitory proteins are multifunctional proteins. The property common to them is the ability to strongly interact with the free available growing sites (Ca, C and O atom) (Figure 2.5) of COM. It is known that COM crystal growth is slow in some directions since certain macromolecules adsorb on it and prevent formation of crystal lattice. Face (-101) of COM crystals is more active as it presents more closely packed calcium atoms and has significantly more adsorptive characteristics for many macromolecules (proteins) [242]. In the present investigation, it was observed that

calcium ions of COM form hydrogen bonding with varied amino acids of active binding sites and carbon of oxalate group gets involved in hydrophobic interactions. It is a fact that hydrogen-bonding are of primary significance in establishing strong complex between ligand and protein active binding site, but nevertheless hydrophobic interactions also act as a stabilizing factor and addition of a hydrophobic group not only allows hydrophobic bonding but also strengthens existing hydrogen bonds and the increased hydrogen bond strength can be an important factor in determining the overall binding energy [243].

The interaction of amino acids is also dependent on the conformation of the active sites, same amino acid in one instance is effectively involved in hydrogen bonding and in other instance same amino acid is involved in week hydrophobic interactions as is shown in the case of active binding site bikunin-1 (Figure 3.18). This dependence is purely steric hindrance, thus suggesting that not all amino acids which could strongly bind with calcium ions, although repeatedly present in the active binding site, interact with COM. Thus there is no advantage of repeated Glu residues until they are structurally available to interact. Strong hydrogen bonding of Glu and Asp with calcium ion of COM crystal supports the hypothesis that negatively charged acidic amino acids which are attracted to positively charged calcium ions [244]. The results presented by CD59-1 binding site supports the findings of Wesson et al. [245] that the charge of the side group was not the sole determinant to cause this effect, as Glu and Asp present in this binding site do not interact with COM. It is further perceived that proteins rich in gamma carboxy glutamic acid (CGU) possess two negative carboxylate groups have better binding to calcium ions of COM [246]. Here again it was observed from the results that although active binding site uripro-1 of protein urinary Prothrombin have repeated CGU monomers, still all the CGU are not involved in COM interactions (Figure 3.21). This evidence further suggests that conformational and interface chemistries interact in a complex manner to inhibit aggregation of COM and an understanding of such interactions may help to determine and control the factors affecting kidney stone formation.

In addition to inhibition of COM by acidic amino acids, certain other amino acids also showed optimal binding with COM unit cell. Osteonectin-2 and uripro-1 active binding site, showed formation of hydrogen bonding by Tyr and Ser, both form hydrogen bond through the hydroxyl group of their side chain with calcium ion. A recent study presented that addition of serine spacer in poly aspartate peptide increased their ability to inhibit COM crystallization [216]. They suggested that the hydroxyl groups (-OH) of serine may have contributed in the interaction by directly binding to calcium ions and form hydrogen bonds. This hypothesis is supported by our finding that the formation of hydrogen bonds is involved between the -OH group of both serine and tyrosine with calcium ion.

Hence, it can be concluded that amino acids interact with calcium ion by forming hydrogen bonds as well as hydrophobic interactions. Although acidic amino acids are primarily involved in establishing strong binding with COM but involvement of other amino acids is also important as it strengthen this interaction.

### *4.4. In vivo antilithiatic properties of DAP*

The antilithiatic activity of DAP was further confirmed in rat model to evaluate its efficacy *in vivo*. The protein was injected intraperitonealy (1 mg/kg and 2 mg/kg body weight) in stone forming animals and both the doses showed positive results towards decreasing COM crystals in a dose-dependent manner.

Determination of creatinine clearance more consistently predicts renal insufficiency than serum creatinine determination alone [247]. Creatinine clearance measures the volume of blood plasma that is cleared of creatinine per unit time. Clinically, creatinine clearance is useful measure for estimating the glomerular filtration rate of the kidneys, which is clinically important factor in determining renal functioning. The proper functioning of kidney after EG and $NH_4Cl$ dose is found to get hampered. As observed by Yamaguchi et al [248], the combination of high doses of EG and $NH_4Cl$ in the drinking water induced crystalluria and hyperoxaluria, along with calcium oxalate deposits in the kidney. In addition, deterioration of renal function was observed,

especially more after 11 days. Thus, the renal functioning was more vulnerable after 15 days dose than 9 days dose. To see the effect of DAP after long duration of its dosage and to see its ability to restore renal functioning after a marked deterioration, DAP was given for both 9 and 15 days at the dose of 1 mg and 2 mg per kg body weight. From these experiments, DAP was found to restore renal functioning in stone forming rats in a dose-dependant manner.

Renal dysfunction further diminishes the ability to filter urea and increases serum urea level [249]. The EG treated rats showed more urinary volume. This is an adjustment to filter toxic metabolites from the blood. But still the level of urea in serum was found high in EG and $NH_4Cl$ exposed animals for both 9 and 15 days treatment. Depending on the magnitude of renal dysfunction, the level of serum urea was more after 15 days treatment than after 9 days treatment. After EG and $NH_4Cl$ exposure the serum urea level increased, indicating renal dysfunctioning due to crystal deposition. Here, again rebalancing of serum urea further unveils the potential effect of DAP on maintaining renal functioning. It has been found that external prophylactic agents restore renal functioning by maintaining creatinine clearance and serum urea level in hyperoxaluric rats [250].

Alkaline phosphatase (AP) and lactate dehydrogenase (LDH) are two cytosolic enzymes and their higher activity in the extracellular fluid indicates cell lysis. Similarly, higher amount of AP and LDH in the urine is an indicator of renal cell injury and these enzymes are the injury marker enzymes. The enhanced urinary excretion of renal injury marker enzymes like AP and LDH in urolithiatic animals suggests damage to the brush border membrane of the renal tubules. This damage also appears to associate with the retention and deposition of crystals in the kidneys [251]. Recent *in vitro* studies have suggested that proximal tubule cells, when compared to distal tubule or collecting duct cells, are more sensitive to the toxic effects of both oxalate and calcium oxalate at pathological level [253].

The tissue injury which occurred upon administration of EG and $NH_4Cl$ resulted in increase of COM deposition in kidney tissue (Figure 3.33). The animals given EG and

$NH_4Cl$ dose for 15 days showed much higher excretion of renal injury markers enzymes than 9 days treatment (Figure 3.26 & 3.27). This is because EG results in many other toxic metabolites in addition to oxalic acid and exposure to these toxins for longer duration would results in higher order of renal injury [251]. DAP restored renal injury to the EG and $NH_4Cl$ exposed animals after treatment of both 9 and 15 days. This shows that in addition to reducing COM crystal and oxalate in rat kidneys, DAP has some additional properties of reducing toxic effects of other metabolites of ethylene glycol.

Khan [242] has hypothesized that inflammation in kidney tissue recruit macrophages to the sites of crystal deposition to reduce renal crystal burden and acts as an early defense against stone formation. Increased inflammation in stone forming animals as observed in renal histology is a protective mechanism against crystal deposition. Reduced inflammation in DAP treated stone forming animals depict fewer sites for crystal deposition. Crystal deposition which is mostly present in renal tubules [251], is also shown in our results. Crystal retention within the renal tubules is promoted by renal epithilial injury, which exposes a variety of crystal adhesion molecules like CD44 on its surface [254]. Decreased renal injury upon DAP administeration further decreases sites for calcium oxalate deposition which is evident from the polarization microscopy of renal tissue (Figure 3.33).

It has been documented that COM crystals either in free or aggregated form are found in the urine of urolithiatic patients [255,256]. COM crystals have greater affinity for renal tubular cells than COD and are responsible for the formation of stone in kidneys [257]. In the present study, administration of DAP reduced supersaturation of COM crystals in the urine as compared to the stone forming rats (Figure 3.28 & 3.29). In addition, a significant reduction in the size of COD crystals was also observed in animals given higher dose of DAP (2 mg/kg body weight). The formation of COD crystals in preference to COM crystals is propitious because it protects against stone disease by reducing the attachment of crystals to renal tubular cells.

Our results as shown in urolithiatic group A2 and B2 are in conformity with the dose selection of EG and $NH_4Cl$ based on the model developed by Yamaguchi et al [248]

where the crystal deposition in the kidney and stones attached to the papillary tip were found to be COM in nature, whereas COD were observed in the urine after giving the prescribed dose. This is due to the fact that COM crystals are prevalent in urolithiasis. After nine days treatment with DAP, the crystals excreted with the urine were less in number and that too only COD crystals were present but after 15 days treatment of urolithiatic rats with DAP, more COM crystals were excreted out instead of COD (Figure 3.28 & 3.29). This shows that after giving DAP for longer duration, it flush out COM crystal retained in the kidney tissue.

From above results, it can be strongly emphasized that DAP has an ability to reduce the incidence of crystal deposition *in vivo*. In addition to decreasing COM and COD crystal retention in kidney and their excretion in urine, DAP maintains proper renal functioning. DAP was also found to reduce renal injury which is evident from the restoration of renal marker enzymes (Figure 3.26 & 3.27).

### *4.5. Antioxidant properties of DAP*

Free radicals such as reactive oxygen species are formed during a variety of biochemical reactions and cellular functions such as mitochondria metabolism. Oxidative stress results from an imbalance between formation and neutralization of pro-oxidants. Various pathological processes disrupt this balance by increasing the formation of free radicals in proportion to the available antioxidants. Urinary excretion of renal tubular enzymes which are considered to be markers for renal injury [258] are the consequence of oxidative stress. AP and LDH (renal injury markers) excretion was normalized following DAP dosing in stone forming rats. This shows that DAP reduced renal injury, which further provides sites for CaOx deposition.

Oxalate is readily filterable at glomerulus and secreted by proximal tubules [259,260]. The damage of glomerulus and its capsule following oxalate exposure as shown in figure 3.31, might have been caused by oxalate itself or its derivative(s) acting as free radicals. In DAP treated stone forming animals the normal morphology of

glomeruli was restored. This effect could be attributed to antioxidant properties of DAP which might have reduced oxalate induced free radical damage.

The antioxidant properties of DAP were studied after inducing hyperoxaluria by sodium oxalate dose for 24 hrs. The dose (70 mg/kg body weight) of sodium oxalate was chosen because it is known to cause oxidative stress in kidney tissue [261], before the formation of calcium oxalate crystals. Thus, we could see the effect of DAP on oxidative stress, prior to calcium oxalate formation. In addition, the activity of DAP was also compared to a known antioxidant N-acetylcysteine (NAC) which was taken as a positive control. After 24 hrs treatment, the kidney tissue of rats were homogenised and variuos oxidative stress marker enzymes and lipid peroxidation were studied.

By definition lipid peroxidation is a process whereby free radicals "steal" electrons from the lipids in our cell membranes, resulting in cell damage and increased production of free radicals. Lipid peroxidation (LP) is the mechanism by which lipids are attacked by ROS that have sufficient reactivity to abstract a hydrogen atom from a methylene carbon in the side chain. The greater the number of double bonds in the molecule, the easier is the removal of the hydrogen atom. Thus, polyunsaturated fatty acids are in particular susceptible to lipid peroxidation. All the biological membranes are characterized by the large amount of polyunsaturated fatty acids associated with amphipathic lipids and a variety of membrane proteins. Lipid peroxidation of biological membranes results in loss of membrane fluidity, changes in membrane potential and increased membrane permeability.

In the present investigation, the level of malondialdehyde (MDA), which is an indirect index of lipid peroxidation, was found to be significantly elevated following oxalate exposure (Figure 3.34). So, it can be suggested that oxalate is injurious to renal tissue and the injury is caused by production of reactive free radicals. Oxalate is also known to induce free radical production like hydroxyl radical and peroxyl radical in renal tissue [262]. The reactive oxygen species culminate in phospholipase A2 activation through NF-κB (nuclear factor κB) DNA-binding activity [263], as NF-κB can be activated by the stress of oxidants [264]. NAC having a thiol group reduces the level of

free radicals responsible for the lipid peroxidation and thus decreases the level of malondialdehyde, the end product of lipid peroxidation. Since, DAP also showed decrease in lipid peroxidation, this implies that antioxidant ability of DAP is potent enough to quench oxalate-induced free-radical reaction.

The free radicals like hydroxyl radical, superoxide, hydrogen peroxide and peroxynitrite are generated during normal metabolism and cells contain multiple protective systems, which limit their damaging effects. These include network of protective enzymes and antioxidants, which prevent and intervene in the injurious oxidative reaction initiated by these species. The first line of defense against superoxide is superoxide dismutase (SOD). This enzyme dismutase the superoxide ion to $H_2O_2$ and $O_2$ [265]. Because, SOD enzyme generates $H_2O_2$, it works in collaboration with $H_2O_2$ removing enzymes. Catalase converts $H_2O_2$ to water and oxygen. Catalase is present in the peroxisomes of mammalian cells, and probably serves to destroy $H_2O_2$ generated by oxidase enzymes located within these subcellular organelles. Catalase is a hemoprotein and is responsible for the decomposition of hydrogen peroxide.

The increase in SOD activity after oxalate exposure could be an adaptive response of this enzyme to increased production of superoxide ions produced by activation of NAD(P)H oxidase via cytokine TGF-β1 (transforming growth factor β 1) induction [266]. NAC treatment is known to cause a decrease of TGF-β1 in mouse mesangial cells [267]. Because TGF-β1 activates NAD(P)H oxidase, which is a potent source of superoxide ion, the decrease in TGF-β1 level would result in decreased superoxide radicals and subsequently normalized enzyme activity. DAP also reduced the activity of SOD enzymes which further suggests that DAP could have reduced production of superoxide anion and hence lower the damage likely to result from its activity.

Further evidence of the efficacy of DAP in relieving oxalate-induced oxidative stress includes rebalancing of catalase activity. Because SOD enzyme generates $H_2O_2$, it works in collaboration with $H_2O_2$-removing enzyme catalase. The increased SOD activity in hyperoxaluric rats leads to production of hydrogen peroxide, which is further decomposed by catalase. Thus, catalase activity was also found to increase after oxalate

exposure to abate increased hydrogen peroxide. It has been reported that NAC supplementation reduces $H_2O_2$-induced damage of epithelial cells *in vitro* [268], suggesting that the decrease in catalase activity after NAC dose is an outcome of reduced $H_2O_2$ level. Subsequently, the decrease in catalase activity after DAP administration shows that DAP might have acted akin to NAC. The rebalancing of elevated antioxidant enzyme's activity by DAP treatment further substantiated the protective nature of DAP against free radical induced oxidative stress.

Glutathione (γ-glutamylcysteinylglycine, GSH) is a sulfhydryl (-SH) antioxidant, antitoxin, and enzyme cofactor. Glutathione is ubiquitous in animals, plants, and microorganisms, and being water soluble is found mainly in the cell cytosol and other aqueous phases of the living system [269]. Glutathione often attains millimolar levels inside cells, which makes it one of the most highly concentrated intracellular antioxidants. Glutathione exists in two forms the antioxidant reduced glutathione tripeptide, conventionally abbreviated as GSH and the oxidized form sulfur-sulfur (S-S) linked compound, known as glutathione disulfide or GSSG.

The GSSG/GSH ratio may be a sensitive indicator of oxidative stress. The reduced glutathione molecule consists of three amino acids - glutamic acid, cysteine, and glycine covalently joined end-to-end. The sulfhydryl (-SH) group, which gives the molecule its electron-donating character, comes from the cysteine residue. Glutathione is present inside cells mainly in its reduced (electron-rich, antioxidant) GSH form. In the healthy cell GSSG, the oxidized (electron-poor) form, rarely exceeds 10 percent of total cell glutathione. Intracellular GSH status appears to be a sensitive indicator of the cell's overall health, and of its ability to resist toxic challenge. Experimental GSH depletion can trigger suicide of the cell by a process known as apoptosis [270,271].

Hyperoxaluria induces oxidative stress and it is found that treatment with methionine [142] or glutathione monoester [143] reduced renal CaOx crystal deposits in the kidneys of hyperoxaluric rats. Both methionine and glutathione have sufhydryl (-SH) group. N-acetylcysteine too has an -SH group. It is also found to scavenge oxidants directly and increase intracellular GSH levels [272]. Thus, it was found that the dose of

NAC to hyperoxaluric rats resulted in an increase in the levels of GSH (Figure 3.38). Since, DAP dose also displayed an increase in GSH levels thus it can be stated that DAP might also possess antioxidant properties similar to NAC.

As stated above that the GSSG/GSH ratio (redox-ratio) is treated as a sensitive indicator of oxidative stress, this ratio was found to be increased in hyperoxaluric rats. Animals given NAC and DAP dose exhibited a decrease in this ratio (Figure 3.40) clearly indicating that DAP has similar antioxidant potential in reducing hyperoxaluria induced manifestations in rat kidney as that of NAC.

In a recent report, α-tocopherol was found to increase protein level of calnexin in the renal tissues and transfection of calnexin was protective against oxidative stress *in vitro* in rat renal tubular cells [273]. In another report, a protein restricted diet based on soy protein isolate has been found to increase hepatic expression of calnexin in pigs with superior oxidative stress response [274]. These studies suggest role of calnexin confering oxidative stress resistance by its induction. The mechanism by which DAP might have reduced renal injury is not yet elucidated but may be related to the fact that DAP probably acted against oxidative stress perhaps in the same way as calnexin.

# Summary & Conclusions

Urolithiasis, one of the most painful ailments of the urinary tract disorder, has beset humans from centuries. The formation of such concretions encompasses several physico-chemical events beginning with crystal nucleation, growth, aggregation [275] and ending by retention with renal tubular epithelial surfaces [276]. The mechanisms governing the induction of all these processes remain speculative. Calcium oxalate (CaOx) is the primary constituent of the majority of stones formed in the urinary system of patients with urolithiasis. Calcium oxalate monohydrate (COM), the thermodynamically most stable form, is observed more frequently in clinical stones than calcium oxalate dihydrate (COD) and it has a greater affinity for renal tubular cells, thus responsible for the formation of stones in kidney [257]. In addition to CaOx, another form of calcium deposits, calcium phosphate precipitates, are common in individuals who are older than 35 years and are considered as relatively benign form of renal calcification [254]. The saturation state of body fluids with respect to stone-forming constituents and the presence of various biomolecules (inhibitors/stimulators) in them as well as organic matrix are known to influence mineralization [21,23,224,225]. Certain stone inhibitory biomolecules such as proteins, lipids, glycosaminoglycans and inorganic compounds have been reported [111]. These kidney stone inhibitory biomolecules may keep the crystals from aggregating or accumulating as additional layers and thus prevent their growth.

Development of modern techniques has revolutionized surgical management of the problem. Extracorporeal shock wave lithotripsy (ESWL) is currently the first-line treatment for upper urinary tract calculi. This treatment is not without side effects [277], and kidney damage during ESWL is a clinically significant problem [278]. The mechanisms underlying shockwave-induced renal tubular injury are not completely understood, though shear forces, thermal and cavitation effects, and free radical formation have been postulated [279]. Therefore, it is worthwhile to look for an alternative for the management of urolithiasis. Many medicinal plants have been employed during ages to treat urinary stones though the rationale behind their use is not well established through systematic and pharmacological studies, except for some

composite herbal drugs and plants [183,161]. Interestingly, the areas having high consumption of these plant products, reported a very low incidence of urolithiasis and dietary patterns have been thought to play an important role for varied incidence of urinary calculi in the specific regions [280]

*Dolichos biflorus* is a leguminous pulse crop of subtropics. Its immature seeds are widely consumed as food in south Asian countries including rural areas of India. It is also used in folklore to treat urolithiasis. So far, only few investigators have studied its efficacy on calcium mineralization. More recently, the seeds of *Dolichos biflorus* were tested and compared with Cystone (commercial drug) for their *in vitro* anticalcification activity on calcium phosphate precipitation [186]. The extract of *Dolichos biflorus* showed inhibitory activity almost equivalent to Cystone towards calcium phosphate mineralization. Similar *in vitro* study showed the possibility of more than one biomolecules in *Dolichos biflorus*, possessing the ability to inhibit calcium phosphate precipitation [187]. There are no reports in the literature of the exact clinical role and efficacy of this plant on *in vivo* urolithiasis. In the present study the efficacy of *Dolichos biflorus* towards CaOx and CaP was examined *in vitro* and further the most potent biomolecule responsible for its antilithiatic property was identified and validated in rat urolithiatic model. The whole work is summarized below:

1. Among all the four plants (viz. *Achyranthes aspera*, *Dolichos biflorus*, *Cocos nucifera*, *Tribulus terrestris*), the seeds of *Dolichos biflorus* showed highest percentage of inhibition towards growth & demineralization of calcium phosphate and significantly good inhibition towards initiation of CaP mineral phase formation. Preliminary fractionation on the basis of molecular weight of biomolecules into more than and less than 10kDa fractions showed the antilithiatic activity in both the fractions indicating that there is possibility of more than one biomolecule possessing this ability.
2. An antilithiatic protein was isolated from the seeds of *Dolichos biflorus* inhibiting both calcium oxalate and calcium phosphate crystallization. It was purified by three step purification scheme involving ammonium sulfate fractionation, anion

exchange and molecular sieve chromatography based on its ability to inhibit calcium oxalate crystallization *in vitro*. The *Dolichos biflorus* antilithiatic protein (DAP) showed two bands of molecular weights 58 kDa & 34 kDa which clearly indicate its dimeric nature and a single band on native PAGE indicating its purity.

3. The characterization of *Dolichos biflorus* antilithiatic protein (DAP) showed that DAP has a molecular weight of 98 kDa and isolectric point of 4.79. Amino acid analysis of DAP showed abundant presence of acidic amino acids (Asp and Glu). Further, Matrix-assisted laser desorption/ionization-time-of-flight mass spectrometry (MALDI-TOF MS) of DAP showed similarities (35% sequence coverage) with calnexin (CNX) protein of *Pisum sativum* (CAA76741). The pI of DAP is comparable with CNX, so DAP is probably CNX like protein. Since, a calcium binding site has been identified in the globular domain of CNX, this suggests that DAP might have a calcium binding site which imparts it the ability to inhibit both CaOx and CaP crystallization.

4. The antilithiatic activity of DAP was further confirmed on rat model to evaluate its efficacy *in vivo*. The protein was injected intraperitoneally (1mg/Kg and 2mg/Kg body weight) in stone forming animals and both the doses showed positive results in a dose-dependent manner. DAP was found to restore renal functioning in stone forming rats by maintaining creatinine clearance and serum urea level. The administration of DAP reduced supersaturation of COM crystals in the urine as compared to stone forming rats. In addition, a significant reduction in the size of COD crystals was also observed in animals given higher dose of DAP (2mg/kg body weight). The crystal deposition in the kidney tissue as observed by polarization microscopy, was also reduced in animals given DAP and that too in a dose-dependant manner. Thus, it clearly suggests that in addition to its ability to inhibit crystallization *in vitro*, DAP was also found to be effective in decreasing crystal formation *in vivo* in rat urolithiatic model.

5. DAP was also found to decrease the excretion of renal injury marker enzymes in addition to decreasing calcium oxalate crystals deposition in urolithiatic rats,

implying that DAP also has an ability to mitigate renal injury. Calnexin has shown protective nature against oxidative stress *in vitro* in rat renal tubular cells, DAP might have the similar ability since, it is CNX like protein. To further validate the protective nature of DAP as an antioxidant; its efficacy was compared with a known antioxidant N-acetylcysteine. DAP dose has shown the ability to reduce lipid peroxidation, maintain level of antioxidant enzymes and redox-ratio (GSH/GSSG) comparable to NAC in sodium oxalate induced hyperoxaluria.

Hence, a plant protein from the seeds of *Dolichos biflorus* is shown to possess the ability of inhibiting calcium oxalate crystallization both *in vitro* and *in vivo*. This protein (DAP) is anionic in nature having abundant acidic amino acids, indicating its similarity with calnexin of *Pisum sativum* which belongs to lectin group of proteins, having calcium binding site, so this provides an explanation for its efficacy to reduce CaP and CaOx crystallization. Our present results put forth the possibility of using plant proteins as therapeutic agents to treat urolithiasis. The work presented here will open new vistas for protein therapeutics from medicinal plants for the management of urolithiasis.

# List of Publications

***PUBLICATIONS***

1. Bijarnia RK, Kaur T, Naik PK, Singla SK, Tandon C. *Online Journal of Bioinformatics*. (Accepted). 2008
2. Bijarnia RK, Kaur T, Aggarwal K, Singla SK, Tandon C. *Food and Chemical Toxicology*. 46, 2274-2278. 2008
3. Bijarnia RK, Kaur T, Singla SK, Tandon C. *Drug and Chemical Toxicology*.30, 229-240. 2007
4. Tandon C, Bijarnia RK, Singla SK. *Panjab University Research Journal*. 56, 1-12.

***CONFERENCES***

1. Bijarnia RK, Kaur T, Singla SK, Tandon C. "Comparative analysis of the anti-calcifying properties of different plants". *Emerging Trends in Biochemistry* (Symposium), Panjab University Chandigarh. (2006)
2. Bijarnia RK, Kaur T, Singla SK, Tandon C. "A novel antilithiatic protein from the seeds of Dolichos biflorus". *Biophysics in Medicine & Biology*. Conference Conducted by: Indian Biophysical Society at Panjab University Chandigarh. 2007

***COMMUNICATED PAPERS***

1. Bijarnia RK, Kaur T, Singla SK, Tandon C. "A novel antilithiatic protein from the seeds of Dolichos biflorus: its validation on rat urolithiasis model".
2. Bijarnia RK, Kaur T, Singla SK, Tandon C "Oxalate mediated oxidant-antioxidant imbalance in erythrocytes; role of N-acetyl cysteine.
3. Bijarnia RK, Kaur T, Singla SK, Tandon C "Antioxidant property of protein from the seeds of Dolichos biflorus: its comparison with N-acetyl cysteine"

# Bibliography

[1] Worcester EM, Coe FL. *Prim Care*. **35,** 369-91. 2008

[2] Collins C. Edward. *A Short Course in Medical Terminology*. Lippincott Williams & Wilkins. 2005

[3] Weaver SH, Jenkins P. *Illustrated Manual of Nursing Practice*, 3rd edition, Lippincott Williams & Wilkins. 2002

[4] Stamatelou, Kiriaki K, Francis, Mildred E, Jones, Camille A, Nyberg Jr, Leroy M, Curhan, Gary C. *Kidney Int.* **63**, 1817–21. 2003

[5] Pietrow, Paul K, Karellas, Michael E. *Am Fam Physici.* **74**, 86–94. 2006

[6] Brikowski TH, Lotan Y, Pearle MS. *Proc Natl Acad Sci U S A.* **105**, 9841-6. 2008

[7] Eknoyan, Garabed. *Clin Rev Bone Miner Metabol.* **2,**177–85. 2004

[8] Shah J, Whitfield HN. *BJU Int.* **89,** 801–10. 2002

[9] Basler, Joseph, Ghobriel, Aldo, Talavera, Francisco, Resnick, Martin I., Wolf J, Stuart Jr, Leslie, Stephen W. *Bladder Stones.* 2007

[10] Auge, Brian K, Preminger, Glenn M. *Curr Opi Urol.* **12,** 287–90. 2002.

[11] Ciftçioglu N, Haddad RS, Golden DC, Morrison DR, McKay DS. *Kidney Int.* **67,** 483–91. 2005

[12] Mandel N. *Sem Nephrol*. **16**, 3364 -742. 1996

[13] Keutal HJ, Sing JS.*Urol*. **2**, 115-22. 1964

[14] Boyce WH, Garvey FK. *Am J Medi.* **45,** 673-83. 1968

[15] Atmani F, Khan SR. *Urol Int*. **68**, 54-9. 2002

[16] Dussol B, Geider S, Lilova A, Leonetti F, Dupuy P, Daudon M, Berland Y, Dagorn JC, Verdier JM.. *Urol Res*. **23,** 45-51. 1995

[17] Sakakura T, Fujita K, Yasui T, Sasaki S, Mabuchi Y, Iguchi M, Kohri K. *Urol Res*. **27**, 200-5. 1999

[18] Daskalova S, Kostadinova S, Gauster D, Prohaska R, Ivanov A. *Microb Pathog*. **25**, 197-201. 1998

[19] Ryall RL, Chauvet MC, Grover PK. *BJU Int.* **96**, 654-63. 2005

[20] Tandon CD, Forouzandeh M, Aggarwal S, Jethi RK. *Mol Cell Biochem*. **171**, 29-35. 1997

[21] Tandon CD, Aggarwal S, Forouzandeh M, Jethi RK. *J Cell Biochem*. **68,** 287-97.1998

[22] Costa-Bauza A, Isern B, Perello J, Sanchis P, Grases F. *Scand J U Nephrol*. **39,** 194-9. 2005

[23] Moghadam MF, Tandon C, Aggarwal S, Singla SK, Singh SK, Sharma SK, Varshney GC, Jethi RK. *J Cell Biochem.* **15**, 1261-75. 2003

[24] Chow K, Dixon J, Gilpin S, Kavanagh JP, Rao PN. *Kidney Int.* **65,** 1724-30. 2004

[25] Borges FT, Michelacci YM, Aguiar JA, Dalboni MA, Garofalo AS, Schor N. *Kidney Int*. **68,** 1630-42. 2005

[26] Pillay SN, Asplin JR, Coe FL. *Am J Physiol.* **275**, 255-61. 1998

[27] Ricchiuti V, Hartke DM, Yang LZ, Goldman HB, Elder JS, Resnick MI, Marengo SR *BJU Int*. **90**, 513-7. 2002

[28] Selvam R, Kalaiselvi P. *Urol Res*. **31,** 242-56. 2003

[29] Ozgurtas T, Yakut G, Gulec M, Serdar M, Kutluasy T. *Urol Int*. **72,** 233-6. 2004

[30] Jonassen JA, Cao LC, Honeyman T, Scheid CR. *Nephron Exp Nephrol*. **98,** 61-4. 2004

[31] Benitez IO, Talham DR. *J Am Chem Soc.* **9**, 2814-5. 2005

[32] Guerra A, Allegri F, Meschi T, Adorni G, Prati B, Nouvenne A, Novarini A, Maggiore U, Fiaccadori E, Borghi L. *Clin Chem Lab Med.* **43,** 585-9. 2005

[33] Sakhaee K, Adams-Huet B, Moe OW, Pak CY. *Kidney Int*. **62,** 971-9. 2002

[34] du Toit PJ, Van Aswegen CH, Steinmann CM, Klue L, Du Plessis DJ. *Med Hypotheses.* **49** 57-9. 1997

[35] Subha K, Varalakshmi P. *Mol Biol Int.* **29**, 271-80. 1993

[36] Trinchieri A, Mandressi A, Luongo P, Rovera F, Longo G. *Scand J Urol Nephrol*. **26,** 379-86.1992

[37] Ramello A, Vitale C, Marangella M. *J Nephrol*. **13**, 45-50. 2000

[38] Soucie JM, Coates RJ, McClellan W, Austin H, Thun M. *Am J Epidemiol*. **1**, 487-95. 1996

[39] Taylor EN, Stampfer MJ, Curhan GC. *J Am Nephrol*. **15,** 3225-32. 2004

[40] Massey LK, Liebman M, Kynast-Gales SA. *J Nutr*. **35,** 1673-7. 2005

[41] Moyad MA. *Urol Nurs.* **23,** 69-74. 2003

[42] Sakly R, Fekih M, Ben Amor A, Najjar MF, Mbazaa M. *Ann Urol*. **37**, 217-9. 2003

[43] Chen J, Liu J, Zhang Y, Ye Z, Wang S. *Chin Med J.* **116**, 569-72. 2003

[44] Carvalho M, Ferrari AC, Renner LO, Vieira MA, Riella MC. *Rev Assoc Med Bras*. **50,** 79-82. 2004

[45] Goldfarb DS, Fischer ME, Keich Y, Goldberg J. *Kidney Int.* **67**, 1053-61. 2005

[46] Maloney ME, Springhart WP, Ekeruo WO, Young MD, Enemchukwu CU, Preminger GM. *J Urol*, **173** 2001-4. 2005

[47] Wolf MT, Zalewski I, Martin FC, Ruf R, Muller D, Hennies HC, Schwarz S, Panther F, Attanasio M, Acosta HG, Imm A, Lucke B, Utsch B, Otto E, Nurnberg P, Nieto VG, Hildebrandt F. *Nephrol Dial Transplant*, **20,** 909-14. 2005

[48] Prié D, Huart V, Bakouh N, Planelles G, Dellis O, Gérard B, Hulin P, Benqué-Blanchet F, Silve C, Grandchamp B, Friedlander G. *N Engl J Med*. **347,** 983-91. 2002

[49] Weisinger JR. *Kidney Int.* **49,** 1507-18. 1996

[50] Bid HK, Kumar A, Kapoor R, Mittal RD. *J Endourol*. **19,** 111-5. 2005

[51] Cousin JL, Motais R. *J Physiol.* **256,** 61-80. 1976

[52] Strzelecki T, Menon M. *J Biol Chem*. **15,** 12197-201. 1986

[53] Simmonds HA. *Orphanet Encyclopedia*. 2003.

[54] Skopkova Z, Hrabincova E, Stastna S, Kozak L, Adam T. *Ann Hum Genet*. **69,** 501-7. 2005

[55] Yenchitsomanus PT. *Southeast Asian J Trop Med Pub Health.* **34**, 651-8. 2003

[56] Devuyst O. *Bull Mem Acad R Med Belg.* **159,** 212-7. 2004

[57] Blanchard A, Jeunemaitre X, Coudol P, Dechaux M, Froissart M, May A, Demontis R, Fournier A, Paillard M, Houillier P. *Kidney Int*. **59**, 2206-15. 2001

[58] Pidasheva S, D'Souza-Li L, Canaff L, Cole DE, Hendy GN. *Hum Mutat.* **24,** 107-11. 2004

[59] Meschi T, Schianchi T, Ridolo E, Adorni G, Allegri F, Guerra A, Novarini A, Borghi L *Urol Int*. **72,** 29-33. 2004

[60] Coen G, Sardella D, Barbera G, Ferrannini M, Comegna C, Ferazzoli F, Dinnella A, D'Anello E, Simeoni P. *Urol Int.* **67,** 49-53. 2001

[61] Braun S, Lafrenz R. *Dtsch Tierarztl Wochenschr*. **112**, 70-3. 2005

[62] Cancho Gil MJ, Diz Rodriguez R, Virseda Chamorro M, Alpuente Roman C, Cabrera Cabrera JA, Panos Lozano P. *Actas Urol Esp*. **29**, 373-7. 2005

[63] Nardi AC, Ferreira U, Claro JA, Stopiglia GM, Netto NR Jr. *Int Braz J Urol*. **30**, 142-7. 2004

[64] Bedir S, Kilciler M, Cincik M, Ozgok Y. *Fertil Steril*. **82**, 1687-8. 2004

[65] Aksoy Y, Malkoc I, Atmaca AF, Aksoy H, Altinkaynak K, Akcay F. *Cell Biochem Funct*. **24**, 467-9. 2005

[66] May M, Gunia S, Helke C, Seehafer M, Hoschke B. *Aktuelle Urol.* **35**, 316-9. 2004

[67] Arnott HJ, Pautard FGE. *Biological Calcification: Cellular and Molecular Aspects*, Appleton-Century-Crofts, New York. 1970

[68] Gallaher RN. *Soil Sci Plant Anal*. **6**, 315–30. 1975

[69] Franceschi VR, Horner HT. *Bot Rev*. **46**, 361–427. 1980

[70] Prychid JC, Rudall PJ. *Ann Bot.* **84**, 725–39. 1999

[71] Nakata P. *Plant Sci.* **164**, 901–09. 2003

[72] Horner HT, Wagner BL. *Am J Bot.* **67**, 1347–60. 1980

[73] Webb MA, Cavaletto JM, Carpita NC, Lopez LE, Arnott HJ. *Plant J.* **7,** 633–48. 1995

[74] Webb MA. *Plant Cell* **11**, 751–61. 1999

[75] Nakata PA, McCon M. *Plant Physiol*. **124**, 1097–104. 2000

[76] Kausch AP, Horner HT. *Am J Bot*. **70**, 691–705. 1983

[77] Horner HT, Wagner BL. *Calcium Oxalate in Biological Systems*, CRC Press, Boca Raton. 1995

[78] Webb MA, Arnott HJ. *Scanning Electron Microsc*. **4**, 1759–70. 1983

[79] Mazen AM, Maghraby OMO. *Biol Plant.* **40,** 411–17. 1998

[80] Kausch AP, Horner HT. *Scanning Electron Microsc*. **3,** 263–72. 1981

[81] Modeseni P, Bombardi V, Giordani P, Brunialti G, Corallo A, *Lichenologist.* **32**, 505–12. 2000

[82] Bradbury JH, Nixon RW. *J Sci Food Agric.* **76**, 608–16. 1998

[83] Arnott HJ, Webb MA. *Int J Plant Sci*. **161,** 133–42. 2000

[84] Saltz D, Ward D. *Plant Ecol*. **148**, 127–38. 2000

[85] Kohl FG. *Elwert'sche Verlagsbuchhandlung*. Marburg, Germany. 1889

[86] Haberlandt G**.** *Physiological Plant Anatomy*. Mac-Millan, London. 1914

[87] Demarty M, Morvan C, Thellier M. *Plant Cell Environ*. **7**, 441–48. 1984

[88] Bush DS. Annu. Rev. Plant Physiol. *Annu Rev Plant Physiol Plant Mol Biol.* **46,** 95–122. 1995

[89] Kinzel H. *Flora*. **182,** 99–125. 1989

[90] Vanaman TC, Sharief F, Watterson DM. *$Ca^{2+}$ Binding Proteins and $Ca^{2+}$-Function*. North Holland, New York, Amsterdam, Oxford. 1977

[91] Hepler PK. *Cell Calcium.* **16,** 322–30. 1994

[92] Leigh RA, Tomos AD. *Philos Trans R Soc Lond*. **341,** 75–86. 1993

[93] Fink S. *New Phytol*. **119,** 33–40. 1991

[94] Zindler-Frank E. *Pflanzenphysiol*. **80**, 1–13. 1976

[95] Franceschi VR. *Protoplasma,* **148**, 130–37. 1989

[96] Zindler-Frank E. *Pflanzenphysiol*. **77,** 80–85. 1975

[97] Wang ZY, Gould KS, Patterson KJ. *Int J Plant Sci*. **155**, 342–9. 1994

[98] Foster AS. *Protoplasma.* **46**, 184–93. 1956

[99] Borchert RL. *Bot Gaz*. **145**, 474–82. 1984

[100] Webb MA, Arnott HJ. *Scan Electron Microsc.* **3**, 1109–31. 1982

[101] Spitzer E, Lott JNA. *Can J Bot*. **60**, 1381–91. 1982

[102] Brubaker CL, Horner HT. *Can J Bot*. **67**, 1664–70. 1989

[103] Arnott HJ, Pautard FGE, Steinfink H. *Nature*. **208,** 1197–98. 1965

[104] Frey-Wyssling A. *Am J Bot*. **68**, 130–41. 1981

[105] Volk GM, Lynch-Holm VM, Kostman TA, Franceschi VR. *Plant Biol.* **4,** 34–45. 2002

[106] Bouropoulos N, Weiner S, Addadi L. *Chem Eur J.* **7,** 1881–8. 2001

[107] Lowenstam HA, Weiner S. *On Biomineralization*. Oxford University Press, New York 1989

[108] Aizenberg J, Hanson J, Ilan M, Leiserowitz L, Koetzle TF, Addadi L, Weiner S. *FASEB J.* **9,** 262–8. 1995

[109] Albeck S, Addadi L, Weiner S. *Connec Tissue Res.* **35,** 419–24. 1996

[110] Aizenberg J, Hanson J, Koetzle TF, Weiner S, Addadi L**.** *J Am Chem Soc.* **119,** 881–6. 1997

[111] Ryall RL. *Pediatr Nephrol*. **10**, 656–6. 1996

[112] Weiner S, Addadi L**.** *Trends Biol Sci*. **16,** 252–56. 1991

[113] Guo SW, Ward MD, Wesson JA. *Langmuir.* **18,** 4284–91. 2002

[114] Shiraga H, Min W, VanDusen WJ, Clayman MD, Miner D, Terrell CH, Sherbotie JR, Foreman JW, Przysiecki C, Neilson EG. *Proc Natl Acad Sci USA.* **89,** 426–30. 1992

[115] Hoyer JR, Asplin JR, Otvos L. *Kidney Int.* **60,** 77–82. 2001

[116] Li X, Zhang D, Lynch-Holm VJ, Okita TW, Franceschi VR. *Plant Physiol*. **133**, 549–59. 2003

[117] Jáuregui-Zúñiga D, Reyes-Grajeda JP, Moreno A. *Plant Science*. **168,** 1163–9. 2005

[118] Danpure CJ, Purdue PE. Metabolic and molecular bases of inherited disease. 7th edn. McGraw- Hill, New York. 1995

[119] Hatch M, Freel RW, Vaziri ND. *J Am Soc Nephrol*. **10,** 324-8, 1999

[120] Hackett RL, Shevock PN, Khan SR. *Urol Res.* **22**, 197-203, 1994

[121] Koul H, Kenington L, Nair G, Honeyman T, Menon M, Scheid CR. *Biochem Biophys Res Commun.* **205**, 1632-7. 1994

[122] Koul H, Kenington L, Honeyman T, Jonassen J, Menon M, Scheid CR. *Kidney Int.* **50**, 1525-30. 1996

[123] Khan SR. *Urol Res.* **23,** 71-9. 1995

[124] Khan SR. *Clin Exp Nephrol.* **8**, 75-88. 2004

[125] Khan SR. *Nephron Exp Nephrol.* **98,** 55-60. 2004

[126] Scheid CR, Koul H, Hill WA, Luber-Narod J, Kennington L, Honeyman T, Jonassen J, MenonM. *Kidney Int.* **49**, 413-9. 1996

[127] Thamilselvan S, Hackett RL, Khan SR. *J Urol.* **157,** 1059-63. 1997

[128] Thamilselvan S, Hackett RL, Khan SR. *J Urol.* **164,** 224-9. 2000

[129] Thamilselvan S, Khan SR, Menon M. *Urol Res.* **31**, 3-9. 2003

[130] Khan SR, Kok DJ. *Front Biosci.* **9,** 1450-82. 2004

[131] Khan SR, Byer KJ, Thamilselvan S, Hackett RL, McCormack WT, Benson NA, Vaughn KL, Erdos GW. *J Am Soc Nephrol*. **10**, 457-63. 1999

[132] Miller C, Kennington L, Cooney R, Kohjimoto Y, Cao LC, Honeyman T, Pullman J, Jonassen J, Scheid C. *Toxicol Pharmacol.* **162,** 132-8. 2000

[133] Khan SR, Finlayson B, Hackett RL. *Am J Pathol*. **107**, 59-69. 1982

[134] Khan SR. *Scanning Microsc.* **9,** 89-100. 1995

[135] Fasano JM, Khan SR. *Kidney Int.* **59**, 169-78. 2001

[136] Riese RJ, Mandel NS, Wiessner JH, Mandel GS, Becker CJ, Kleinman JC. *Am J Physiol.* **262**, 177-84. 1992

[137] Verkoelen CF, Van der Broom BG, Houtsmuller AB, Schroeder FH, Romijn JC. *Am J Physiol*. **274,** 958-65. 1998

[138] Bigelow MW, Wienner JH, Kleinman JC, Mandel NS. *Am J Physiol.* **272**, 55-61. 1999

[139] Wiessner JH, Hasegawa AT, Hung LY, Mandel NS. *J Am Soc Nephrol.* **10,** 441-5. 1999

[140] Thamilselvan S, Selvam R. *Indian J Biochem Biophys.* **34**, 319-23. 1997

[141] Kumar S, Selvam R. *J Nutr Biochem.* **14**, 306-9. 2003

[142] Selvam R, Ravichandran V. *Indian J Exp Biol.* **31,** 882-7. 1993

[143] Muthukumar A, Selvam R. *Mol Cell Biochem.* **185,** 77-84. 1998

[144] Ito Y, Yasui T, Okada A, Tozawa K, Hayashi Y, KohriK. *J Urol.* **173**, 271-5. 2005

[145] Toblli JE, Ferder L, Stella I, De Cavanagh MVE, Angerosa M, Inserra F. *J Urol.* **168,** 1550-5. 2002

[146] Antus B, Exton MS, Rosivall L. *Int J Immunopathol Pharmacol.* **14**, 25-30. 2001

[147] Umekawa T, Chegini N, Khan SR. *Kidney Int.* **61,** 105-12. 2002

[148] Pearle MS. *Curr Opin Nephrol Hypertens.* **10,** 203-9. 2001

[149] Gürocak S, Küpeli B. *J Urol.* **176,** 450-5. 2006

[150] Eisenberg DM, Kessler RC, Foster C, Norlock FE, Calkins DR. *N Engl J Med.* **328**, 246-52. 1993

[151] Eisenberg DM, Davis RB, Ettner SL, Appel S, Wilkey S, Van Rompay M, Kessler RC. *JAMA.* **280**, 1569-75. 1998

[152] Brevoort P. *Herbal Gram.* **36**, 49-57. 1996

[153] Johnston B. *Herbal Gram.* **40**, 52. 1997

[154] Akerele O. *Policy and implementation: International Traditional Health Newsletter*. World Health Organization, Switzerland. 1985

[155] Farnsworth NR. *Bioactive compounds from plants (Ciba Symposium 154)*. Wiley, NY. 1990

[156] Ohkawa T, Ebisuno S, Kitagawa M, Morimoto S, Miyazaki Y. *J Urol.* **129**, 1009-11. 1983

[157] Ohkawa T, Ebisuno S, Kitagawa M, Morimoto S, Miyazaki Y, Yasukawa S. *J Urol.* **132**, 1140-45. 1984

[158] Ebisuno S, Morimoto S, Yoshida T, Fukatani T, Yasukawa S, Ohkawa T. *Br J Urol.* **58**, 592-5.1986

[159] Grases F, Masarova L, Costa-Bauzá A, March JG, Prieto R, Tur JA. *Planta Med.* **58**, 509-12. 1992

[160] Grases F, March JG, Ramis M, Costa-Bauzá A. *Phytotherapy Res.* **7**, 146-9. 1993

[161] Grases F, Ramis M, Costa-Bauzá A, March JG. *J Ethnopharmacol.* **45**, 211-14. 1995

[162] Koide T, Yamaguchi S, Utsunomiya M, Yoshioka T, Sugiyama K. *Int J Urol.* **2,** 81-6. 1995

[163] Yasui T, Fujita K, Sato M, Sugimoto M, Iguchi M, Nomura S , Khori K. *Urol Res.* **27**, 194-9.1999

[164] Calixto JB, Santos ARS, Filho VC, Yunes RA. *Med Res Ver.* **18**, 225-8.1998

[165] Freitas AM, Schor N , Boim MA. *BJU Int.* **89**, 829-34. 2002

[166] Santos AR. *J Pharm Pharmacol.* **46**, 755-9.1994

[167] Alexander HC, Nestor S. *Nephron.* **81**, 393-7.1999

[168] Ballabh B, Chaurasia OP, Ahmed Z, Singh SB. *J Ethnopharmacol.* **118,** 331-9. 2008

[169] Bhaskar R, Varalakshmi P , Amsaveni R. *Indian drugs*. **29**, 254-8.1992

[170] Anand R, Patnaik GK, Kulshreshtha DK , Dhawan BN. *Ind J Exp Biol.* **32,** 548-52.1994

[171] Sangeeta D, Sidhu H, Thind SK , Nath R. *J Ethnopharmacol*. **44,** 61-6.1994

[172] Prasad KVSRG, Bharathi K, Srinivasan KK. *Ind J Phy Pharmacol*. **33**, 337-41.1993

[173] Kailash P, Varalakshmi P. *Indian J Exp Biol*. **30**, 440-2.1992

[174] Poonguzhali PK, Chegu H. *Br J Urol*. **74,** 23-5.1994

[175] Grases F, Costa-Bauza A. *Br J Urol.* **66,** 240-4. 1990

[176] Muangman V, Viseshsindh V, Ratan-Olarn K, Buadilok S. *J Med Assoc Thai*. **78,** 310-3. 1995

[177] Grases F, Melero G, Costa-Bauza A, Prieto R, March JG. *Int Urol Nephrol.* **26,** 507-11.1994

[178] Melzig MF. *Wien Med Wochenschr*. **154,** 523-7. 2004

[179] Suki WN. *Verh K Acad Geneeskd Belg*. **52,** 203-21. 1990

[180] Ellison DH. *Ann Intern Med*. **114,** 886-94. 1991

[181] Grases F, Conte A. *Urol Res*. **20,** 86-8. 1992

[182] Singh CM, Sachan SS. *J Nepal Pharm Assoc.* **7**, 81-5.1989

[183] Jethi RK, Indoo Bala Sofat, Bindia Duggal, Mridula Mahajan. *Probe*. **24**, 32-7. 1984

[184] Mitra SK, Gopumadhavan S, Venkatarangannna MV, Sundaram R. *Phytother Res.* **12**, 372-4. 1998

[185] Schwartz BF, Schenkman N, Nguyen R, Stoller ML. *Urology.* **56,** 912-4. 2000

[186] Garimella TS, Jolly CI, Narayanan S. *Phytother Res*. **15**, 351–5. 2001

[187] Peshin A, Singla SK. *Indian J Exp Biol*. **32**, 889–91. 1994

[188] Kabra SG, Kabra V, Banerji P, Jain LK, Bhargava A, Chaturvedi RP. *Ind J Exp Biol*. **16**, 212. 1978

[189] Trinder P. *Analyst.* **85**, 889-94. 1960

[190] Gomori MD. *J Lab Clin Med.* **27**, 955-60. 1941

[191] Chutipongtanate S, Nakagawa Y, Sritippayawan S, Pittayamateekul J, Parichatikanond P, Westley BR, May FE, Malasit P, Thongboonkerd V. *J Clin Invest*. **115**, 3613–22. 2005

[192] Nakagawa Y, Kaiser ET, Coe FL. *Biochem Biophys Res Commun*. **84**, 1038–44. 1978

[193] Trease GE, Evans WC. *Pharmacognsy*. Macmillian publishers, Canada. 1989

[194] Harborne JB. *Phytochemical methods*. Chapman and Hall, London. 1973

[195] Sofowara A. *Medicinal plants and Traditional medicine in Africa.* Spectrum Books Ltd, Nigeria. 1993

[196] Lowry OH, Rosbrough NJ, Farr AL, Randall RJ. *J Biol Chem*. **193**, 265–75. 1951

[197] Laemmli UK. *Nature*. **227**, 680–5. 1970

[198] Yang VC, Langer R. *Anal Biochem*. **147**, 148–55. 1985

[199] Elkin RG, Wasynczuk AM. *Cereal Chem*. **64**, 226–9. 1987

[200] Tazzoli V, Domeneghetti C. *American Mineralogist*. **65**, 327-34. 1980

[201] Wallace AC, Laskowski RA, Thornton JM. *Protein Engineering*. **8**, 127-34. 1995

[202] Guvench O, Weiser J, Shenkin PS, Kolosswary I, Still WC. *J Comput Chem.* **23**, 214-21. 2002

[203] Wu X, Milne JLS, Borgnia MJ, Rostapshov AV, Subramaniam S, Brooks BR. *J Struc Biol*. **141**, 63-76. 2003

[204] Todorov NP, Mancera RL, Monthpux PH. *Chem Phys Let.* **369**, 257-63. 2003

[205] Reynolds CH. *J Chem Info Comp Sci*. **35**, 738-42. 1995

[206] Bonsnes RW, Taussky HH. *J Biol Chem*. **158**, 581–9. 1945

[207] Marsh WH, Fingerhut B, Miller H. *Clin Chem*. **11**, 624–7. 1965

[208] Vassault A. *Methods of enzymatic analysis.* verley Chemie. 1992

[209] Bessey OA, Lowry OH, Brock MJ. *J Biol Chem*. **164**, 321. 1946

[210] Buege JA, Aust SD. *Methods Enzymol.* **52**, 302-10. 1978

[211] Kono Y. *Arch Biochem Biophy.* **186**, 189-215. 1978

[212] Luck H. *Methods of enzymatic analysis*. Acadmic press, New york. 1971

[213] Takeuchi K, Okada M, Ueshima K, Ohuchi T, Okabe S. *Digestion.* **54**, 91-7. 1993

[214] Zahler W, Cleland WW. *J Biol Chem*. **243**, 716-9. 1968

[215] Addadi L, Weiner S. *Proc Natl Acad Sci U S A*. **82**, 4110-4. 1985.

[216] Wang L, Qiu SR, Zachowicz W, Guan X, DeYoreo JJ, Nancollas GH, Hoyer JR. *Langmuir.* **22**, 7279-85. 2006

[217] Wang XP, Yang RM. *Eur Neurol.* **50,** 153-7. 2003

[218] Christina AJM, Ashok K, Packialakshmi M, Tobin GC, Preethi J, Murugesh N. *Methods Find Exp Clin Pharmacol*. **27**, 633–8. 2005

[219] Atmani F, Farell G, Lieske JC. *J Urol.* **172**, 1510 –4. 2004

[220] Joshi VS, Parekh BB, Joshi MJ, Vaidya AD. *Urol Res.* **33**, 80–6. 2005

[221] Kumar P, Despande PS, Singh CM. *Bull Med Ethnobot Res*. **2**, 277–84. 1981

[222] Zerwekh JE, Holt K, Pak CY. *Kidney Int.* **23**, 838–41. 1983

[223] Coe FI, Parks JH, Nakagawa Y. *Semin Nephrol.* **11**, 98–109. 1991

[224] Aggarwal S, Tandon C, Forouzandeh M, Singla SK, Kiran R, Jethi RK. *Ind J Biochem Biophy*. **42**, 113 –7. 2005

[225] Aggarwal S, Tandon C, Forouzandeh M, Singla SK, Kiran R, Jethi RK. *Mol Cell Biochem*. **210**, 109 –19. 2000

[226] Qui SR, Wierzbicki A, Orme CA, Cody AM, Hoyer JR, Nancollas GH. *PNAS USA*. **101**, 1811–5. 2004

[227] Degen E, Williams DB. *J Cell Biol.* **112**, 1099-115. 1991

[228] Wada I, Rindress D, Cameron PH, Ou W-J, Doherty JJ, Louvard D, Bell AW, Dignard D, Thomas DY, Bergeron JJM. *J Biol Chem*. **266**, 19599-610. 1991

[229] Sambrook JF. *Cell*. **61**, 197-9. 1990

[230] Gilchrist JS, Pierce GN. *J Biol Chem*. **268,** 4291-9. 1993

[231] Smith MJ, Koch GL. *EMBO J*. **8**, 3581-6. 1989

[232] Fliegel L, Burns K, MacLennan DH, Reithmeier RA, Michalak M. *J Biol Chem*. **264**, 21522-8. 1989

[233] Kretsinger RH, Rudnick SE, Sneden DA, Schatz VB. *J Biol Chem*. **255**, 8154-6. 1980

[234] Schrag JD, Bergeron JJ, Li Y, Borisova S, Hahn M, Thomas DY. *Mol Cell*. **8**, 633–44. 2001

[235] Leach MR, Cohen-Doyle MF, Thomas DY, Williams DB. *J Biol Chem*. **277**, 29686–97. 2002

[236] James DW, Ghosh M, Etzler ME. *Plant Physiol*. **77**, 630–4. 1985

[237] Lieske JC, Toback FG. *Semin Nephrol*. **16**, 458-73. 1996

[238] Lieske JC. Norris R, Toback FG. *Am J Physiol*. **273**, 224–33. 1997

[239] Gul A, Peter R. *Urol Res.* **35**, 65–71. 2007

[240] Kassack MU, Hogger P, Gschwend DA, Kameyama K, Haga T, Graul RC, Sadee W. *Am Assoc Pharmaceuti Sci*. **2**, 2-8. 2000

[241] Harriman DJ, Lambropoulos A, Deslongchamps G. *Tetrahedron Letters*, **48**, 689. 2007

[242] Khan SR. *Int J of Urol*. **59**, 59-71. 1997

[243] Williamson MP, Williams DH. Euro J Biochem. **138**, 345-48. 1984

[244] Sheng X, Jung T, Wesson JA, Ward MD. Proceed Nat Aca of Scie U.S.A. **102**, 267-72. 2005

[245] Wesson JA, Worcester EM, Kleinman JG. *J Urol*. **163,** 1343-8. 2000

[246] Ryall RL, Fleming DE, Grover PK, Chauvet M, Dean CJ, Marshall VR. *Mol Urol*. **4**, 391-402. 2000

[247] Maithel SK, Pomposelli FB, Williams M, Sheahan MG, Scovell SD, Campbell DR, LoGerfo FW, Hamdan AD. *Am J Nephrol*. **26,** 612-20. 2006

[248] Yamaguchi S, Wiessner JH, Hasegawa AT, Hung LY, Mandel GS, Mandel NS. *Int J Urol*. **12**, 290–8. 2005

[249] Cao ZG, Liu JH, Radman AM, Wu JZ, Ying CP, Zhou SW. *Zhongguo Zhong Yao Za Zhi*. **28**, 1072–107. 2003

[250] Bijarnia RK, Kaur T, Aggarwal K, Singla SK, Tandon C. *Food and Chemical Toxicology*. **46**, 2274-8. 2008

[251] Khan SR, Glenton PA, Byer KJ. *Kidney Int*. **70**, 914–23. 2006

[252] Wang L, Guan X, Tang R, Hoyer JR, Wierzbiciki A, De Yoreo JJ, Nancollas GH. *J Phy Chem B*. 112, 9151-7. 2008

[253] Thamilselvan S, Hackett RL, Khan SR. *J Am Soc Nephrol*. **14,** 452-6. 1999

[254] Verkoelen CF. *J Am Soc Nephrol.* **17**, 1673-87. 2006

[255] Robertson WG, Peacock M, Nordin DEC. *Lancet*, **2**, 21–3. 1969

[256] Mandel NS, Mandel GS. *J Urol.* **142**, 1516–21. 1989

[257] Schroder FH. *Kidney Int*. **48**, 129–38. 1985

[258] Khan SR, Shevock PN, Hackett RL. *J Urol*. **142**, 846–9. 1989

[259] Larsson L, Tiselius HG. *Metab*. **13**, 242-50. 1987

[260] Weinman EJ, Frankfurt SJ, Ince Am, Sansom S. *J Clin Invest*. **61**, 801-6. 1978

[261] Farooq SM, Ebrahim AS, Subramhanya KH, Sakthivel R, Rajesh NG, Varalakshmi P. *Mol Cell Biochem.* **284,** 95–101. 2006

[262] Selvam R. *Urol Res*. **30,** 35–47. 2002

[263] Lappas M, Permezel M, Georgiou HM, Rice GE. *J Clin Endocrinol Metab*. **89**, 2365-72. 2004

[264] Siebenlist U, Franzoso G, Brown K. *Annu Rev Cell Biol*. **10**, 405-55. 1994

[265] Fridovich I. *Annu Rev Biochem*. **44**, 147-59. 1975

[266] Rashed T, Menon M, Thamilselvan S. *Am J Nephrol*. **24**, 557-68. 2004

[267] Shan Z, Tan D, Satriano J, Silbiger S, Schlondorff D. *Kidney Int.* **46,** 388-95. 1994

[268] Cotgreave IA, Moldeus P. *Bull Eur Physiopathol Respir.* **23,** 275–7. 1987

[269] Kosower NS**,** Kosower EM. *Int Rev Cytol*. **54,** 109-60. 1978

[270] Duke RC, Ojcius DM, Young JD. *Sci Am*. **276**, 79-87. 1996

[271] Slater AFG, Stefan C, Nobel I. *Toxicol Letts*. **82/83,** 149-53. 1995

[272] Roederer M, Staal FJ, Raju PA, Ela SW, Herzenberg LA, Herzenberg LA. *Proc Natl Acad Sci USA*. **87,** 4884-8. 1990

[273] Lee W, Akatsuka S, Shirase T, Dutta KK, Jang L, Liu Y. *Arch Biochem Biophy*. **453**, 168-78. 2006

[274] Schwerin M, Dorroch U, Beyer M, Swalve H, Metges CC, Junghans P. *FASEB J*. **16**, 1322–4. 2002

[275] Lieske JC, Deganello S. *J Am Soc Nephrol*, 10, 422–29. 1999

[276] Lieske JC, Swift H, Martin T, Patterson B, Toback FG. *Proc Natl Acad Sci USA*. **91**, 6987–91. 1994

[277] Terlecki RP, Triest JA. *Urol*. **70**, 898–99. 2007

[278] Li X, He D, Zhang L, Xue Y, Cheng X, Luo Y. *Urol Res*. **35**, 193–9. 2007

[279] Moran ME, Hynynen K, Bottaccini MR, Drach GW. *J Urol*. **142**, 388-92. 1990

[280] Grases F, Costa-Bauza A, Prieto RM. *Nutr J*. **5**, 23-7. 2006